Politecnico di Bari

Repository Istituzionale dei Prodotti della Ricerca del Politecnico di Bari

Intelligent Systems for Industry 4.0: Decision Support Systems and Immersive Human-Computer Interfaces

(Article begins on next page)

10 April 2024

LIBERATORIA PER L'ARCHIVIAZIONE DELLA TESI DI DOTTORATO

Politecnico di Bari

Al Magnifico Rettore
del Politecnico di Bari

Il sottoscritto Gianpaolo Francesco Trotta nato a San Giovanni Rotondo il 04/10/1987

residente a Cassina de Pecchi (MI) Via Roma, 32 e-mail gianpaolofrancesco.trotta@poliba.it

iscritto al 3° anno di Corso di Dottorato di Ricerca in Ingegneria Meccanica e Gestionale ciclo XXXI

ed essendo stato ammesso a sostenere l'esame finale con la prevista discussione della tesi dal titolo:
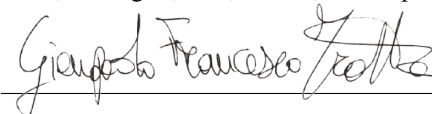
Intelligent Systems for Industry 4.0 Decision Support Systems and Immersive Human-Computer Interfaces

DICHIARA

1) di essere consapevole che, ai sensi del D.P.R. n. 445 del 28.12.2000, le dichiarazioni mendaci, la falsità negli atti e l'uso di atti falsi sono puniti ai sensi del codice penale e delle Leggi speciali in materia, e che nel caso ricorressero dette ipotesi, decade fin dall'inizio e senza necessità di nessuna formalità dai benefici conseguenti al provvedimento emanato sulla base di tali dichiarazioni;
2) di essere iscritto al Corso di Dottorato di ricerca Ingegneria Meccanica e Gestionale ciclo XXXI, corso attivato ai sensi del "*Regolamento dei Corsi di Dottorato di ricerca del Politecnico di Bari*", emanato con D.R. n.286 del 01.07.2013;
3) di essere pienamente a conoscenza delle disposizioni contenute nel predetto Regolamento in merito alla procedura di deposito, pubblicazione e autoarchiviazione della tesi di dottorato nell'Archivio Istituzionale ad accesso aperto alla letteratura scientifica;
4) di essere consapevole che attraverso l'autoarchiviazione delle tesi nell'Archivio Istituzionale ad accesso aperto alla letteratura scientifica del Politecnico di Bari (IRIS-POLIBA), l'Ateneo archivierà e renderà consultabile in rete (nel rispetto della Policy di Ateneo di cui al D.R. 642 del 13.11.2015) il testo completo della tesi di dottorato, fatta salva la possibilità di sottoscrizione di apposite licenze per le relative condizioni di utilizzo (di cui al sito http://www.creativecommons.it/Licenze), e fatte salve, altresì, le eventuali esigenze di "embargo", legate a strette considerazioni sulla tutelabilità e sfruttamento industriale/commerciale dei contenuti della tesi, da rappresentarsi mediante compilazione e sottoscrizione del modulo in calce (Richiesta di embargo);
5) che la tesi da depositare in IRIS-POLIBA, in formato digitale (PDF/A) sarà del tutto identica a quelle **consegnate**/inviate/da inviarsi ai componenti della commissione per l'esame finale e a qualsiasi altra copia depositata presso gli Uffici del Politecnico di Bari in forma cartacea o digitale, ovvero a quella da discutere in sede di esame finale, a quella da depositare, a cura dell'Ateneo, presso le Biblioteche Nazionali Centrali di Roma e Firenze e presso tutti gli Uffici competenti per legge al momento del deposito stesso, e che di conseguenza va esclusa qualsiasi responsabilità del Politecnico di Bari per quanto riguarda eventuali errori, imprecisioni o omissioni nei contenuti della tesi;
6) che il contenuto e l'organizzazione della tesi è opera originale realizzata dal sottoscritto e non compromette in alcun modo i diritti di terzi, ivi compresi quelli relativi alla sicurezza dei dati personali; che pertanto il Politecnico di Bari ed i suoi funzionari sono in ogni caso esenti da responsabilità di qualsivoglia natura: civile, amministrativa e penale e saranno dal sottoscritto tenuti indenni da qualsiasi richiesta o rivendicazione da parte di terzi;
7) che il contenuto della tesi non infrange in alcun modo il diritto d'Autore né gli obblighi connessi alla salvaguardia di diritti morali od economici di altri autori o di altri aventi diritto, sia per testi, immagini, foto, tabelle, o altre parti di cui la tesi è composta.

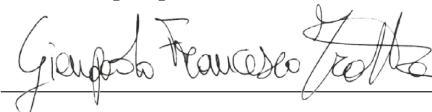Luogo e data Cassina de Pecchi, 19/12/2018   Firma _____

Il/La sottoscritto, con l'autoarchiviazione della propria tesi di dottorato nell'Archivio Istituzionale ad accesso aperto del Politecnico di Bari (POLIBA-IRIS), pur mantenendo su di essa tutti i diritti d'autore, morali ed economici, ai sensi della normativa vigente (Legge 633/1941 e ss.mm.ii.),

CONCEDE

- al Politecnico di Bari il permesso di trasferire l'opera su qualsiasi supporto e di convertirla in qualsiasi formato al fine di una corretta conservazione nel tempo. Il Politecnico di Bari garantisce che non verrà effettuata alcuna modifica al contenuto e alla struttura dell'opera.
- al Politecnico di Bari la possibilità di riprodurre l'opera in più di una copia per fini di sicurezza, back-up e conservazione.

Luogo e data Cassina de Pecchi, 19/12/2018   Firma _____

Department of Mechanics, Mathematics and Management

MECHANICAL AND MANAGEMENT ENGINEERING

Ph.D. Program

SSD: ING-IND/15–DESIGN AND METHODS FOR INDUSTRIAL ENGINEERING

Final Dissertation

Intelligent Systems for Industry 4.0: Decision Support Systems and Immersive Human-Computer Interfaces

by

Eng. Trotta Gianpaolo Francesco

Supervisors:

Prof. Eng. Vitoantonio Bevilacqua, PhD

Prof. Eng. Michele Fiorentino, PhD

Prof. Eng. Antonio E. Uva, PhD

Coordinator of Ph.D. Program:

Prof. Eng. Giuseppe Pompeo Demelio, PhD

Course n°31, 01/11/2015-31/10/2018

Department of Mechanics, Mathematics and Management

MECHANICAL AND MANAGEMENT ENGINEERING

Ph.D. Program

SSD: ING-IND/15–DESIGN AND METHODS FOR INDUSTRIAL ENGINEERING

Final Dissertation

Intelligent Systems for Industry 4.0: Decision Support Systems and Immersive Human-Computer Interfaces

by

Referees:

Prof.

Prof.

Supervisors:

Prof. Eng. Vitoantonio Bevilacqua, PhD

Prof. Eng. Michele Fiorentino, PhD

Prof. Eng. Antonio E. Uva, PhD

Coordinator of Ph.D. Program:

Prof. Eng. Giuseppe Pompeo Demelio, PhD

Course n°31, 01/11/2015-31/10/2018

SUMMARY

The aim of this PhD thesis is the design, development and evaluation of intelligent systems for Industry 4.0. In particular, because of the interest in innovative solutions for advanced services in manufacturing and bioengineering fields, the goal of the proposed solutions is the design, development and evaluation of intelligent systems following the four main principles of Industry 4.0: interoperability, information transparency, technical assistance and decentralized decisions. The focus is mainly on the technical assistance principle, which describes how assistance systems could support humans by comprehensively aggregating and visualising information via immersive and innovative human-computer interfaces when making informed decisions, solving urgent problems and conducting a range of unpleasant tasks.

In manufacturing, the time to train operators for a task, rather than the time to solve a maintenance problem for a component on a manual working station, plays a vital role in the efficiency and efficacy of an industrial environment. Therefore, considering the innovative principles of Industry 4.0, the leading research question is as follows: How should we design and develop an immersive human-computer interface to allow the operators, without any wearable device, to quickly learn the tasks required during their work? A use case based on the application of a spatial (or projected) augmented reality system was investigated. This PhD work presents the approaches used to design the manual working station and to implement the algorithms used to recognise and track the objects on the station and opportunely project the information about a specific task. Moreover, in an industrial environment, the evaluation of postures performed by operators during their work has a crucial impact on the operators' health and, in this case, on the efficiency and efficacy of industrial processes. Therefore, the central research question is as follows: How should we implement and validate a real-time system to detect awkward postures? This PhD dissertation presents the approach employed to design the system using a depth camera sensor, such as Kinect v2, and to validate it using a standardised vision system used for motion analysis in clinical examinations, such as the BTS platform.

The industrial bioengineering field is strictly correlated to the manufacturing area, concerning both technologies and techniques used to design and implement systems to support physicians during clinical and diagnostic examinations or surgical operations. In the context of this PhD work, computer vision algorithms and decision support systems able to detect and recognise tumours starting from medical images, also known as computer-aided diagnosis frameworks, were implemented to support physicians in their diagnostic decisions. Moreover, signals acquired using sensors during the clinical examination are opportunely elaborated to use them for training decision support systems

that recognise the severity of the certain neurological diseases. In this way, the problems created by the observational nature of this kind of examination are fixed, and the systems implemented help the clinicians make more precise decisions about disease severity. Finally, immersive human-computer interfaces used for comprehensively overlapping information (e.g., 3D reconstruction of a tumour) in the real world were designed and developed to help surgeons during surgical operations.

After an introduction of Industry 4.0, the dissertation is organised into two main parts, which discuss the two topics covered during the PhD research. The dissertation ends with the conclusions and future works . In detail, the second chapter, entitled Design, Development and Evaluation of Intelligent, Immersive and Innovation Human-Computer interfaces in an Industrial Scenario for Maintenance Services, is related to the discussion of immersive and innovative techniques and technologies used to improve the work quality, concerning postures in the workplace and time to finish a training task. The third chapter, entitled Intelligent Support in Industrial Bioengineering: Decision Support Systems and Immersive Human-Computer Interfaces Application, is related to the discussion of decision support systems to support clinicians during diagnostic or clinical examinations and a mixed reality system to support surgeons during surgical operations.

Contents

List of figures

List of tables

Chapter 1

1 Industry 4.0: a definition

1.1 Introduction

Industry 4.0, also known as 'The Fourth Industrial Revolution', affects entire industries by transforming the way goods are designed, manufactured, delivered and paid.

Due to the techniques and technologies introduced by this revolution, the manufacturing industry is not the only industry enduring this transformation; the service industry is changing the way services are designed and provided. The fourth industrial revolution, different from the previous industrial revolutions, was predicted a priori and not ex-post [1]. This a priori prediction allows companies and research institutes to actively shape the future. In 2011, Germany was the first to introduce an initiative, called Industrie 4.0, as part of its high-tech strategy to establish the idea of a fully-integrated industry [2]. In contrast, Italy waited until 2015 to present a national plan for Industry 4.0.

The main factor causing the fourth revolution is the rapid technological progress that introduces a range of new business potentials and opportunities: Internet of Things (IoT), Internet of Services (IoS), cyber-physical systems (CPS) and smart factories are becoming more relevant and changing the existing approaches of value or service creation. In particular, in [3] the authors explain the IoT and IoS in the manufacturing processes causing the fourth industrial revolution. While the IoT allows objects (e.g., sensors, actuators, mobile phones, wearable devices) and 'things' (i.e., interactions and collaboration with people) to reach the common goal, the IoS enables companies that provide services to offer their products via the internet. Another critical component of Industry 4.0 is the CPS. The system allows the physical world to fuse with the virtual world (made of thinking objects or intelligent services) and humans who interact both with the physical and virtual world. In [4] the authors propose a five-level CPS structure, the 5C architecture, which provides a step-by-step guideline for developing and deploying a CPS for manufacturing applications.
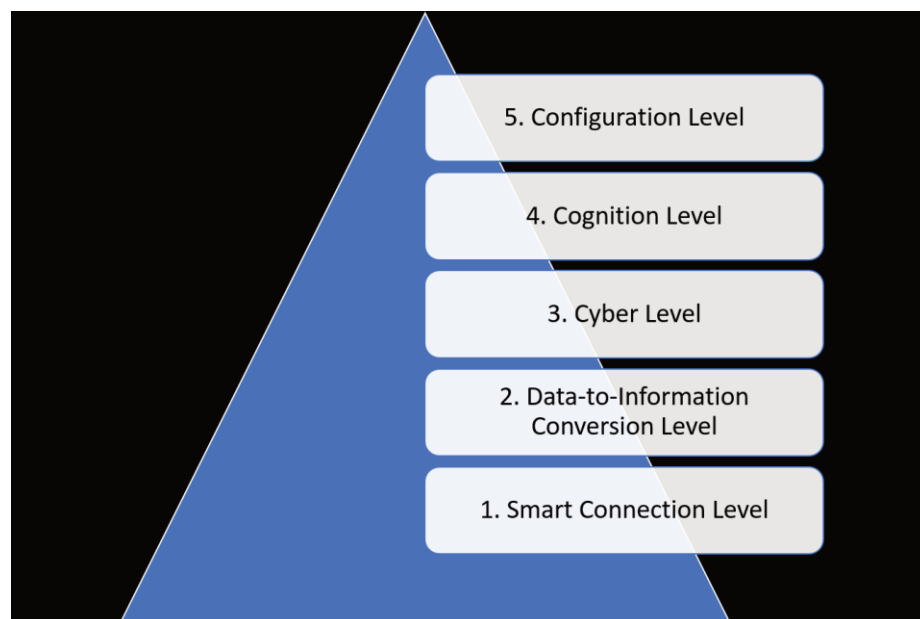
Figure 1 - 5C architecture for the implementation of a Cyber-Physical System

As presented in Figure 1, the architecture proposed consists of the following

- Smart connection layer (condition-based monitoring): represents the first step for developing a CPS and concerns the accurate and reliable processes for acquiring data from machines, humans and resources (the players of a complex industrial environment).
- Data-to-information conversion level (prognostics and health management): concerns the second level of a CPS architecture that creates smart machines using data acquired from the previous level and by applying inferred algorithms to evaluate the machines' health value.
- Cyber level (cyber-physical system, self-compare): this level uses the information from every connected machine to form the machine network and to perform specific analytics used to extract additional information that provides better insight over the status of each machine. Therefore, the cyber level is useful to predict the future behaviour of the machinery.
- Cognition level (decision support system): displays the correct information derived from previous levels to expert users. Proper presentation of the acquired knowledge to expert users supports correct decisions.
- Configuration level (resilient control system): the feedback from cyberspace to physical space. This level acts as a general control to make a machine self-configure and self-adapt.

Finally, the smart factory is the main feature of Industry 4.0. As the authors [5] explain, in a smart factory, people and machines interact to execute a task due to a system working in the background that can consider context information, like the position and status of objects. A system should support people and machines obtaining information both from the physical world (e.g., position of an object) and the virtual world (e.g., simulation model, electronic documents) to be context-aware. Therefore, considering the definitions of CPS, IoT and IoS, the smart factory, as a complex workplace in which humans and machines interact to reach goals, can be defined as a factory in which CPS and IoT and IoS systems communicate to efficiently and effectively support people and machines in the execution of their tasks.

Without a clear definition of Industry 4.0, companies face several difficulties when trying to develop ideas or take actions. Therefore, with regard to the previous considerations, Industry 4.0 could be defined as a set of technologies, techniques and concepts of a value chain organisation. In a modular smart factory of Industry 4.0, a CPS monitors physical processes, creates virtual copies of a physical world and makes decisions in cooperation with people and machines in real time over the IoT system. Via the IoS system, both internal and decentralised services could be offered and utilised both by people and machines. Therefore, to support companies and academic researchers in identifying possible Industry 4.0 pilots, in [1], the authors try to derive six design principles from the Industry 4.0 components (Table 1):

The first component is interoperability. In Industry 4.0, companies rather than in an intelligent workplace in which people and machines interact with a CPS able to manage thinking object use, also, IoS services the interoperability plays a crucial role.

Each module of a smart factory should operate with the others to assist people and machines during their work.

Second, virtualisation is the means by which the CPS can monitor physical processes. Using sensors data from the IoT infrastructure, with the virtualisation, the CPS creates

a virtual copy of the physical world to manage the cooperation between people and machines.

Third, in decentralisation, the central control of several systems that have to communicate and interact with each other is replaced, in an Industry 4.0 context, with decentralised control. The decentralisation principle allows a smart factory to train CPS to make correct decisions considering all the features coming from the modules of the entire systems. However, to avoid uncontrollable situations, the systems able to make decisions on their own must be designed to support people in their work and not replace them. This aspect is crucial in the healthcare field. For example, in a context in which a CPS can make decisions based on a patient's vital parameters, it is necessary to design and implement an alert system to notice an expert domain decision.

For the forth competent, real-time capability, an intelligent system is defined as a system able to analyse, in real-time, considerable information from several sources. It is important to avoid delays in crucial decisions that could compromise the efficiency and efficacy of the entire process.

Fifth, service orientation allows the entire smart factory to be a workplace in which each module is connected and interacts with the others; only an IoS system could be utilised. Since modules are often not internally reachable, the IoS system must offer the services both internally and across company borders.

Regarding the sixth component, modularity, a factory could be defined as smart if it is flexible and adapts itself to change requirements. A modular system is the only way to reach the goal. Therefore, only a smart factory, consisting of several modules, could adjust itself to improve product characteristics, for example.

Table 1 - Design principles of Industry 4.0 components

	CPS	IoT	IoS	Smart Factory
Interoperability	X	X	X	X
Virtualisation	X			X
Decentralisation	X			X
Real-Time Capability				X
Service Orientation			X	
Modularity			X	

Overall, the following are the abilities with which an Industry 4.0 scenario must be provided:

- The ability of machines, devices, sensors and humans to interact with each other via IoT and IoS,
- The ability of the CPS to create a virtual copy of the physical world via an aggregation of raw sensor data or higher-value context information,
- The ability of support systems to help people by aggregating and visualising information for making informed decisions and solving urgent problems,
- The ability of CPS to support people by conducting a range of tasks,
- The ability of CPS to make a decision on its own and to perform its tasks as autonomously as possible.

1.2 Challenges

As described in Section 1.1, the core of the Industry 4.0 strategy is based on intelligent manufacturing or, in general, on intelligent systems using CPS technology to decentralise production, to personalise products or services and to increase people's participation. In this way, each part of the system (people and machines) can interact to efficiently and effectively create products and services. In [6] the Germany strategic plan to implement Industry 4.0 is described. In particular, are highlighted the main points of this plan.

Building a network.

The core of the foundation of Industry 4.0 is the CPS. This system implements the connection between thinking objects and incorporates several functions, such as computing, communications, precision control, interaction, coordination and autonomy. The CPS can implement these functions only by creating a virtual copy of the physical world.

Researching two major themes.

The first theme is the smart factory, which is key to future intelligent infrastructure. The smart factory is focused on intelligent systems and processes and the implementation of networked distributed production facilities. However, the intelligent production is focused on human-computer interaction and advanced technologies. The main goal of the intelligent production is the use of innovative techniques and technologies, which can be applied to a process to create a highly flexible, personalised and networked industrial

chain. In general, not just the human-computer interactions can be applied; thing-to-thing interactions are also necessary to create better services to meet customers' needs. Therefore, the common concept between smart factory and intelligent production is the combination of smart devices with information communication technology (ICT).

Realisation of three integration.

Horizontal integration aims to achieve the cooperation between enterprises for providing real-time products and services. Horizontal integration is possible by applying integration between a resource and an information network. Vertical integration refers to a network of intelligent factories to update the traditionally fixed production processes, such as assembly-line production. Finally, end-to-end integration refers to the design and the implementation of the interconnected CPSs, each of which is implemented at a terminal and has a digital value chain that communicates and interacts with other CPS terminals. In general, a terminal can be a man, a machine, or a service. These interconnections allow the entire system to achieve complete horizontal, vertical and end-to-end integration.

Against these backdrops, the challenges of Industry 4.0 can be summarised in eight planning objectives:

1. System standardisation and implementation of a reference architecture: a set of standards needs to be designed and developed to create a network between different infrastructures and companies that must be connected and integrated.
2. Efficient management: with the introduction of large and complex systems, appropriate plans need to be made and an efficient model needs to be designed and developed to optimise the management.
3. Implementation of a broadband infrastructure to enforce strict criteria on communications networks that must be reliable, comprehensive and high quality.
4. Safety and security: the interactions between people and machines in these new scenarios have not posed a threat to people and the environment; on the contrary, the introduction of intelligent systems needs to be designed and implemented for the improvement of working conditions regarding safety, health and security.
5. Organisation and design of work to achieve humane, automated, green production and management.
6. Staff training and continuing professional development: with the introduction of these technologies, staff training and continuing professional development need to be fast and accurate. For example, new technologies such as virtual reality could be useful for training operators in a virtual safe place.
7. Establishing a regulatory framework: the introduction of the new technologies introduces new issues, such as in enterprise data, liability, personal data and trade restrictions. Therefore, appropriate means of control need to be actuated.
8. Improving the efficiency of resource use while reducing and balancing resource utilisation on the environment caused by pollution and destruction.

The interaction between people and machines must be implemented in every step of the production process assuming that, in the future, the individual worker will have more responsibility and a larger operating area. Therefore, the role of the worker will be to creatively solve issues and problems inside the CPS [7]. Figure 2 provides an example of an adapted production strategy in which the infrastructure of the entire system is designed to allow the interaction between human and intelligent systems.
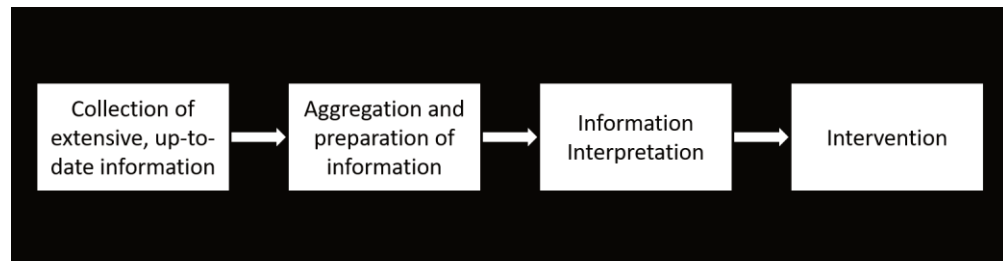
Figure 2 - Example of Human as a monitor of the production strategy and last instance in the decision-making process

The previous flowchart is applicable in every field in which human, computer, machines and thinking objects interact and communicate. Therefore, the concepts of Industry 4.0 are, in general, suitable for the fields of healthcare, agriculture and energy, as well as manufacturing.

1.3 Technologies and Techniques

Overall, the enabling techniques and technologies refer to a series of wide and multi-disciplinary characteristics applicable to complete a task [8]. To design and implement intelligent systems for Industry 4.0, several techniques and technologies could be used (Figure 3).

Figure 3 - Enabling techniques and technologies for Industry 4.0

Additive Manufacturing

Additive manufacturing is a technique introduced in recent years and applied as a production technology [9–12]. Also known as rapid prototyping, additive manufacturing is used in several applications and business models for direct part production. The application fields are the aerospace industry [13], the medical industry [14], and the engineering industry [15–21]. The Industry 4.0 paradigm introduces the customisation of products and real-time monitoring of engineering systems to gain lifecycle data. Intelligent systems, such as sensors and actuators connected to build a system to support humans in several tasks, are key enablers for smart control of an industrial value chain. Therefore, additive manufacturing contributes to the success of the application of Industry 4.0 principles through its layer-by-layer fabrication methodology for enabling the production of smart structures. The integration of sensors and actuators through additive manufacturing suggests a great potential to improve process performances in many fields of application for many products. For example, to satisfy the requirements for the centralisation of the patient in the medical field, it is possible to create biomechanical devices for a specific patient's anatomy. These devices would be equipped with several sensors connected in a body area network [22–25]. Furthermore, additive manufacturing has applications in the machine tool industry to predict maintenance [26, 27] and in metal forming tools to monitor the process temperature and wear [28].

Mixed, Augmented and Virtual Reality

Among the enabling technologies used to implement an Industry 4.0 scenario in several application fields, augmented reality (AR) and, in particular, mixed reality (MR) have proven to be suitable tools in recent years. [27, 29, 37, 38, 30–35, 35, 36]. The main goal of systems that use these technologies is to enable workers to collaborate, to interact with information collected and interpreted using an intelligent system or decision support system and to monitor and control part of or an entire physical system.

The advantage of AR over virtual reality (VR) is that the worker or the operator perceives the instructions without needing to change from a real context to a virtual one. The main application concerns the support of workers in maintenance, repair, and control tasks through instructions with textual, visual or auditory information. However, in conjunction with the introduction of the Industry 4.0 paradigm, the set of application fields had increased and is clearly of great interest in the medical field [39–45]. The benefit of using this technology is both in remote and in local assistance. Companies that have machines installed in remote locations need to monitor, operate and repair those machines with the minimum number of people on-site. Therefore, AR or MR can help by allowing collaboration between workers in different places. [46–51]. Likewise, these technologies could help support workers in the decision machining in real scenario, combining their experience with information extracted in real time from databases and overlapping opportunely in the real world.

The last described scenario concerns the quick access to documentation, like manuals, drawings or 3D models, both for training an operator by giving step-by-step instructions to develop specific tasks [52–55] and for reducing the time and effort dedicated to manually checking the well-trained operators [49]. Most of the AR solutions in literature employ head mounted displays (HMDs), which have several drawbacks, including ergonomics, cost, limited field of view, low resolution, encumbrance and weight. The use of spatial (or projected) augmented reality systems (SAR) is the key to solving this issue.

SAR is based on digital projectors that superimpose virtual data (e.g., text, symbols, indicators) directly onto the real environment [56]. However, projected AR, like all new technologies, requires feasibility studies and optimisation processes before it can be introduced into the industrial environment. One of the most important issues is the correct visualisation of technical information. In particular, in [29] the authors evaluated the possibility to project text directly onto workbench surfaces (without the need to calibrate the scene), comparing users' performance with that of a normal LCD monitor [57] because, , in a real working environment, the operator stands in front of the workbench and is currently assisted by instructions on monitors usually placed on their workbenches or tool carts.

The design of an AR-based system should include the following aspects [58]:

- The final application must provide added-value services;
- Functional discontinuities in the operating modes should be avoided;
- Cognitive discontinuities between the old and the new operating practice must be reduced;
- If the operator wears an HMD or similar technology, the system should be designed to reduce physical side-effects, such as headaches, nausea or visual loss acuity;
- The systems should be designed to avoid unpredicted effects of the devices used by operators, such as distractions, surprises or shocks;

- The designer must consider the user's perception regarding ergonomics and aesthetics;
- The user interaction must be natural and user-friendly.

Not only in the manufacturing field could an augmented reality solution be used to implement an Industry 4.0 scenario. For example, in the bioengineering field, imaging technology is important as most medical applications use imaging techniques in various forms. These medical applications use these techniques on the image outputs from X-Ray, MRI and CT scans to develop systems for image-guided surgery or post-operative imagery. [59–65]. Using these systems and AR or MR techniques, a surgeon can visualise the affected area in the correct position directly on the patient's body during a surgical operation [58]. Currently, most of the work using MR conducted in the medical field is for training purposes. Sappenfield et al. [44] used the mixed reality simulator to perform training on how to access the subclavian vein. The authors found having a navigable 3D scene benefited the medical staff

Promising results with regards to training are also provided by [66], where CBCT DICOM files are segmented and rendered as animated 3D models in a HoloLens, an HMD for MR, environment. The presence of 3D animations rendered in the real world is believed to boost medical understanding in radiology. The important technical outcome of these types of systems is that it is possible to both visualise DICOM content in this environment and apply animations to them without affecting the rendering

Initial trials for the introduction of HoloLens in a surgery room was advanced by [67], where a full MRI scan of a brain was displayed through the glasses. To track the patient during the operation, an additional tracking sensor was introduced. Although limited, this paper indicates the specialists' great appreciation for and interest in new visualisation techniques and underlines how, as of 2017, visualisation is still a bottleneck for biomedical imaging.

Finally, Virtual Reality (VR) [68]. The updates in computing technology allow VR to be used for both professional and public applications, such as for car [69–72], design and construction, in architecture and civil engineering [73, 74] and for educational purposes [75].

In manufacturing, the use of VR technologies can reduce the time necessary for developing machine tools. Machine prototypes built in this way can support human validation of the designed solution's functionality and evaluation of the results of simulations such as stress analysis, kinematics and dynamics. [76]. In particular, the concept of a virtual factory, with the introduction of Industry 4.0, is the natural consequence of VR use in manufacturing. A virtual factory is a simulated model consisting of several sub-models. Each sub-model represents a production cell of a factory. In this way, a simulated model for testing a manufacturing system can be designed and controlled [77]. The goal of this simulation is to find a problem to fix and thus improve the layout of sub-models in the context of the virtual factory. Another application of VR in manufacturing is training workers.

The main goal is to avoid the risk of use for both humans and machines [78]. Moreover, in the medical field, there are several studies in which VR is applied for training in surgery, for treating mental health problems and for analysing human movement and muscle function. For example, in [79] the authors used VR for visualising muscle activation. The system analysed human movement and muscle functions by computing, in real time, kinematic joints and kinetics for full body models and dimensions and force evaluation in muscle elements. With the introduction of VR, the

software can create interactions between humans and biomechanical data during patient examination or treatment.

Moreover, for surgery training [80], a virtual environment with a stereovision system and haptic interfaces can help users acquire technical skills involved in craniotomy-based procedures. However, in this particular field, several studies are presented on the different state-of-the-art areas of surgery [80–86]. Several studies addressed treating mental health problems as well [87]. In particular, in [88] four patients with diagnosed claustrophobia were tested. In this study, a reduction of claustrophobia symptoms after three-month treatment was observed. Moreover, the same virtual treatment for other types of phobias was positive [89–92].

Industrial Internet

The Industrial Internet of Things (IIoT) is a collection of technology used in an Industry 4.0 scenario, specifically in smart manufacturing [93]. Born from a convergence of industrial systems with ICT, sensors and communication systems [94] ., IIOT is derived from a more abstract idea, called IoT, which integrates computing and communications technology, and is expanded to include the many 'things' used both in the home [95] and at work [96].

The IoT started with the idea of tagging and tracking 'things' using low-cost sensors. However, with the introduction of smartphones, this paradigm evolved due to the perfect union between low-cost computing and pervasive broadband networking. Technically, the IoT consists of several physical artefacts that contain embedded systems of electrical, mechanical, computing and communication technologies that enable internet-based communication, using several well-known communication protocols, such as Internet Protocol and data exchange.

A consequence of the application of the IoT paradigm in industrial processes is the launch of IIoT. Although IIoT follows the same core definition of IoT, the 'things' and goals are different. The IIoT, for example, consists of sensors, actuators, robots, milling machines, 3D-printers, assembly line components, chemical mixing tanks, engines, healthcare devices, planes, trains and automobiles. An important part of IIoT is the operational technology that refers to hardware and software systems found within the industrial environment. [97]. These systems, such as a programmable logic controller, distributed control systems and human-machine interfaces are also known as industrial control systems [98–100], and the main goal is to control the several processes and procedures that occur in an industrial environment. However, these are traditional systems that with the introduction of the internet-based communication technologies, can be integrated into manufacturing organisations' information technology systems and infrastructures. Only with the union between operational technology and information technology (the core of the IIoT) will an Industry 4.0 scenario answer the needs of future systems in every application field [101].

Cloud Manufacturing

Cloud-based manufacturing (CBM) [102] is a new paradigm that contributes to the success of Industry 4.0. The goal of this paradigm in an Industry 4.0 scenario is to design networked manufacturing for enhance efficiency in a cyber-physical production line, reduce product lifecycle costs and optimise the resource allocation in response to variable-demand customer-generated tasking [103]. The features of CBM are networked manufacturing, scalability, agility, ubiquitous access, multi-tenancy and virtualisation, Big Data and IoT. With these characteristics, a CBM system could be meant as an everything-as-a-service (infrastructure-as-a-service, platform-as-a-service, software-as-a-service) system. [104–107]. A consequence of CBM is the Cloud-based Design and Manufacture (CBDM) [108] which focuses on the product realisation processes using an integrated cloud computing model. In other terms, the goal of a CBDM system is to enhance a CBM system by integrating it with cloud-based design concepts along with social product development.

Big Data Analytics and DSS

Several companies in different application fields understand it is crucial to have data analytics capabilities of driving digital transformation. Therefore, skills concerning the development of algorithms for interpreting data must be required.

In particular, in the manufacturing field, big data analytics (BDA) and technologies allow the support of real-time collection of data from several sources, for comprehensive analysis of the data and for real-time decision making to improve manufacturing flexibility, product quality, energy efficiency and maintenance processes [109–113]. Currently, healthcare organisations involving both single-physician offices with multi-provider groups and large hospital networks with accountable care organisations stand to realise significant benefits by using big data for effectively digitising or combining them. [114, 115]. It seems that existing analytical techniques can be applied to the vast amount of existing (but currently unanalysed) patient-related medical data to reach a deeper understanding of outcomes to be applied at the point of care. Potential benefits could include following up on specific diseases. In general, BDA in healthcare could contribute to evidence-based medicine. The goal is the analysis of much structured and unstructured medical data to match treatments with outcomes, device and remote monitoring for capturing, in real-time, large volumes of fast-moving data from several devices placed at home or in hospital and, finally, patient profile analytics for applying several analyses to patient profiles to improve care and lifestyles.

In general, a big data system (BDS) for healthcare, and for other application fields, consists of four main parts:

- Big data sources generally involve web and social media data, machine-to-machine data, big transaction data, biometric data, human-generated data related to clickstream and interaction data from Facebook, Twitter, LinkedIn, blogs, and health plan websites, smartphone apps, data read from remote sensors, meters, and other vital sign devices. Moreover, data types and sources include health care claims and other billing records increasingly available both in semi-structured and unstructured formats, fingerprints, genetics, handwriting, retinal scans and other medical images, blood pressure and other similar types of data. Finally, data types and sources encompass unstructured and semi-structured data such as physician's notes, paper documents and e-mail.
- Big data transformation is a component that consists of a data warehouse able to store several types of data. To properly cluster and analyse the data stored in

the data warehouse, a data transformation process should be applied. For this scope, the open-source Apache Foundation project, Hadoop, should be used to analyse data and to create N datasets used as input in an Ensemble Support Vector Machine (ESVM). Hadoop has two primary components: Hadoop File System and MapReduce programming framework. The main feature of Hadoop is that the file system and MapReduce co-deploy such that a single cluster is produced and the storage system is included in the processing system [116].

- Big data tools and platforms are a component that uses structured or semi-structured data from the big data transformation component as input. In general, this component performs the implementation of an ESVM [117], which implements a DSS based on several datasets collected in a proper data warehouse.

- Big data analytics is the core of the entire system and allows a result aggregation to comprehensively describe the analyses performed using the previous components of the system. These components include an interface to interact with humans who must make decision based on the results of BDS.

The main features of a BDS are volume, velocity, variety and veracity. In detail, a big data system creates and accumulates an incredible amount of several types of data over time. Advances in data management, particularly virtualisation and cloud computing, are currently facilitating the development of platforms for more effective capture, storage and manipulation of large volumes of data. Moreover, data are accumulated and analysed in real-time and at a rapid pace, or velocity. In many situations, the application of these features in a big data system could be the difference between success and failure. For example, in the medical field, the ability to retrieve, analyse, compare and make decisions based on output values could help physicians create a diagnostic report in a brief period due to the MapReduce ESVM approach used to predict the disease severity of patients. Big data is extensive because the information comes from several different sources. The recent exploiting of these sources for analytics means that structured data (which previously held unchallenged dominance in analytics) is now joined by unstructured data (text and human language) and semi-structured data (XML, RSS feeds). There is also data that is hard to categorise, as it comes from audio, video, and other devices.

Moreover, multidimensional data can be drawn from a data warehouse to add historical context to big data. Multidimensional data is a far more eclectic mixture of data types than analytics has ever involved. Therefore, with big data, variety is just as wide as volume. Also, variety and volume tend to fuel each other [118]. The quality of data acquired from different sources is highly variable, and success or failure decisions depend on having accurate information. Unstructured data imply all often incorrect. The veracity hypnotises a scaling up in the performance of techniques and technologies to use in a big data management system. Big data analytics could be executed across several servers, or nodes, in distributed processing and by considering the use of the paradigm of parallel computing and of the approach called 'divide and process'.

Moreover, models and techniques need to consider the characteristics of BDA. Traditional data management hypnotises the warehoused data is certain, precise, and clean. High-quality data enable improving the coordination of processes in different application fields, avoiding errors and reducing costs.

Simulation and prototype

The main goal of simulation and prototype technologies and techniques is to mirror the physical world in a virtual one. This feature is crucial for a CPS implemented in an Industry 4.0 scenario. In general, a physical world includes machines, products and humans. The virtualisation of the world allows workers to test and optimise processes in a simulated manner and apply the changes in the physical world. There are several simulation studies used for observing the behaviour of machines and operators in manufacturing: movements [119, 120], connectivity with robotic arms [121, 122], real-time tracking [123, 124], energy efficiency [125, 126], deadlock prevention [127, 128], and the use of virtual engineering objects for industrial design and manufacturing [129–133]. Also, in this case, the application fields are many, and since there is great interest in the medical field, the practical knowledge of these techniques from manufacturing is shifted to bioengineering to reach the same goal [134–137].

Robotic Systems

This complex system in which machines and humans interact to reach a common goal consists of modern robots characterised by autonomy, flexibility and cooperation. Currently, robots interact with one another and work safely with humans, even learning from them [138, 139].

In general, the use of robots in a system offers cost advantages when performing most of the processes in an intelligent environment. For example, the use of the programmable dual-arm robot is proposed in [9] for material distribution in the assembly line. This study focused on the safe operation of the robot through monitoring the environment while the robot was working. Several procedures were implemented to avoid unsafe behaviour. For example, if any disturbance, such as humans or equipment, enters the robot's virtual space (safety eye), the system stops the robot's movement with a sound anticipating some complicity [140, 141]. At this point, an operator could remove obstacles before the robot resumes working. Since manufacturing tasks are becoming individualised and flexible, robots in the smart environment should perform tasks collaboratively without reprogramming. The way is a ubiquitous interaction between robot and robot and human and robot as described in [142–144].

Cyber Security

A CPS consists of millions of embedded sensors and communications devices. This type of infrastructure is weak regarding risks associated with the increasing use of data or concerning systemic breaches [145]. Therefore, a cyber-physical manufacturing systems may face the threat of cyber-attacks. Generally, malicious software affects and spreads from one machine to another through communication systems to modify the manufacturing processes or destroy data, leading to product quality defects or a complete shutdown. Therefore, the implementation of an intelligent algorithm to avoid these situations is critical in an Industry 4.0 scenario because industrial data is highly sensitive, encapsulating various aspects of the industrial operation, such as information about products, business strategies and companies [113].

1.4 Application Fields

According to the previous chapters, the key instruments for enhanced value creation when adopting the Industry 4.0 paradigm are platform-based cooperation and a dual innovation strategy to answer these questions: how should we manage the close cooperation required between the actors of a value chain? How can we help achieve the breakthrough for the Internet of Everything even though it will need to be built onto the existing infrastructure in our developed economies? In Section 1.1, the goals of the CPS were described. In particular, the virtual copy of the physics world needs to be completed to allow all a system's modules to collaborate with each other to achieve a goal. The continuing convergence of the real and the virtual worlds will be the main driver of innovation and change in all economic sectors. The IoT, data and services play a vital role in mastering the energy transformation, developing and designing an innovative and optimal mobility and logistics sector, providing support to improve processes and systems in the healthcare field and enhancing the value chain of the manufacturing industry [146].

The IoT, data and services or 'Internet of Everything', with a CPS and smart factory are the players of the forth industrial revolution. If an object used in manufacturing is described as smart, it follows the Industry 4.0 paradigm: the object can communicate and interact with other actors of the value chain to reach the goal of making a decision and supporting humans in their work. The potential of IoT, IoS, CPS and smart factories becomes particularly apparent when different, formerly separate, fields of application converge.

Today, these fields have new relationships, interdependencies and interactions with each other (Figure 4).
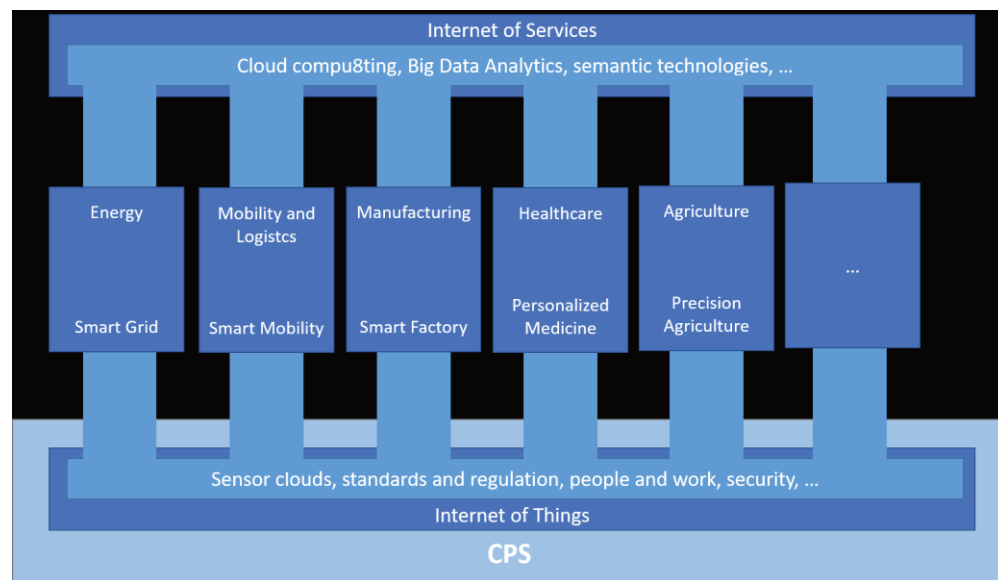
Figure 4 - Modules of Industry 4.0 applied to several fields

Energy

Modern electricity production is increasingly decentralised [147] but is more dependent on the weather conditions. However, several types of research are focused on this issue. For example, in [148] an approach to assess distribution system reliability in different weather conditions is presented. In general, these problems are related to smart grids: a solution to manage the energy acquired by several sources that incorporate both industrial generating facilities and private consumers. A smart grid is a combination of energy technology and ICT, and with the introduction of the Industry 4.0 paradigm, several new approaches could be used to perform new measurements, controls and automatism across the entire distribution grid [149, 150].

Moreover, the implementation of the Industry 4.0 paradigm in the energy field introduces the new business model and new distribution to provide consumers with incentives to change their energy consumption patterns. The principal result of the application of the Industry 4.0 paradigm in the energy field is the Internet of Energy (IoE) [151]. The optimisation of the processes to produce, store and consume energy is the main goal of the IoE. This goal is reached by introducing CPS, IoT, IoS and smart factories to update the concept of the smart grid. In fact, while the smart grids, and in particular smart cities, are introduced to create a sustainable model for cities able to preserve their citizens' quality of life, the IoE can be used to change, for example, the transport processes from design logistic processes, through real-time optimisation, to update the model day after day [152].

Mobility and Logistics

As it has always been an efficient logistics and mobility, allow communities to grow economically. The key is an efficient transport system [153]. The previous introduction of digitalisation [154] and the more current introduction of Industry 4.0 [155] allows the implementation of new methods to move, store, realise and supply freight through the world. Trends, such as urbanisation and growth in global trade, as well as rapid growth in e-commerce, have led to an increase in transport requirements. The Industry 4.0 techniques and technologies allow services to be based on quality, reliability, efficiency and sustainability: requirements dictated by society [156]. Several scenarios could be designed and implemented to improve the transport services applying IoT, IoS, CPS and smart factories. For example, the integration of manufacturing and logistics via the Industry 4.0 paradigm could allow the production of manufacturing to respond instantaneously to supply variability, but this is realisable only if supply chains are networked with manufacturing facilities in real time. Another key to the implementation of an intelligent transport system derived from the concept of decentralisation introduced by digitalisation and Internet 4.0. In this context, the decentralised structures and processes make it possible to manage a large complex logistics system. Therefore, to make logistics and transport systems more efficient, real-time systems able to record events and status using Industry 4.0 principles and technologies will allow fast detection of any disruption to the system, thereby enabling support for human operators to rapidly solve issues [146, 157].

Agriculture

The connectivity of tools used in agricultural practices is the key to enabling the development of the precision agriculture paradigm conceptualised a decades before the introduction of Industry 4.0 [158–160]. However, the Industry 4.0 paradigm introduced new principles that created challenges for enabling data exchanges and for investing in new infrastructures. The goal is to design and implement new scenarios able to support humans in several tasks [161, 162]: to optimize routes for tractor drivers, to optimize the efficiency and productivity by means of smart sensors and, in general, to reduce the need of a human workforce by means of automation of vehicles, robots and other machinery. The key to this transformation is the ability to collect and manage a huge quantity of data with the production with several techniques introduced by the big data concept, a technology of Industry 4.0. Therefore, the development of these new tools and practices in agriculture relies strongly on the development of connected objects [163].

Manufacturing

The manufacturing field is the first area in which the Industry 4.0 paradigm was applied [3]. The digitalisation and the introduction of the forth industrial revolution principle applied to manufacturing are characterised by flexible control of production and associated areas.

This goal is reached by designing a CPS system linked to and that interacts with IoT and IoS in real time. The result of the application of Industry 4.0 principles in this field is smart factories: the industrial environment in which human-machine, human-resource, resource-machine and machine-machine interactions allow humans, machines and resources to communicate with each other as naturally as in a social network. Therefore, the implementation of interactions between players in a factory is the main goal Industry 4.0 principles must reach to improve the value chain.

By applying these principles, products are uniquely identifiable, may be located at all times and have their history known, as well as their current status and alternative routes to achieve their target state. Autonomous, distributed machines, robots, transport and warehousing systems that control and configure themselves according to the needs of the current situation negotiate with each other to establish who has spare capacity at any given moment [146]. There are several applications of intelligent systems in the manufacturing field, each of which is different not in their goals but in the technologies and techniques used to reach those goals. For example, in [142] the authors present a framework that consists of an industrial network, cloud and supervisory control terminals. Each terminal can be a machine, conveyors and products. After the framework description, the authors perform a classification of the smart objects into various type of agents, and they define a coordinator in the cloud. Therefore, in this work, the technologies and techniques of cloud-based manufacturing, described in Section 1.3 are used to achieve high efficiency of the processes by mean of the implementation of an autonomous decision framework and distributed cooperation between agents.

The smart factory result is characterised by a self-organised multi-agent system assisted by big data (see Big Data Analytics and DSS section) feedback and coordination. In the end simulations (see Simulation and prototype section) were performed and the results assess the effectiveness of the proposed negotiation mechanism and deadlock prevention. Moreover, many applications for adaptive maintenance and training using mixed, virtual or augmented reality (see Mixed, Augmented and Virtual Reality section) are implemented considering the Industry 4.0 principles [164].

Healthcare

In healthcare, particularly in the bioengineering field, the digitalisation and the introduction of intelligent knowledge-based systems have a lasting impact on peoples' lives and the healthcare system itself. The two main goals in this area are prevention and personalisation.

Several applications were designed and developed to implement a patient-centred healthcare system in which, for each patient, information about factors such as genetic make-up, a wide range of physiological parameters, diagnostic or clinical examination are combined. This huge amount of data is then transformed using intelligent algorithms to support physicians accessing a suitable set of information that is more useful for that specific type of patient. Therefore, personalised medicine is the way to reach these main goals [165, 166, 175–184, 167, 185–191, 168–174]. An Industry 4.0 scenario, including all methods, techniques, technology and principles could be implemented to improve the healthcare industry. In fact, currently, many studies focus on the design of a CPS, the core of an Industry 4.0 scenario, applied to personalised medicine [192–196]. In particular, a medical cyber-physical system is a healthcare critical integration of a network of medical devices designed to face several challenges, including inoperability, security and privacy and high assurance in the system software. Moreover, the IoT, data, services and DSS provide physicians with information about patients' personal health to allow the selection of a more precise treatment.[146].

1.5 Conclusion

In this first chapter, the Industry 4.0 paradigm was described. Starting from the main principles that must be implemented in an Industry 4.0 scenario, the chapter focused on the challenges, the application fields and the enabling techniques and technologies of Industry 4.0.

In addition to the manufacturing industry, particularly maintenance, a great emphasis is placed on industrial bioengineering applications. Since 2011, when the German government introduced the Industry 4.0 paradigm, the practical knowledge acquired by manufacturing fields has transferred to other fields, such as bioengineering. Therefore, the innovation of this PhD work is, firstly, the application fields in which an Industry 4.0 scenario could be designed and implemented following all the main principles and, secondly, the technologies used to optimise a process or a task both in manufacturing and in bioengineering. The discussion in this first chapter allows for an understanding of the great impact on peoples' lives and works that an Industry 4.0 scenario could have. The goal of intelligent systems for Industry 4.0, described in the next chapters, is to ensure an intelligent interaction between information, decision support systems, immersive technologies and humans to improve the quality of the technical assistance, one of the four main principles of Industry 4.0.

Chapter 2

2 Design, Development and Evaluation of Intelligent Human-Computer Interfaces in an Industrial Scenario for maintenance services

2.1 Introduction

2.1.1 Objectives and research questions

The objective of this part of the work is the design, development and evaluation of Intelligent Human-Computer Interfaces in an Industrial Scenario for maintenance services. In particular, two uses case will be described and discussed. The first one concerns the application of the Spatial (or Projected) Augmented Reality (SAR) technology to allow the design of an intelligent system for adaptive maintenance. Meanwhile, the second one concerns the development and validation of Computer Vision-based system able to support a RULA expert rater to evaluate the exposure to risk factors in workplaces.

Looking at the different phases of the product lifecycle and how AR has already been used for each, those that are less dependent from the product itself, are manufacturing, commissioning and inspection, and maintenance. In particular, in those three phases, except for certain product categories (e.g. cars, planes, plants), the product is handled into a Manual Working Station (MWS). Common operations that are accomplished into an MWS are assembly, welding (especially spot welding), packing, testing, repairing, inspecting. In all these tasks, the worker has to follow some strict procedures and s/he is supported by information that can be provided in an AR mode, with all the benefits, which are widely discussed in the literature [132, 197–203]. The motivation for the optimism regards the introduction of AR technologies in industrial sector arises from the literature where is described how AR instructions significantly reduced participants' overall execution time and error rate in manual assembly tasks.

Despite the steady improvement in working conditions, according to the Sixth European Working Conditions Survey [204], exposure to repetitive arm movements and tiring positions remains a common issue. Taking into account worker's health and also welfare costs, it is mandatory to apply policies aimed at minimising risks belonging to the work-related musculoskeletal disorders (WMSDs). WMSDs include "all musculoskeletal disorders that are induced or aggravated by work and the circumstances of its performance" [205]. The best applicable practice to prevent WMSDs consists in the evaluation of the exposure to risk factors in the workplace and in planning an eventual ergonomic intervention as the workplace redesign. Many methods have been developed with this goal. They can be classified into three groups: i) self-report; ii) direct measurement, and iii) observational methods [206]. Self-reports methods suffer from non-objective factors and are affected by intrinsic limits of subjective evaluations [207, 208]. Direct methods use data from sensors attached to the worker's body, but they are typically more expensive, intrusive, and time-consuming [209–211]. Observational methods, which are widely applied in industry, consist of direct observation of the worker during his work shift. A detailed review of the most common observational methods can be found in [212] where OWAS, revised NIOSH, RULA, OCRA, REBA, LUBA, and EAWS are compared. In industrial practice, posture data are collected through subjective observation or estimation of body-joint angles in pictures/videos. These methods have the main disadvantage to require a field expert who performs a time-consuming analysis of the postures. Therefore, a method based on Computer Vision techniques using low-cost and calibration-free depth camera is required to suggest a semiautomatic

approach to observational methods aiming to support an expert rater during the valuation of postures.

2.1.2 Contribution

The main contributions of the presented works regard the study of the implemented systems to optimise methods for future update and to use the methodologies in the bioengineering field. In particular, concerning the design and development of the SAR system for MWS, the interaction between the system and the database in which are stored all information about the task and the calibration process are investigated. On the other hand, regarding the system based on Computer Vision techniques to evaluate posture in the workplace, a validation procedure based on an expensive device used in the clinical application (BTS Bioengineering platform [213]), is performed to validate the system implemented and based on low-cost device.

2.1.3 Part outline

In the paragraphs that follow, I will present state of the art about immersive Human-Computer Interfaces for Industry 4.0, in part explained in previous paragraphs (seeMixed, Augmented and Virtual Reality). Also, an introduction on Human Ergonomics and Motion Analysis in which I'll focus mainly on the aspects concerning the health of a worker and how the techniques used and standardised in the clinical application can be used to validate systems and instruments for the industrial scenario will be discussed. Moreover, I'll describe the two systems designed, implemented and evaluated, Finally, a common conclusion in which I'll focus on how same technologies can be used to help humans both in bioengineering and manufacturing field.

2.1.4 Human-Computer Interfaces for Industry 4.0

Following the Industry 4.0 principles, each player of an intelligent environment consists of modules to interact with other players. A player is not only a machine, but can be a resource or a human or, in general, intelligent objects.

An intelligent environment can be described as a cyber-physical structure in which humans should be integrated to realise their individual skills and talents fully. Therefore, a cyber-physical structure can be described as a network of relationships between humans and CPS consists of physical and virtual components [214]. The interaction between humans and physical or virtual components of CPS occurs both by direct manipulation of the virtual of physical components and by means of human-computer interfaces. In this contest, the role of the worker is to dictate a production strategy and supervise the implementation of the self-organising production processes. Therefore, the classic workplace becomes less significant due to extensive networking and mobile real-time information availability. The result of the application of this type of paradigm is that the workers assume more responsibility on a larger operating area since that their decision and monitoring processes can be executed on site or from afar. In this way, the worker takes on the role of the creative problem solver and his/her work is characterized by constructive planning activities or mental work. The novel role of human workers must be combined with the implementation of organisational and technological material and methods. Firstly, the need to fit qualifying strategies creates a need to find a resource that solves problems with an interdisciplinary approach that is necessary for an Industry 4.0 scenario. On the other hand, the need of human-technology solutions provides the creation of a networked and decentralised manufacturing system, the main result of the implementation of Industry 4.0 principles.

The CPS implementations with their abilities to gather, exchange and process data are leading to increasing the requests for managing information in every application fields of Industry 4.0. The result is an emerging need for requirements concerning the acquisition, aggregation, representation and re-use of data. In order to control and manage processes in these innovative systems, human workers must easily interact, in a distrusted manner, with all the necessary interfaces for visualising current production processes and the resulting data. On the other hand, each component of CPS must be able to collect data originate from a multitude of different data sources by means of standardised and platform-independent interfaces. Human workers must be able to interact with this component using mediating interfaces such as VR or AR. In particular, as described in Mixed, Augmented and Virtual Reality paragraph, VR allows the user to simulate and explore the behaviour of the CPS-based production system. On the other hand, the AR, which represents the computer-aided enhancement of human perceptions by means of virtual objects placed in the real world, allows the user to interact with CPS directly or to view information to make a decision on a specific process. There is a lot of information that could be visualised in the field of view of the human's works. Therefore the CPS must have such component able to evaluate information with which the human workers have to interact to make an intelligent decision. These components, also called, Decision Support Systems (DSS) are necessary components in a CPS, as described in paragraph 1.1. To implement these types of interactions, the IoT or IoS parts of an Industry 4.0 scenario, must be designed on a network in which each intelligent object has to be able to interact with each other following a precise standard for information access and exchange. By implementing the network of thinking objects and the interfaces for the interaction between data and human workers, the aggregated and pre-processed information can be directly accessible by human workers by means of mediating interfaces [215]. Therefore, several scenarios can be designed:

- maintenance by providing interactive and virtual instructions [216–218];
- quality control monitoring or, in general, production processes monitoring by means of an intelligent retrieval and allocation of information, such as the status of a CPS [219–221];
- planning and simulation of production processes to understand and optimise the behaviour of the CPS. In this scenario, the objectives must be both the design of information and virtual objects handling to be as user-friendly as possible and the implementation of the scenario by following specific requirements especially concerning robustness and security [222–224].

In general, interaction must be intuitive. This means that the same experiences gained while dealing with real objects can be transferred to the virtual/digital world. Tradition user interfaces are characterised by an unimodal interaction, in which the user, by means of several input devices such as a keyboard, mouse, joystick, etc., can give a command to the system that replies with the visualisation of the command result (generally, on a screen). The use of innovative multi-touch and voice control devices allows for improved ease of use, which will be updated by users personal experience [225]. However, the need to introduce innovative user interfaces collides with the strictly specific requirements of the environment in which the interfaces have to be used (industrial environment, operating room, etc.). For example, the most important form of interaction is the touchscreen interaction. However, only with the introduction of the Dispersive Signal Technologies (DST) [226], smartphones or tablets have been introduced in an industrial field since DST allow the human worker to interact with the touch screen when wearing gloves. Other problems such as dust and water splash must be solved to introduce smartphones or tablets in an industrial environment but already exists some hardware solutions. Voice control is another type of interaction that allows human workers to interact with systems even if their attention or haptic capabilities are fully busied [227]. Moreover, natural gestures interfaces are like voice control interfaces since it is particularly intuitive and immediate. Recognizing hand position and movements, natural gestures interfaces could be image or device based. In the device-based version, wearable sensors, such as acceleration or position sensor, have to be worn to record users' movements. On the other hand, image-based systems use camera sensors object recognition and image processing techniques to recognise the gesture, posture, hand position, etc. [7].

Natural User Interface (NUI) is a goal of the Human-Computer Interface (HCI). The true meaning of what NUI is has evolved along with the introduction of the new technologies. For example, the Graphic User Interfaces (GUIs) are considered an NUI compared to command-line interface and Gesture UI, by means of technologies such as Kinect, is considered an NUI advanced over GUI [228]. A meaning of NUI could be gestures, touch, speech and haptics that support user interaction with a system via the human body [229, 230]. For example, in [231] the authors described the concepts regarding touch, tap and swipe on a flat screen with the disappearance of buttons. The new technologies, such as AR, VR and voice commands produce a new definition of NUI. Nowadays user interfaces are based on vision, hearing and tactility. However, to improve the experience new technologies are implemented by enabling thermal, wind and pressure stimuli based on the sense of touching. For example, in [232] the authors demonstrate how the addition of thermal and wind stimuli in a virtual reality scenario improves the sense of presence for a specific simulation. Moreover, in [233, 234] the authors design thermal and pressure feedback for mobile devices to reach haptic interfaces. The common goal of these studies is the extension of user interfaces with peripheral modalities beyond vision and hearing. Other senses such as olfaction and gustation

are also important for a human to interact with the world since that plays an important role in human emotion, memory and social interaction [235]. However, there are few works in the state of the art that explore the interfaces to support olfaction and gustation. For example, a study that demonstrates how people could use smell to tag photos compare with text label is presented in [236]. Another study designs and built an olfactory display system that distributes spatially on the touch screen several types of odours [237]. Finally, a team of researchers present an olfactory display based on biometric data in [238]. However, the most important study concerning olfaction is [239] in which Obres et al. identified 10 categories of smell experience that are useful to encourage the HCI community to design and implement devices for the improvement the simulation of olfaction in a simulated world. The research in the olfactory interfaces has encouraged the design and implementation of devices to simulate the sense of taste [240–242]. The common goal of these studies is to investigate the implications of gustatory experience by designing and implementing devices to allow users to taste dispensed flavours by touching the tongue to the screen or by developing a digital taste interface that simulates several tastes on the tongue via thermal or electrical stimuli. However, these types of interactions are still limited [243].

2.1.5 Human Ergonomics and Motion Analysis technologies

The applications of human motion analysis are growing fast in the areas including but not limited to healthcare [244, 245], virtual reality [246], sport [247], etc. [248], over the past decades. Human motion tracking systems generate real-time data that represent human movement and posture. The tracking system can be classified according to the motion capture techniques as optical and non-optical. Non-optical systems, or sensor-based systems, include the inertial, magnetic and mechanical motion capture techniques. These systems have the disadvantage of being intrusive, which can affect the performance of the system and limit its application. Optical-based systems utilize data captured from one or more cameras (infrared or video camera) to triangulate the three-dimensional position of a subject according to marker-based or markerless techniques. Systems such as Optitrack (http://optitrack.com/), VICON (http://www.vicon.com/), and BTS (www.btsbioengineering.com/) are vision-based tracking systems with markers. Instantaneous bone position and orientation and joint kinematic variable estimations are accurately addressed in the framework of rigid body mechanics (Figure 5).
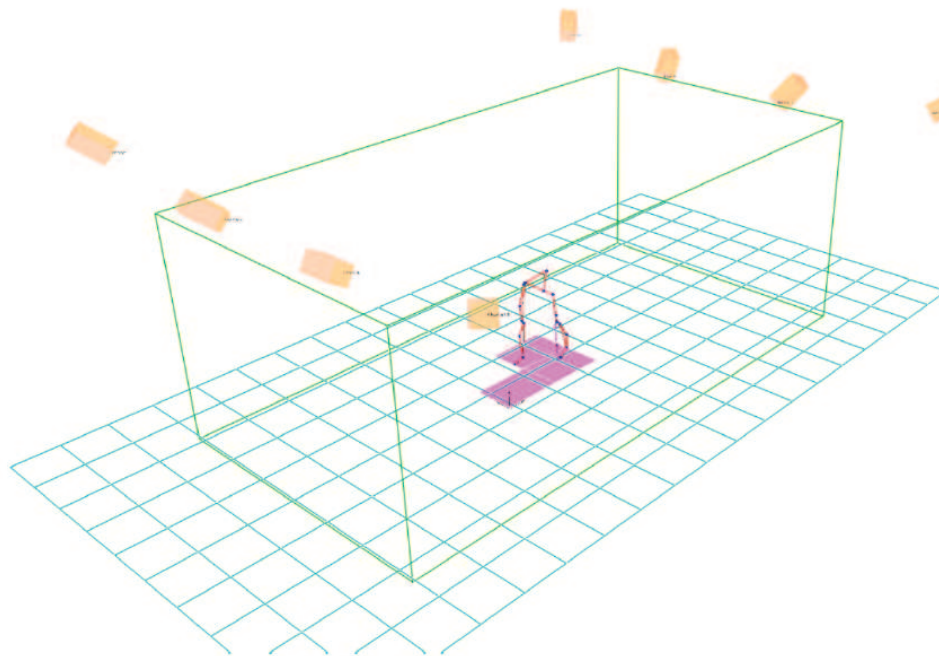
Figure 5 – 3D tracking during Gait Analysis Processing in BTS Smart Clinic environment: infrared cameras (orange), force platforms (magenta), biomechanical model (red segments), calibrated volume (green parallelepiped).

In particular, by using a combination of several markers in a specific pattern, the software can identify rigid bodies or skeletons. By putting at least 3 markers on the rigid body in a unique and non-symmetric pattern, the motion capture system is able to recognize the object and determine its position and orientation. A skeleton is a combination of rigid bodies and/or markers, and rules for how they relate to each other. Several pre-defined skeleton models for the human body exist in the motion capture software, but it is possible to set up user-defined skeletons or models depending on the needs of the researchers. Commercial systems available offer the combination of hardware and software to: acquire the position of the passive markers placed on the body segments (capture), reconstruct the trajectories of each marker (tracking) and - if required - elaborate the three-dimensional data (analyse) according to a specific medical protocol [249, 250].

The posture analysis field is really crucial in an industrial environment in which the human workers are undergone to repetitive movements during work tasks. Therefore, several observational methods used by experts are introduced to avoid posture problems. However, observational methods like OWAS, NIOSH, OCRA, and EAWS, even if supported by depth cameras user data, still require a heavy intervention by a field expert to estimate the required parameters (e.g. forces, loads, static/repetitive muscular activity etc.). The ISO standard 11228-3:2007(E) [251] suggests the use of a simplified method in the early stage of the analysis and, if critical conditions are detected, provides the OCRA method to be applied for additional investigation. Among the simplified methods for rapid analysis of mainly static tasks, the RULA, acronym of Rapid Upper Limb Assessment, is one of the most popular [252]. The main weakness of RULA is related to the inter-rater reliability. In [253] the authors found just "fair" inter-rater reliability of the RULA grand-score (ICC<0.5) among four trained raters. Dockrell et al. [254] proposed an investigation of the reliability of RULA that demonstrated higher intra-rater reliability than inter-rater reliability implying that serial assessments would be more consistent if carried out by the same person. Bao et al. [255] showed that, if a "fixed-width" categorization strategy is used when classifying the angles between body segments, the inter-rater reliability grows with the amplitude of the width. Moreover, larger body parts as shoulder and elbow, allow better estimation than smaller ones, as wrist and forearm [256, 257].

The introduction of low-cost and calibration-free depth cameras, such as the Microsoft Kinect v1 sensor, provided easy-to-use devices to collect data at high frequencies. Several authors studied the accuracy of kinematic data provided by the Kinect v1 device in various application domains [209, 258–261]. The results showed that Kinect v1 is accurate enough to capture human skeletons in a workplace environment. The accuracy and robustness of the provided joint positions (skeleton tracking) are promising for applications that require to fill in an ergonomic assessment grid [262, 263]. Patrizi et al. [264] compared a marker-based optical motion capture system with a Kinect v1 for the assessment of the human posture during work tasks. However, three main technical problems arose in the works using Kinect v1: the lack of wrist joints tracking, the influence of the environment lighting conditions, and the self-occlusions (in postures such as crossing arms, trunk bending, trunk lateral flexion, and trunk rotation). The Kinect v2, presented in 2013, uses a different technology (time-of-flight), and according to the specifications, it outperforms the previous version. It tracks 25 body joints including wrists; it is more robust to artificial illumination and sunlight [265] and more robust and accurate in the tracking of the human body [266]. Conversely, a study [210] found the non-trivial result that Kinect v1 outperforms v2 as regards average error of joint position (76 mm vs 87 mm) in seated and standing postures. These results feature the Kinect v2 sensor to be a promising tool for postural analyses, especially for the metrics whose calculation is based on angular thresholds that tend to minimize the effect of joint angle errors.

2.2   Usable AR-based system for adaptive maintenance

The Manual Working Station (MWS) applications are crucial in an Industry 4.0 scenario. Some requirements must be respected to develop applications for industrial augmented reality [267], i.e.:

- reliability: high accuracy, fall-back solutions;
- user-friendliness: AR system safe and easy to set up, learn, use, and customize;
- scalability: setup easy to reproduce and distribute in large numbers.

The MWS scenario is effortlessly reproducible in a laboratory. Therefore, is simple to look for all the possible bottlenecks and try to solve them in order to have a reliable application. By testing the application with focused user tests, and thanks to their feedbacks, it would be possible to create a user-friendly solution. Finally, about the scalability, the aim to find all the hardware and software solutions that are the less dependent as possible to the product and operations to be accomplished in the MWS is investigated. Most of the AR solutions in literature employ Head Mounted Displays (HMDs), which have several drawbacks in terms ergonomics, cost, limited field of view, low resolution, encumbrance and weight [268, 269].

2.2.1   Research question

The main research question is about the usability of a projected AR on MWS. The goal is to design and develop a system able to give, in a proper manner, all the necessary information directly on the real environment by means of digital projectors to superimpose virtual data (text, symbols, indicators, etc.) [56]. However, projected AR, like all new technologies, requires some feasibility studies and optimization processes before it can be introduced in the industrial environment. One of the most important issues is the correct visualization of technical information, and then, an evaluation of users' performance deriving from the use of a normal LCD monitor [57] compared with projected AR must be performed. This because, in a real working environment, the operator stands in front of the workbench and is currently assisted by instructions on monitors usually placed on their workbenches or on tool carts.

2.2.2   Materials

From state of the art, the first lesson learned is that Head-Worn Displays (HWD) should not be used in an MWS scenario for adaptive maintenance. The worker does not have a real perception of the objects that s/he is handling, and this could be very dangerous. Furthermore, HWDs are connected via cable to the computer where the application is running. This physical link, along with wearing issues may cause ergonomic problems. Moreover, the projection of text on real industrial workbench surfaces produces the same performance of text displayed on an LCD monitor (except for the blue text) [57]. Furthermore, reading of text projected on wooden surfaces is better than the reading of text displayed on an LCD monitor. Vision-based tracking methods are highly sensitive to lighting changes [270]. For this reason, fine control of the environmental lighting should be taken into account. This led to the need for an external lighting system. As regards contents, the experience acquired demonstrates that the use of animated 3D virtual objects is not essential. The time required to create an animation is often more than the benefit that the animation gives, especially for experienced workers. This encouraged the design and development of projective AR and the consequent use of 2D graphics signs to indicate objects or operations to accomplish in the real scene. The main technical features defined for the prototype are:

- A light frame to be clasped on a normal workbench of a Manual Working Station; the dimensions of the reference workbench are 1200 mm (L) × 1000 mm (D). The frame should be designed to hold multiple cameras and projectors at an adjustable distance.
- A turntable where the product to be assembled/maintained should be fixed. In many cases, this additional frame is already present to facilitate the operators in the maintenance tasks. The need to use it in this system concerns the possibility to locate the tracking markers. This is because marker position on the product may vary during the working steps, e.g. assembly.
- The optical tracking is based on fiducial markers that are glued on the turntable. A multi-marker technique is used with the markers placed so that it is always visible from the camera at least one of them.
- An additional lighting system must be provided, to have uniform lighting on the markers.
- The virtual contents that the projector should display are 2D graphic signs as circles, arrows, squares, crosshairs, etc.
- The user interface is projected directly on the workbench and contains a menu with the tree of the operations performed/to perform and the possible subtasks of the current operation.
- The contents navigation could be done with virtual buttons or other Natural User Interfaces like voice recognition and gesture recognition [129].

2.2.3 Methods

The application framework developed for this prototype is based on the general structure of an assembly/maintenance manual. A reorganisation of the information about the maintenance steps in a tree-like structure with different levels of detail should be evaluated [132]. This allowed the technicians to gain in efficiency as compared to paper manual, skipping well-known details while accessing specifics only if needed (learning, troubleshooting, etc.). Therefore, the following four commands may be sufficient to navigate the manual effectively:

- Next. A maintenance task, at the current level of detail, is clear or completed. The user wants to access the information about the next task at the same level of detail.
- Previous. The user wants to access the information about the previous task at the same level of detail.
- Go down (to a lower level). More detailed information is required; therefore, the current task is expanded in a more detailed sequence of sub-tasks (e.g., unknown task or troubleshooting).
- Go up (to an upper level). The user needs fewer details. Therefore s\he navigates through a sequence of less detailed tasks.

Going up to the first level brings the user to the root node of the manual. Considering this structure of manual, the user of the application can go back and forth from a step to the previous/following, up a level to go the main menu, down a level to access further details for that step.

The system architecture is schematized in Figure 6.
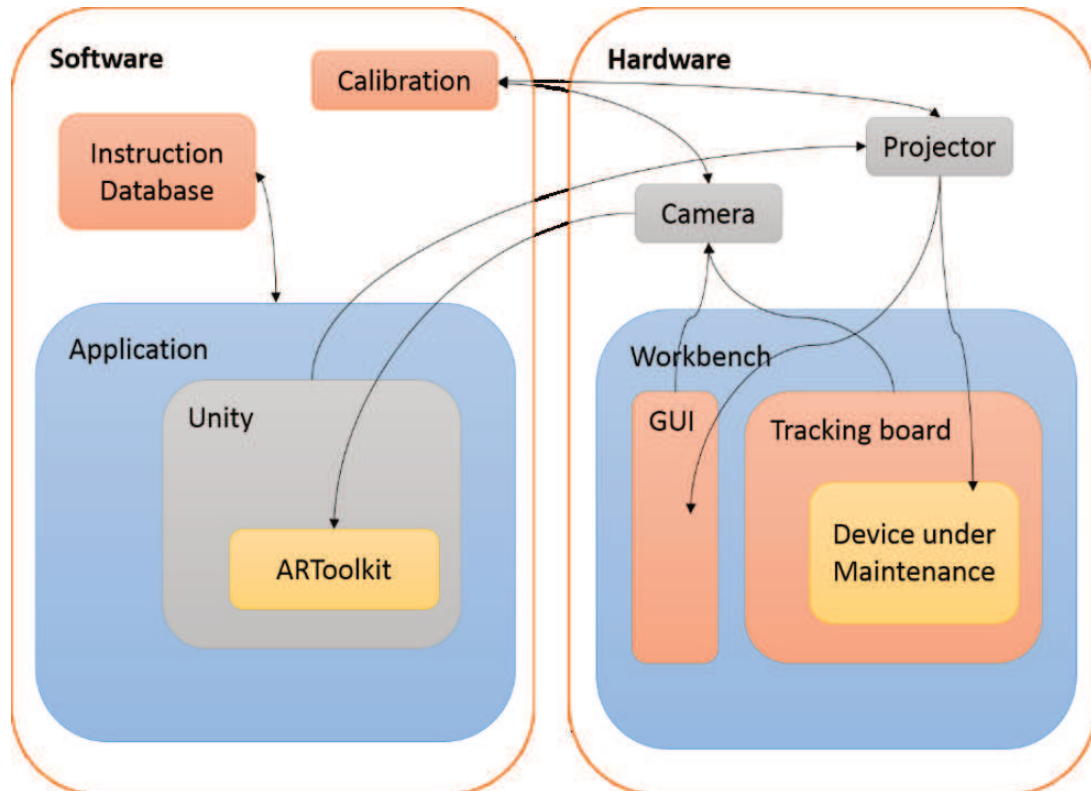
Figure 6 - System architecture

The hardware side is composed by a camera for tracking and a projector for visualizing info on the workbench. The device under maintenance is located on a tracking board with optical markers which is supported by four wheels allowing for easy translation and spinning on the workbench. The beamer projects also a GUI for managing the procedure and the info. The software side, running on one PC, is composed by an application based on Unity 3D and the tracking module based on AR Toolkit. In the framework, each working step is a Unity scene file that includes all the contents needed for the display of the information, namely CAD models of the virtual objects, their placement on the scene (position/orientation), their possible animation, a text list of tools needed, and text instructions. Each scene component is conveniently stored in a SQL database managed by a MySQL RDBMS, linked using a MYSQL connector for Unity 3D. Each interaction between the operator and the system correspond to a SQL query. The result of a query is a collection of data used to instantiate at run-time a scene component. According to the requirements, the physical structure is designed by means of CATIA (Figure 7), using a teamwork approach.
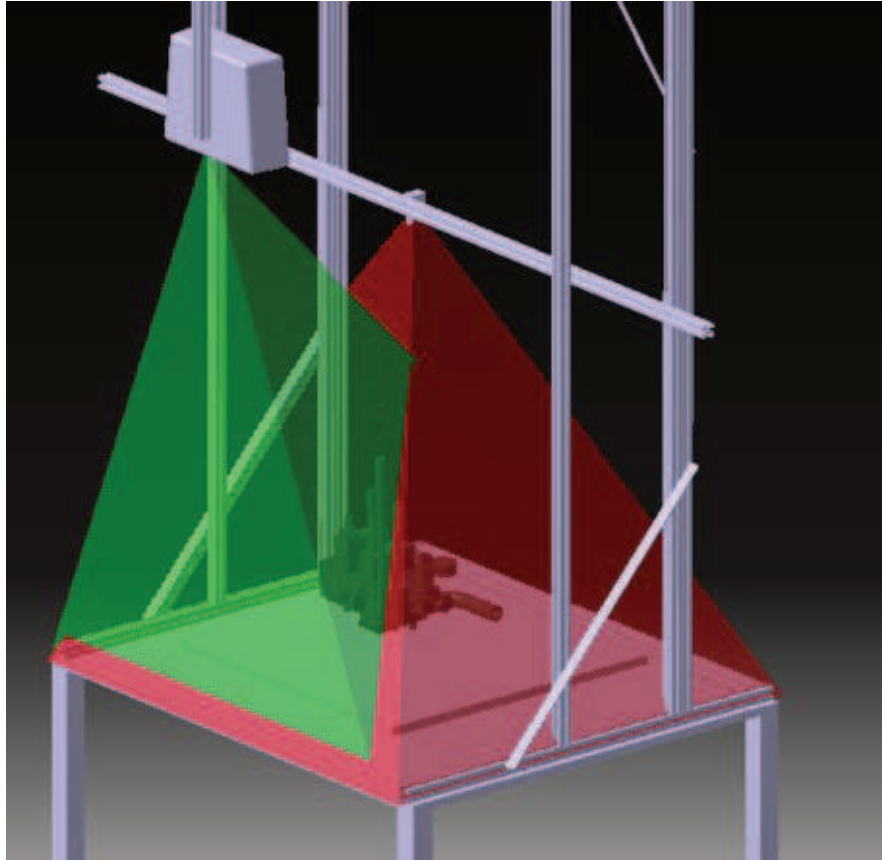
Figure 7 - Projected AR workbench CAD design

Physical setup

As workbench, a white table adjustable in height (the height was set at 750 mm from the floor), 1200 mm large and 1000 mm deep is used. The components are installed on a physical structure realized with Bosch Rexroth aluminium profiles 30 × 30 (shown in Figure 8) allowing a very good physical stability of the structure.

Figure 8 - The prototype

As for tracking board, a square table (side 650 mm) where we put on the product to be maintained is used; it can freely move on the table due to four wheels mounted beneath the base. At the corners of the table, four 140 mm markers used for the tracking are fixed. In this way, the markers move jointly to the product, but they are not fixed on it, so this solution is scalable to different products to be maintained. Benq W1080ST + projector mounted at a distance of about 1300 mm from the table and from the side of the user is used. In this way, the projector illuminates mainly the area in front of the user. The distance from the table is set in order to illuminate all the width of the table, whereas part of the height is not illuminated. The resolution used is 1600×1200. The projector was fixed at the end of an aluminium bar whose height can be changed, in order to have a scalable solution, i.e. the same frame even if we change the projector can be used. The projector used in this prototype was set at the height of 1330 mm. For tracking purpose, an Imaging Source DFK 23U445 (1/3" CCD sensor, resolution 1280×960, USB 3.0) with a 4 mm optic is used. The camera was mounted on a horizontal bar at the height of 1000 mm from the table to frame the entire table. Two lamps (30 W energy-saving, 5200 K), mounted inside an aluminium reflector (Ø 26 cm) with a diffuser to have a softer light and very uniform illumination, at the height of 1150 mm are added.

Graphical User Interface

The designed Graphical User Interface (see Figure 9) includes the following elements:

- Graphic signs (arrows, circles, etc.) are projected to point at the parts of the product where to operate. Their placement is computed in the authoring phase by overlapping the virtual object on the CAD model of the object to be maintained. The CAD model is also used in the Unity scene as occlusion model to have a more realistic rendering of the scene.
- A text box at the bottom of the table with instructions for the operator. A navigation tree, to understand which step of the maintenance procedure the operator has reached and if there are any sublevels for that step.
- At what point of the procedure is the operator, and if there are sublevels for that step.
- A panel with the list of needed tools; in this panel, also additional information or images can be provided.
- Indicators of the marker occluded for the navigation of the user interface.
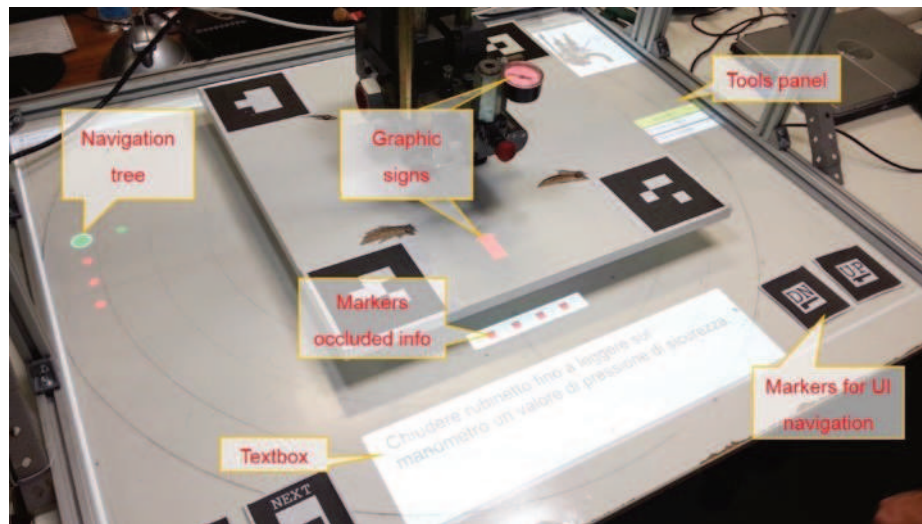
Figure 9 - The Graphical User Interface

As to the interface navigation, a technique based on marker occlusion is used. Four different markers for the four directions of the application are used: next, previous, up to a level, down a level. When the user occludes with his/her hand the marker, the corresponding trigger is activated, and the corresponding scene is loaded. A control on the GUI to check if a marker has been occluded is developed. It consists of four squares; a square is red if the related marker is not occluded, green otherwise. Just as an example, on each new step, the system suggests the operator move the rotating base in order to adjust the point of view to optimize the projected information. A virtual red circular arrow indicates the direction of rotation, and it disappears when the correct position of the rotating base is reached (see Figure 10).
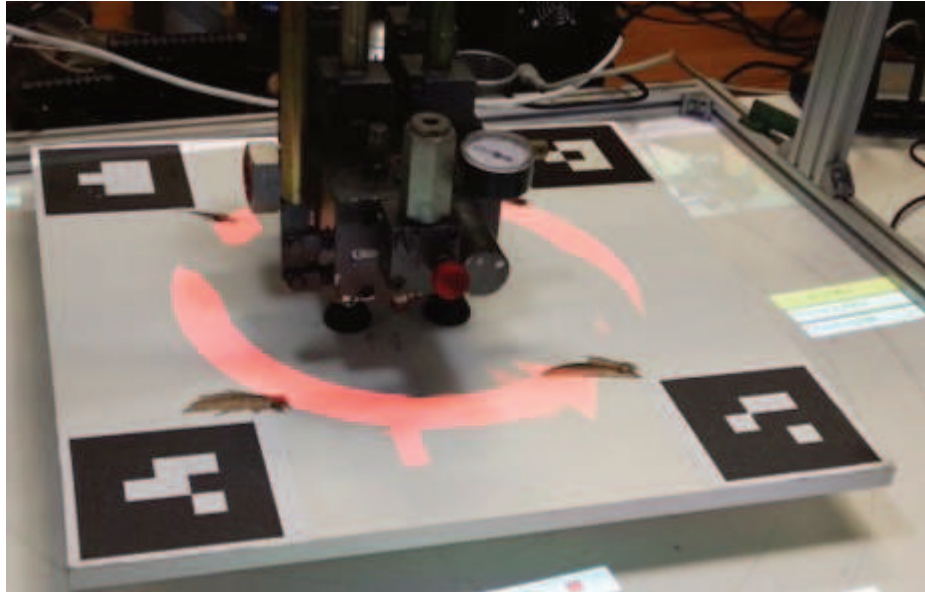
Figure 10 - The red circular arrow suggests the operator rotate counterclockwise the rotating base

2.2.4 Innovative Results and Discussion

As a first test case, the maintenance procedure of an oleo dynamic valve (model GMV 3010 ¾") is implemented. The maintenance procedure was quite simple with four macro steps, with several sub-levels. Nevertheless, the test case was able to test the functionality of the complete system. In this case, a working volume of about 600 mm (L) × 500 mm (D) × 600 mm (H) is measured. Common assembly/maintenance instructions usually contain information about the localization of the sub-product involved in the operation (e.g., a screw), the tools needed, and the operation itself to accomplish. The system proved to be very effective to locate specific points or objects in our product, for example, heads of screws, holes, sensors, buttons, etc. However, these points must lie on a surface, which is directly illuminated by the projector. As to the interface navigation, in this initial prototype, a reliable solution is not properly designed and created. This type of navigation of the interface it is not reliable because an occlusion occurs whenever something (often user's arm) stands between the marker and the camera, leading to frequent false positives (unwanted triggers). Therefore, several research activities as future works can be described, in particular:

- For the localization tasks of points directly illuminated by the projector, the accuracy of the system in the localization of these points to determine the dimensions of the virtual objects to use, have to be measured.
- Find which is the virtual object that ensures higher reliability and is more user-friendly: circle/square, filled/empty, fixed/flashing.
- For those points that do not lie on a surface directly illuminated by the projector (e.g., vertical objects, undercut points, etc.), two possible solutions can be tested: (1) use of multiple projectors; (2) use of a portable camera coupled with a pico-projector, to be handled by the operator as a torchlight.
- As regards tools, the information can be showed in different ways: the simpler are codes of the tools or images projected on the table. Nevertheless, if a set of the working tools in a wall stand is presented, a projector in front of the tools and project a graphic sign to locate the tools needed could be mounted. For the reliability of this system, all the tools must be put back at their correct place after their use. Therefore, it is possible to position a

camera near the projector to compare, using simple imaging processing techniques, the actual image of the tools with a reference one with all the tools at their correct place. In this way, if a tool has not been put back in its correct position after the operation, a warning message would be shown to the operator.

- As regards information on the operation to perform, this can be provided in different ways: text, arrows (for example to indicate un/screwing, insertion, and extraction). As to the text, the optimal location and formatting should be found. As to arrows, position, type, colour, dimensions, animation should be determined.
- In the system requirements, only 2D information are specified. If 3D animations are really needed, they could be displayed as a video projected on the table (no AR).
- The more reliable and user-friendly way to navigate the User Interface among those proposed in the description of the prototype has to be found: voice recognition, gesture recognition, hand recognition, others [271].
- Finally, in order to have also a more scalable solution, the frame creating a less heavy and intrusive as possible structure has to be optimised.

Concluding, the design and development of a prototype for effective use of the AR in the industrial world, in particular for Manual Working Stations, is described in this paragraph (Usable AR-based system for adaptive maintenance). It consists of an aluminium frame with a camera and a projector that dynamically projects information on the real object to be maintained on the workbench. The virtual environment engine uses the frames captured by the camera as input to its tracking algorithm; it computes in real time the position and the orientation of the object. In the meanwhile, the projector displays the information in the desired position even if moving the target object. The data structure of a database for the managing of AR instructions is designed, and the information stored in the DB can be interactively requested from the AR application. With this work, the basis for the development of an effective AR application for the industrial environment are created. However, further tests and experiments should be done to implement reliable, user-friendly and scalable solutions.

2.3   Real-Time System for Posture Workplace Evaluation

The evaluation of the exposure to risk factors in workplaces and their subsequent redesign represent one of the practices to lessen the frequency of work-related musculoskeletal disorders. In this section K2RULA, a semi-automatic RULA evaluation software based on the Microsoft Kinect v2 depth camera, aimed at detecting awkward postures in real time, but also in the off-line analysis is described. The tool is validated with two experiments. In the first one, the K2RULA grand-scores is compared with those obtained with a reference optical motion capture system and a perfect statistical match according to the Landis and Koch scale (proportion agreement index ¼ 0.97, k ¼ 0.87) is found. In the second experiment, the agreement of the grand-scores returned by the proposed application with those obtained by a RULA expert rater is evaluated, finding again a statistical perfect match (proportion agreement index ¼ 0.96, k ¼ 0.84), whereas a commercial software based on Kinect v1 sensor showed a lower agreement (proportion agreement index ¼ 0.82, k ¼ 0.34).

2.3.1 Research question

As described in paragraph 2.1.5 , many methods have been developed with the goal of postures evaluation. They can be classified into three groups: i) self-report; ii) direct measurement, and iii) observational methods [184]. These methods have the main disadvantage to require a field expert who performs a time-consuming analysis of the postures. The introduction of low-cost and calibration-free depth cameras such as Kinect v1 and Kinect v2 provides easy-to-use devices to collect data at high frequencies and suggests a semiautomatic approach to observational methods. The results of the application of these devices acquired by state of the art show that the Kinect v2 sensor can be a promising tool for postural analyses, especially for the metrics whose calculation is based on angular thresholds that tend to minimize the effect of joint angle errors, as RULA. However, some of the results reported in the literature are controversial, since they are sensitive to the specific setup and to the postures adopted for the validation. Therefore, there is still need for further tests to strengthen the knowledge and the main research question is: is it possible to effectively use the Kinect v2 data for an early screening of exposure to WMSDs risk? The typical application scenario can be derived by the ISO standard 11228-3:2007(E), e.g. the workspace is continuously monitored by a depth camera connected to an automatic RULA evaluation system and, if critical conditions are automatically detected, additional investigations (e.g. OCRA) can be carried out.

2.3.2 Methods

K2RULA software

K2RULA software is implemented by using C#, Windows Presentation Foundation libraries (.NET framework) and Microsoft Kinect for Windows SDK 2.0. The GUI of the K2RULA tool allows the user to select the video stream to be visualized (depth or infrared), and to activate a secondary window for the RBG stream (Figure 11). The button "Real Time RULA" evaluates the RULA grand-score of the current posture. Furthermore, playback control buttons allow the execution of an offline analysis of a recorded file.
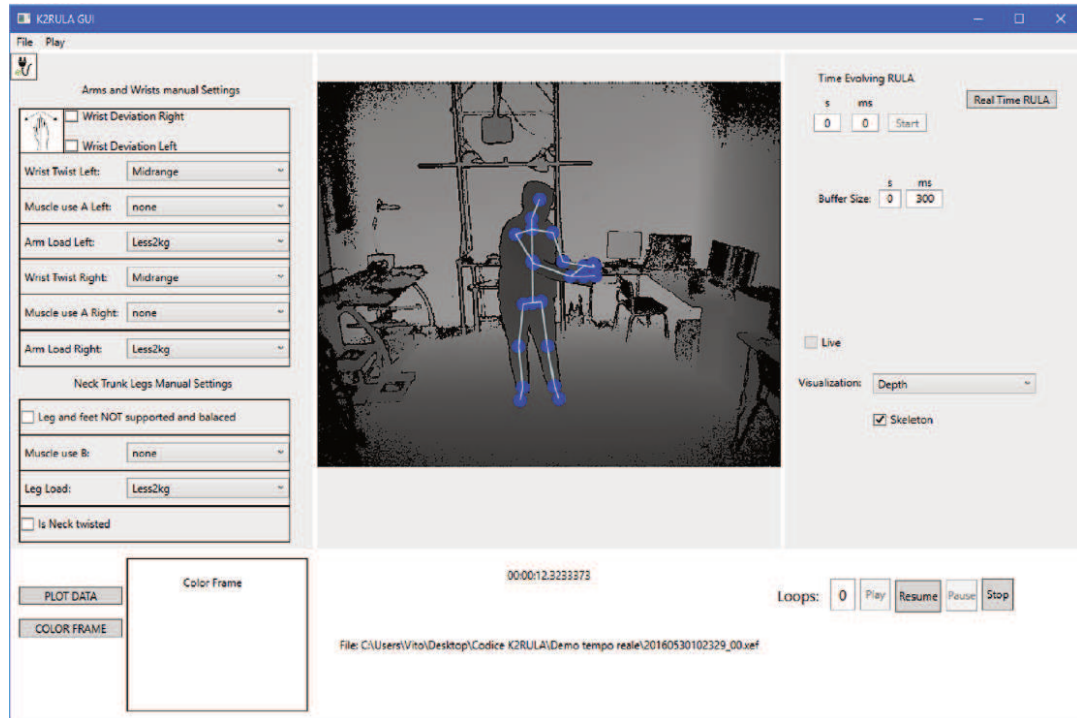
Figure 11 - GUI of the K2RULA software

The RULA method

The RULA method consists in the fulfilment of an assessment grid, where the human body is divided into two sections (Section A: upper arm, lower arm, and wrist; Section B: neck, trunk, and legs). A score is calculated using three tables. The first two tables give the posture scores of the body segments. Each one of these scores is then corrected according to the frequency of the operations and the force load on the limbs. The third table takes as input the previous scores and returns a grand-score. An action level list indicates the intervention required to reduce the risks of injury of the operator:

- 1-2 grand-score: the posture is acceptable if it is not maintained or repeated for long periods,
- 3-4 grand-score: the further investigation is needed, and changes may be required,
- 5-6 grand-score: investigation and changes are required soon,
- 7 grand-score: investigation and changes are required immediately.

Data retrieval

The Kinect tracking algorithm returns a hierarchical skeleton composed of joint objects (Figure 12).
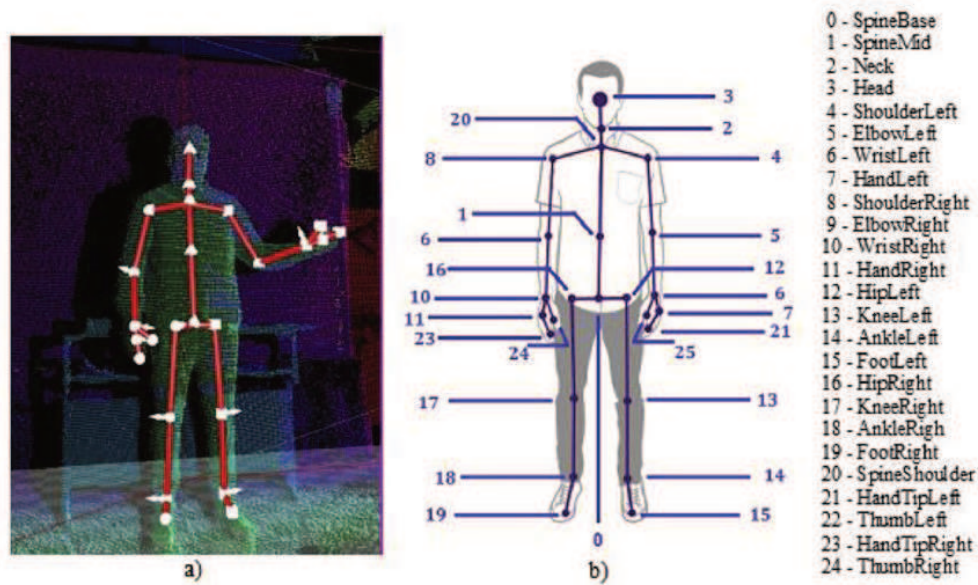
Figure 12 - The skeleton returned by Kinect for Windows SDK 2.0. a) Depth map and skeleton visualised by the Microsoft Kinect Studio v2.0; b) joints position with respect to the body as reported by Microsoft HIG (http://download.microsoft.com/download/6/7/6/676611b4-1982-47a4-a42e-4cf84e1095a8/kinecthig.2.0.pdf)

Each joint position is calculated in real time as the average of the positions stored in a 300 ms memory buffer (about 10 valid frames at 30 Hz) to minimize jittering. If the sensor is not able to track a joint (e.g. occlusion), its position is inferred (inferred joints) from the surrounding joints by the Microsoft SDK. The K2RULA algorithm requires only 19 of the 25 tracked joints. RULA parameters are trivially evaluated from geometrical angles between the joints. However, for some angles, additional processing is necessary. A trunk vector as the vector connecting the spine base (from Windows SDK nomenclature) to the spine shoulder must be defined, respectively approximately corresponding to the mid-posterior superior iliac spine [272] and the incisura jugulars [272]. For the upper arms flexion/extension the angle between the trunk vector and the vector corresponding to the projection of the upper arms on the sagittal plane is computed. The latter is evaluated as the one passing through the trunk vector and perpendicular to the straight line connecting the shoulders. The upper arms abduction is evaluated with the angle between the trunk vector and the vector corresponding to the projection of the upper arms on the plane passing through the trunk and parallel to the straight line connecting the shoulders. For the shoulder abduction, the angle between the vector connecting the spine shoulder to the neck and the vector connecting the spine shoulder to the shoulder under analysis are computed. To evaluate the working position of the lower arm with respect to the midline of the body and the side of the body, the relative positions of the projections of the wrist, spine shoulder and shoulder on the straight line connecting the shoulders are analysed (Figure 13).
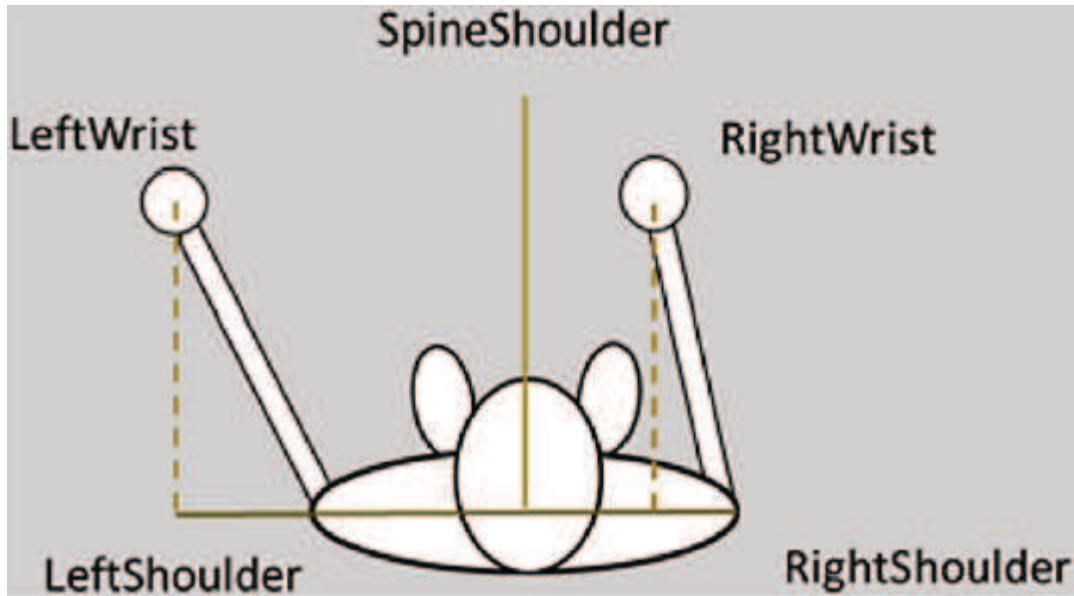
Figure 13 - Lower arms working position assessment geometrical construction

As regards the wrist location, the adduction/abduction angle is evaluated approximatively. The angle between the vector connecting the elbow to the wrist and the vector connecting the wrist to the hand tip are computed. The grid assessment requires taking into account the trunk twisting and bending state. A test to evaluate the correlation between directions for the skeleton object normal and the three joints in the trunk, concerning the twisting state of the body, is performed (Figure 12). Hence, the angles between the normal to the ankles (directed towards the outside of the body) and the normal to the trunk, directed towards the sensor are calculated (Figure 14).
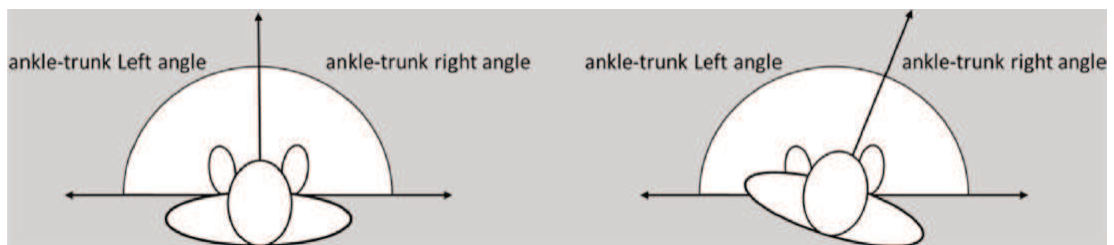
Figure 14 - Trunk twisted detection scheme

To detect the trunk bending state, the angle between the straight line passing through the hip joints and the direction normal to the horizontal plane are evaluated. The trunk flexion degree is trivially assessed by the angle between the direction perpendicular to the horizontal plane and the trunk vector. The neck flexion/extension computing the angle between the normal to the trunk vector in the sagittal plane and the projection in this plane of the vector connecting the spine shoulder to the head are assessed. This solution leads to an overestimation of the neck back flexion with respect to visual inspection. Therefore, a positive bias of five degrees in the computation of the angle on a heuristic base is added. The neck bending computing the angles between the vector connecting the spine shoulder to the head and each one of the vectors connecting the spine shoulder to the shoulders are detected. Despite the improvements in joint detection provided by Kinect v2, the accuracy is not sufficient to detect some important parameters for some joints, such as the wrist and neck twist. In addition, K2RULA is not able to evaluate other factors, such as the load on arms and the kind of muscle use, that affect the RULA grand-score. As solution, default settings are implemented and provided a simple GUI for the operator to set them (Figure 15).

Figure 15 - Window Interface for manual settings and default values

Functionalities

The "Real Time RULA" button activates the display of the RULA scores panel (Figure 16).
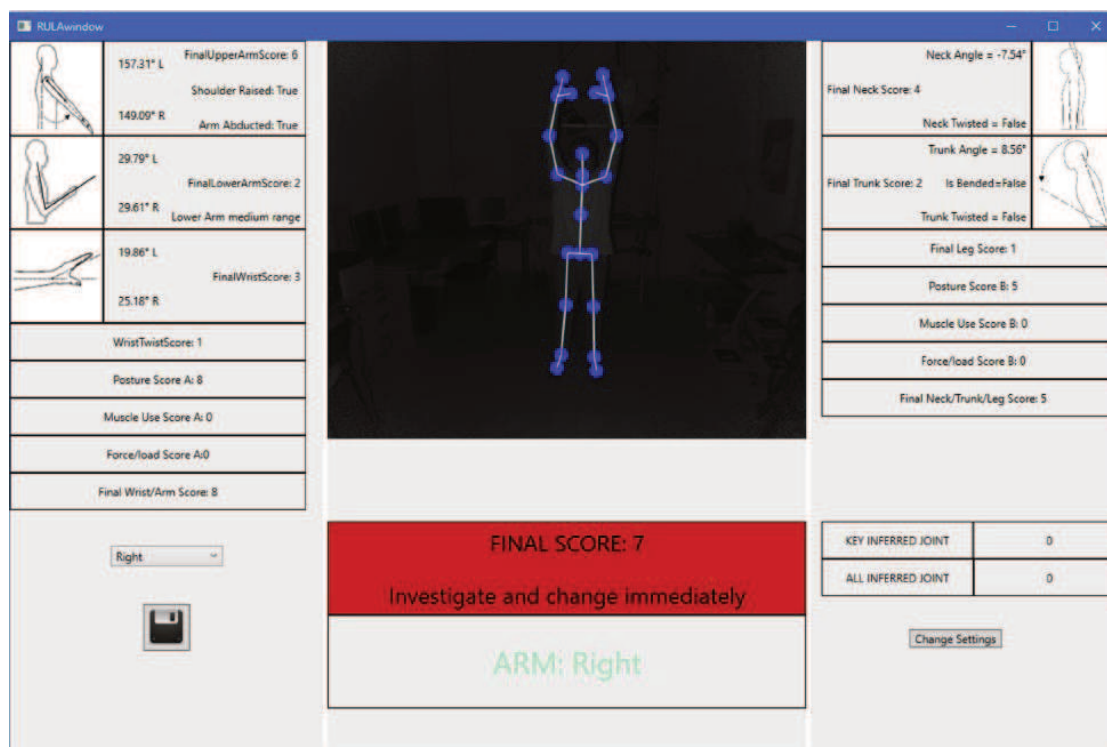
Figure 16 - The RULA scores panel

This window provides the scores of each body section for both sides, the computed angles, and the grand-score, and saves the report on a text file. The action level is visualized with a colour-coded background varying from green (grand score 1-2) to red (grand score 7). Furthermore, the inferred joints are evidenced with red circles on the skeleton to highlight the reliability of the assessed scores. Another functionality of K2RULA is to process a recorded file continuously in the standard Microsoft format (.xef). The software calculates the grand-score for each of the frames and generates a report, exportable in a comma-separated values file while visualizing an interactive timeline plot. By clicking on one point of the graph, a pop-up label displays the RULA grand-score for that instant (Figure 17).
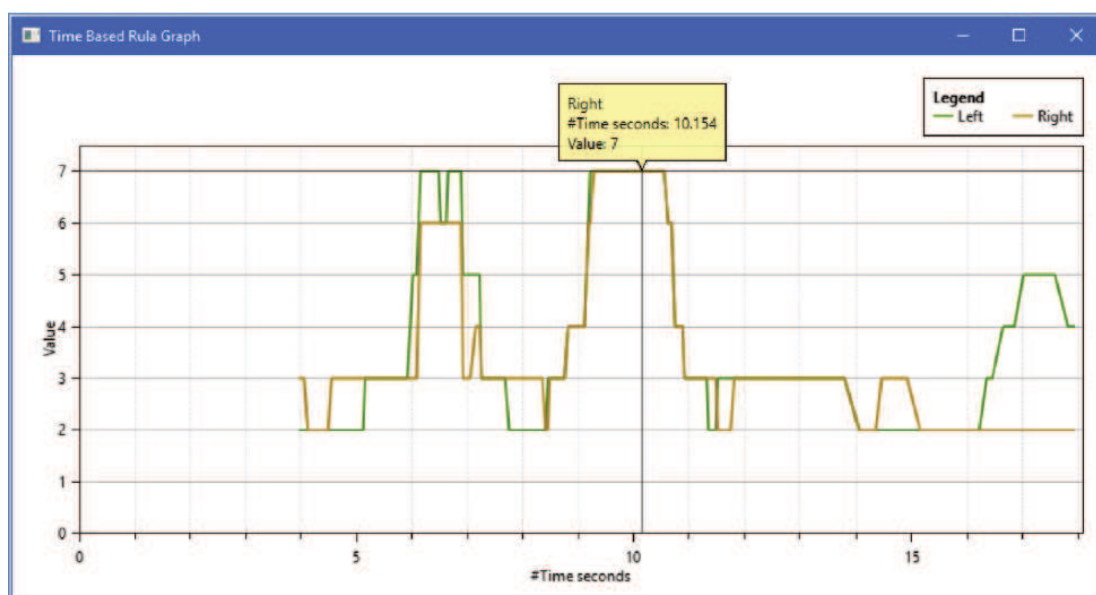
Figure 17 - Grand-scores plot for an offline analysis on a recorded file: postures at second 6-7 and 9-11 are critical and require further analysis

This functionality allows to evaluate the working activities continuously and to spot for critical conditions.

Experiment 1: validation with an optical motion capture system

In this experiment, we studied the agreement between the K2RULA tool and a reference tracking system. The hypothesis 1 is: K2RULA RULA grand-scores are in accordance with an optical motion capture system.

To run K2RULA, a Kinect v2 connected to a PC with a CPU Intel® Core™ i5-4200 2.50 GHz, 4 GB RAM, GPU NVIDIA GeForce GT 740 M, OS Windows 8 is used. The reference tracking system is a BTS SMART-DX 5000 optical motion capture systems [273] composed by 8 infrared digital cameras, with an acquisition frequency of 100 Hz, and one PC with a CPU Intel® XEON E5640 2.67 GHz, e 3 GB RAM, OS Windows XP. The SMART Suite software for raw data acquisition and processing [273] is used.

15 static postures are selected: nine of them (Figure 18) from the EAWS form (https://vdocuments.site/eaws-form-v134-en.html), and six (Figure 19) extracted from a booklet of the European campaign against musculoskeletal disorders [274].
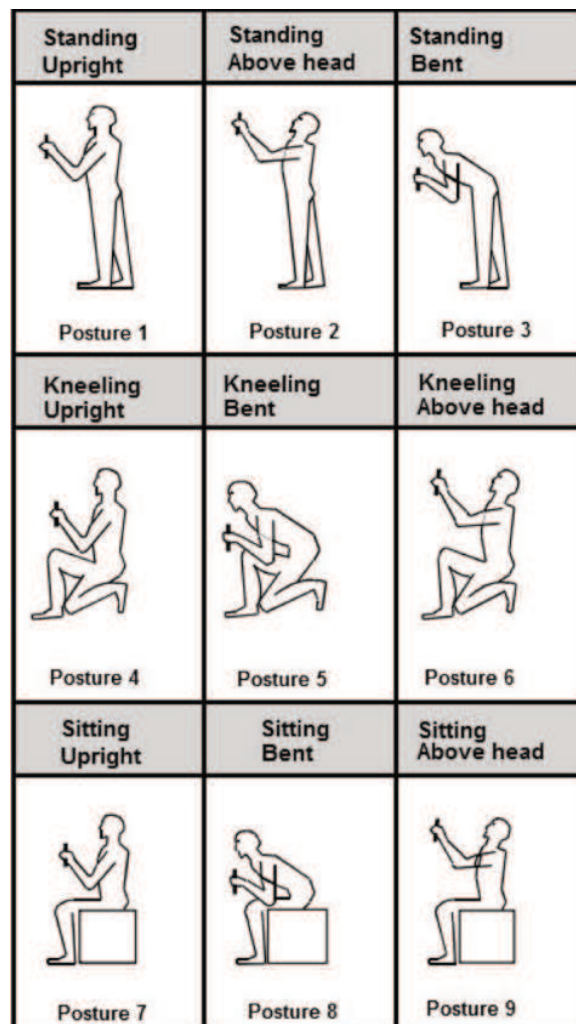
Figure 18 - Postures belonging to the EAWS form v. 1.3.4
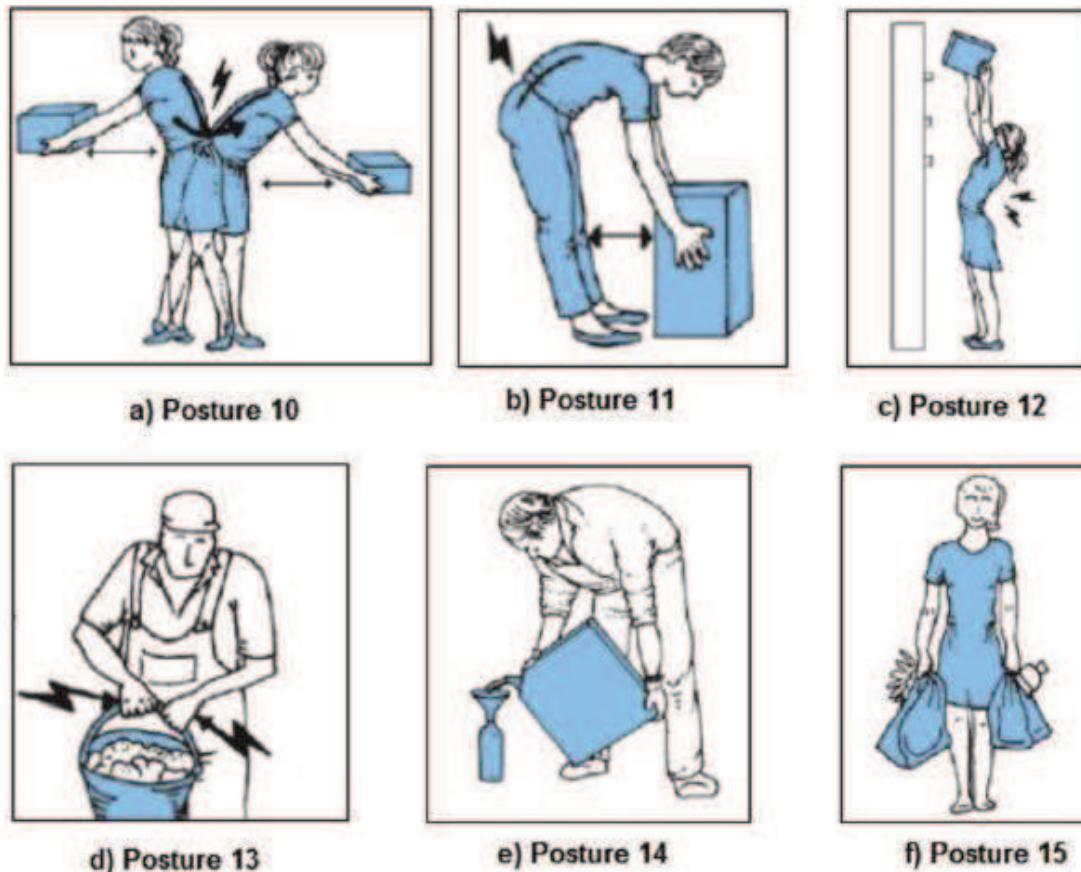
Figure 19 - From image a) to e) the five most common awkward postures, in image f) the posture used as the basis for comparison.

A volunteer (male, age 26, height 180 cm, and weight 80 kg) as an actor to simulate the aforementioned postures is recruited. Eighteen markers (1.0 cm diameter reflective spheres) on anatomical landmarks, as suggested in [272] (see Table 2 and Figure 20) are positioned.

Table 2 - The anatomical landmarks for reflective markers positioning, the Kinect-identified joint names and their motion tracking system-based counterparts.

Body part	Anatomical landmarks	Kinect-identified joint names	Motion tracking system-based counterparts
Head	Left/Right Temporal Region (LTR/RTR)	Head	(LTR + RTR)/2
Torso	Left/Right Medial end of the Clavide (LMC/RMC)	Not present	(LMC + RMC)/2
Neck	C7	Neck	(C7 + (LMC+RMC)/2)/2
Left shoulder	Left Acromion (LA)	Left Shoulder	LA
Right shoulder	Right Acromion (RA)	Right Shoulder	RA
Let elbow	Left Lateral Humeral Epicondyle (LLHE), Left Medial Humeral Epicondyle (LMHE)	Left Elbow	(LLHE + LMHE)/2
Right elbow	Right Lateral Humeral Epicondyle (RLHE), Right Medial Humeral Epicondyle (RMHE)	Right Elbow	(RLHE + RMHE)/2
Left wrist	Left Radial Styloid (LRS), Left Ulnar Styloid (LUS)	Left Wrist	(LRS + LUS)/2
Right wrist	Right Radial Styloid (RRS), Right Ulnar Styloid (RUS)	Right Wrist	(RRS + RUS)/2
Left hip	Left Anterior Superior Iliac Spine (LASIS)	Left Hip	LASIS
Right hip	Right Anterior Superior Iliac Spine (RASIS)	Right Hip	RASIS
Sacrum	Sacrum (S)	Spine Base	S
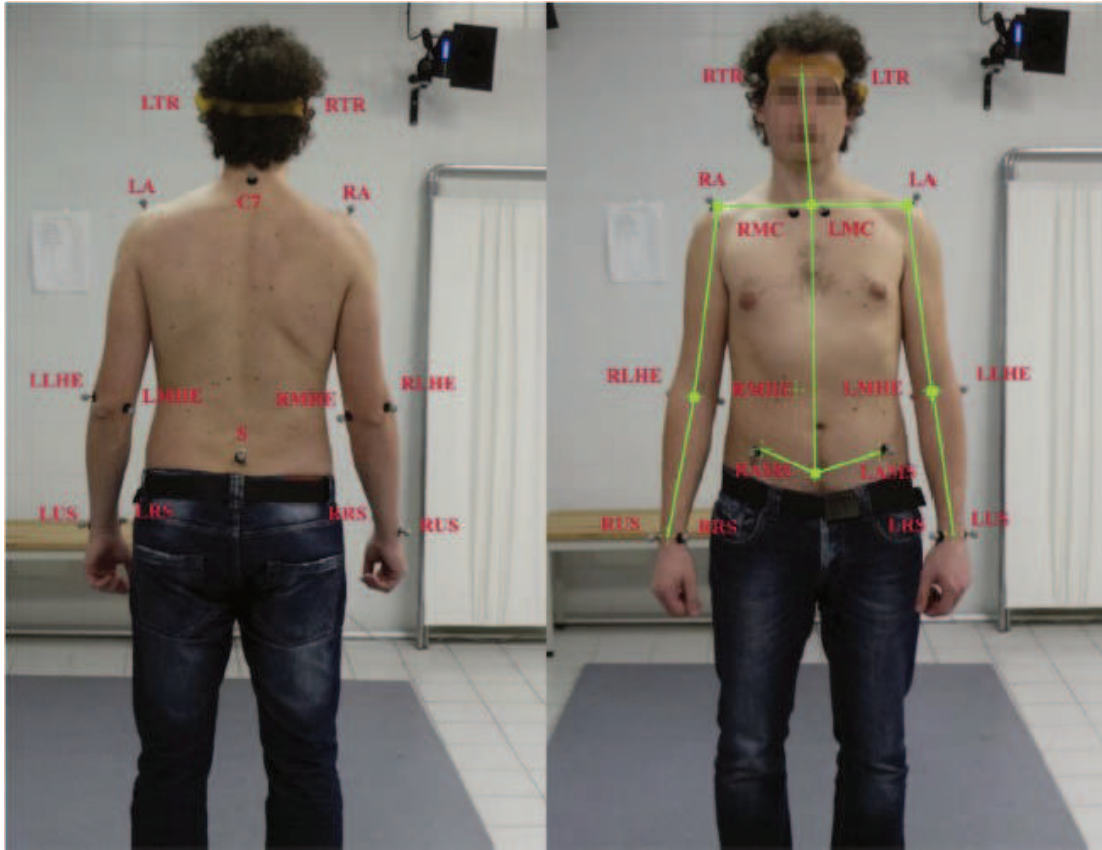
Figure 20 - The anatomical landmarks for reflective markers positioning, on the right the skeleton body model generated with the 3D CAD tool is overlaid in green

Specific landmark choices are referred to the literature: head [209], shoulders and neck [275], elbows [276, 277], wrist centres [277, 278], and the pelvis girdle [279]. The Kinect is positioned in front of the actor at a distance of about 240 cm and at the height of 180 cm from the ground. The actor is in the centre of the area framed by the optical motion capture system in a laboratory with controlled lighting conditions (400lx). Simultaneously, the static postures with both the tracking systems and synchronized them according to the same event-based procedure as in [209] are recorded.

Data analysis

The coordinates from the optical motion capture system in a 3D CAD parametric model (Autodesk Inventor professional 2017) are imported, and the required angles are measured. Then the RULA grand-scores using the RULA Employee Assessment Worksheet [280] are computed. The agreement between the two systems by using two-dimensional contingency tables [281] is assessed. The proportion agreement index (p0), and the strength of agreement on a sample-to-sample basis as expressed by linear weighted Cohen's kappa are computed.

Results

Figure 21 shows the RULA grand-scores for the body left and right side obtained with the K2RULA and the optical motion capture system. These results indicate the "perfect" agreement between the two systems (see Table 3) in the Landis and Koch scale [282].
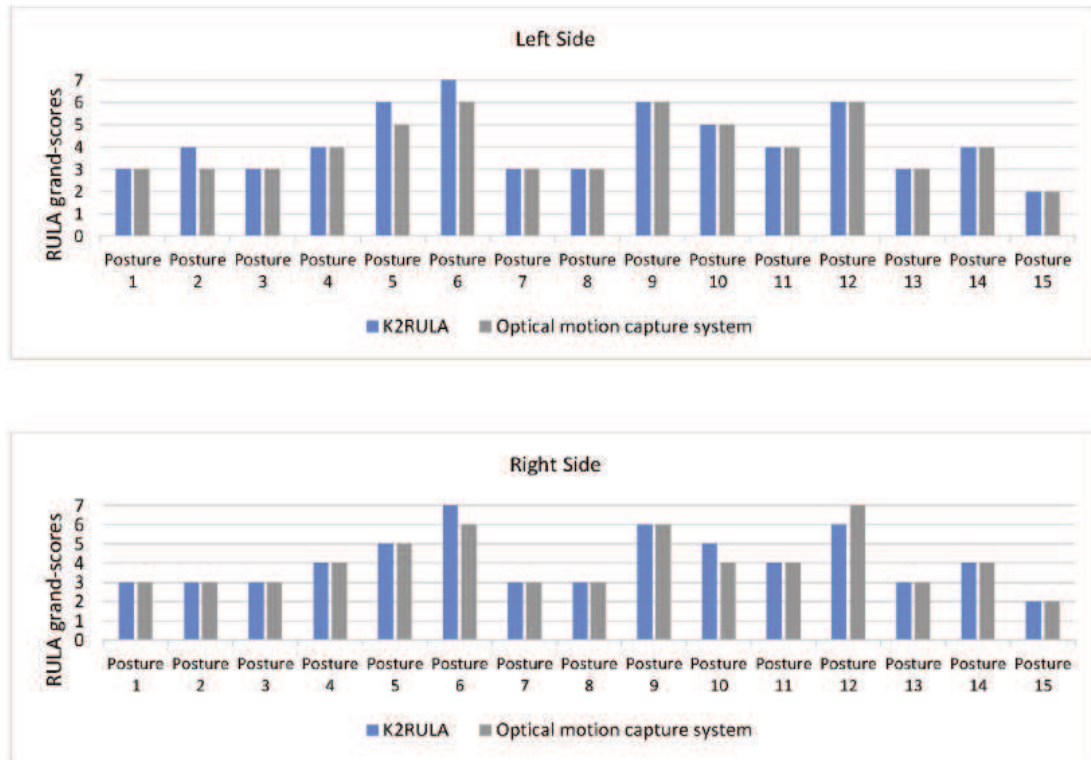
Figure 21 - RULA grand-scores for the body left and right side

Table 3 - Observed agreements between the K2RULA and the optical motion capture system, linear weighted Cohen's kappa and Z-test results

Body scale	P_o	Cohen's Kappa	Agreement (Landis and Koch scale)	z (k/sqrt(var))	p-value	Null hypothesis
Left	0.97	0.87	Perfect	4.38	<0.0001	Reject
Right	0.97	0.87	Perfect	4.78	<0.0001	Reject

To validate the statistical significance of this result, the null hypothesis that the observed agreement is accidental, by referring to the value of the critical ratio z to tables of the standard normal distribution is tested. Rejecting the null hypothesis (p < 0.001) for both the body left and right side, allowed us to confirm the hypothesis 1: K2RULA grand-scores are in accordance to the RULA assessments obtained with an optical motion capture system.

Experiment 2: validation with RULA expert and comparison with the Jack TAT

In the second experiment, the K2RULA tool with a human RULA expert and with the Jack TAT are compared. Two hypotheses, for this experiment, are defined:

- hypothesis 2: K2RULA grand-scores are in agreement with the ones obtained by the RULA expert;
- hypothesis 3: the K2RULA provides better results than the Jack Task Analysis Toolkit.

Equipment

Data with a Kinect v2, a Kinect v1, and video with a Webcam Logitech® Hd Pro C920 are simultaneously collected. Two identical PCs (CPU Intel® Core™ i5-4200 2.50 GHz, 4 GB RAM, GPU NVIDIA GeForce GT 740 M, OS Windows 8) ran the K2RULA and the TAT software tool version 8.0.1 (based on Kinect v1).

Procedure

The same 15 static postures of experiment 1 are used. A RULA expert (an occupational doctor working for INAIL, 1 with more than 10 years of practice) and one volunteer (male, age 28, height 170 cm, weight 72 kg) as an actor are recruited. During the experiment, the two Kinect sensors and the video camera (one above the other) are positioned in front of the "actor" as in the previous experiment in a laboratory with controlled lighting conditions (400lx). While the actor was keeping each static pose for a few seconds, each posture is recorded. The RULA grand-scores using both the K2RULA and the Jack-TAT are assessed. The RULA expert analysed offline the recorded video of each posture and assessed the RULA grand-scores.

Data analysis

The comparison between the two Kinect based (KB) methods using as baseline the expert evaluation are carried out, as in [263]. The agreement between results as done in experiment 1 are assessed.

Results

Figure 22 shows the RULA grand-scores for the K2RULA and the Jack-TAT compared with the expert evaluation as a baseline. These results indicate "perfect" agreement between the expert and the K2RULA and just "fair" agreement between the expert and the Jack-TAT (see Table 4).
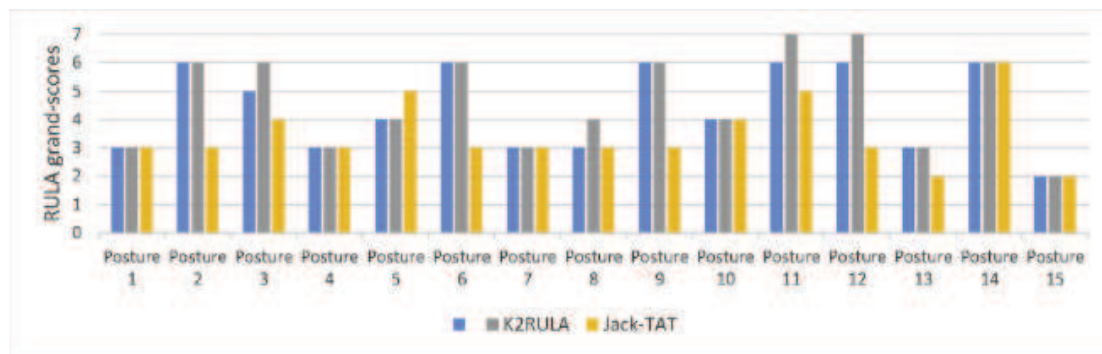
Figure 22 - Kinect-based methods vs Expert evaluation

Table 4 - Observed agreements, linear weighted Cohen's kappa and Z-test results

Methods	P_o	Cohen's Kappa	Agree-ment (Landis and Koch scale)	z (k/sqrt(var))	p-value	Null hy-pothesis
Expert-K2RULA	0.96	0.84	Perfect	3.87	<0.0001	Reject
Expert-Jack	0.82	0.34	Fair	0.82	0.412	Accepted

To validate the statistical significance of these results, the null hypothesis that the observed agreement is accidental is tested. Rejecting the null hypothesis (p < 0.001) for the agreement between the expert and the K2RULA the hypothesis 2 can be confirmed: K2RULA grand-scores are in agreement with the ones obtained manually by the RULA expert. On the contrary, accepting the null hypothesis (p = 0.412) for the agreement between the expert and the Jack-TAT the hypothesis 3 can be confirmed: K2RULA provides better results than the Jack Task Analysis Toolkit.

2.3.3 Innovative Results and Discussion

In the first experiment, the RULA grand-scores, returned by the two methods, were identical in 24 postures of the 30 considered. This result is in accordance with the outcomes presented by Plantard et al. in [283]. The only six differences were due to detection of the arm abduction and the trunk flexion where K2RULA overestimated the grand-score (+1). The RULA assessment method, based on wide angle ranges, effectively compensates the joint position differences between the two tracking systems, indeed present as reported in the literature. In the second experiment, the Kinect-based methods reported exactly the expert grand-scores for postures one, four, seven, eight, ten, and fourteen (Figure 22). In posture two, Jack-TAT underestimated the ergonomic risk, returning a low score for the neck. Analysing the video frame, the neck appears back flexed. Jack-TAT was not able to detect this situation. In posture six, the operator is kneeling with outstretched hands high above the level of the shoulders. The neck and forearm have high scores, involving a high ergonomic risk. The expert and K2RULA returned the same severe grand-score. Jack-TAT gave a lower grand-score. Jack-TAT showed some problems with kneeling postures and sometimes it was not able to track the skeleton. In posture nine, the operator sits with both arms raised over shoulder height. The expert and K2RULA returned the same grand-score whereas Jack-TAT gave a lower one. Posture ten is characterized by the trunk rotation and by the left arm crossing the sagittal plane. K2RULA and the expert gave the same score for each body section. Jack-TAT, in this case, returned the same grand-score, but this correspondence is just accidental as Jack-TAT underestimates the arm section and overestimates the neck section. In posture eleven, the trunk is highly flexed forward. The K2RULA returned the highest grand-score since it detected even a small twisting and a bending of the trunk. In posture twelve, Jack-TAT did not detect the neck back flexion and underestimated the arm section. Jack-TAT seems to underestimate the ergonomic risk frequently returning a grand-score lower than the one estimated by the expert (mean error $\varepsilon = -0.933$, error std. dev. s = 1.34). K2RULA slightly overestimates the risk (mean error $\varepsilon = 0.267$, error std. dev. s = 0.44). However, this overestimation is conservative and hence consistent with the goal of this tool. K2RULA showed a "perfect" agreement with respect to the expert ($P_0 = 0.96$, k = 0.84). The results showed a slightly better

agreement than that obtained by Plantard et al. in [283], although their data were acquired in real work conditions.

The K2RULA is tested in a laboratory set-up with controlled lighting conditions and without occluding objects. This is the best working condition for the Skeleton Tracking algorithm for Kinect v2 [266] and Kinect v1 , and the results suffer only from the actor's body self-occlusions. Further investigations are needed to evaluate the behaviour of K2RULA in a real working environment. Moreover, the hands configuration plays a key role. Therefore, methods to track hands with or without wearable sensors must be investigated in the future. The availability of data acquired by hand tracking algorithms would probably allow the implementation of methods and tools able to assess fatigue indexes more detailed than the RULA score, such as OCRA index, moving from static postures analysis to continuous measurement.

Concluding, in this section is described a real-time semi-automatic RULA evaluation system based on Kinect v2. It allows to speed up the detection of critical conditions and to reduce the subjective bias. K2RULA is able to analyse off-line data and to save the results for deeper ergonomic studies. The proposed tool is validated with two experiments, using as a baseline an optical motion capture system and a RULA expert, proving the reliability of K2RULA as a faster alternative to classical visual inspection evaluation. The system is also compared with commercial software, the Jack-TAT, based on the Kinect v1 sensor. In summary:

1. K2RULA grand-scores are equivalent to the assessments obtained with an optical motion capture system;
2. K2RULA grand-scores are in perfect agreement with a RULA expert evaluation;
3. K2RULA outperforms the Jack-TAT tool, based on Kinect v1.

The proposed system can be effectively used as a fast, semi-automatic and low-cost tool for RULA analysis.

2.4 Conclusions

In this second chapter, two designed and developed intelligent applications are described. Two articles are published, one on the "International Conference on Augmented Reality, Virtual Reality and Computer Graphics" [29] and the other one on the international journal "Applied Ergonomics" [284]. Starting from these studies, other applications are developed in the bioengineering field, and they will be described in the next chapter.

Although the applications described in this chapter are not thought for an Industry 4.0 scenario, the conclusion is that could be intended as applications that could be used in a complex scenario consisted of a CPS, IoT and IoS services. The common goal of this applications is the Technical Assistance (one of the four principles of Industry 4.0) in the manufacturing field.

The first application regards the design, and the development of an Intelligent Manual Working Station (MWS) consists of a workbench, a projector, a camera and a set of markers linked to a machine that hosts a database in which are stored the necessary information to implement a Spatial (or Projected) Augmented Reality System. The goal is the Technical Assistance intends as the optimisation of the necessary procedures applied by a new worker that has to learn his/her work on the MWS. Moreover, the system could also be used to avoid the use of a physical manual during maintenance applications without the use of wearable devices that could hinder natural movements of the worker. Further update and tests should be done to understand the validity of the

proposed system. However, it could be contextualised in an Industry 4.0 scenario. By considering the architecture of a Cyber-Physical System (Figure 1), the system could be intended as a part of CPS and could be placed in the 4th level of the 5C architecture. The 4th level is called Cognition Level. The goal of the level is to show the right information derived from previous levels (Cyber, Data-to-Information Conversion and Smart Connection Levels) to users. Therefore, after the validation of the system, future work could consider the design and implementation of a network that linked all the MWSs. All data exchanged by machines could be useful to improve the system and to predict the future behaviour of it by means of the implementation of the Data-to-Information Conversion and CPS Levels that apply inferred algorithms considering previous data. Finally, the Configuration Level could make every MWS self-configuring and self-adapting.

The second application concerns the design, and the development of an intelligent system consists of a computer and a depth sensor (Kinect v2) to implement a support system for RULA experts that have to evaluate the posture that workers assume during work. The great advantage of the use of this type of application in an Industry 4.0 scenario, is that the system, consists of several equal systems linked together, could collect data and retrieve results automatically to an expert rater that could decide to accept the support or to perform further analysis to make a better decision. To contextualise the system in an Industry 4.0 scenario, same considerations done on the previous work could be made.

Chapter 3

3 Intelligent Support in Industrial Bioengineering: Decision Support Systems and Immersive Human-Computer Interfaces applications

3.1 Introduction

3.1.1 Objectives and research questions

The objective of this last part of the work is the design, the development and the evaluation of intelligent applications to support human worker in Industrial Bioengineering scenarios. In particular, three use cases will be described: the first one concerns the design and development of DSSs for supporting expert neurologists to evaluate the severity of Parkinson and Blepharospasm. A healthcare network based on Big Data Analytics (BDA) is theorised, and a low-cost Computer Vision system is designed to acquire, during a standard neurological examination, all the necessary features to train DSSs based on Support Vector Machine (SVM) and Artificial Neural Networks (ANNs). The goal, in this case of Parkinson, is to classify the disease's severity following a standardized severity scale called Unified Parkinson's Disease Rating Scale (UDPRS). In the case of Blepharospasm, several videos from a camera RGB regarding the examination of the different patient are evaluated. Starting from these videos, several features are extracted from training two Artificial Neural Networks (ANNs) to count the main three symptoms of this disease's severity: blinks, brief spasms and prolonged spasms. The algorithms are designed following a standardized severity scale used by neurologists to perform observational examinations. The second use case, concerning the design and the development of Computer-Aided Diagnosis (CAD) frameworks, based on the evaluation of medical images from several and different sources, to support experts domain to detect and recognise cancer. The last use case concerns the system implemented in collaboration with the Technology University of Graz and University Hospital of Graz. Starting from the images resulting from a Positron Emission Tomography (PET) and a CT (Computed Tomography), the first part of the system concerns the detection and the 3D reconstruction of Maxillo-Facial tumours. An automatic registration procedure during a surgical operation to overlap the tumours on the correct position in the world space by means of Microsoft HoloLens is designed and implemented. Finally, a survey is submitted to a team of expert surgeons of the University Hospital of Graz that tried the system. The goal is to understand if the automatic overlapping of a tumour causes an improvement of the surgical procedures.

Concluding, all of these designed and developed applications that I will describe in the next sections, could be a crucial part in a Medical Cyber-Physical System (MCPS). As described in paragraph 1.1, a Cyber-physical system (CPS) is a fundamental part of an Industry 4.0 scenario. The main goal of a CPS is the virtualisation of the physical world. It consists of embedded computers and networks able to monitor and control the physical processes through feedback loops. The idea is to create an interconnection of intelligent objects and systems to execute critical tasks. Therefore, the CPS concept could also be applied to social services, in particular in medical and healthcare applications [114]. In order to improve this field, infrastructure and computing framework are required and is called Medical Cyber-Physical System which integrates the cyber and the real world with systems for decision making and other healthcare applications [285, 286]. In the following paragraphs, designed and developed intelligent applications to support physicians in diagnostic, clinical and surgery applications are described.

3.1.2 Contribution

The main contributions of the presented works regard the design and the development of intelligent systems in the bioengineering field to support physicians, in different medical areas, in their tasks. In particular, concerning the design and the development of

- the support systems to evaluate the severity of Parkinson's and Blepharospasm's diseases;
- the CAD frameworks to support clinicians to detect and recognise a tumour;
- the Mixed Reality system to overlap a tumour during surgical operations,

My contributions are:

- design of Computer Vision-based system by means of low-cost devices (Kinect v2, MyO Armband, et.) to acquire some important motor features during neurological examinations;
- design and implementation of intelligent algorithms (based on SVM and ANN) to detect and count symptoms of the diseases;
- design and implementation of CAD frameworks based on Machine Learning and Deep Learning algorithms;
- design and Implementation of an Immersive Human-Computer Interfaces in Mixed Reality, by means Microsoft HoloLens, to automatically overlap reconstructed maxillo-facial tumours on the face of the patient during surgical operations.

3.1.3 Part outline

In the paragraphs that follow, I will present all the systems previously introduced. For each system, an introduction will contextualise the problem and the techniques that I will describe to answer to the research question. I'll focus mainly on the machine learning and deep learning techniques used to support physicians in neurological and diagnostic examinations implementing DSS and CAD Frameworks. Concerning the last implemented system, I'll describe all the steps to implement a Mixed Reality system in maxillo-facial surgery: starting from the tumour detection and 3D reconstruction and ending with the procedures applied to overlap a tumour on the real face of the patient. In particular, these techniques, that are often used in manufacturing for training purposes, can be applied in the bioengineering field. The chapter ends with a common conclusion that stands out how, in general, this software could be contextualised in an Industry 4.0 scenario applied in the healthcare field.

3.2 Decision Support Systems in Neurological Examinations

Nowadays, healthcare organizations involving both single-physician offices with multi-provider groups and large hospital networks with accountable care organizations stand to realize significant benefits by using big data for effectively digitizing or combining them [115]. It seems that existing analytical techniques can be applied to the vast amount of existing (but currently unanalysed) patient-related medical data to reach a deeper understanding of outcomes to be applied at the point of care. Potential benefits could include following up specific diseases as well as Parkinson or Blepharospasm pathologies. In general, Big Data Analytics (BDA) in healthcare could contribute to evidence-based medicine for analysing a lot of structured and unstructured medical data to match treatments with outcomes, device/remote monitoring for capturing, in real-time, large volumes of fast-moving data from several devices placed at home or in hospital and, finally, patient profile analytics for applying several analyses to patient profile to improve cares and lifestyles.

3.2.1 Research Question

In this part of PhD work is suggested a Healthcare network based on BDA for Parkinson and Blepharospasm diseases to support clinicians in the objective assessment of the typical Parkinson and Blepharospasm motor issues and alterations by means of a Support Vector Machine (SVM) and Artificial Neural Network (ANN). Meanwhile, the healthcare network is only theorised, the intelligent applications to evaluate diseases severities are designed and developed, and the results of experiments will be described in the Innovative Results paragraph of this section.

3.2.2 Healthcare Network

The network architecture aims to suggest a solution which avoids the situation in which a patient has to go to his healthcare, as shown in Figure 23 (a). For this purpose, a healthcare network based on a Big Data System (BDS) is proposed and properly described, as shown in Figure 23 (b).
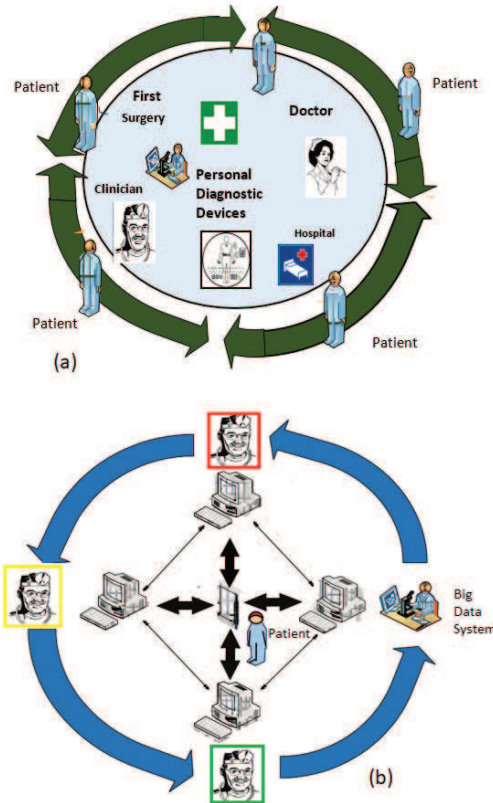
Figure 23 - a) Traditional healthcare network; b) Proposed healthcare network based on a Big Data System

The considered BDS should be composed of four main elements:

   I.   Big Data Sources.
   II. Big Data Transformation.
   III. Big Data Tools&Platforms.
   IV. Big Data Analytics for Parkinson's disease.

As shown in Figure 24 volume, velocity, variety and veracity are features of a big data system and, in particular, they are features of a big data system in healthcare [114].
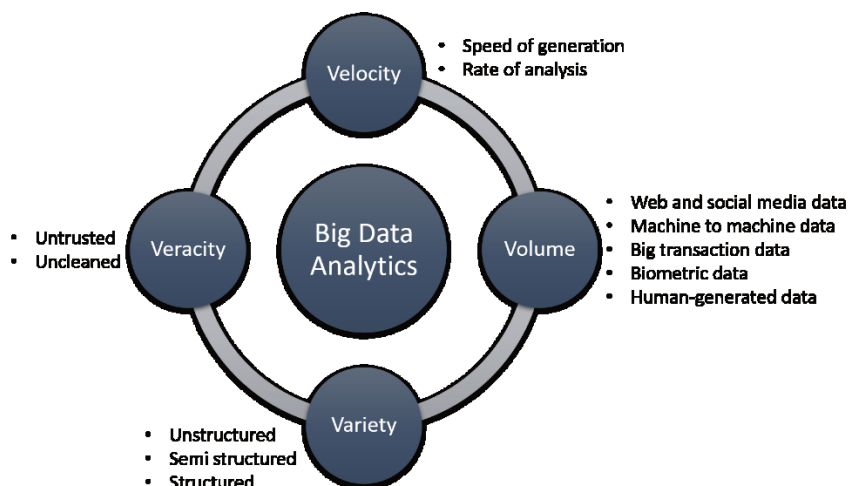
Figure 24 - The 4 'Vs' of Big Data Analytics in healthcare

In detail, volume: a big data system creates and accumulates over time an incredible amount of health-related data such as personal, medical records, radiology images, clinical trial data, 3D imaging, genomics and biometric sensor readings. Biometric data from sensors and other types of common data, such as clinicians' notes, video, images, are considered in this work. Advances in data management, particularly virtualization and cloud computing, are currently facilitating the development of platforms for more effective captures, storages and manipulations of large volumes of data [39];

velocity: data are accumulated and analysed in real-time and at a rapid pace, or velocity. In many medical situations, the application of this features in a big data system could make the difference between life and death. For example, the ability to retrieve, analyse, compare and make decisions based on output values could help physicians to have a diagnostic report in a brief period of time thanks to the MapReduce ESVM (MRESVM) or ANN approach used to predict the disease severity of patients;

variety: one of the things that make big data really big is that they are coming from several different sources. The recent exploiting of these sources for analytics means that so-called structured data (which previously held unchallenged hegemony in analytics) is now joined by unstructured data (text and human language) and semi-structured data (XML, RSS feeds). There's also data that's hard to categorize, as it comes from audio, video, and other devices. Moreover, multidimensional data can be drawn from a Datawarehouse to add historical context to big data. It is a far more eclectic mixture of data types than analytics has ever involved. So, with big data, variety is just as wide as volume. In addition, variety and volume tend to fuel each other [287]. In this work a lot of data from several sensors and application are stored and processed;

veracity or "data assurance": the quality of healthcare data is highly variable, and life or death decisions depend on having accurate information. Unstructured data imply all often incorrect. The Veracity hypnotizes a scaling up in the performance of techniques and technologies to use in a big data management system. Big data analytics in healthcare could be executed across several servers, or nodes, in distributed processing and by considering the use of the paradigm of parallel computing and of the approach called 'divide and process'. Moreover, models and techniques need to take into account the characteristics of BDA. Traditional data management hypnotizes the warehoused data be certain, precise, and clean. High-quality data enable improving the coordination of care, avoiding errors and reducing costs. Due to the fact that BDA has to be exactly specified for each field of application a detailed BDS suitable for PD is herein proposed

and reported in Figure 25 but could also be applied for Blepharospasm considering only a different type of machine learning method (ANN). The proposed healthcare network is described as reported in Figure 26.

Figure 25 - Block diagram of the considered Big Data System
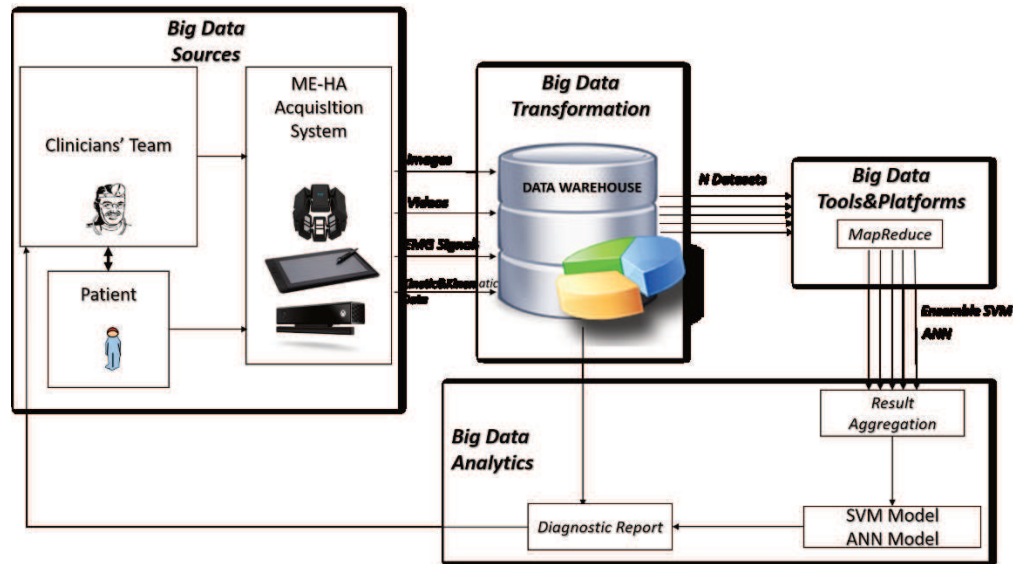
Figure 26 - Block diagram of the proposed Healthcare Network based on Big Data Analytics for Parkinson and Blepharospasm disease

More in detail, the Big Data Source component, consists of three main sub-components (patient, clinicians' team and the acquisition system). The interaction between these sub-components has several heterogeneous data such as images, videos, electromyographic data, kinetic and kinematic data and, clinicians' notes, patient personal data, etc. as outcomes. In particular, the acquisition system is designed and developed to acquire and evaluate several features both from a motor impairment examination and a handwriting analysis. The Big Data Transformation component consists of a Datawarehouse that could store structured, semi-structured and unstructured data that coming from the first component. In particular, since unstructured data is random and difficult to analyse, structured data, already tagged and easily sorted, and semi-structured data that contains tags to separate data elements [266] are stored in a Datawarehouse. The Big Data Tools&Platforms is a component that uses structured or semi-structured data from the Big Data Transformation component as input. This component should perform the implementation of an ESVM [117] based on several datasets collected in a proper Datawarehouse. However, several SVM and ANN models, without aggregation, will be described in the next section and are designed and implemented to be used together in the future. Finally, a diagnostic report based on the output of the SVM and ANN models is feedback to clinicians.

In general, the performance exhibited by such a classifier is strictly dependent on its topology, expressed in terms of the number of hidden layers, number of neurons per layer and activation function per layer. In fact, the overall performance of the ANN depends on how the neurons in the hidden layers (the layers between the input layer and the output layer) process the weighted input information coming from the previous

layers. The improvement of the computational capabilities of the processing systems allowed the researchers to investigate how deeper (high number of hidden layers) and/or wider (low number of hidden layers with a lot of neurons) ANN architectures may improve the state-of-the-art in classification and pattern recognition problems. Identifying the optimal ANN topology is a task of crucial importance; incoherent choices are done in the design phase, in fact, can lead to classification models unstable and with limited performance [288].

The optimal neural network topology was designed implementing evolutionary algorithms. According to Bevilacqua et al. [289], a mono-objective genetic algorithm (MOGA) is used as an optimization strategy to design the best ANNs with optimal topologies. To do this, a binary chromosome of 30 bits was assembled to describe the following features characterizing an artificial neural network topology:

- first hidden layer, the number of neurons ranging in the interval [1-256], coded with 8 bit;
- second and third hidden layer, the number of neurons ranging in the interval [0-255], coded with 8 bit for each layer;
- first, second and third hidden layer, activation function [0-3], coded with 2 bit for each activation function of each layer.

The four activation functions coded in the chromosome are the log-sigmoid (logsig); the hyperbolic tangent sigmoid (tansig), the pure linear (purelin) and the symmetric saturating linear (satlins), whereas the activation function utilised in the output layer is the softmax function (softmax). The solution computed with the genetic algorithm is the optimal ANN topology that after training, validation and test for a given number of iterations nIT of different permutations of the input dataset showed the highest mean accuracy av_ACC. In detail, according to the confusion matrix shown in the following table, if TP(i), TN(i), FP(i) and FN(i) are the number of true positives, true negatives, false positives and false negatives, respectively, predicted with the specific ANN topology for the ith permutation of the input dataset, the accuracy ACC(i) is defined as the ratio between the sum of the true predictions and the sum of all the predictions (the true and the false ones):

Table 5 - Confusion matrix utilised to classify the predictions of the specific ANN topology for the ith permutation of the input dataset

		True condition	
		Positive	**Negative**
Predicted	**Positive**	TP	FP
Condition	**Negative**	FN	TN

$$ACC(i) = \frac{TP(i) + TN(i)}{TP(i) + TN(i) + FP(i) + FN(i)}$$

Therefore, the mean accuracy denoted as av_ACC can be computed as:

$$av\_ACC = \frac{\sum_{i=1}^{n_{IT}} ACC(i)}{n_{IT}}$$

In addition to ACC(i) and av_ACC, the specificity SSPP(i), the sensitivity SSEE(i), for the ith permutation of the input dataset, and the average values of these quantities can be computed:

$$\begin{cases} SSPP(i) = \dfrac{TN(i)}{FP(i) + TN(i)} \\[2mm] av\_SSPP = \dfrac{\sum_{i=1}^{n_{IT}} SSPP(i)}{n_{IT}} \\[2mm] SSEE(i) = \dfrac{TP(i)}{TP(i) + FN(i)} \\[2mm] av\_SSEE = \dfrac{\sum_{i=1}^{n_{IT}} SSEE(i)}{n_{IT}} \end{cases}$$

3.2.3 Parkinson Disease

Parkinson's disease (PD) is currently one of the most spread neurodegenerative disorders. In detail, it is a degenerative brain disorder characterized by a loss of midbrain dopamine (DA) neurons [263] and the main clinical PD symptoms related to body movements involve tremor, rigidity, bradykinesia, and gait abnormalities. Unfortunately, no definitive treatment is at the moment available. Nevertheless, it has been proved that the quality of life of patients can be increased by means of other novel therapies. Physician evaluations are commonly based on historical information from the patient, regarding motor function during activities of daily living and clinic observation, using clinical rating scales [264] and the number of patients is growing as well as the amount of medical data [265]. On this proposal, healthcare networks for PD already exist [266], but the vast volume of existing medical data leaves the most of them still unanalysed. In general, Big Data Analytics (BDA) in healthcare could contribute to evidence-based medicine for analysing a lot of structured and unstructured medical data to match treatments with outcomes, device/remote monitoring for capturing, in real-time, large volumes of fast-moving data from several devices placed at home or in hospital and, finally, patient profile analytics for applying several analyses to patient profile to improve cares and lifestyles. Therefore, in this chapter, several intelligent systems to support neurologists, during the neurological examination, in the objective assessment of the typical PD motor issues and alterations, by means of several devices, are designed, developed and evaluated.

3.2.3.1   Materials and Methods

The motor exercises considered in the acquisition system are a subset of exercises described in the Unified PD Rating Scale (UPDRS) reviewed by the Movement Disorder Society in 2007 [290] and that consists in four parts: Part I (non-motor experience in daily living), Part II (motor experience in daily living), Part III (motor examination), and Part IV (motor complications). Nowadays there are several scientific results supporting its validity. Subjectivity and low efficiency are inevitable as most of the diagnostic criteria use descriptive symptoms, which cannot provide a quantified diagnostic basis. In particular, main problems regard the evaluation of the severity of specific symptoms such as freezing of gait, dysarthria [291], tremor [292], bradykinesia and dyskinesia [293]. Another interesting research field focuses on the analysis of different common life tasks such as handwriting, which is a highly over-learned fine and complex manual skill involving an intricate blend of cognitive, sensory and perceptual-motor components [294]. For these reasons, the presence of an abnormality in the handwriting process is a well-known and well-recognized manifestation of a wide variety of neuro-motor diseases. There are two main difficulties related to handwriting which affect PD

patients: (i) the difficulty in controlling the amplitude of the movement, i.e., a decreased letter size (micrography) and failing in maintaining stroke width of the characters as writing progresses, and (ii) the irregular and bradykinetic movements, i.e., increased movement time, decreased velocities and accelerations, and irregular velocity and acceleration trends over time. For these reasons, in literature, there are several works investigating the possibility of differentiation between PD patients and healthy subjects by means of computer-aided handwriting analysis tools [295].

By considering the current state of the art, important novel contributions are here described with designing and evaluating two specific systems for PD patients: a vision-based system able to capture specific movements of different main MDS-UPDRS [185] scale exercises and a handwriting analysis tool able to extract biometric signals related both to pen movements and muscular activity. Furthermore, a specific set of features extracted from the previous system set-up is evaluated. The Motor Examination – Handwriting Analysis (ME-HA) acquisition system consists of several instruments:

- Microsoft Kinect: attached to a telescopic bar along the vertical axis to enable users to change its orientation and position so that it can recognize movements [284];
- passive reflective markers to track the position of fingers and toes;
- the Myo armband: a wearable gesture control and motion control device consisting of 8 electromyographic sensors used as sEMG bracelet sensor for acquiring sEMG signals from 8 different points of the forearm;
- the WACOM Cintiq 13" HD used as graphics tablet providing co-located visual feedback to acquire pen tip position (planar x-y coordinates) and pressure, and the tilt of the pen with respect to the writing surface.

Several features based on all tasks performed by each patient have to be derived; thus, proper acquisition system needs to be designed and developed by means of these instruments. In particular, several systems based on the third part of MDS-UPDRS regarding the motor examination and the handwriting analysis can be designed.

Finger-to-nose task

Participants. 17 subjects were recruited: 6 PD patients and 11 Control volunteers. PD patients are balanced in gender and ranged in age from 58 to 81 years old (m: 73,5 sd: 10,7). Also, the control subjects are balanced in gender but ranged in age from 21 to 33 years old (m: 26,1 sd: 3,8).

The Kinect® sensor is placed at the height of 80 cm above the patient's head. So, from a raised position it can capture a patient's location and the hand involved in the experiment. In addition, Kinect® has been preferred to normal RGB cameras because it captures 3-dimensional information, using a depth sensor. It consists of an infrared camera, which involves realizing calculations using a different wavelength than the traditional RGB camera. Finally, it is a relatively low-cost technology, which makes the whole system extremely cheap. The kinetic tremor is evaluated which measures smooth, coordinated movement of the upper limbs by having each of the examinees touch the tip their nose with their index finger (Figure 27).
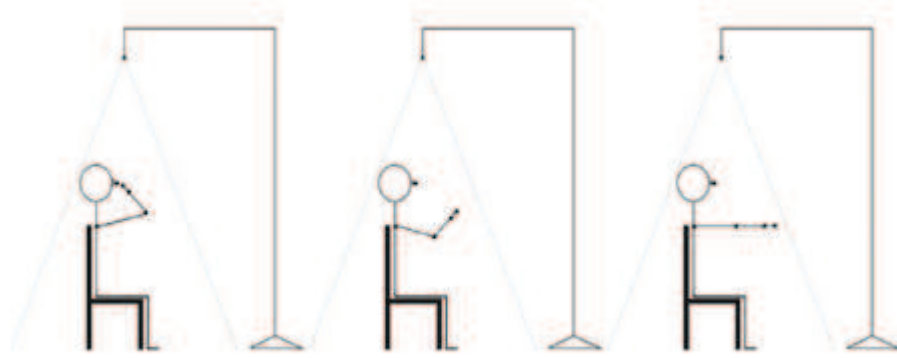
Figure 27 - Example of the exercise execution

In every examination, all features required for the classification have been evaluated by means of a reflector marker placed on a finger of each patient. In Fig. 6 an example of a typical trajectory during the exercise for PD and Control is depicted.
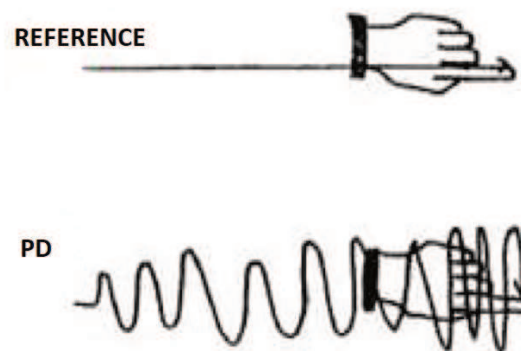
Figure 28 - Example of trajectory difference between PD and ideal one

Medical specialists usually observe significant features useful for evaluating tremor only on the basis of their own experience, i.e., by adopting a qualitative and subjective approach in their evaluation. Some of these features useful for evaluating tremor include average amplitude, maximum amplitude, frequency, and are subsequently determined and analysed by this system. A cloud of points, each one representing the spatial position of the marker over three axes (X, Y, and Z) is acquired during the finger-to-nose experiment; this cloud is extracted from images captured at a frame rate of 30 Frame Per Second (FPS).

The linear regression is used to find the reference line for the specific test; this line is used to evaluate the tremor amplitude as the distance between this reference line and the index finger trajectory, point by point for each frame. A typical fluctuation pattern of a PD patient frame by frame is shown in Figure 29.

Figure 29 - Fluctuation pattern of a PD patient

More in detail the Principal Components Analysis (PCA) is used to fit a linear regression [296]. PCA minimizes the perpendicular distances from the data to the fitted model. This is the linear case of what is known as Orthogonal Regression or Total Least Squares and is appropriate when, as in this case, there is no natural distinction between predictor and response variables, or when all variables are measured with error. This contrasts with the usual regression assumption that predictor variables are measured exactly, and only the response variable has an error component.

The figures (Figure 30, Figure 31) shown an example of a cloud of points and the respective fit line.
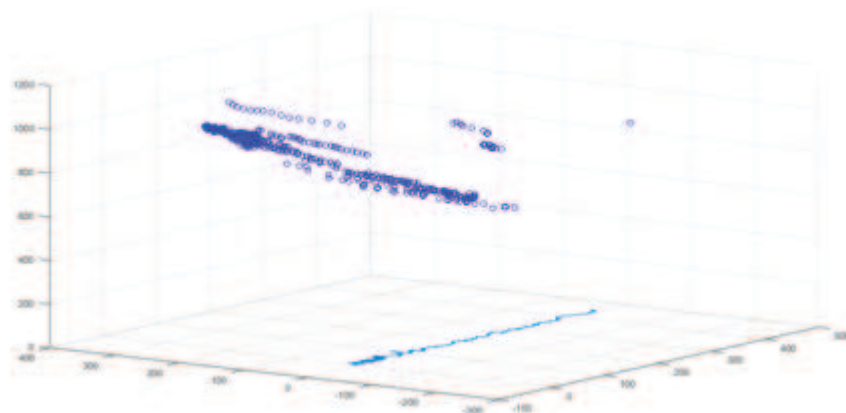
Figure 30 - Cloud of points of index finger trajectory
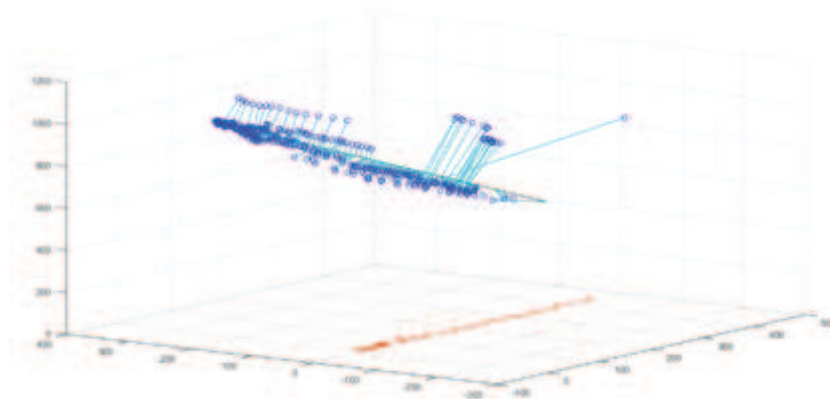
Figure 31 - Reference line of index finger trajectory

As third feature, frequency is considered. In particular, the average tremor frequency of patient per second is used. The peaks of the amplitudes during the task is evaluated by means of the reference line obtained with linear regression previously described. Each peak is considered as a change of direction on the three-reference axis. Then, an evaluation of the number of tremors during the exercise and the medium frequency of tremors per second for each patient is performed.

During the experiment, some marker tracking errors are detected. These errors are due to the lighting conditions that can interfere with the infrared sensor of Kinect® acquisition system or to reflective objects in the Kinect® field of view that produce detection mistakes as shown in Fig.6.
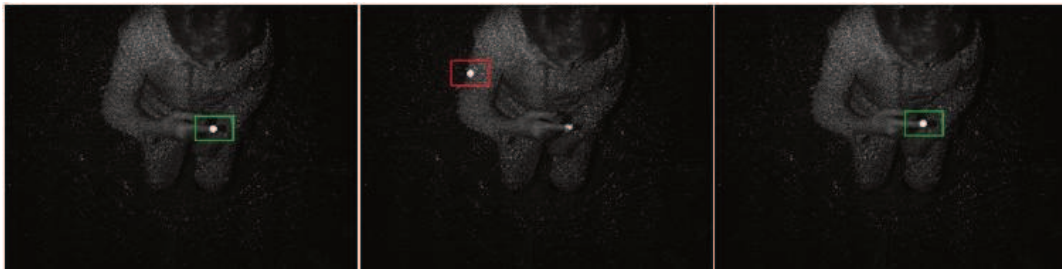
Figure 32 - Example of system acquisition: correct tracking in the 1st and 3rd image; an example of the tracking error in the 2nd image

The selected data are filtered by means of a low-pass filter to remove the peaks of amplitude over 20 cm. This threshold is chosen because it's twice as much the maximum severity of the MDS-UPDRS. Therefore, a fluctuation over this threshold is considered as acquisition system error.

An SVM classifier [297] to discriminate the PD patients from control subjects is designed. SVM is a binary classifier whose goal is to find the best linear decision surface that separates the training features space. SVMs have high generalization capability because they can be extended to separate space of non-linear input features. The performances are discussed in paragraph 3.2.3.2.

Finger and Foot Tapping tasks.

Participants. Thirty-three PD patients (mean age 71.6 years, SD 9.0, age range 54-87) and twenty-nine healthy subjects (mean age 71.1 years, SD 9.2, age range 57-90) participated in the experiments after giving a written informed consent. The 33 PD patients were examined by a medical doctor and rated according to MDS-UPDRS Part IV for motor complications that consider a scoring with five level (Normal, Slight, Mild, Moderate and Severe). In detail, fourteen (mean age 67.2 years, SD 9.8, age range 54-81) and nineteen (mean age 74.1 years, SD 7.1, age range 63-87) patients are classified as mild and moderate PD patients, respectively. None of the patients is classified as either slight or severe PD patient.

Two separate vision-based systems able to acquire the movement of the thumb, the index finger and the toes are developed. Both acquisition systems are based on passive markers made of reflective material and the Microsoft Kinect RGBD camera (Figure 33).

Figure 33 - Left image shows a healthy subject wearing the two passive finger markers. The images reported on the right show the foot of a subject doing the foot tapping exercise while he is wearing a passive marker on the toes

The Finger Tapping exercise set up considers the examination of both hands separately. While the subject is seated in front of the camera he has to tap ten times the index finger on the thumb quickly. During the task, the subject wears two thimbles made of a reflective material on both the index finger and thumb.

Meanwhile, in the Foot Tapping exercise setup, the feet are tested separately. The tested subject sits in a straight-backed chair in front of the camera and has both feet on the floor. He is then instructed to place the heel on the ground in a comfortable position and then tap the toes ten times as big and as fast as possible. A system of stripes with reflective material is positioned on the toes.

The two vision-based acquisition systems use passive reflective markers to track the position of the thumb, the index finger and the toes. After the movement acquisition, an image processing phase is needed to recognize the marker in each acquired video frame and compute the 3D position of a centroid point associated with the specific marker. This post-processing phase has been conducted using the OpenCV library running the flowing steps on each image frame:

- conversion to a grayscale image;
- extraction of the pixels associated with the reflective passive markers with a thresholding operation;
- blurring and thresholding operations in sequence;
- eroding and dilating operations in sequence;
- dilating and eroding operations in sequence.

After the post-processing phase, all the found blobs are extracted using an edge detection procedure. Only the blobs having sizes comparable with markers' size are kept for the next analysis. As a final step, the centroid of each blob (only one blob for the foot tapping and two blobs for the finger tapping) is computed. Given the position of the centroid, its depth information and the intrinsic parameters of the used camera, have been computed the 3D position of the centroid associated with each tracked marker in the camera reference system. Such centroid has then considered as the position of the specific finger or of the foot's toes.

The entire post-processing analysis described above produces the 3D positions of toes' marker (Foot Tapping) and of the two fingers' markers (Finger Tapping). Given the position of each marker we then extracted the following signals over time (Figure 34):

- d1(t) - the distance between the two fingers' markers over time (Finger Tapping);
- d2(t) - the distance between the position of the toes' marker over time and the position of the same marker when the toes are completely on the ground (Foot Tapping).
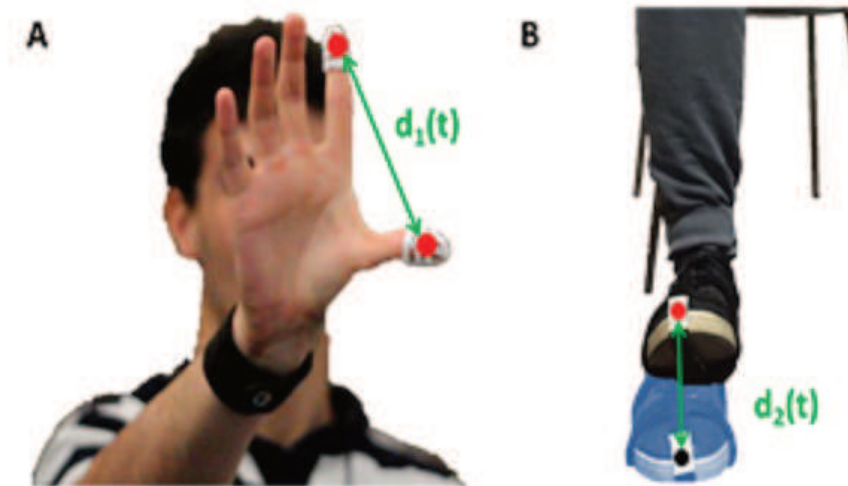
Figure 34 - a) Finger Tapping: the signal d1(t) is the distance between the two centroids (red filled circles) of the passive finger markers; b) Foot Tapping: the signal d2(t) is the distance between the centroid of the toes' marker and the centroid of the same

Both signals have been normalized to make them range in [0,1]. Given the entire acquired signal, all the single trials (ten finger tappings and ten-foot tappings) have been extracted for each side. The same set of features for both computed signals are extracted, i.e. d1(t) and d2(t). The set of the extracted features contains features of the time domain, space domain and frequency domain. In particular, the features are:

- meanTime: averaged execution time of the single exercise trial;
- varTime: variance of the execution time of the single exercise trial;
- meanAmplitude: averaged space amplitude of the single exercise trial;
- varAmplitude: variance of the space amplitude of the single exercise trial;
- tremors: number of peaks detected during the entire acquisition;
- hesitations: number of amplitude peaks detected in the velocity signal during the entire acquisition;
- periodicity: periodicity of the exercise computed as reported in [298];
- AxF: (amplitude times frequency) the averaged value of the division between the amplitude peak reached in a single exercise trial and the time duration of the trial.

The results and relative discussions are described in the paragraph 3.2.3.2.

Handwriting Analysis.

Participants. 32 participants (21 males, 11 females, age: 71.4 ± 8.3 years old) took part in the experimental tests. The age-matched control group is composed of 11 healthy subjects (4 males, 7 females, age: 70.2 ± 10.2 years old), whereas the PD group is composed of 21 subjects (17 males, 4 females, age: 72.1 ± 8.3). According to the degree of the disease, the PD group is, then, divided into two subgroups: mild and moderate. The mild group is composed of 12 patients (9 males, 3 females, age: 70.5 ± 10.0) and the moderate one is composed of 9 patients (8 males, 1 female, age: 73.8 ± 6.0).

This technique is based on a model-free technique that allows the extraction and the classification of particular features starting from the assumption that the characteristics (or features) of one or more particular biometric signals or parameters can synthesize and represent a particular aspect of the user's handwriting. The analysis requires the application of processing algorithms on signals generated starting from a specifically created pattern and can succeed to extract the features of interest.

The exercise, in particular, requires the writing of a specific pattern and the recording of two different main sources of information. The system set-up is reported in Figure 35 and includes the MyoTM Gesture Control Armband (www.myo.com) used as sEMG bracelet sensor for acquiring sEMG signals from 8 different points of the forearm and the WACOM Cintiq 13" HD (www.wacom.com/en-ch/products/pen-displays/ Cintiq-13-HD) used as graphics tablet providing co-located visual feedback to acquire pen tip position (planar x-y coordinates) and pressure, and the tilt of the pen with respect to the writing surface.
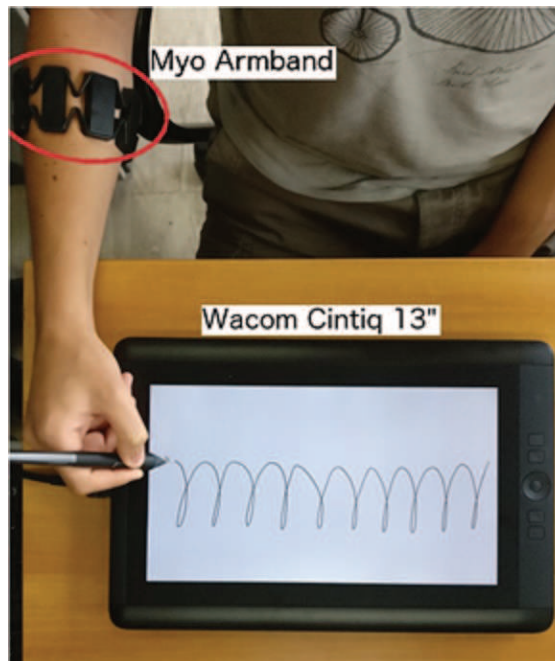
Figure 35 - The system set-up used for the experimental tests to validate the proposed approach

Three writing patterns (WPs) corresponding to as many writing tasks are selected. They were properly differentiated according to the writing size and as the size constraint (one task is size unconstrained, while the other two have a visual reference as for size constraint):

- task number 1 - a five turn-spiral drawn in an anti-clockwise direction (WP1);
- task number 2 – a sequence of 8 "l" with a size of 2.5cm (a 2.5 cm visual marker reference is displayed on the left of the tablet screen) (WP2);
- task number 3 – a sequence of 8 "l" with a size of 5cm (a 5 cm visual marker reference is displayed on the left of the tablet screen) (WP3).

The acquisition setup allows the synchronous recording of two main sources of information and signals representing different aspects of handwriting: the sEMG of the forearm and the pen data from the tablet. The features related to handwriting are extracted from biometric signals acquired during the handwriting tasks. In particular, it is possible

to group the proposed features into two categories: sEMG related and pen tip related features.

sEMG related features. These features are related to the muscular activity of the subject and are extracted from the sEMG signals acquired at the subject's forearm:

- Root Mean Square (RMS) features extracted for each sEMG channel. RMS is computed as the square root of the mean of the sample squares.
- Zero Crossing (ZC) features, an index related to the signal sign variation. To normalize the features among the subjects, its value is divided by the length of the signal.

Pen tip related features. These features are extracted from the signals generated by a graphics tablet during the handwriting task:

- Cartesian and XY features are referred to the pen tip position and are extracted starting from the XY axes position: Cartesian and XY (i) velocity, (ii) acceleration, and(iii) jerk. This led to a total of nine signals.
- Pen tip pressure feature, a scalar feature and corresponds to the pressure applied by the pen tip on the surface of the tablet.
- Azimuth and altitude feature: the azimuth feature is the value of the angle between a reference direction (e.g., the Y axes of the tablet) and the pen direction projected on the horizontal plane. The altitude feature is the value of the angle between the pen direction and the horizontal plane.

Pattern-specific features associated with a specific writing pattern (WP). For letter-based WPs, the features are mainly related to the writing size, whereas, for the spiral-based WPs, the features are mainly related to the writing precision. For the features extracted from the letter-based WPs, the upper and the lower peaks of the Y coordinate of the pen tip position are computed and, then, used as input data of a linear regressor. Finally, the angle α between the R-up and R-low regression line and the coefficient of determination ($R2$) are computed and selected as features. For spiral WPs, instead, the feature extracted is an index representative of the variability of the strokes. For each point P of the X-Y pen tip position, the vector $\vec{r}$ with respect to the spiral centroid point C, having oran igin in P is computed. The angle β between $\vec{r}$ and the direction vector $\vec{d}$ tangent to the spiral in P is, then, calculated. The spiral precision index feature is the standard deviation of the β angles computed for each point P.

To reduce the number of features to be classified and to infer which of them are the most representative of the subject's status, a classification decision tree technique based on Gini's diversity index is used. To classify the extracted features, Artificial Neural Network (ANN) based classifier is used. The optimal topology for an ANN classifier is found by exploiting a Multi-Objective Genetic Algorithm (MOGA) and by maximizing the average test accuracy on a set of training, validation and test iterations for each ANN topology using permutations of the dataset [289]. The experiments aim to fulfil two main objectives: the separation between (i) PD patients from healthy subjects, and (ii) mild and moderate PD patients. The performance for both the MOGA algorithm and the ANN-based classification are evaluated in terms of accuracy, specificity and sensitivity and are discussed in paragraph 3.2.3.2.

Gait Analysis.

Participants. Thirty elderly participants from a local clinical centre (Medica Sud s.r.l., Bari, Italy) are recruited: 14 healthy subjects (10 male and 4 female, 73.57 ± 6.47 years, range 65-82 years) and 16 idiopathic Parkinson patients (13 male and 3 female, 74.94 ± 7.68 years, range 63-87 years). Right, and left sides of each patient are considered separately. All participants provided written informed consent. The subjects are asked to walk straight towards the device, with their normal walking rhythm (Figure 36). Several trials are acquired for each patient, changing the starting foot, to have at least one gait cycle for each side without errors.

The Kinect sensor samples at a frequency of approximately 30 Hz and video frames are captured both in colour and depth. Using captured frames, the Kinect SDK segments and tracks human skeletons and gives the output of a human skeleton represented by 25 nodes or control points in the Kinect's own reference frame known as the skeleton space. Motion analysis data collection started with the subject standing in a T-pose for one second to facilitate the skeleton tracking. Subjects then walked toward the Kinect sensor, which was placed 3.5 m away from the subject's starting point at the height of 0.75 m. The 3.5-m distance is selected to guarantee that the recorded gait cycle, which began when the subject was about 2.5–3 m from the Kinect, did not include the acceleration/deceleration phases of walking that are anticipated during the initiation or completion of the gait task (Figure 36).
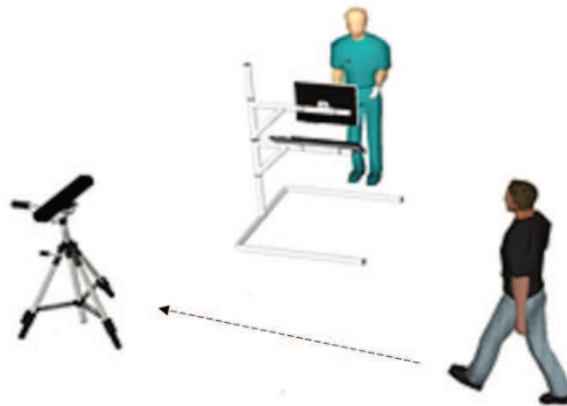
Figure 36 - Representation of the proposed set-up in the clinical centre. The dotted black line indicates the walking direction (one-way walk)

Three categories of features are considered:

- Temporal: to assess the duration of gait phases in seconds and in percentage compared to the duration of the gait cycle (Stance and Swing Phase/Time, Double Support Phase, Stride Time);
- Spatial: to estimate length, width and velocity of movements, normalized by the height or the lower limb length of the subject (Stride Cadence/Length/Velocity, Step Length/Width, Swing Velocity);
- Angular: to assess the degree of rotation for specific postures and movements, typical of Parkinsonian patients (Trunk/Neck Flexion, Pisa Syndrome, Arm Swing).

The dataset resulting from the previous analyses is constituted by sixteen different features, grouping, for each subject, gait parameters. For each patient, several gait cycles are extracted, to have more reliable values.

The values included in each dataset record refer to average measures on all the gait cycles considered for the single subject. For each approach, classification is carried out, before with all the features and then with several sets of selected features, identified using the Open Source Machine Learning Software Weka. All the analyses are conducted following two different classification strategies based on supervised learning. In particular, Support Vector Machines (SVMs) and Artificial Neural Networks (ANNs) are used, which are state-of-the-art classifiers that have gained popularity within pattern recognition tasks [289, 299, 300].

Considering the easy tuning of training parameters, SVMs classifiers [301] is considered to realize a preliminary inspection of the processed data. SVM is a classifier whose goal is to find the best decision hyper-plane that separates the training features space. SVMs have high generalization capability because they can be extended to separate space of non-linear input features. Evolutionary approaches, and optimization strategies based on probabilistic graphical models, for the design of classification architectures, are becoming very popular thanks to their ability to automatically optimize the classifiers topologies to improve the overall classification performance. A Genetic Algorithm able to search for ANN topologies for multi-class discrimination is used. In both the ANN and SVM strategies, the performance of the classifiers are evaluated in terms of Accuracy, Specificity and Sensitivity and are discussed in paragraph 3.2.3.2.

3.2.3.2 Innovative Results

Finger to nose task.

Different types of SVM classifiers are designed and implemented. However, the best results are achieved using the cubic SVM (Table 6). To avoid data overfitting, 5-fold cross-validation is used. As the dimension of the dataset is relatively small, multiple tests to get more reliable results are realisable.

Table 6 - Confusion Matrix from cubic SVM applied to features extracted during finger to nose task

		True condition	
		Positive **(PD patients)**	**Negative** **(Healthy subjects)**
Predicted **Condition**	**Positive** **(PD patients)**	10	1
	Negative **(Healthy sub-jects)**	1	16

The SVM approach yielded an average accuracy of around 82%, showing the existence of good separation between the two classes (Parkinson and healthy subjects). The confusion matrix of the best SVM model is shown in Table 6, and the performance indexes are reported in the following equations:

$$Accuracy = \frac{TP + TN}{TP + TN + FP + FN} = 0.93,$$

$$Sensitivity = \frac{TP}{TP + FN} = 0.91,$$

$$Specificity = \frac{TN}{TN + FP} = 0.94$$

However, a low number of instances in the dataset suggests to further investigate these results.

Finger tapping and foot tapping tasks.

All the extracted features can be used both to classify a subject either as healthy or PD affected and to infer the severity of the disease. In particular, discrimination between mild and moderate PD patients is performed.

Three different binary support vector machine (SVM) classifiers are designed and implemented and are based on following three set of features:

- Set 1: all the finger tapping features;
- Set 2: all the foot tapping features;
- Set 3: both finger and foot tapping features;

The training process is based on 5-fold cross-validation and evaluates in sequence the following types of SVM classifiers: (1) linear SVM, (2) quadratic SVM, (3) cubic SVM, (4) Gaussian SVM.

Several results are evaluated for these exercises. In particular, considering only the finger tapping features to discriminate healthy subjects from PD patients, the results are that the best classifier is the Gaussian SVM with an accuracy of 71.0 %, a sensitivity of 75.7 % and a specificity of 65.5 %.

Table 7 - Confusion matrix of "Healthy subjects vs PD patients" classification with finger tapping features

		True condition	
		Positive (PD patients)	**Negative** (Healthy subjects)
Predicted Condition	**Positive** (PD patients)	25	10
	Negative (Healthy subjects)	8	19

Moreover, considering foot tapping features, the results are that the best classifier is the Gaussian SVM with an accuracy of 85.5 %, a sensitivity of 91.0 % and a specificity of 79.0 %.

Table 8 - Confusion matrix of "Healthy subjects vs PD patients" classification with finger tapping features

		True condition	
		Positive (PD patients)	**Negative (Healthy subjects)**
Predicted Condition	**Positive (PD patients)**	30	6
	Negative (Healthy subjects)	3	23

Finally, considering both finger and foot tapping features, the results are that the best classifier is the Quadratic SVM with an accuracy of 87.1 %, a sensitivity of 87.8 % and a specificity of 86.0 %.

Table 9 - Confusion matrix of "Healthy subjects vs PD patients" classification with both finger tapping and foot tapping

		True condition	
		Positive (PD patients)	**Negative (Healthy subjects)**
Predicted Condition	**Positive (PD patients)**	29	4
	Negative (Healthy subjects)	4	25

This first analysis indicates that the selected set of features from the movement acquired during both exercises (Finger Tapping and Foot Tapping) can be used to capture the abnormal motor activity of a PD patient with great results.

Focusing on the results of Mild PD patients and Moderate PD patients the results are following described.

Considering only the finger tapping features, the best classifier is the Gaussian SVM with an accuracy of 57.0 %, a sensitivity of 100 % and a specificity of 0 %.

Table 10 - Confusion matrix of "Mild PD patients vs Moderate PD patients" classification with finger tapping features

		True condition	
		Positive (Moderate PD patients)	**Negative (Mild PD patients)**
Predicted Condition	**Positive (Moderate PD patients)**	19	14
	Negative (Mild PD Patients)	0	0

Moreover, considering only the foot tapping features, the best classifier is the Gaussian SVM with an accuracy of 81.0 %, a sensitivity of 84.0 % and a specificity of 78.0 %.

Table 11 - Confusion matrix of "Mild PD patients vs Moderate PD patients" classification with foot tapping features

		True condition	
		Positive (Moderate PD patients)	**Negative (Mild PD patients)**
Predicted Condition	**Positive (Moderate PD patients)**	16	3
	Negative (Mild PD Patients)	3	11

Finally, considering both finger and foot tapping features the results are that the best classifier is the Gaussian SVM with an accuracy of 78.0 %, a sensitivity of 89.0 % and a specificity of 64.0 %.

Table 12 - Confusion matrix of "Mild PD patients vs Moderate PD patients" classification with both finger tapping and foot tapping features

		True condition	
		Positive (Moderate PD patients)	**Negative (Mild PD patients)**
Predicted Condition	**Positive (Moderate PD patients)**	17	5
	Negative (Mild PD Patients)	2	9

This second analysis indicates that the set of features selected from the movement acquired during both exercises (finger and foot tapping) lead to a good "Mild PD patients vs Moderate PD patients" classification results. But, it is worth noting that the "Mild PD patients vs Moderate PD patients" classification scores are slightly lower than the "Healthy subjects vs PD patients" classification ones. It is also worth noting that the foot-tapping features are the most important ones to achieve the best accuracy and specificity levels, and that finger tapping features are completely not representative of the motor differences between mild and moderate PD patients. Concerning the "Mild PD patients vs Moderate PD patients" classification, from what emerged in this second analysis the final results are that finger tapping features lead to lower accuracy and specificity levels. Only when the finger tapping features are used together with the foot tapping features the SVM classifier present a better sensitivity level at the expense of both the accuracy and specificity.

Handwriting analysis.

As described previously, three writing patterns (WPs) leading to as many writing tasks are used: a five-turn spiral drawn in an anticlockwise direction (WP1), a sequence of 8 Latin letter "l" with a size of 2.5cm (WP2) and with a size of 5cm (WP3)

The experiments aim to fulfil two main objectives: the separation between (i) PD patients from healthy subjects, and (ii) mild and moderate PD patients. The features extracted during the experiments are grouped in three datasets: (i) dataset A with 41 features, (ii) dataset B with 43 features and (iii) dataset C with 43 features extracted from WP1, WP2 and WP3, respectively. Then, a feature selection algorithm is applied on the three datasets to select and reduce the number of the features. This led to the creation of six new, different feature datasets: dataset with all features included in set A, B and C (Case 1, 2 and 3, respectively) and dataset with only the features resulting from the feature selection algorithm applied on dataset A, B and C (Case 4, 5 and 6, respectively).

Since 250 iterations of the net training procedure for each case are performed, the performance results have been reported in percentage (standard deviation in brackets).

Objective 1 - Separating PD patients and healthy subjects:

- for dataset A (WP1-41 features-Case 4), the 6 selected features are: one RMS value, 3 ZC values, the mean cartesian velocity and acceleration on X axes;
- for dataset B (WP2-43 features-Case 5), the 6 selected features are: the mean jerk on Y axes, 3 ZC values, the mean cartesian acceleration and velocity on X axes;
- for dataset C (WP3-43 features-Case 6), the 7 selected features are 2 RMS values, one ZC value, the mean cartesian velocity, the altitude STD, the azimuth RMS and the mean velocity on X axes.

The best accuracy value (96.85%) is achieved in case 6 (classification on the data set composed of the selection of 7 features from the dataset of 43 features extracted from WP3, i.e., the sequence of 8 Latin letter "l" with a size of 5cm). In case 6, three out of seven features are related to sEMG signals (RMS and ZC), whereas the other features were related to pen tilt and velocity.

Objective 2 - Separating mild and moderate PD patients:

- for dataset A (WP1-41 features-Case 4), the 6 selected features are: 2 RMS values, 2 ZC values, the mean pressure and the mean altitude;
- for dataset B (WP2-43 features-Case 5), the 5 selected features are: 2 RMS values, 2 ZC values and the mean cartesian velocity;
- for dataset C (WP3-43 features-Case 6), the 5 selected features are 2 RMS values, one ZC value, the mean cartesian velocity on X axes and the mean pressure.

The best accuracy value (96.00%) is achieved in Case 4 (dataset A-6 features selected over 41 features extracted from WP1, i.e., the spiral WP). In Case 4, four out of six features are related to sEMG signals (RMS and ZC), whereas the other features are related to pen tilt and pressure.

The obtained classification accuracy for all three cases for both objectives, instead, are reported in Table 13.

Table 13 - Accuracy and standard deviation values obtained for each case

	Case	Objective 1	Objective 2
All Features	1	90.76% (0.0764)	94.34% (0.0626)
	2	92.98% (0.0523)	87.26% (0.0850)
	3	95.95% (0.0479)	91.86% (0.0830)
Selected Features	4	93.78% (0.0566)	96.00% (0.0658)
	5	91.58% (0.0526)	86.71% (0.0837)
	6	96.85% (0.0405)	91.66% (0.0858)

As it can be observed, the obtained accuracy values x for both objectives are high (86 < x < 97) and present a limited standard deviation d (d < 0.09), thus demonstrating the repeatability of the classification performances and the stability of the optimal topology ANN architectures. It is worth to observe also that the highest values of resulting accuracy have been obtained for both objectives for the classification of the selected features. The obtained results confirm the relevance of the sEMG signals not only in PD-healthy differentiation but also in differentiating mild and moderate PD patients. Furthermore, the results confirm the choice of acquiring signals also related to pen tilt, pressure and velocity.

Gait analysis.

Two different subgroups for the classification analysis are analysed as follow:

- Case A: Healthy (14) versus Parkinson's Disease (16). Dataset consists of a total of 30 records, 16 PD patients and 14 older age normal subjects. Right, and left sides of each patient are considered separately in the study. So, the final dataset is composed of 60 instances.
- Case B: Mild (9) versus Moderate/Severe (7) Parkinson's Disease. Dataset consists of a total of 16 records, 9 slight and 7 moderate PD patients. Right, and left sides of each patient were considered separately in the study. So, the final dataset is composed of 32 instances.

All the participants were able to complete both clinical and instrumented evaluations. The results obtained with both SVM and optimized ANN classifiers are reported and compared following. In detail, the comparison is evaluated analysing the average values of Accuracy, Sensitivity and Specificity across 250 different training iterations.

Table 14 - ANN and SVM performance comparison with only selected features

		Accuracy	Sensitivity	Specificity
Case A (9 Features)	SVM	0.785 ± 0.034	0.817 ± 0.049	0.748 ± 0.055
	ANN	0.894 ± 0.082	0.870 ± 0.127	0.918 ± 0.110
Casa B (6 features)	SVM	0.887 ± 0.039	0.789 ± 0.060	0.963 ± 0.051
	ANN	0.950 ± 0.071	0.900 ± 0.157	0.990 ± 0.043

The results showed that the ANN classifier performed the best in both cases and in both configurations (all features versus reduced features). In particular, when diagnosing PD, the ANN reached 89,4 % (± 8,6 %) of Accuracy, 87,0 % (± 12,7 %) of Sensitivity and 91,8 % (± 11,1 %) of Specificity with only 9 selected features; while, the ANN reached 95,0 % (± 7,1 %) of Accuracy, 90,0 % (± 15,7 %) of Sensitivity and 99,0 % (± 4,3 %) of Specificity with 6 selected features in classifying mild to moderate PD patients.

3.2.4 Blepharospasm Disease

Blepharospasm (BSP) is adult-onset focal dystonia with phenomenologically heterogeneous effects including, but not limited to, blinks, brief or prolonged spasms and narrowing or closure of the eyelids. In spite of the clear and well-known symptomatology, rating objectively the severity of this dystonia is a rather complex task as BSP symptoms are so subtle and hardly perceptible, that even expert neurologists can rate the gravity of the pathology in the same patients differently. Software tools were then developed to support neurologists in the rating procedure. Currently, a computerized video-based system is available that is capable to determine the eye closure time objectively, but that cannot distinguish the typical symptoms of the pathology. Therefore, the main research question is: by means of ANN, could blinks, brief and prolonged spasms be recognized to support neurologists for evaluating the disease severity? The software described below, based on standard video-recordings from commonly available video cameras, is capable not only to measure the per cent time of eye closure but also to recognize blinking, brief and prolonged spasms, that are the typical facial movements taking place in patients with blepharospasm. The proposed software is a practical system very suited for the clinical context where the environmental conditions cannot be easily standardized; it appears a promising tool for supporting/assisting physicians to rate the blepharospasm severity according to the Blepharospasm Severity Rating Scale (BSRS) [267].

3.2.4.1   Materials and Methods

Participants. Nine patients with BSP are recruited (3 women and 6 men, average age 69.55-8.94 years).

The protocol adopted to evaluate the blepharospasm severity consists of an examination recording with a digital video camera (Canon, Legria HFM306, 3.3MP Full HD CMOS, HD Video Lens (up to 18x zoom), DIGIC DV III) at 29.97 frames per second. An experienced neurologist, revising the video-recordings, identified dystonic spasms and blinks and evaluated the overall Severity Index (SIn) of the recruited patients applying the Blepharospasm Severity Rating Scale (BSRS). The neurologist classified the BSP symptoms observed in the recruited patients, as follows (Figure 37).
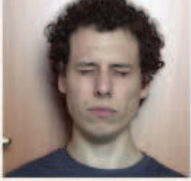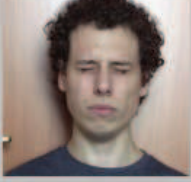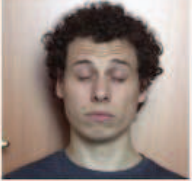
Symptom	Duration	Features	
Open eyes	-	-	
Blink	< 1s	transient eyelid drop without any lowering of the eyebrow	
Brief spasm	0.3 to 3 s	lowering of the eyebrow and narrowing/closure of the eyelid rim	
Prolonged spasm	> 3 s	lowering of the eyebrow and narrowing/closure of the eyelid rim	
apraxia of eyelid opening		raising of the eyebrow above the superior orbital margin	

Figure 37 - Typical symptoms observed in patients with blepharospasm

1) A sudden Orbicularis Oculi (OO) muscle contraction causing lowering of the eyebrow and narrowing/closure of the eyelid rim is classified by the neurologist as a spasm. In turn, the spasm can be classified into:

1a) brief spasm, i.e. a spasm-inducing a brief eyelid closure lasting 0.3 to 3 s;

1b) prolonged spasm, i.e. a spasm-inducing a prolonged eyelid closure with a duration of more than 3 s.

2) A bilateral, synchronous short duration (<1 s) OO muscle contraction causing a transient eyelid drop, - but without any lowering of the eyebrow -, is classified by the clinician as a blink.

3) Delay in reopening the eyelids after involuntary closure associated with no overt OO contraction and raising of the eyebrow above the superior orbital margin was classified as apraxia of eyelid opening.

The following clinical test is performed to determine the severity index SIn, according to the BSRS scale, of the patients. Participants were seated on a chair placed in front of the video camera with the feet resting on the floor and the hands on the knees (Figure 38).
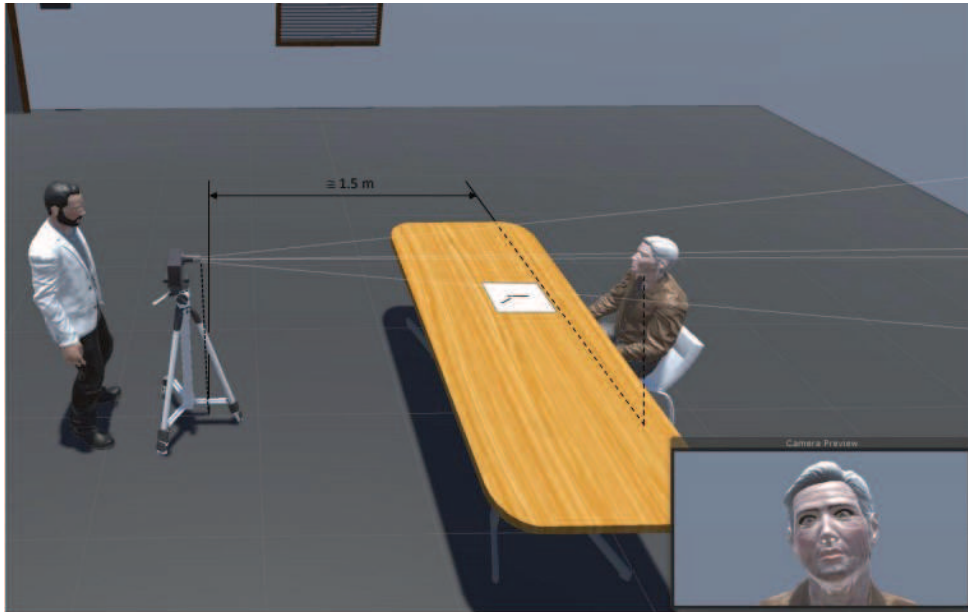
Figure 38 - Set-up utilized to acquire the facial expressions of the patient during the clinical test

The camera objective is zoomed in so that the resulting field of view was entirely occupied by the patient's head with her/his shoulders. Video-recordings had an approximately 5-minute total duration and were performed according to the protocol described in a previous study [302]. In the first three minutes, a training phase for the clinician takes place; in fact, the neurologist asks the patient to perform some tasks that carefully observes, thus acquiring a deep knowledge of the modalities with which the BSP symptoms take place in the patient. During the last two minutes of the test, the patient is asked to remain at rest with the eyes open and fixing a specific point located in front of her/him. In this time interval, the clinician recognizes and counts blinks, brief and prolonged spasms, apraxia of the eyelid opening.

In detail, the adopted clinical test is articulated in the following steps:

(i)   in the first 10 s, the patient is at rest with the eyes open;

(ii)   the patient is asked to voluntarily and forcefully close and to open the eyes 5 times, one cycle per second, approximately (in reality, the time necessary to perform the requested task very often depends on the patient and the severity of the dystonia);

(iii)   again, for 10 s the patient is at rest with the eyes open;

(iv)   the patient is asked to voluntarily and gently close and open the eyes 5 times, one cycle per second;

(v)   again, for other 10 s the patient is at rest with the eyes open;

(vi)   the neurologist poses the following questions: Are you capable to avoid closing the eyes? How? With the sole force of will? Or, do you need to touch eyes, face or neck?

(vii)   the patient has 50 s time to give a response to the questions posed;

(viii)   the patient is asked to write on a sheet of paper a stereotyped sentence (e.g., "Today is a nice sunny day") 3 times;

(ix)   The patient remains at rest for at least 150 s, with the eyes open and fixing a specific point located in front of her/him. In the last 120 s the neurologist "manually" counts the number of blinks, brief and prolonged spasms, apraxia of eyelid opening.

The first three (approximately) minutes of the test include the steps (i) to (viii), whereas during the last two (approximately) minutes only the step (ix) is performed. It is worthy to note that the tasks performed in the steps (ii) and (iv) are of crucial importance for the neurologist. In fact, voluntary and forceful closure of the eyes can give useful information on how a spasm occurs in the patient. Similarly, voluntary and gentle closure of the eyes is a sort of simulation of a blink and therefore can instruct the clinician on how this event can take place in the patient.

A software tool is developed, based on the dlib library [303] and implementing the face detector (A) and the face pose estimator (B) algorithms, in order, to measure the duration of the time interval in which the patient's eyes are closed and to automatically recognize three of the four BSP symptoms described above, namely: 1a) blinks, 1b) brief and 2) prolonged spasms; the last symptom, the apraxia of eyelid opening, is neglected in this study phase. The schematic shown in Figure 39 briefly summarizes the principal steps followed to develop and validate the software.

Recruitement of the 9 patients [1]

Clinical test and video frame acquisition [2]

Observation of the video-frames and [3]
assessment of the severity index (SIn) values
with the BSRS scale

Implementation of the face detector
algorithm [4]

Implementation of the face pose
estimator [5]

Implementation of the correction
tool T_{corr} [6]

Face pose estimator algorithm re-training [7]

Extraction of ROIs [8]

Classification of ROIs [9]

Calculation of the co-occurrence matrix [10]

Identification of the five triangles and
computation of the geometrical
dimensions [11]

Classification of spasm/
no spasm events [12]

Generation of two datasets DS1 and DS2 [13]

Topology optimization and training of the NN for
the classification of the eye state (open/closed) [14]

Topology optimization and training of the NN for
the classification of the spasm/no spasm event [15]

Assessment of the optimized neural networks in
the last two minutes of the clinical test [16]

Generation of two datasets DDSS1 and DDSS2 [17]

Computation of the arrays A_{spasm} and $A_{eye-state}$ [18]

Differentiation between blinks, brief and prolonged
spasms [19]

Validation of the software [20]

sensitivity (SE) [21]
specificity (SP)

Figure 39 - Schematic of the steps followed to develop and validate the proposed software

(A) Face detector algorithm. For each of the acquired frames (during the clinical test, Figure 39, Blocks [1], [2] and [3]), the face detector algorithm, which is based on the traditional Histogram of Oriented Gradients (HOG) feature combined with a linear classifier, and a sliding window detection scheme, identifies the bounding box in which the patient's head can be inscribed (Figure 39, Block [4]). Preliminary analyses revealed that the face detector is significantly robust with respect to variable head movement and variable lighting conditions during the video recording. For each of the recruited patients, the percentage of frames εFD, in which the face detector algorithm is capable of reliably identifying the face of the patient, is computed, - with respect to the total number of frames acquired for the same patient -. The average value of εFD computed over all the patients is 99.960 % whereas the lowest one resulted in 99.948 %. Table 15 lists, for each patient, the number of frames acquired during the last (about) two minutes of the clinical test, (i.e. in the time interval where the patient remains at rest with the eyes open and fixing a point) and the corresponding value of εFD.

Table 15 - Values obtained for εFD, the percentage of video frames where the face of the patient is detected with the face detector algorithm

Patient	Total number of analysed video-frames	Number of video-frames in which the patient's head is detected	εFD
P1	3897	3897	100.000
P2	3927	3925	99.949
P3	3927	3925	99.949
P4	3837	3835	99.948
P5	3867	3865	99.948
P6	3897	3895	99.949
P7	3927	3926	99.974
P8	3867	3865	99.948
P9	3897	3896	99.974
Average			99.960

(B) Face pose estimator algorithm. The face pose estimator detects the position of 68 facial landmarks distributed in different points of the patient's face, such as the edges of the mouth, the eyes, the eyebrows, the nose, etc. (Figure 39, Block [5]; Fig. 4 (a)). In detail, the pose estimator algorithm first identifies the position of specific face points that allow defining the principal facial features, then predicts the location of the 68 facial landmarks in real-time [304]. The pose estimator is created by using dlib's implementation of the study in [304] and trained on the iBUG 300-W face landmark dataset [305].

The two above described algorithms were implemented to process the video frames acquired from all the patients. For each of the analysed frames, first the face of the patient is detected via the face detector algorithm, then the location of the 68 facial landmarks through the face pose estimator. Preliminary analyses revealed that, after a training phase, the face pose estimator algorithm is always capable of identifying the location of all the 68 landmarks in all the videos recorded. However, due to head

movements and variable lighting conditions, the face pose estimator sometimes could not predict the location of some facial landmarks (Figure 40(b)) correctly.
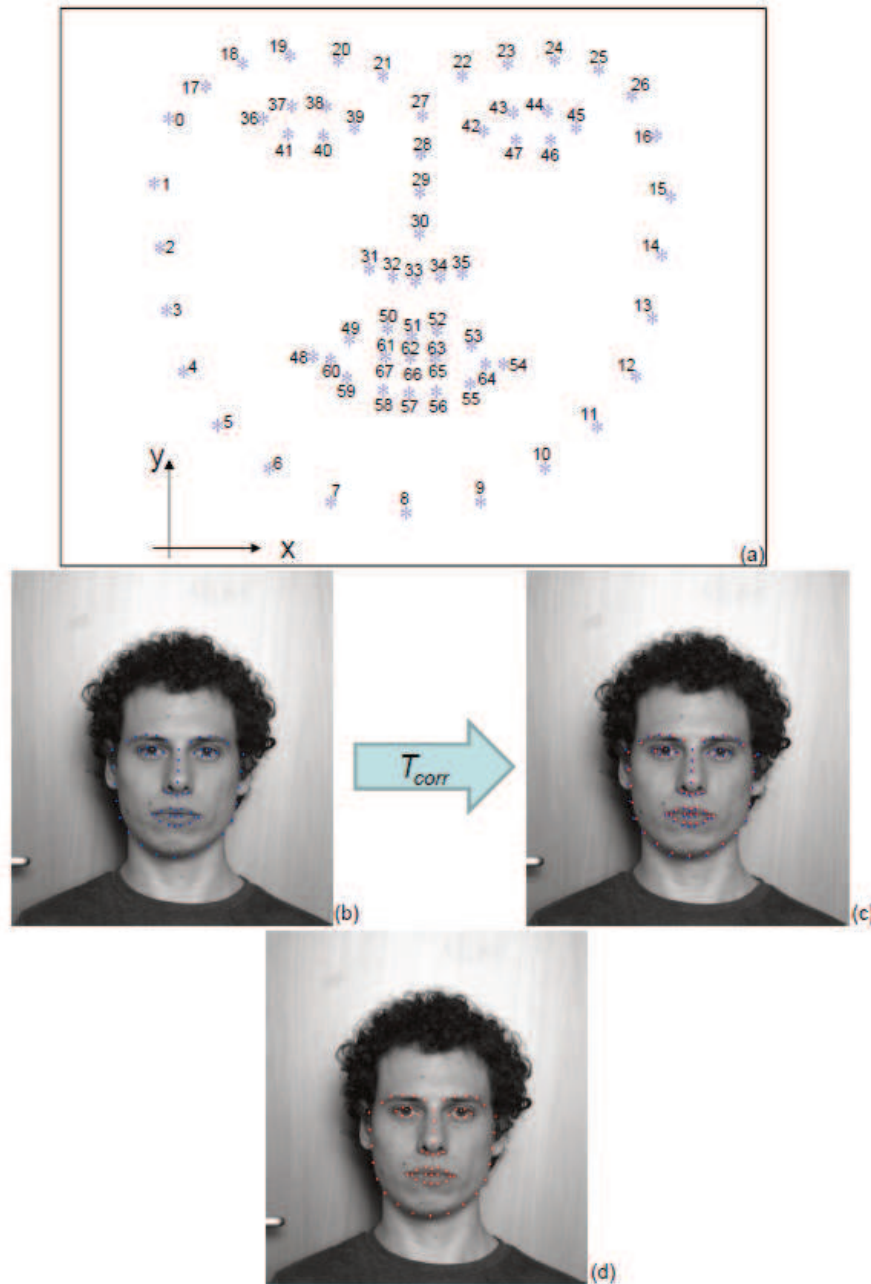
Figure 40 - (a) Schematic of the 68 facial landmarks placed by the face pose estimator algorithm. Implementation of the algorithm on one of the acquired frames before (b) and after (c) applying the correction tool Tcorr. The final results of the implementation of Tcorr tool (d) is represented by more stable and more correctly positioned facial landmarks. The red and blue points represent the facial landmarks correctly and not correctly positioned, respectively.

A correction tool Tcorr is hence developed that allows the re-training of the pose estimator utilizing the facial landmarks correctly re-located (Figure 39, Block [6]). The core of Tcorr is imglab: a dlib simple graphical tool for annotating images with object bounding boxes and optionally their part locations. Tcorr requires the clinician to choose a random number of frames, - at least thirty,- recorded during the first three minutes of the clinical test, retracting the patient with the eyes in several states (eyes closed during a spasm, eyes closed during a blink and eyes open). For each frame, the

clinician can drag and drop, in a correct position, all the facial landmarks not correctly positioned. Implementing Tcorr led to a better face pose estimator algorithm re-training thus making it capable of predicting with higher accuracy the location of the 68 facial landmarks (Figure 39, Block [7]; Figure 40(b), (c) and (d)).

To detect the BSP symptoms, an algorithm is developed to crop the Region of Interest (ROI) around the eyes of each patient. To do this, specific facial landmarks predicted with the facial pose estimator algorithm is utilized to define the rectangular bounding box delimiting each eye (Figure 39, Block [8]). Concerning the right eye, the points 36 and 39 were utilized to determine the horizontal dimension of the rectangle (Figure 41).
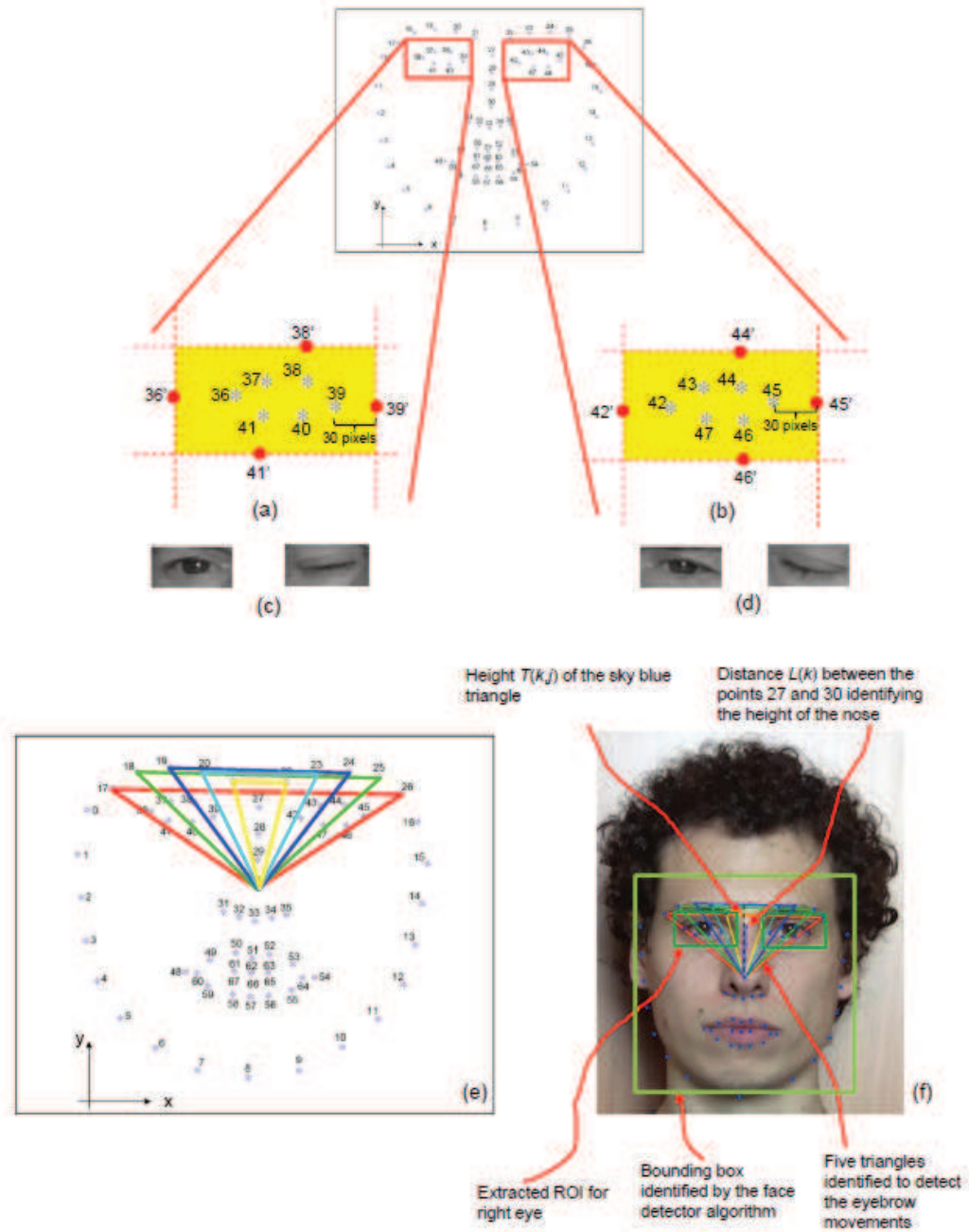
Figure 41 - (a) Regions of Interest (ROIs) extracted around the right (a) and the left (b) eye. Examples of ROIs extracted for the right (open and closed) (c) and the left (open and closed) (d) eyes. The five triangles - with one of the vertices on the tip of the nose and the others defined by the facial landmarks located on eyebrows – identified (on the schematic € and on the face of the patient (f)) to detect the eyebrow movements.

In detail, the horizontal dimension of the ROI goes from the point 36' placed 30 pixels at the left of point 36 to the point 39' placed 30 pixels at the right of point 39 (Figure 41(a)). The vertical dimension of the rectangle is defined through the points 38 and 41. Again, 30 pixels are added above and below the points 38 and 41, respectively, thus identifying 38' and 41'. The same procedure as that adopted for the right eye is also utilized for the left eye (Figure 41(b)). The points utilized to define the horizontal and the vertical dimension of ROI are, in this case: 42 and 45; 44 and 46, respectively, to which a 30-pixel padding margin is added, as for the case of the right eye. For each video frame, two ROIs were extracted, - one for each eyes-, resized to 64×32 pixels and saved in grey scale. In general, the dimension of each extracted ROI depends on the eye size and therefore is patient-dependent. The resizing procedure allows having all the ROIs with the same dimensions, which is an essential requirement for the successive computation procedures described below.

The algorithm to crop the ROI frame by frame was implemented on the video registered from all the patients during the first three minutes of the clinical test, i.e., in the time interval where the clinician asks the patient to perform some tasks and deeply observes her/his "response". Two folders are then created, one to gather the ROIs with open eyes, the other, the ROIs with closed eyes (Figure 39, Block [9]; Figure 41 (c) and (d)). Then, the same neurologist that assessed the severity index SIn (according to the BSRS scale) of the recruited patients manually classified/labelled the obtained ROIs moving each one in the correct folder. It is worthy to note that, although this classification must be done for all the ROIs extracted, the described procedure is rather easy to accomplish and requires a relatively small amount of time. In the first three minutes of the clinical test, the patient gently or forcefully closes the eyes; most of the frames (and hence ROIs) with open (or closed) eyes are close in time, and therefore it is rather easy, for the neurologist, to gather frames with the same eye state. For all the ROIs extracted and labelled, the co-occurrence matrices of oriented gradients were computed for the classification of the eye state (Figure 39, Block [10]). Indeed, the typical descriptive feature implemented in computer vision for the eye state classification is represented by the histogram of oriented gradients (HOG), which is a useful and commonly utilized tool suffering from the limit of local gradient information. The co-occurrence matrix of oriented gradients is proved to enhance the capability to describe the global gradient information of eye images thus allowing to classify with higher accuracy, - compared to the classical HOG -, the eye state[306]. This matrix is a 4D array with dimensions levels-of-grey × levels-of-grey × number-of-distances × number-of-angles. The value that the co-occurrence matrix assumes for example at the coordinates xx, yy, zz and ww is the number of times the grey level yy is present at the distance zz and at the angle ww starting from the grey level xx. Following the study reported in [306], a number of grey levels equal to 8, a distance equal to 1 pixel (hence, the number of distances is 1) and an angle equal to 0 radians (therefore, the number of angles is 1 are fixed. Therefore, the dimensions of the computed co-occurrence matrices, - which represent the number of features that will be given in input to the artificial neural network described below-, are: $8 \times 8 \times 1 \times 1$ for a total number of features nFeye-state equal to nFeye-state = 64.

In order to detect the eyebrow movements related to the spasm events, an algorithm is developed that measures the height of the five triangles with one of the vertices on the tip of the nose (i.e. the point 30) and the others defined by the pairs of facial landmarks symmetric with respect to the sagittal plane and located on the eyebrows (Figure 39, Block [11]; Figure 41 (e) and (f)). In detail, to avoid sudden changes of the height of the triangle due to possible rotations of the patient's head, the height of the triangles was normalized with respect to that of the nose, that is the distance between the points 27

and 30 (Figure 41(f)). For each acquired frame k, the normalized height Y(k,j) of the j_{th} triangle (j=1, 2, ..., 5), the average normalized height value $\bar{Y}(k)$ and the standard deviation $\sigma(Y(k))$ were computed as:

$$
\begin{cases}
Y(k,j) = \dfrac{T(k,j)}{L(k)} & j = 1, 2, \dots, 5 \\[2ex]
\bar{Y}(k) = \dfrac{1}{5} \displaystyle\sum_{j=1}^{5} Y(k,j) \\[2ex]
\sigma(Y(k)) = \sqrt{\dfrac{\sum_{j=1}^{5}[Y(k,j) - \bar{Y}(k)]^2}{5}}
\end{cases}
$$

where, T(k,j) is the eight of the j_{th} triangle, and L(k) is the distance between the points 27 and 30. Figure 42 and Figure 43 show the average normalized height of triangles $\bar{Y}(k)$ typically registered during a blink and a spasm, respectively.
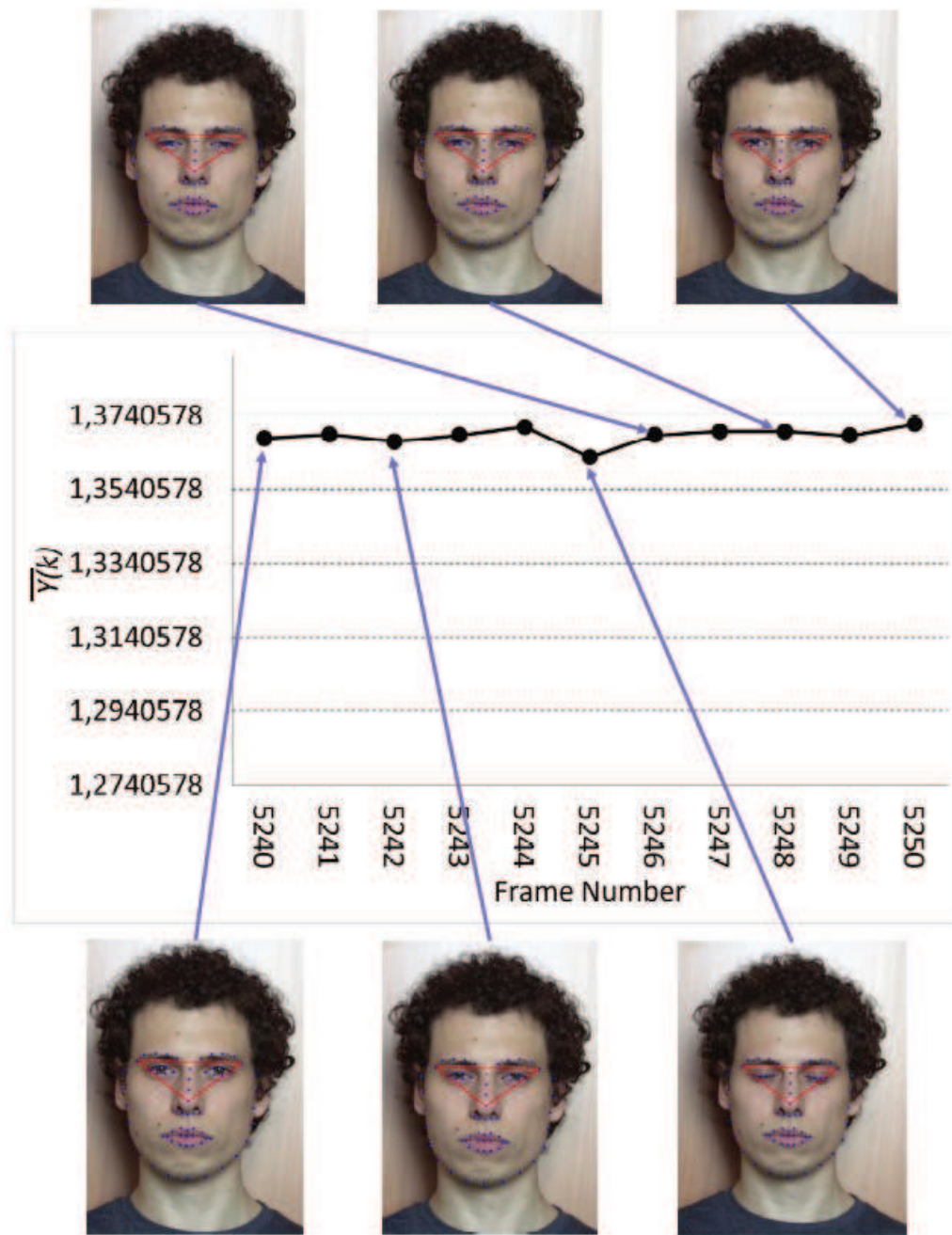
Figure 42 - Typical values of the average normalised height $\bar{Y}(k)$ of triangles registered during a blink
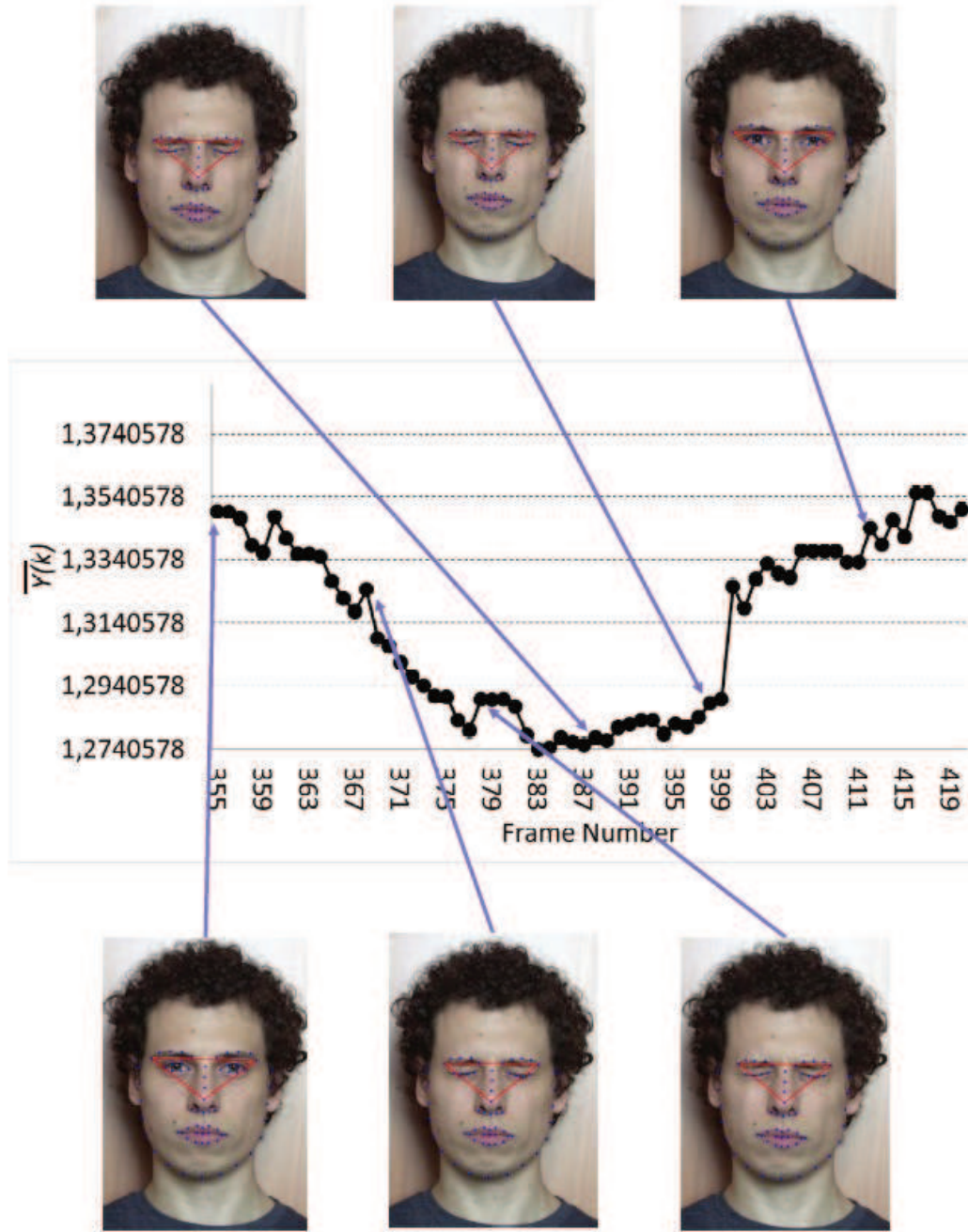
Figure 43 - Typical values of the average normalised height $\bar{Y}(k)$ of triangles registered during a spasm

It is interesting to see how in case of blinking (Figure 42) the average height of the triangles remains practically constant, whereas a large decrease of $\bar{Y}(k)$ occurs during a spasm (Figure 43).

Therefore, the number of features nFspasm, - given in input to the artificial network described below - is, nFspasm = 7, i.e., the five normalized heights Y(k,j), the average normalized height $\bar{Y}(k)$ and the standard deviation σ(Y(k)). Also in this case, two folders were created, 'Spasms' and 'No spasms' (Figure 39, Block [12]). All the frames acquired in the step (ii) (in which the patient is asked to voluntarily and forcefully close and open the eyes 5 times) where the patient's eyes are closed are labelled as 'spasm'; on the contrary, the frames acquired before or after step (ii) with the patient's eyes open are labelled as 'no spasm'. It is worthy to note that, for how it is defined, the spasm

event requires the eyes being closed, which is the reason why the frames (acquired during the step (ii)) where the eyes are closed are classified as 'spasms'. The strategy of including in the folder 'No spasms' the frames with open eyes is justified by the fact that when the patient has the eyes open certainly the height of the five triangles does not change in time (which is the basic requirement for having the 'no spasm' event). For instance, preliminary analyses revealed that considering the step (iv) where patients are asked to voluntarily and gently close and open the eyes five times, -practically, this is sort of simulation of a blink-, the height of triangles can change even significantly. Some patients, in fact, due to the pathology, are not able to "gently" close and open the eyes and, having difficulties in re-opening the eyes, often moved the eyebrows. To avoid these issues, in the folder 'No spasms' the only frames recorded in the first three minutes of the clinical test with the eyes open are included.

Two Datasets (DS) were finally generated (Figure 39, Block [13]): the first dataset DS1 including 30160 entries and regarding the classification of the eye state (in detail, 16576 entries were labelled as 'closed eyes' and 13584 as 'open eyes'); the second dataset DS2 including 11266 entries and regarding the classification spasm/no spasm events (4474 entries were labelled as 'spasm', the remaining 6792 as 'no spasm'). It is worthy to note that, for each video frame, two entries can be obtained regarding the classification of the eye state, - one entry for each extracted ROI -, and one entry regarding the classification spasm/no spasm events. Each entry of DS1, in turn, includes nFeye-state = 64 features, while each entry of DS2, includes nFspasm = 7 features. Table 16 lists, for each patient, the number of entries obtained for each of the two datasets.

Table 16 - Entries obtained from each patient and given in input to the neural network

Patient	Entries 'closed eyes.'	Entries 'open eyes.'	Entries 'spasm.'	Dataset eye state: Total entries 'closed eyes' + 'open eyes'	Dataset spasm/no spasm: Total entries 'spasm' + 'open eyes'
P1	2666	1950	978	4616	1953
P2	1544	1634	421	3178	1238
P3	2930	848	788	3778	1212
P4	1666	2112	785	3778	1841
P5	2634	784	341	3418	733
P6	1162	1596	301	2758	1099
P7	1068	1750	279	2818	1154
P8	1736	1022	325	2758	836
P9	1170	1888	256	3058	1200
				30160	11266

The two data sets DS1 and DS2 are given as input to Artificial Neural Networks (ANNs), which are models constituted by a large number of processing units (neurons), used to solve specific classification or patterns recognition problems. Thanks to their capability "to learn" the hidden relationships between the input pattern and the output target, ANNs have been widely used to solve problems in different fields, from medical to control and manufacturing.

ANNs are utilized to classify the blinks automatically, the brief and prolonged spasms observed in the nine recruited patients with BSP (Figure 39, Blocks [14] and [15]). The training algorithm chosen for weights (W, Figure 44) and bias (b, Figure 44) update is the resilient backpropagation algorithm [307].
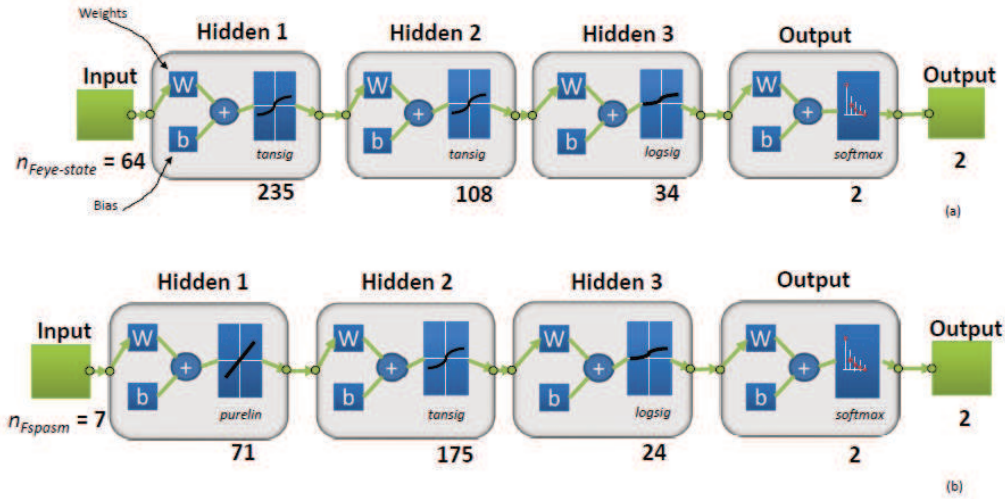
Figure 44 - Neural networks with optimised topology utilised to classify the eye state (a) (open or closed) and the spasm and the no spasm event (b)

The parameters utilised in the genetic algorithm are: an initial population with 100 individuals randomly generated, where, each individual corresponds, practically, to a candidate ANN topology; crossover with 2 points, with a probability of 0.8; mutation with a probability of 0.2; selection system: elitism.

In this case, the number of iterations is set to nIT = 200. Training, validation and test datasets were obtained from the two input datasets (i.e., DS1 and DS2); in detail, 60% of the samples are utilised for training, 20% for validation and 20% for the test.

The genetic algorithm previously described is implemented to determine the optimal topology of two artificial neural networks: the ANN for the classification of the eye state and the ANN for the classification of the spasm/no spasm events. The optimal ANN topology computed by the genetic algorithm for the eye state classifier included (Figure 44(a)) four layers with 235, 108, 34 and 2 neurons for the first hidden, the second hidden, the third hidden and the output layer, respectively. Furthermore, the genetic algorithm found the following activation functions: tansig for the first and the second hidden layer, logsig for the third hidden layer. For the output layer, as stated above, the softmax function is utilized. Concerning the optimal topology of the neural network for the classification of the spasm/no spasm event, it included four layers with (Figure 44(b)): 71, 175, 24 and 2 neurons for the first hidden, second hidden, third hidden and the output layer, respectively. The activation functions predicted by the genetic algorithm are purelin, tansig and logsig, for the first, the second and the third hidden layer, respectively. Again, softmax is utilized for the output layer.

The average values of accuracy (ACC), specificity (SSPP) and sensitivity (SSEE) with the standard deviations computed over the nIT = 200 iterations for the optimal ANN topologies are listed in Table 17.

Table 17 - Values of av_ACC, av_SSPP and av_SSEE computed ver the nIT = 200 iterations for the optimal ANN topologies

	Eye state	Spasm/no spasm event
av_ACC ± std	0.9641 ± 0.0015	0.9290 ± 0.0051
av_SSPP ± std	0.9643 ± 0.0002	0.9507 ± 0.0007
av_SSEE ± std	0.9637 ± 0.0026	0.8743 ± 0.0136

The assessment of the two optimized neural networks is performed with the frames acquired in the last two minutes of the clinical test when patients are asked to remain at rest with the eyes open and staring at a specific point located in front of them (Figure 39, Block [16]). For each acquired frame, the ROIs are cropped, the co-occurrence matrix is computed, and the heights of the five triangles are identified.

In detail, two different Datasets (DDSS) are created (Figure 39, Block [17]): the first dataset DDSS1 is given in input to the neural network for the classification of the eye state, the second DDSS2 to the neural network for the classification of the spasm/no spasm events. DDSS1 includes a number of entries equal to twice the number of frames acquired in the two minutes (for each frame, in fact, two ROIs can be extracted), DDSS2, the number of frames acquired in the two minutes. Again, each entry of DDSS1 includes nFeye-state = 64 features (i.e., the dimensions of the co-occurrence matrix), whereas each entry of DDSS2 includes nFspasm = 7 features (i.e., the number of triangle heights considered). Then, the following workflow is implemented:

- Giving in input DDSS1 to the first optimized neural network for the classification of the eye state, the frames containing closed eyes are first identified. Then, for each frame, the co-occurrence matrix, for both the right and the left eye, is computed. However, if one of the two co-occurrence matrices is predicted to be 'closed eye', the other one is automatically hypothesized to be 'closed eye'. This is because the BSP is focal dystonia with bilateral and synchronous symptoms that simultaneously affect the right and the left eyes [308–310]. Therefore, the output of this first classification is an array Aeye-state, - with the length equal to the number of frames acquired in the two minutes of the clinical tests, assuming, for each frame number, one of the following possible values: 0 in the case of open eyes and 1 in the case of closed eyes (Figure 39, Block [18]; Figure 45).
- Giving in input DDSS2 to the second optimized neural network, the frames where a lowering of the eyebrows takes place, are detected. The output of this second classification is an array Aspasm, with the same length of the previous array, which assumes, for each frame, one of the two possible values: 1 if an eyebrow narrowing occurs, 0 otherwise (Figure 39, Block [18]; Figure 45).
- Finally, the spasms from the blinks are distinguished. It is worthy to note that the requirements for a symptom to be classified as spasm are the eyes closure, the lowering of the eyebrows and a duration of at least 300 ms, which corresponds to the time necessary to acquire about 10 frames with the camera utilized to video record the patients. A symptom with a duration shorter than this cannot be classified as a spasm but as a blink [311]. Furthermore, as stated above, a spasm lasting less than 3 s (i.e., the time to acquire about 100 frames) must be classified as brief spasm, or as a prolonged spasm if its duration is longer than this time. Therefore, the frames where Aeye-state assumes the value 1 (i.e. 'eyes closed') are considered and, in correspondence of these frames, the values of Aspasm are observed too. If a set of less than 10 consecutive frames (i.e. a set with a number of consecutive

frames nc-frames < 10) is characterized by Aeye-state = Aspasm = 1, then the entire set is classified as a blink. Instead, if a set includes more than 10 and less than 100 consecutive frames (i.e. $10 \leq$ nc-frames <100) with Aeye-state = Aspasm = 1, then the set is classified as brief spasm. If the condition Aeye-state = Aspasm = 1 is satisfied for a number of consecutive frames greater than 100 (i.e. $100 \leq$ nc-frames), then the set is classified as prolonged spasm. Finally, all the sets of consecutive frames with Aeye-state = 1 & Aspasm = 0, are classified as blink (Figure 39, Block [19]; Figure 45).
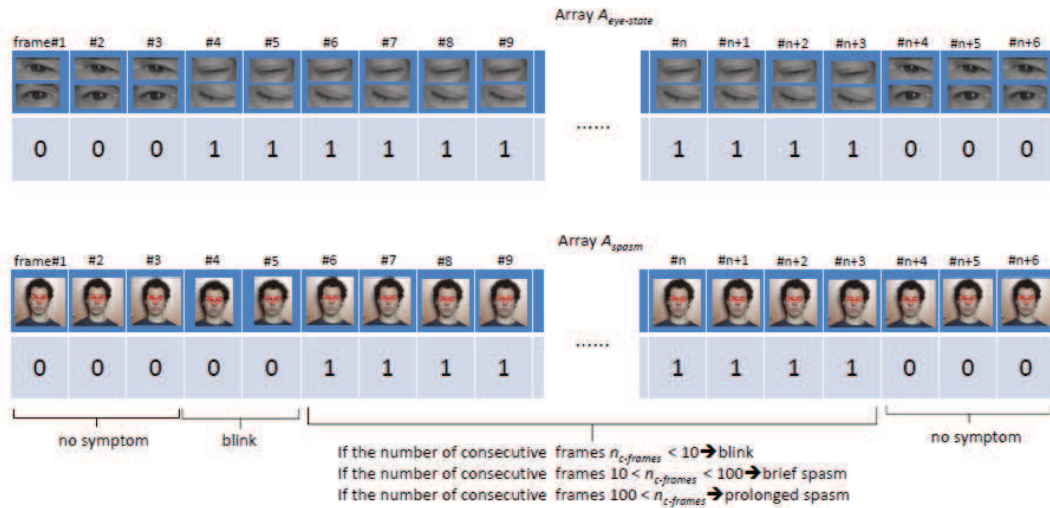
Figure 45 - Giving in input the datasets DDSS1 and DDSS2 to the two optimised and trained neural networks, two arrays are computed: Aeye-state and Aspasm. Comparing the values assumed by Aeye-state and Aspasm the blepharospasm symptoms are classified

Validation procedure.

The last two minutes of the videos registered for the nine patients during the clinical test ARE segmented via the developed software into a number of clips lasting 10 to 20 s. Each clip IS trimmed to include just one of the following symptoms/events: brief spasm, prolonged spam, blink and no involuntary eye closure (Figure 39, Block [20]). Four folders are then created and named: Blinks, Brief_spasms, Blinks+brief_spasms, Prolonged_spasms which included, each, the clips reproducing the symptom corresponding to the name of the folder. Furthermore, in the four folders, clips detected by the software and reproducing no involuntary eye closure are also included. Therefore, for instance, the folder Blinks included all the clips detected by the software and reproducing blinks as well as some of those reproducing no involuntary eye closures. Similarly, the folder Blinks+brief_spasms included the clips reproducing brief spasms, those reproducing the blinks and, finally, some of those reproducing no involuntary eye closures. These folders are then given to the expert neurologist that watched all the video clips, thus identifying the specific reproduced symptoms. The sensitivity SE and the specificity SP (Figure 39, Block [21]) of the software are then assessed. In detail, regarding the folder Blinks, if ns is the number of clips identified by the software and reproducing blinks, nn the number of clips identified by the neurologist and reproducing the same symptom, then the sensitivity is given by the ratio SE = nn/ns×100. The same procedure is adopted to compute values of SE related to the other symptoms. Similarly, with reference to the folder Blinks, if nas is the number of clips detected by the software as reproducing no blink symptoms and nans the correspondent number determined by

the neurologist, then the specificity SP is given by SP = nas/nans×100. The same procedure is followed in assessing the specificity SP related to the other symptoms.

3.2.4.2 Innovative Results

The values of SE and SP computed for each detected symptoms are diagrammed in Figure 46.
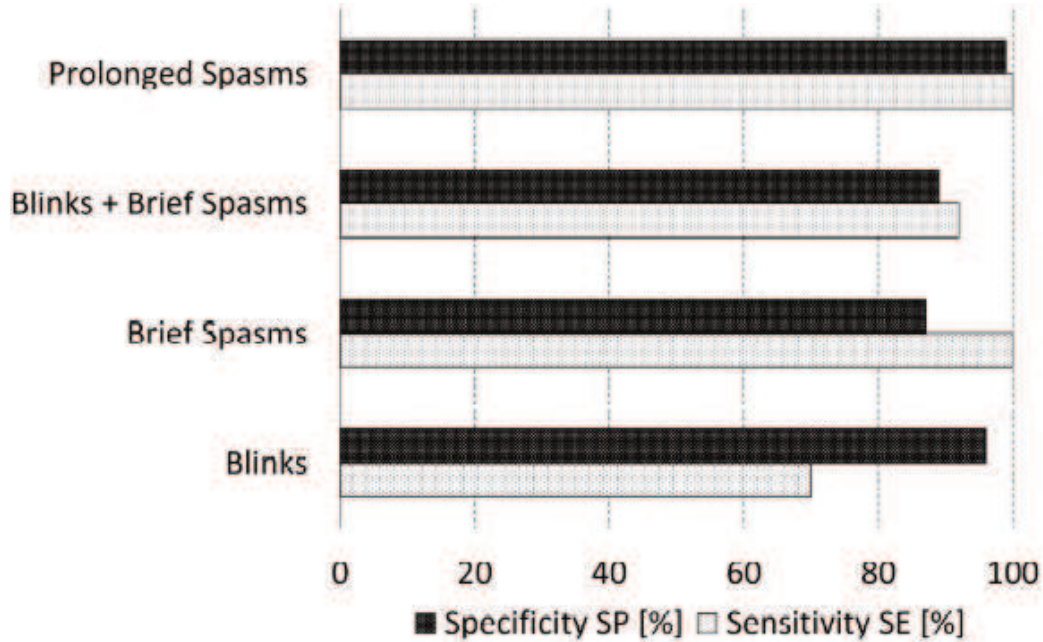
Figure 46 - Values of sensitivity SE and specificity SP obtained with the proposed software for the different investigated symptoms

The sensitivity SE of the software is excellent for prolonged spasms and satisfactory for brief spasms (Figure 46). Smaller values of sensitivity are, instead, found in the case of blinks; a confusion related to the imperceptible difference between blinks and brief spasms is probably responsible for this result. A proof of this is given by the satisfactory level of sensitivity computed in the case blinks, and brief spasms are combined in the same folder. The high levels of specificity SP demonstrate the capability of the proposed software to distinguish the non-pathologic conditions.

The clinimetric properties of the proposed software are assessed as well. In detail, for each patient, all the frames, - recorded in the last two minutes of the clinical test - where the eyes are closed, are considered. Therefore, to determine the percentage of closure time for the investigated symptoms, the frames (with closed eyes) are distinguished depending on the symptom and counted. If fblink, fbsp, fpsp is the number of frames reproducing blinks, brief spasms, prolonged spasms, respectively, and ftot the total number of frames registered in the last two minutes, the percentages of closure time for blinks tblink, brief spasms tbsp and prolonged spasms tpsp can be computed as follows:

$$\begin{cases} t_{blink} = \dfrac{f_{blink}}{f_{tot}} \times 100 \\ t_{bsp} = \dfrac{f_{bsp}}{f_{tot}} \times 100 \\ t_{psp} = \dfrac{f_{psp}}{f_{tot}} \times 100 \end{cases}$$

The values of percentage of closure time are computed for all the patients and put in correlation with the severity index values SIn evaluated by the expert neurologist according to the Blepharospasm Severity Rating Scale (BSRS) scale (Figure 47(a)).
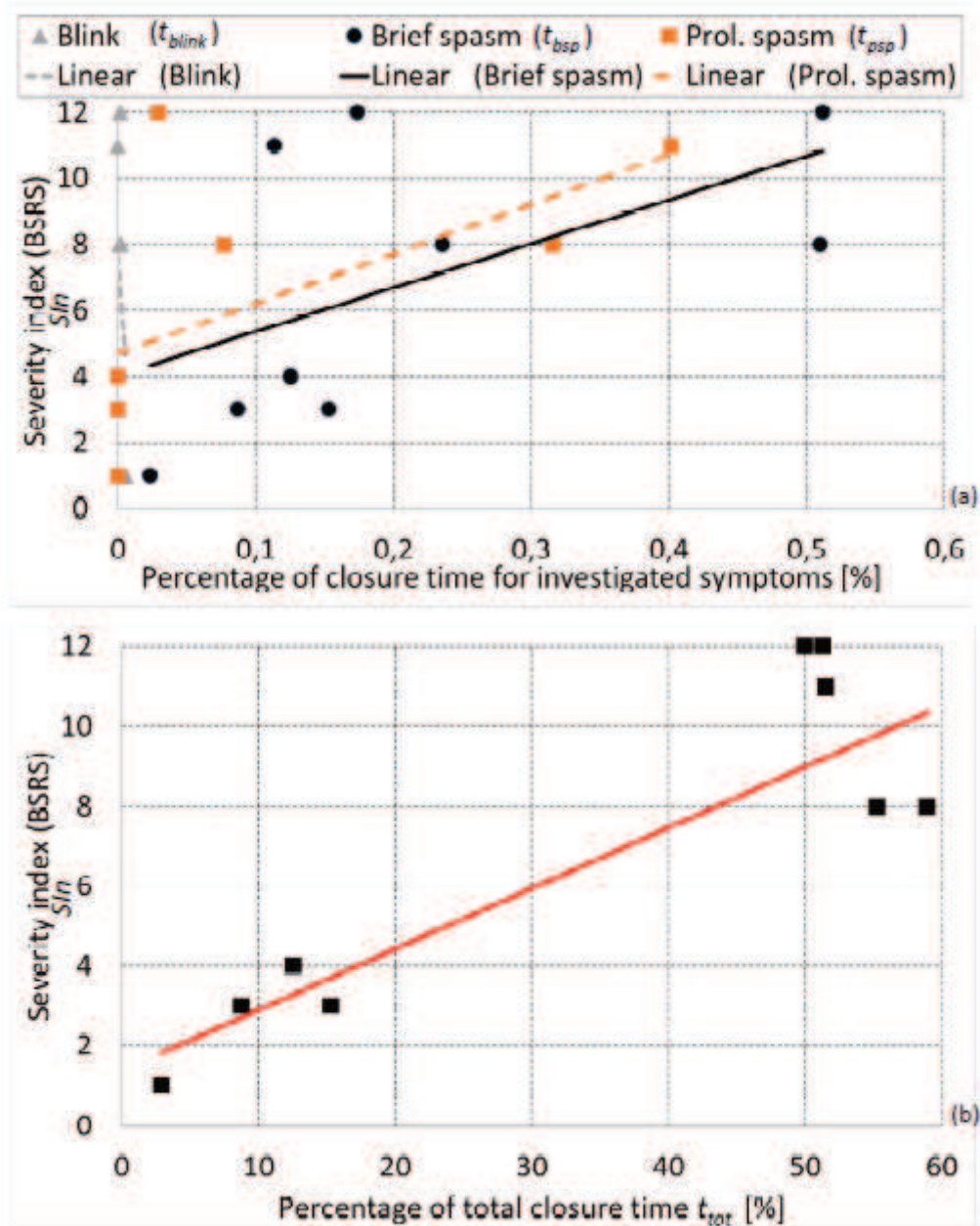
Figure 47 - Correlation between (a) the severity index SIn, determined by the expert neurologist and the percentages of closure times for the investigated symptoms; (b) the severity index SIn determined by the expert neurologist and the total closure time

The blepharospasm severity rating scale includes 6 items [302] to each of which a score S must be assigned.

Item A1 concerns the type of eyelid spasm occurring in the patient.

- If brief spasm (duration < 3 sec) with complete rim closure take place - score $S(A1) = 1$;
- If prolonged spasm (duration ≥3 sec) with partial rim closure take place - score $S(A1) = 2$;

- If prolonged spasm (duration ≥3 sec) with complete rim closure take place - score S(A1) = 3.

Item A2 concerns the apraxia of eyelid opening.

- If apraxia is present - score S(A2) = 2;
- If apraxia is absent - score S(A2) = 0;

Item A3 concerns the spasms occurring during the writing of the stereotyped sentence.

- If the spasms of the orbicularis oculi occur - score S(A3) = 1
- If the spasms of the orbicularis oculi do not occur - S(A3) = 0;

Item A4 concerns the average duration of the prolonged spasms.

- If the average duration is 3 to 4-sec - score S(A4) = 1;
- If the average duration is 3.1 to 5-sec - score S(A4) = 2;
- If the average duration is larger than 5-sec - score S(A4) = 3;

Item B1 regards the frequency of blinks + brief spasms.

- If 1 to 18 blinks + brief spasms take place per minute - score S(B1) = 1;
- If 19 to 32 blinks + brief spasms take place per minute - score S(B1) = 2;
- If more than 32 blinks + brief spasms take place per minute - score S(B1) = 3;

Item B2 regards the frequency of prolonged spasms.

- If 1 to 3 prolonged spasms take place per minute - score S(B2) = 1;
- If 3.1 to 7 prolonged spasms take place per minute - score S(B2) = 2;
- If more than 7 prolonged spasms take place per minute - score S(B2) = 3.

The total score is given by the sum:

$$SIn = S(A1) + S(A2) + S(A3) + S(A4) + S(B1) + S(B2)$$

For how the software was designed, it is not capable of evaluating the Items A2 and A3. Therefore, the measurable severity index SIn_m, that can be automatically determined by the software is given by:

$$SIn\_m = S(A1) + S(A4) + S(B1) + S(B2)$$

Interestingly, high Spearman correlation coefficients are computed for a brief (Spearman rho 0.684, p-value 0.042) and prolonged (Spearman rho 0.783, p-value 0.022) spasms. A very low correlation coefficient is instead found in the case of the blinks (p-value n.s.), which indicates that no clear correlation exists between tblink and the severity index SIn values. In reality, it is worthy to note that the severity index values. SIn reported in the diagram, take into account, in addition to blinks, also other symptoms. Considering that the weight that blinks have on this severity scale is very small compared to the weight of the other symptoms (practically, the only item B1 partially depends on the number of blinks) one can understand that blinks only in a very marginal way affect the severity index values, which justifies the absence of correlation.

The values of the severity index (BSRS) are put in correlation also with the percentage of total closure time. If ftotce is the total number of frames registered in the last two minutes of the clinical tests and characterized from having closed eyes, the percentage of total closure time ttot can be computed as:

$$t_{tot} = \frac{f_{totce}}{f_{tot}} \times 100$$

The values of the severity index (BSRS) are diagrammed in function of ttot; a linear regression line is also included in the diagram (Figure 47(b)). A significant correlation coefficient is found between the severity index SIn values and ttot (Spearman rho 0.735, p-value 0.038).

It is worthy to note that the proposed software is not capable of evaluating the index severity values SIn according to the Blepharospasm Severity Rating Scale (BSRS). The BSRS scale, in fact, includes 6 items, to each of which a score S must be assigned according to specific criteria. Among the others, the BSRS includes the item A2 that regards the apraxia of eyelid opening and the item A3 that concerns the spasms occurring during the writing of the stereotyped sentence (i.e. the step (viii)). For how the system is designed, it is not capable of assigning a score for the items A2 and A3. However, considering the only 'measurable' items, and summing up the scores given to each of the measurable items, the software gives in output values of (measurable) severity index SIn_m that are consistent with those correspondent determined by the expert neurologist (Spearman rho 0.863, p-value 0.003) (Figure 48).
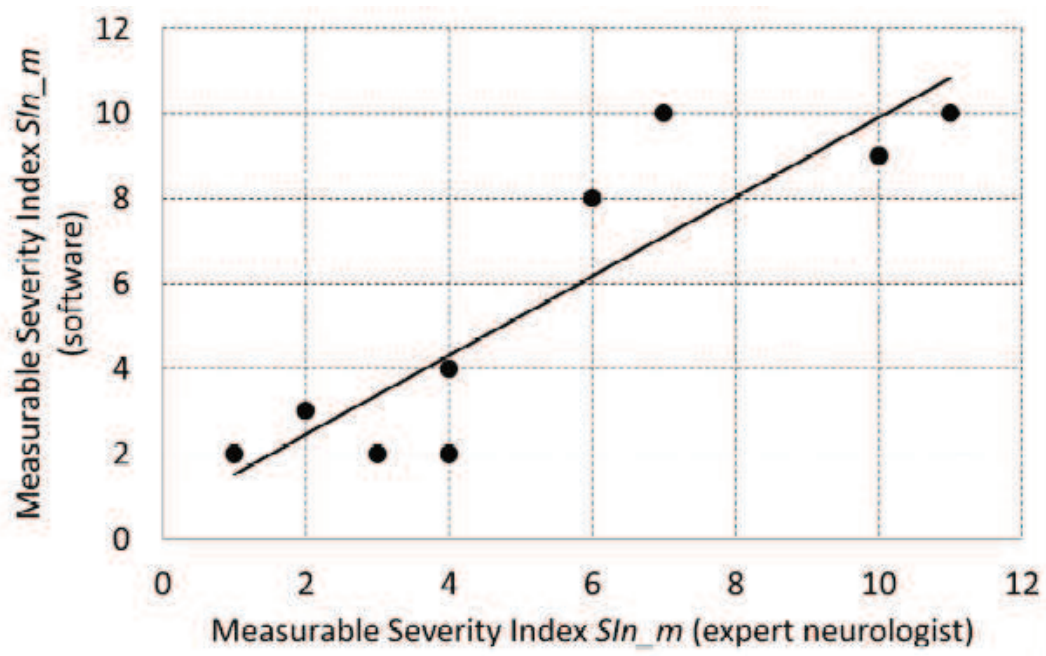
Figure 48 - Correlation between the measurable severity index SIn_m computed by the software and that determined by the expert neurologist

Significant values of the Spearman correlation coefficients can also be found considering the score -given to individual 'measurable' items -, computed by the software and the score determined by the expert neurologist (Table 18).

Table 18 - Spearman correlation coefficients between the scores (assigned to the different items) computed by the software and those determined by the expert neurologist

Item	Features	Spearman rho	p-value
A1	Type of eyelid spasm	0.793	0.019
A2	Apraxia of eyelid opening – Not measurable by the proposed software	---	---
A3	Spasms occurring during the writing of the stereotyped sentence – Not measurable by the proposed software	---	---
A4	The average duration of the prolonged spasms	0.806	0.009
B1	Frequency of blink + brief spasms	0.676	0.046
B2	Frequency of prolonged spasms	0.756	0.030
Total 'measurable' severity index SIn_m	SIn_m = S(A1) + S(A4) + S(B1) + S(B2)	0.863	0.003

The proposed software tool presents some limitations. First, while the software exhibits large values of sensitivity SE in distinguishing brief spasms, prolonged spasms and blinks + brief spasms, the values of SE computed for blinks are, in reality, smaller. This can be justified by the argument that the software sometimes confuses blinks with brief spasms. However, it is worthy to note that the difference between the symptom of the blink and the symptom of the brief spasm is subtle and, as often occurs in the clinical practice, the task of distinguishing the two symptoms is complex to be accomplished even for the neurologist. This is true especially in the case the brief spasms have a duration close to the threshold value of 300 ms [311] which represents, de facto, the time duration that distinguishes the brief spams from the blinks. During the clinical evaluation, the neurologist does not measure the time physically and hence can do the 'error' of confusing the two symptoms. The proposed software, instead, taking into account the exact number of frames included in the set reproducing the symptom under investigation can measure the time with an accuracy of about 0.03 s. Furthermore, the distinction of blepharospasm symptoms is often subtle and imperceptible. It is commonly known, in fact, that different expert neurologists can assign different severity index SIn values to the same patients. Further investigations should be carried out on this topic.

The second limitation of the study is represented by the time necessary to implement the software on the specific patient, which includes: 1) the time necessary to utilize the correction tool Tcorr (where the neurologist has to drag and drop the incorrect facial landmarks on about thirty acquired frames); 2) the time necessary to re-train the face pose estimator after implementing Tcorr; 3) the time necessary to extract, from the acquired frames, all the entries to give in input to the neural networks. Preliminary investigations revealed that for an experienced neurologist all these tasks require approximately and averagely 30 minutes. However, considering that an experienced neurologist spends about 60-90 minutes per patient to observe all the acquired video clips, one can conclude that implementing the software allows saving more than 0.5 hours of time per patient. Furthermore, it is worthy to note that the proposed software is not conceived to 'replace' the neurologist but to 'assist/support' her/him in the procedures of the

definition of the BSP severity. From this point of view, the limitation of the time necessary to implement the software is relatively relevant and is abundantly counterbalanced by the important advantage to make objective the process of evaluating the BSP symptoms.

The third limitation of the study is the rather low acquisition frequency (about 30 frames per second) of the CCD camera utilized to video-record the clinical tests performed on the patients. Certainly, the use of CCD with higher acquisition frequency would allow following the facial movements taking place in BSP symptoms with higher detail.

Despite these limitations, a correlation exists between the total closure time ttot and the severity index values SIn (Figure 47), which is consistent with the results of Peterson et al. [312]. Furthermore, a very high level of εFD, the percentage of video frames where the face of the patient is detected with the face detector algorithm, is found. The lowest percentage of face-found frames was εFD = 99.948 % which is higher than that (93 %) found by Peterson et al. [312]. Furthermore, it is worthy to note that, currently the only computerized and automatic system capable of rating the blepharospasm severity is represented by the toolbox CERT [312] that is capable of measuring the eyes closure time but that cannot recognize and hence count the specific BSP symptoms. Finally, the implementation of Tcorr led to correctly determine the position of the facial landmarks, which allowed the definition of 'stable' triangles for the identification of the spasms.

3.2.5 Discussion and Conclusion

The proposed model of a Healthcare Network based on Big Data Analytics for Parkinson's and Blepharospasm's disease should be capable to transform the way healthcare providers use sophisticated technologies to gain insight from their clinical and other data repositories and make satisfying decisions. Moreover, the use of machine learning algorithms contextualized in the proposed Big Data System can support clinicians in their decisions and in monitoring the follow up of each patient's disease. In this paragraph the attention is focused on the design, development and evaluation of Decision Support Systems (DSS) that trained with data from different sources could support physicians and, in particular, neurologists. It is worthy to note that, this kind of healthcare network could be compared with an Industry 4.0 scenario applied to medicine. Whereas the (Medical) Cyber-Physical System consists of all the developed DSS, the IoT and IoS infrastructure consists of all the components that a network based on Big Data Analysis should have to improve the quality of service. The previous description is a description of an Industry 4.0 scenario that often is applied in the manufacturing field. However, nowadays, always more often this architecture is applied in different application fields in which, an intelligent services digitalisation supports the work of experts domain. Although this section is focused only on the implementation of DSS, in future, attention will be focused on issues such as guaranteeing privacy, safeguarding security, establishing standards and governance, thus improving tools and technologies always more. Therefore, the proposed Healthcare Network should be more accurately implemented, tested and validated.

3.3   CAD Frameworks in Diagnostic Examinations

In the last decades, the amount of deaths due to cancer has significantly increased, overcoming the number of deaths caused by heart attacks and stroke, as emphasized in the reports of the World Health Organization [313]. In detail, in several industrialized countries there are specific neoplasias with a high incidence, where an early non-invasive diagnosis and staging can luckily prevent bad prognosis in some of these cases. The three tumour forms considered have been evaluated among the top ten in the world for an estimated number of deaths [314]. This can be well noticed in Figure 49 where, in 2012, the amount of deaths for a liver tumour has been estimated at the second position all over the world, the amount of deaths for a breast tumour is at the fifth position, whereas the number of deaths due to leukaemia has the tenth value in the world.
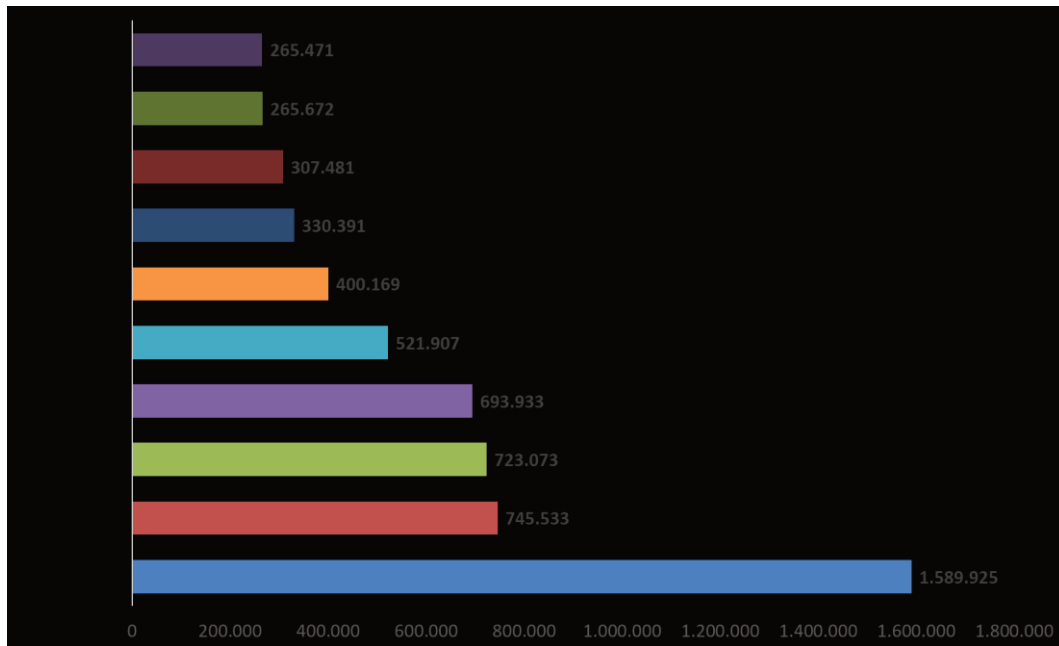
Figure 49 - Estimated number of deaths caused by tumours worldwide in 2012

On this proposal, a first basic concept can be pointed out: Image Diagnostics is a great choice for its high ability to stage the course of each of the considered three diseases, without being excessively invasive [315]. In detail by considering:

- breast cancer: (i) in tomosynthesis it is important to note that doses of ionizing radiation far below those released in the conventional Computed Tomography (CT) are released [316]; (ii) in Magnetic Resonance (MR) ionizing radiation is not considered [317];
- hepatocellular carcinoma (HCC): in CT with contrast medium, the contrast medium is very characteristic and therefore able to reduce the frequency of subsequent examinations [318];
- leukaemia: in the peripheral strips, the method of capturing the images is absolutely non-invasive because it requires only a blood draw [319].

Medical imaging is a fundamental methodology for representing the internal organs of the human body, allowing non-invasive and accurate diagnosis of several diseases, including neoplasias [320]. On this proposal, it should be pointed out that there are different imaging techniques able to highlight the characteristics of the human body, on the basis of the sensors used to acquire information and produce the representation of each internal organ. Moreover, beside the diagnostic capabilities, medical imaging is

also crucial for staging and monitoring the clinical course of each disease under investigation [321].

All the previously described advantages led the scientific community to study and develop a large number of automatic systems, based on medical imaging, with the aim of supporting physicians in diagnosing, staging and monitoring different pathologies. On this proposal, a large number of works focused on Computer Aided Diagnosis (CAD) systems can be found in the literature. Figure 50 shows the number of publications per year from 2006 to 2016 in the field of medical imaging, highlighting the popularity achieved by CAD systems in recent years.
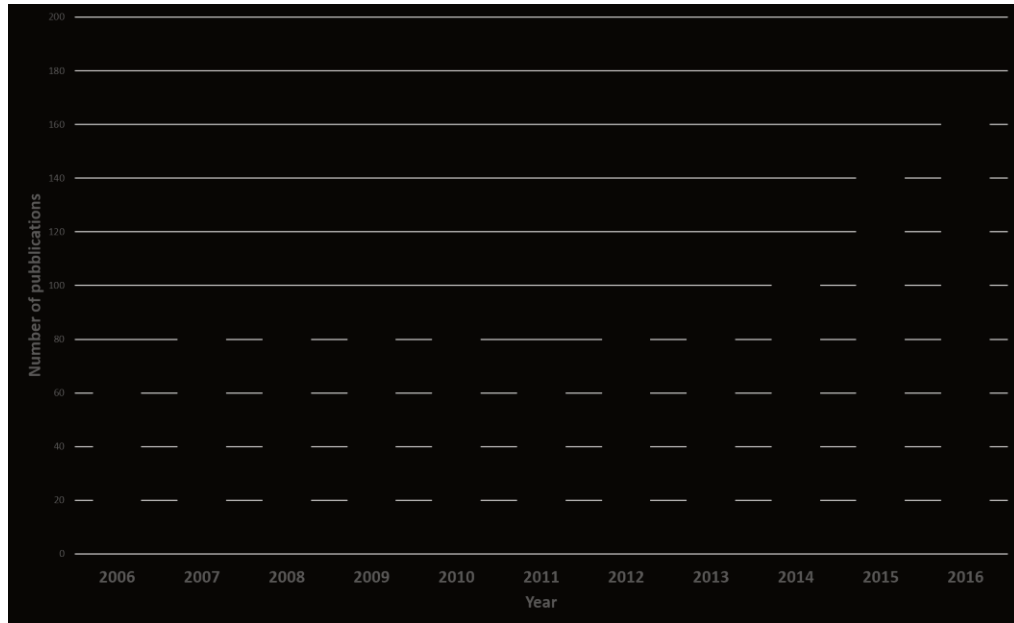
Figure 50 - Number of publications per year from 2006 to 2016. Topic: Computer-Aided Diagnosis & Medical Images.

In fact, as reported in [322], CAD systems can support clinicians in diagnosing, offering a cheap and suitable alternative to a double data reading, intended as a mean for reducing errors.

Standard workflow of Computer Assisted Frameworks

All the CAD systems based on medical imaging share an analogous workflow able to classify a particular tumour starting from an acquisition procedure, independently from the disease under investigation. The chain represented in Figure 51 shows the essential steps needed to perform the classification task.

Figure 51 - Traditional workflow implemented by CAD systems

It has to be noted that the pipeline is usually composed by the following four phases: (1) Image Acquisition, (2) Image Segmentation, (3) Features Extraction, (4) Classification.

Image acquisition. Thanks to the increasing availability of computational resources, new medical imaging technologies have been developed and commercialized during the last decades. Valuable tools, such as Computed Tomography, MR imaging, Digital Subtraction Angiography, Doppler Ultrasound-imaging, as well as various imaging techniques based on nuclear emission, such as Positron Emission Tomography (PET) or Single-Photon Emission Computed Tomography (SPECT), have all been added to imaging tools of radiologists' toward an ever more reliable detection and diagnosis of diseases [323]. It can be noted that the optimal acquisition device can be selected on the basis of the investigation objective, in order to highlight specific areas of the human body. Concerning breast cancer, the tomosynthesis provides for a lower release of ionizing radiation if compared to conventional CT, together with Magnetic Resonance imaging that does not exhibit any ionizing radiation. Moreover, CAD systems for detecting breast tumours can support in differentiating benign and malignant forms with high accuracy and reduced times [316]. As a consequence, they are clinically very useful to reduce the number of biopsies of benign lesions and can offer a second reading to assist physicians in avoiding misdiagnosis. Concerning with liver cancer, the most modern triphasic techniques with contrast medium allow to be given a more accurate ability to recognize HCC lesions and stage the evolution of lesions more accurately for analogous doses, avoiding to repeat frequently CT examinations [318]. Regarding with leukaemia, minimally invasive strategies, such as those related to simple blood sampling supported by imaging for more accurate classification of leukocyte forms and their counting allow the implementation of innovative CAD Frameworks.

Image Segmentation. It is well known that segmentation is a crucial task in medical image processing, as the accuracy of this step can directly affect other post-processing tasks, such as image analysis and feature extraction [324]. After the acquisition of images, a pre-processing phase is needed for the improvement of their quality, eventually using techniques for removal of artefacts [325]. This is a crucial step in order to reach an optimal result in the subsequent phases since the outcomes of this phase affect the performance of the whole workflow. In fact, as far as medical imaging is concerned, in literature, there is a huge number of useful algorithms for the pre-processing of images [326], which are frequently coupled with segmentation algorithms, e.g. edge-based or feature-based segmentation techniques, for different aims, such as object recognition [327]. Although image processing includes different steps, segmentation is the most important one in medical imaging, aiming at separating images into regions that are meaningful for a specific task, such as the detection of organs or the computation of some metrics. Segmentation approaches can be classified into several categories on the basis of the involved features and the typology of the implemented techniques. It has to be noticed that the features of interest include pixel intensities, gradient amplitudes, or measures of texture. Segmentation techniques applied to these features can be broadly classified into three categories: region-based, edge-based, or classification techniques [328]. On the basis of the previous categorization, region-based and edge-based segmentation techniques explore intra-region similarities and inter-region differences between features, whereas a classification technique assigns class labels to individual pixels or voxels based on feature values by considering the 2D or 3D space, respectively. As reported in [329], grey-level thresholding is a simple but effective segmentation method. Thresholding may be performed at the global or local level, i.e., thresholds can be selected equal to a constant value throughout the image, or spatially varying by computing different thresholds for each subsection of the image. Thresholding methods can also be categorized as point-based methods or region-based ones; region-based methods compute the value of a proper threshold not only on the basis of the grey-level of an

individual pixel but also considering the properties of its neighbourhood. Whether local or global thresholds, point-based or region-based ones, they are typically estimated from the intensity histograms by means of different approaches. In some cases, a priori knowledge could be necessary to perform an efficient segmentation, due to the fact that noise, artefacts or other issues could make segmentation a tricky task, not easily achievable using only information coming pixel values. In [330] these problems are overcome by considering deformable and active models or atlas-based methods. Classification algorithms are frequently used for segmentation too. Supervised approaches for segmentation requires training data from users to let classifiers to learn how to label each pixel of the input images. On the other side, unsupervised classifiers are based on cluster analysis to discriminate natural structures in the input images starting from the data used for training. In recent years, however, segmentation methods based on Deep Learning (DL) strategies have been introduced [331]. The described pre-processing phases are preparatory for the extraction of ROIs containing the areas to be classified. In the most of cases, the segmentation task provides a binary mask as an outcome, which is then superimposed on the input image with the aim to filter-out all the undesired areas [332]. The detected ROIs are subsequently processed and classified on the basis of the approach considered in the subsequent phase. More in detail, a further step for the extraction of features is necessary in case of traditional approaches for classification, e.g. by means of Artificial Neural Networks (ANNs) or Support Vector Machines (SVM), whereas, if considering Deep Learning networks, e.g. Convolutional Neural Networks [333], a subsequent step for the extraction of features is not necessary, since these architectures directly process images as inputs. Medical imaging is essential in many fields of medical research and clinical practice because it greatly facilitates early and accurate detection and diagnosis of diseases. Processing methods for enhancing morphological features of masses and other abnormalities in medical images are also very useful [334]. For example, in [335], the goal of the analysed method consists in enhancing the morphological features of a region containing a lesion with high suppression of surrounding tissues. The described morphological method involves two steps: (1) selective extraction of target features by mathematical morphology and (2) enhancement of the extracted features by two contrast modification techniques. The effectiveness of the method is evaluated in quantitative terms by means of the contrast improvement ratio. Results clearly show that the method outperforms the conventional contrast enhancement methods. The effectiveness and usefulness of the proposed method have been further demonstrated by the application to three types of medical images: a mammographic image, a chest radiographic image, and a retinal one. As a conclusion, it can be affirmed that the proposed method enables the specific extraction and enhancement of mass lesions, which is essential for a clinical diagnosis based on medical image analysis. Thus, the method can be expected to achieve an automatic detection and recognition of lesions' locations and a quantitative analysis of their morphology. Concerning liver segmentation, processing algorithms can be categorized according to the amount of the inputs from the involved user: handcrafted, semi-automated and fully automated [336]. Handcrafted segmentation is considered as the "gold standard" in clinical practice and research, but it is expensive and time-consuming. The increase of automated segmentation approaches has revealed to be quite robust, but in some cases may suffer from certain segmentation pitfalls. Thus, emerging applications of segmentation include surgical planning and integration with MRI-based biomarkers.

Feature extraction. In this section, the importance of identifying and extracting appropriate sets of features from images, capable of characterizing and discriminating classes of interest, will be discussed [337]. For example, the segmentation of breast cancer could take advantage by combining morphological features with texture ones. In [338], the authors have developed a fully automated, three-stage segmentation method that includes clustering, active contour, and specularities detection stages. After segmentation, morphological features describing the shape of a suspected mass are extracted. Texture features are also extracted from a band of pixels surrounding such a mass. Stepwise feature selection and linear discriminant analysis (LDA) are employed in the morphological, texture, and combined feature spaces for designing the classifier. The improvement obtained by supplementing texture features with morphological ones in classification reveals statistically significant. In the analysed work, the leave-one-case-out discriminant score from different views of a mass is combined to obtain a summary score for classifying a mass as malignant or benign. In [339], a Computer-Aided Diagnosis system based on shape analysis is proposed, which proves to be highly accurate in evaluating breast tumours. However, the training time of the classifier to diagnose breast tumours reveals considerable. The extraction of morphologic features can also require a lot of computation. Hence, to develop a highly accurate and quick CAD system, texture and morphologic features of ultrasound breast tumour imaging are combined to evaluate breast tumours and reveal that the proposed system reduces the training time compared to systems based only on the morphologic analysis. According to the literature, there are several sets of features that could be used to characterize ROIs. From a general point of view, the features may be distinguished between global and local, based on the localization of the information used to compute: global features are a function of the whole processed image, whereas local features are a function of a local image region. By considering global features, the most used are Haralick features [340] (Figure 52), Local Binary Patterns (LBP) [341] and Threshold Adjacency Statistics (TAS) [342]. On the other side, the most used set of local features are the Speeded-Up Robust Features (SURF) [343].

Angular Second Moment	$\sum_i \sum_j p(i,j)^2$
Contrast	$\sum_{n=0}^{N_g-1} n^2 \{\sum_{i=1}^{N_g} \sum_{j=1}^{N_g} p(i,j)\}, |i-j| = n$
Correlation	$\frac{\sum_i \sum_j (ij)p(i,j) - \mu_x \mu_y}{\sigma_x \sigma_y}$ where μ_x, μ_y, σ_x and σ_y are the means and std. deviations of p_x and p_y the partial probability density functions
Sum of Squares: Variance	$\sum_i \sum_j (i-\mu)^2 p(i,j)$
Inverse Difference Moment	$\sum_i \sum_j \frac{1}{1+(i-j)p(i,j)}$
Sum Average	$\sum_{i=2}^{2N_g} i p_{x+y}(i)$ where x and y are the coordinates (row and column) of an entry in the co-occurence matrix, and $p_{x+y}(i)$ is the probability of co-occurence matrix coordinates summing to $x+y$
Sum Variance	$\sum_{i=2}^{2N_g} (i-f_8)^2 p_{x+y}(i)$
Sum Entropy	$-\sum_{i=2}^{2N_g} p_{x+y}(i) log\{p_{x+y}(i)\} = f_8$
Entropy	$-\sum_i \sum_j p(i,j) log(p(i,j))$
Difference Variance	$\sum_{i=0}^{N_g-1} i^2 p_{x-y}(i)$
Difference Entropy	$-\sum_{i=0}^{N_g-1} p_{x-y}(i) log\{p_{x-y}(i)\}$
Info. Measure of Correlation 1	$\frac{HXY - HXY1}{max\{HX,HY\}}$
Info. Measure of Correlation 2	$(1 - \exp{-2(HXY2 - HXY)})^{\frac{1}{2}}$ where $HXY = -\sum_i \sum_j p(i,j) log(p(i,j))$, HX, HY are the entropies of p_x and p_y, $HXY1 = -\sum_i \sum_j p(i,j) log\{p_x(i)p_y(j)\}$, $HXY2 = \sum_i \sum_j p_x(i)p_y(j) log\{p_x(i)p_y(j)\}$
Max. Correlation Coeff.	Square root of the second largest eigenvalue of Q where $Q(i,j) = \sum_k \frac{p(i,k)p(j,k)}{p_x(i)p_y(k)}$

Figure 52 - The statistics that can be calculated from the co-occurrence matrix with the intent of describing the texture of the image

Other kinds of descriptors useful for the characterization of neoplasias or lesions are based on the description of shapes that can be computed from Regions of Interest. In Figure 53 some examples of tumour classification which starts with shapes in benign and malignant cases are represented [344].
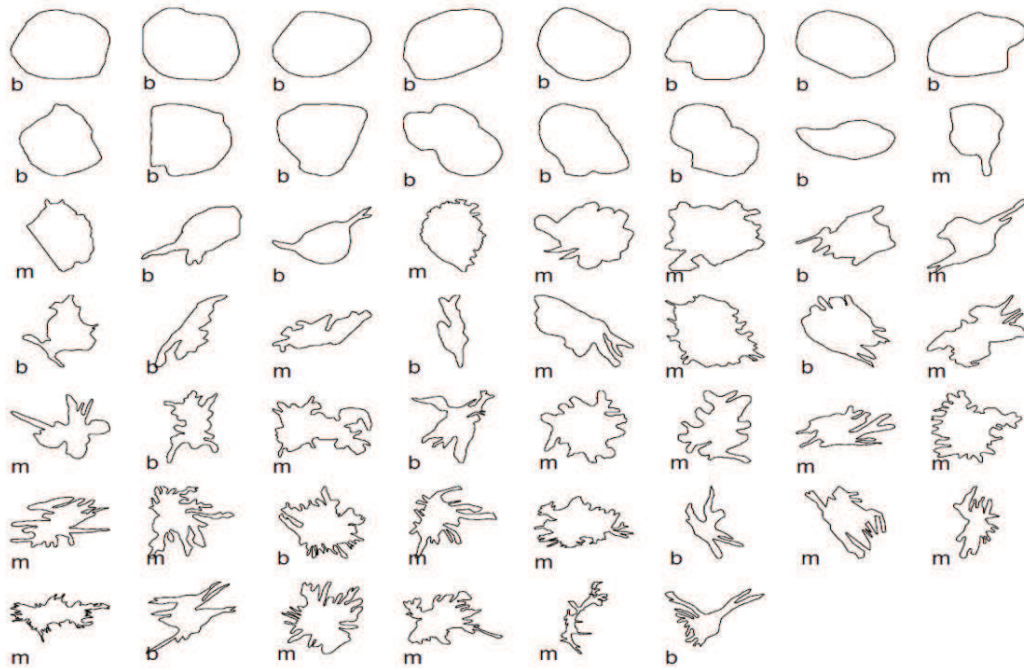
Figure 53 - Tumour diagnosis from contours of breast masses: (b) benign masses, (m) malignant tumours

Regardless of their nature, extracted features could be over the number effectively required for the classification task. This high dimensionality of the created dataset could lead to not-negligible problems in the subsequent classification phase, which could affect performance during both the design phase (for both training time and computational resources) and the classification phase with a reduced quality concerning the most common metrics of rating. For these reasons, before proceeding to the design phase of the most appropriate classifier for a given task, the dataset is processed to identify a new feature space, reduced or transformed with respect to the previous one, while maintaining the same informative contents of extracted data. In this regard, several techniques allow to properly process a dataset in order to reduce its dimensionality, leading to a general increase in the performance of the subsequent classifier, such as feature selection methods based on Information Gain [345], or other feature extraction methods, e.g. Principal Component Analysis (PCA) or Independent Component Analysis (ICA) [346].

Classification. In the last years, a relevant number of studies have been proposed, from a classification point of view. In most cases, the design of CAD systems is based on a supervised learning approach, using Artificial Neural Networks (ANNs) or Support Vector Machines (SVMs), as well as Swarm Intelligence (SI) or simpler Linear Discriminant Analysis (LDA) classifiers built on radiologists' gold standard labelling [347]. In particular, ANNs may be classified in several ways, on the basis of:

- the task for which each ANN is designed (e.g. pattern association, clustering);
- the partial/full degree of connectivity of neurons in the network;
- the direction of the flow of information within networks (recurrent and non-recurrent);
- the type of learning algorithm based on a set of systematic equations that use obtained outputs along with an arbitrary performance measure to update the internal structure of the ANN;
- the learning rule;

- the degree of learning supervision needed for training each ANN.

In particular, supervised learning involves the training of an ANN with the correct classification (i.e., target outputs) being given for every example, and using the deviation error of the ANN solution from corresponding target values to determine the required amount by which each weight should be adjusted. On the other side, unsupervised learning does not require the knowledge of a correct answer for training examples. In fact, corresponding networks arrange data samples into clusters based on their similarity or dissimilarity by exploring the underlying structure in data and the correlation between the various examples themselves [348]. It is well known that the development of Artificial Neural Networks requires partitioning of the parent database into:

- training set: it should include all the data belonging to the problem domain and is used during the training phase to update the weights of the network by evaluating the classification error;
- validation set: it is used after selecting the best network to examine the network further or confirm its accuracy before being implemented in the neural system and/or delivered to the end user;
- test set: it is used during the learning process to check the network response using data not included in the training set.

The data used in each set (training, validation and test) should be different from each other. There are no mathematical rules, but only some rules of thumb derived from experience and analogy between ANNs and statistical regression for the determination of the required sizes of the training, validation and test set. In particular, Cross-Validation (CV) is a popular strategy for algorithm selection. The main idea is to split parent dataset once or several times for estimating the risk of each algorithm. The popularity of CV mostly comes from the "universality" of the data splitting heuristics. Nevertheless, some CV procedures have been proved to fail for some model selection problems, depending on the goal of model selection, estimation or identification. The advent of new competitive imaging modalities for the same diagnostic problem has led to performing many studies involving comparisons of the information obtained from these imaging techniques. Several papers use Receiver Operating Characteristic (ROC) curves for comparison [349]. The intuitive result is that the area under the ROC curve represents the probability that a random pair of normal and abnormal images will be correctly ranked as to their disease state. In particular, this probability only conveys the intrinsic potential for discrimination with equally weighted sensitivity, and specificity is emphasized. Other external decision factors that influence diagnostic performance include the real mixture of diseased and non-diseased patients and the relative costs of the two types of diagnostic errors.

In scientific literature, two different classes of ANNs can be identified on the basis of the number of hidden layers: Shallow and Deep Neural Networks. In details, ANNs with a single hidden layer are named Shallow Neural Networks, whereas a Deep architecture has a number of hidden layers greater than one (Figure 54 adapted from Nielsen [350] under Creative Commons Attribution-Non Commercial 3.0 Unported License).
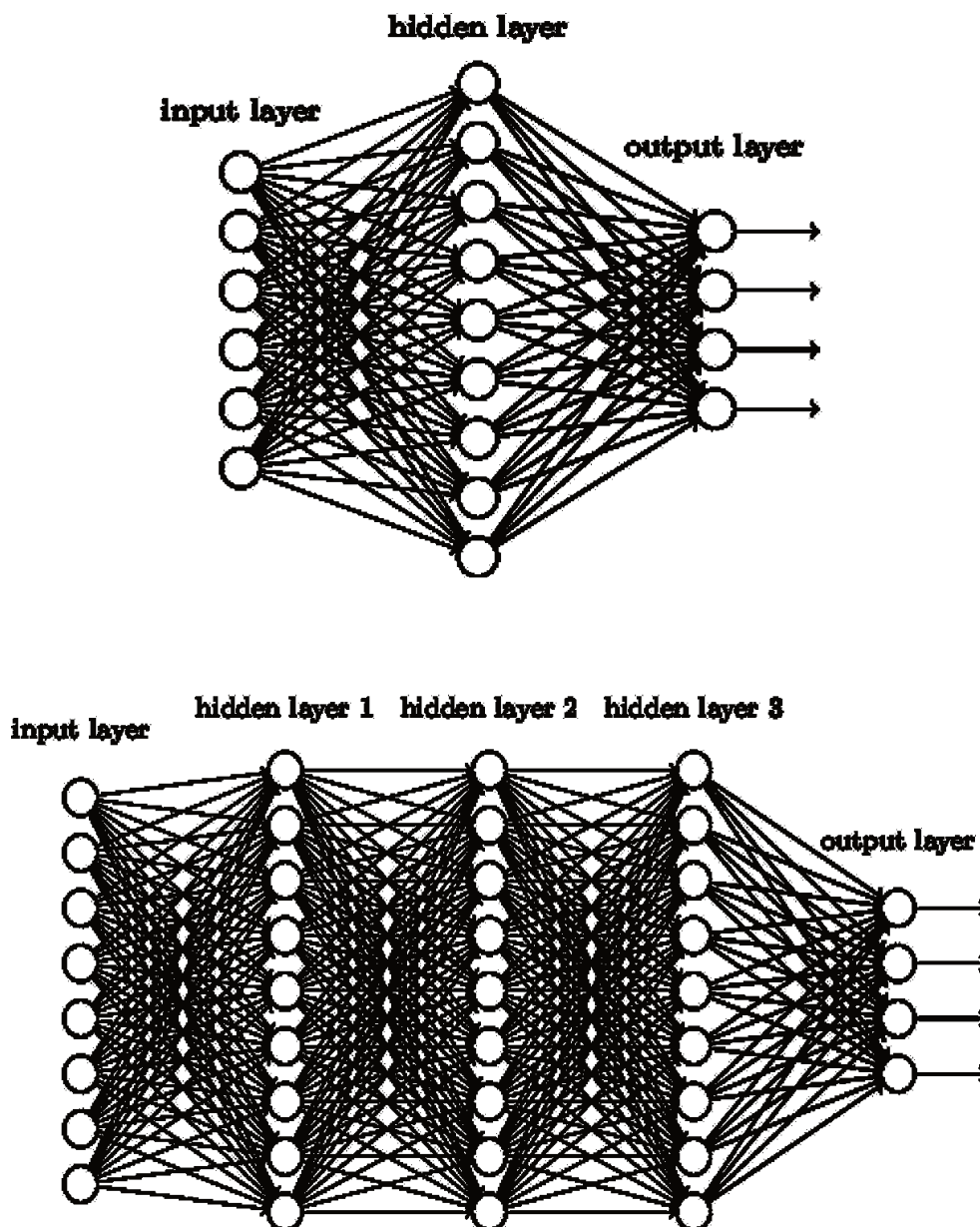
Figure 54 - Architectural differences between (a) shallow and (b) deep neural network

Regarding deep architectures, different strategies have been introduced in the literature so far; the success of deep networks in image processing is mainly due to the spread of Convolutional Neural Networks (CNNs). These kind of architectures are able to classify, i.e. make a decision, working directly on a raw image given as input to the network. In fact, a CNN is capable of extracting some descriptors (feature learning capability) of an image automatically, thus eliminating the development of algorithms for the processing of images for the extraction of the so-called "hand-crafted" features [351] necessary for a classical classifier, such as ANN or SVM. The general architecture of a Convolutional Neural Network is shown in Fig. 6 [352]; it is a combination (which depends on the specific implementation) of convolutional layers, REctified Linear Unit (RELU) layers and pooling layers followed by a fully connected layer (as in traditional multi-class ANNs).
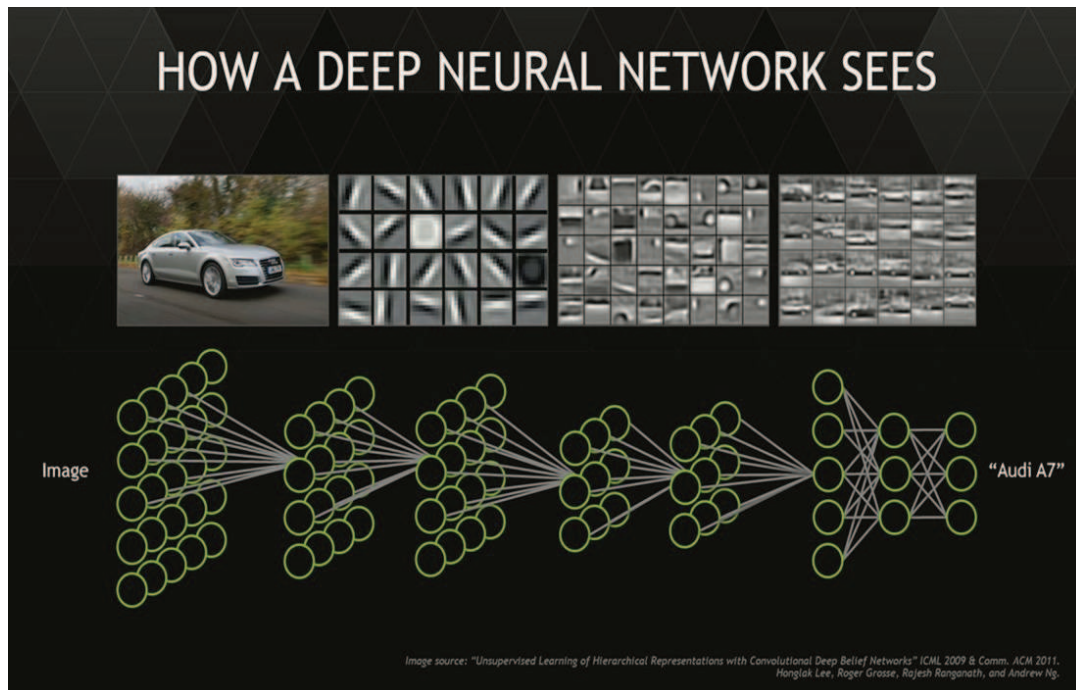
Figure 55 - A representation of the CNN layers

Thanks to their architectures, convolutional layers in CNNs allow obtaining different sets of descriptors for input images, thus obtaining different levels of abstraction for images representation based on the depth of the network. According to literature and given enough neurons, a sufficiently wide shallow neural network could approximate any function, so there is not a specific motivation to prefer Deep Neural Networks at all. In addition, the quality of the final generalisation properties of ANNs strictly depends on the significance and classes-balance of the available training data [353]. However, it is well known that a huge number of neurons in a single layer architecture increases the number of parameters to be tuned during the training phase, with the risk of overfitting data. Making ANNs deeper by adding multiple layers, enables the classifier to learn features at different levels of abstraction depending on the number of hidden layers. This can lead to stronger capabilities of generalisation.

Convolutional Neural Networks are powerful architectures that can be used in three different ways:

- Training from scratch: as for ANNs, Convolutional Neural Networks may be created from scratch, designing the overall architecture and providing enough samples as input for training. This process generally takes a lot of time using large datasets with several classes.
- Transfer Learning or Fine-Tuning: this approach enables to use an available pre-trained model for classification purposes different from the original ones. In details, it is possible to fine-tune the classification layer of a CNN to predict new classes given as inputs.
- Feature Extractors: in this case, it is possible to remove the classification layer from the CNN and consider outputs as features describing each input image as automatically computed by the network. This process is iterative; thus it is possible to remove more intermediate layers on the basis of the desired level of abstraction of the features.

3.3.1 Research Question

Computer Aided Diagnosis (CAD) systems can support physicians in classifying different kinds of breast cancer, liver cancer and blood tumours also revealed by images acquired via Computer Tomography, Magnetic Resonance, and Blood Smear systems. In this regard, this part of the PhD work focuses on papers dealing with the description of existing CAD frameworks for the classification of the three mentioned diseases, by detailing existing CAD workflows based on the same steps for supporting the diagnosis of these tumours. In detail, after an appropriate acquisition of the images, the fundamental steps carried out by a CAD framework can be identified as image segmentation, feature extraction and classification. In particular, specific CAD frameworks are considered, where the task of feature extraction is performed by using both traditional handcrafted strategies and Convolutional Neural Networks-based innovative methodologies, whereas the final supervised pattern classification is based on neural/non-neural machine learning methods. Then, the performance of three selected case studies are carefully reported, designed with the aim of showing how final outcomes can vary according to different choices in each step of the adopted workflow. More in detail, these case studies concern with breast images acquired by Tomosynthesis and Magnetic Resonance, hepatocellular carcinoma images acquired by Computed Tomography and enhanced by a triphasic protocol with a contrast medium, peripheral blood smear images for cellular blood tumours and are used to compare their performance.

3.3.2 Breast Cancer

The high incidence of breast cancer, which at the moment corresponds to more than 25% of female cancers [314], and the ever-increasing life expectancy of the population require an accurate assessment of the clinic state of the breast gland with imaging techniques. In this field, mammography represents the gold standard imaging tool [354]; in fact, mammographic examinations are used in several screening programs thanks to the capability to perform a very early detection, whereas Magnetic Resonance (MR), Computer Tomography (CT) or Digital Breast Tomosynthesis (DBT) techniques are necessary to perform a more in-depth analysis of risky cases, or for the follow-up of treated patients. In recent years, several works have been presented dealing with breast lesions detection and classification considering deep strategies for classification [355–357].

In the following sections, two works for detecting and classifying breast lesions will be described. In particular, a supervised approach for detecting and classifying breast lesions from MR images will be introduced in paragraph 3.3.2.1, whereas a supervised approach based on deep architectures for the extraction of features in order to classify using simpler non-neural strategies will be discussed in paragraph 3.3.2.2.

3.3.2.1　Magnetic Resonance

In this paragraph, a CAD system for detecting and classifying breast lesions in images acquired via Magnetic Resonance is presented. The workflow is reported in Figure 56Figure 56 - Workflow for breast lesion classification and will be described.
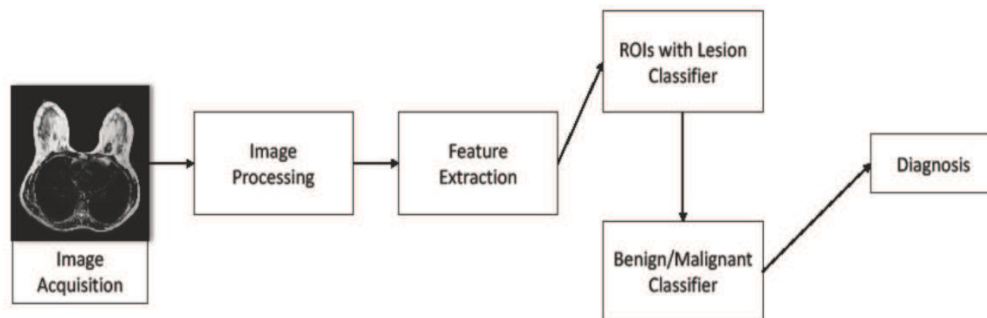
Figure 56 - Workflow for breast lesion classification

3.3.2.1.1　Materials and Methods

The acquisition phase is conducted following the standard procedure for breast cancer diagnosis, which consists of as follows:

- Transverse short TI inversion recovery (STIR) turbo spin-echo (TSE) sequence (TR/TE/TI = 3.800/60/165 ms, Field of View (FOV) =250x450 mm (APxRL), matrix 168x300, 50 slices with 3-mm slice thickness and without gaps, 3 averages, turbo factor 23, resulting in a voxel size of 1.5 x 1.5 x 3.0 mm3; acquisition time: 4 minutes);
- Transverse T2-weighted TSE (TR/TE = 6.300/130 ms, FOV = 250x450 mm (APxRL), matrix 336x600, 50 slices with 3-mm slice thickness and without gaps, 3 averages, turbo factor 59, SENSE factor 1.7, resulting in a voxel size of 0.75x0.75x3.0 mm3; acquisition time: 3 minutes);
- Three-dimensional dynamic, contrast-enhanced (CE) T1-weighted high resolution isotropic volume (THRIVE) sequences (TR/TE= 4.4/2.0 ms, FOV = 250x450x150 mm (APxRLxFH), matrix 168x300, 100 slices with 4-mm slice thickness, spacing

between slices: 2 mm; turbo factor 50, SENSE factor 1.6, 6 dynamic acquisitions, resulting in 1.5 mm3 isotropic voxels, a dynamic data acquisition time of 1 min 30 s, and a total sequence duration of 9 min).

In details, the first step consists in a pre-processing phase of the acquired images; then, after a simple rescaling of the grey level of pixels, an algorithm for masking the presence of thorax in all the slices is performed, aiming at filtering out all the anatomic structures external to the breast. In this regard, as shown in Figure 57, three points are computed to generate a parabola having its vertex coincident with the sternum (point A) and passing through the side edges of the chest (points B and C).
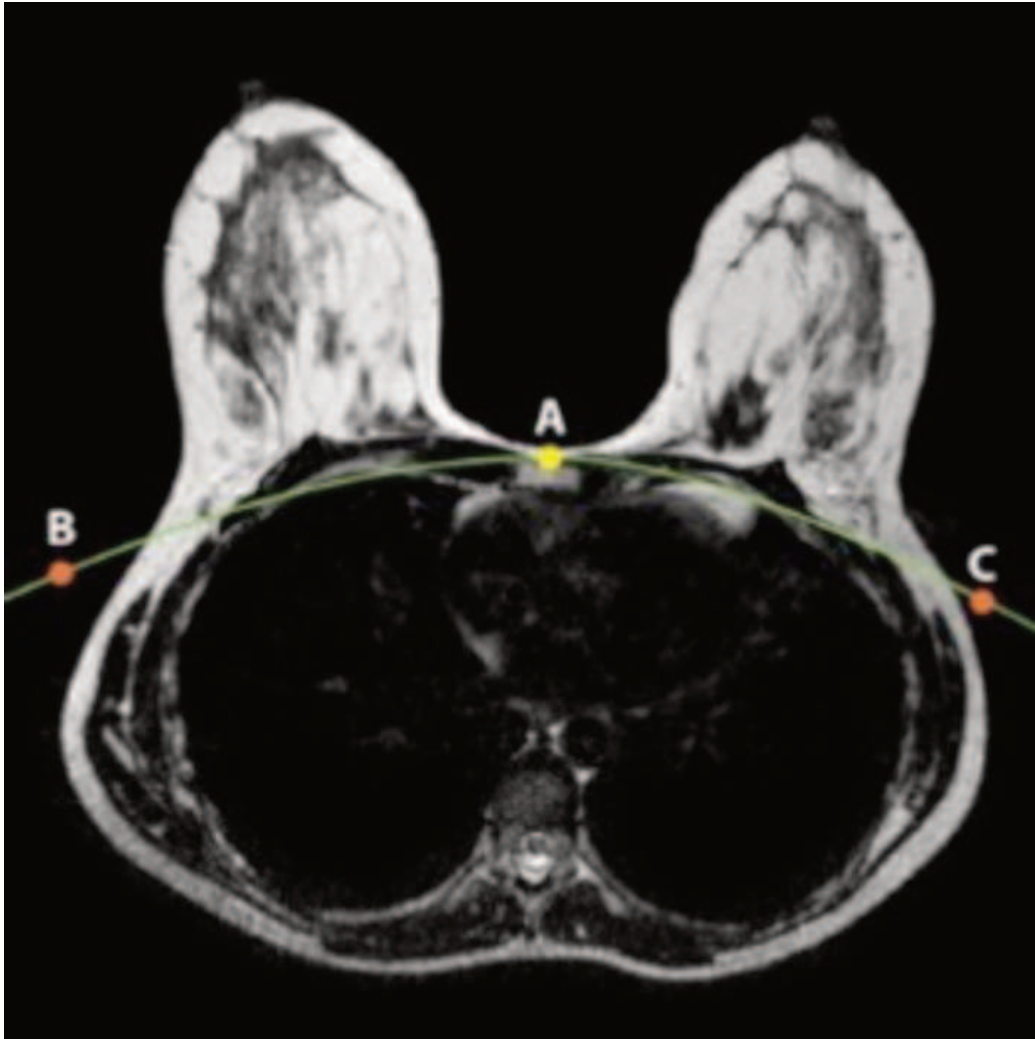
Figure 57 - Output image of the algorithm for thorax masking. The reference points for parabola generation are A, B and C

A segmentation phase, necessary for the removal of all the uninteresting parts of the image, is subsequently performed. In particular, a thresholding operation is implemented considering the 95th percentile of the grey level histograms of the images acquired without Contrast Medium (CM). Then, areas with a diameter below 5 mm are removed, and the obtained mask is applied to the starting image in order to extract the regions of interest. The remaining areas are characterized considering 10 different features describing the shape of the extracted ROIs. After the extraction of the features, two Artificial Neural Networks can be designed using an evolutionary strategy, as reported in [289]. The first ANN is designed to discriminate among lesions and other structures, such as vessels

(Figure 58), whereas the second one is used to classify benign/malignant lesions by taking the same set of features of the regions classified as lesions in the previous step.
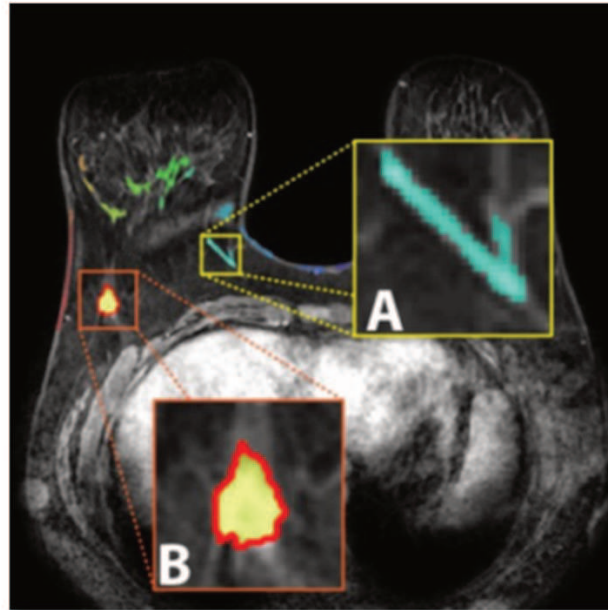
Figure 58 - The classification result for the discrimination between lesions and other structures. A indicates a vessel, whereas B a lesion

In particular, regarding the first classifier, the generated dataset is balanced with a Synthetic Minority Over-sampling Technique (SMOTE) to increase the number of patterns characterizing lesions until the number of negative cases to achieve better classifier performance.

3.3.2.1.2   Innovative Results

In both cases, performances are measured in terms of Accuracy, Sensitivity and Specificity. Obtained results in both cases are reported in Table 19 and Table 20, respectively.

Table 19 - Results obtained for the discrimination between ROIs with and without lesions

	Min	Max	Mean
Accuracy	0.9624	0.9849	0.9736 ± 0.0044
Sensitivity	0.9592	0.9958	0.9791 ± 0.0075
Specificity	0.9459	0.9892	0.9684 ± 0.0075

Table 20 - Results obtained for the discrimination between benign and malignant lesions

	Min	Max	Mean
Accuracy	0.7308	1	0.8977 ± 0.0584
Sensitivity	0.6923	1	0.8908 ± 0.1021
Specificity	0.7692	1	0.9046 ± 0.0875

In details, these tables show Accuracy, Sensitivity and Specificity as mean values obtained performing 100 iterations of training, validation and test of ANN, considering a different random permutation of the input dataset at each iteration.

The reported results show that a supervised machine learning approach for the detection of breast lesions from MR images and the subsequent classification benign/malignant lesions is consistent, and shows good performance, especially from the perspective of False Negative reduction.

3.3.2.2 Digital Tomosynthesis

Digital Breast Tomosynthesis (DBT) has been recently introduced for breast cancer screening and detection and consists of a promising innovative radiological technique for early diagnosis and staging. DBT produces a limited angle cone beam in tomosynthesis of the breast glands and has demonstrated to have a higher accuracy if compared to the most commonly used bi-dimensional imaging techniques, such as mammography, CT or MR [358]. Thanks to this innovative technology, a 3D model of the breast is created, also reducing the effect of tissue superimposition [359], improving the visualization of masses and architectural distortions. In particular, the edges of breast lesions are better defined, and this leads to an improvement of the final diagnosis. In this paragraph, a CAD system to support the classification of three kinds of lesions is designed. An image-processing step performing segmentation is needed to extract candidate ROIs containing suspicious lesions (Figure 59).
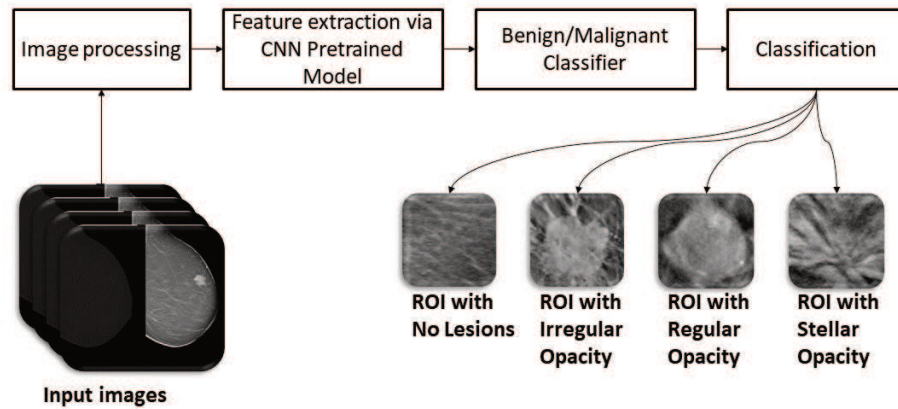
Figure 59 - Workflow for breast lesion classification

3.3.2.2.1   Materials and Methods

The extracted ROIs are labelled according to the classification in 4 classes provided by radiologists:

1. None: segmented ROI not containing any kind of lesion (Figure 60(a));
2. Ori: segmented ROI containing an irregular opacity (Figure 60(b));
3. Oro: segmented ROI containing a regular opacity (Figure 60(c));
4. Ost: segmented ROI containing a stellar opacity (Figure 60(d)).
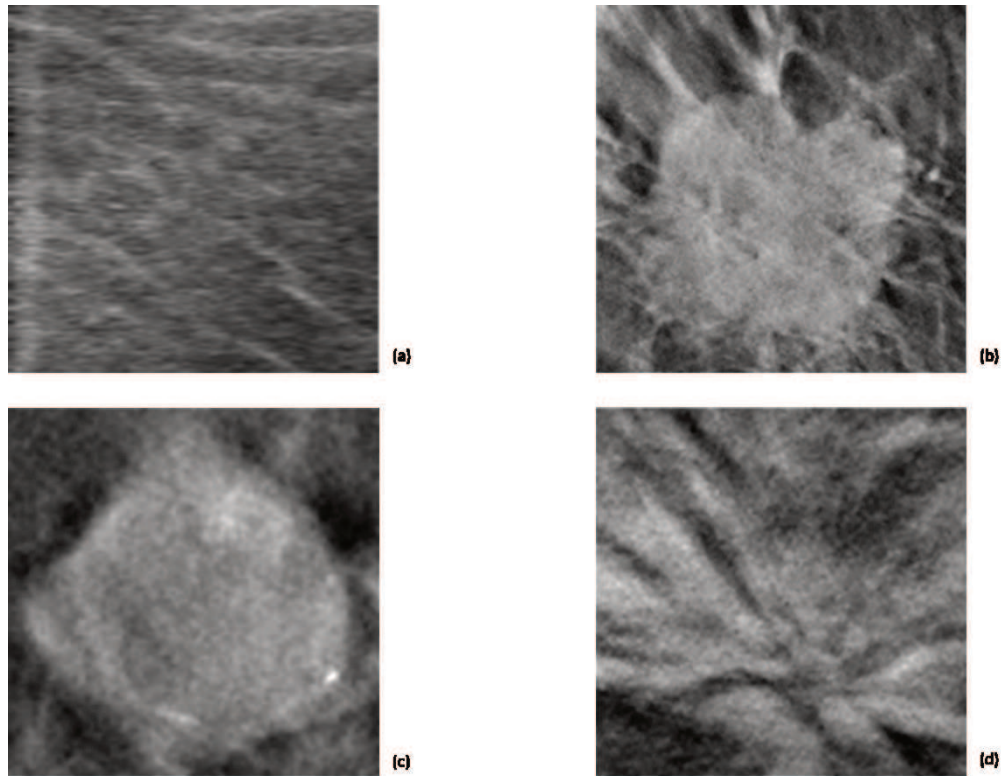
Figure 60 - Images extracted after the segmentation phase: (a) ROI without lesions; (b) ROI with an irregular opacity; (c) ROI with a regular opacity; (d) ROI with stellar opacity

The extraction of features describing the segmented ROIs is performed following two different approaches:

- Several pre-trained models of Convolutional Neural Networks are used as automatic features extractors by pruning the CNN architectures at certain levels of depth;
- hand-crafted morphological and textural features are computed using the Grey Level Co-occurrence Matrix (GLCM) [360].

3.3.2.2.2   Innovative Results

Since several strategies for feature extraction are used, also the classification step is performed following different approaches. In particular, two Artificial Neural Networks are designed by considering an evolutionary approach to discriminate among the four classes taking the hand-crafted features as inputs. In a first step, the classes named Ori, Oro and Ost have been grouped into a single one (P - Positive), whereas the second class is None (N - Negative); in this case, a binary classifier is used and obtained performance are reported in Table 21.

Table 21 - Results obtained for binary classification

	Accuracy	Sensitivity	Specificity
Mean	84.19%	85.90%	82.82%
Standard Deviation	3.06	5.33	5.17

Subsequently, the second ANN is used to discriminate among the four classes, but the obtained Accuracy reveals lower than the one obtained via a binary classifier (74.84%

± 4.89). This behaviour reveals predictable and reasonable, considering the way in which ANNs are designed and optimized: the extraction process of the most discriminant features heavily influences the overall capabilities of the classifier. In this case, the features used as inputs showed good results to discriminate binary class samples, while these did not provide enough information to correctly describe all the different kinds of lesions in the multi-class approach.

Regarding CNNs as feature extractors, several pre-trained models have been developed, which are: GoogLeNet, ResNet, AlexNet, VGG-very deep, VGG-F, M and S [361–364]. In the second approach, the dataset is constituted by the set of features extracted by the CNN models. The output of the CNN models, or rather, their final activations, is used to train several non-neural learners, which were: Linear Support Vector Machine (Linear SVM) [365], K-Nearest Neighbor (KNN) [366], Naive Bayes [367], Decision Tree [368] and Linear Discriminant Analysis (LDA) [369].

In order to improve overall performance, several tests for dataset processing have been carried out on all considered CNN architectures; in particular, Activation Normalization and Image Augmentation are explored leading to a slight improvement in all architectures. Finally, since VGG-F, VGG-S and VGG-S show the higher mean accuracies and the lowest processing time, they are considered for final evaluation. Results reported in Table 22 show that Naive Bayes classifier is not recommended in this classification; Decision Trees enable to improve the mean accuracy in comparison to Naive Bayes, but they are far to be considered as reliable classifiers.

Table 22 - Results of the selected pre-trained CNNs used as features extractor, training several networks with normalisation and augmented images

	KNN	LDA	LINEAR SVM	NAÏVE BAYES	DECISION TREE
VGG-F	91.63 ± 0.41	64.57 ± 0.66	67.29 ± 2.02	43.82 ± 0.59	59.68 ± 1.07
VGG-M	90.74 ± 0.48	66.25 ± 0.60	69.50 ± 2.16	42.85 ± 0.57	57.03 ± 0.98
VGG-S	92.02 ± 0.48	65.24 ± 0.80	68.84 ± 1.89	44.89 ± 0.60	56.16 ± 0.93

Performances have been furtherly increased via the linear classifiers SVM and LDA, but better results have been obtained from KNN classifiers. In this case, mean performance has reached significant levels of accuracy, specificity and sensitivity with low variability. Furthermore, it is worth to mention that the values of sensitivity and specificity for positive samples reveal higher than 95% to substantiate the high level of performance in terms of accuracy, as reported in Table 7 where results are calculated using a 1-vs-all approach.

Table 23 – Sensitivity (SE) and specificity (SP) for the lesions evaluated through a 1-vs-all approach

	Ori vs All		Oro vs All		Ost vs All	
	SE	SP	SE	SP	SE	SP
VGG-F	98.67%	97.07%	96.01%	95.98%	97.24%	96.93%
VGG-M	98.14%	96.64%	95.00%	95.76%	97.18%	96.62%
VGG-S	98.36%	97.13%	95.61%	96.33%	96.67%	97.25%

3.3.3 Liver Carcinoma

As for breast cancer, liver cancer shows an extremely high mortality worldwide [314]. In recent years, several works have been presented dealing with the detection and classification of hepatic tumours considering different strategies for classification. Different machine learning techniques for the diagnosis of liver disease and hepatitis disease are developed in [370]. It is observed that Functional Trees (FTs) provide 97.10% of correctness for a liver disease diagnosis. The implemented feedforward neural network correctly classifies hepatitis disease by providing a value of 98% of accuracy. Moreover, in [371] a Deep Convolutional Neural Network (DCNN) is developed to segment liver in CT slices via an automatic procedure. The same model has been subsequently employed for the classification of lesions, by considering images from the previous classification as inputs. All developed models have been evaluated on the Liver Tumour Segmentation Challenge dataset (LiTS) for liver segmentation tasks [372]. In the reported paper, a DICE coefficient [373] equal to 0.67 is reached, but classification performance for lesions are still low.

In [374] a novel application of Convolutional Neural Networks is presented to segment liver tumours. In this work, the method is tested on 30 CT images using a leave-one-out cross-validation. Reported experiments show that CNN models produce an accurate and robust liver tumour segmentation. If compared to traditional machine learning methods, such as AdaBoost and SVM, the CNN method seems to perform in a better way. Limitations of CNNs are still found on segmenting tumours with inhomogeneous density and unclear boundary, principally like under-segmentation in each a tumour adjacent to structures with similar densities.

In [375], several recent Computer Aided Diagnosis (CAD) systems used in the diagnosis of liver diseases have been discussed. This article investigates the various CAD systems used for the classification of liver diseases using CT scan images. The reported description of the tumour segmentation process focuses on the algorithm used to classify a tumour and the corresponding results for all considered works. However, this article does not consider the most modern deep learning classification techniques.

A pilot study for hepatocellular carcinoma grading and the evaluation of microscopic vascular invasion is proposed in [376] where a shallow artificial neural network is compared to linear models. The results obtained from ANN in terms of AUC and Accuracy are higher than the ones obtained from a linear logistic model in both HCC grading and MVI presence evaluation.

In [377], 164 liver lesions (80 malignant tumours and 84 haemangiomas) are evaluated. The suspicious tumour region in the digitized CT image is manually selected and extracted as a circular sub-image. The proposed pre-processing adjustments for sub-images are used to equalize the information needed for a differential diagnosis. The auto-covariance texture features of sub-images are extracted, and a support vector machine classifier identifies a tumour as benign or malignant. The value of accuracy of the proposed diagnosis system for classifying malignancies is 81.7%, the value of sensitivity is 75%, that of specificity is 88.1%, the positive predictive value is 85.7%, and the negative predictive value is 78.7%.

In the following sections, two specific works for detecting and classifying hepatocellular carcinoma will be analysed and discussed. In particular, a supervised approach based on the extraction of hand-crafted features for detecting and classifying HCCs obtained via a triphasic CT protocol and a second approach based on a supervised Convolutional Neural Network.

3.3.3.1   Hand-Crafted Features

In [378] the considered acquisition system is based on CT, which is, as is well known, a medical imaging technique that is widely used for Hepatocellular Carcinoma detection. CT images, as well as MR ones, are always required to determine the disease extension. In fact, both these techniques are considered as gold standards for non-invasive evaluation of focal and diffuse diseases of the liver and biliary tract. The CT scans used in the reported work have been acquired with a 320 slices Scanner (Toshiba Aquilion One) after an automated injection of 1.5 ml/kg of iodinated contrast medium (Iomeprole 400 mgI/ml) through a 16G Needle in antecubital vein at a flow rate of 4ml/sec with the following protocol:

1. arterial dominant phase acquired 20 seconds after the aortic peak calculated by a bolus tracking system with a ROI positioned in the abdominal aorta at a trigger density of 150 Houns field Units (HU) (Figure 61(a));
2. portal phase acquired 70 seconds after contrast injection;
3. equilibrium phase acquired 180 seconds after contrast injection Figure 61(b)).
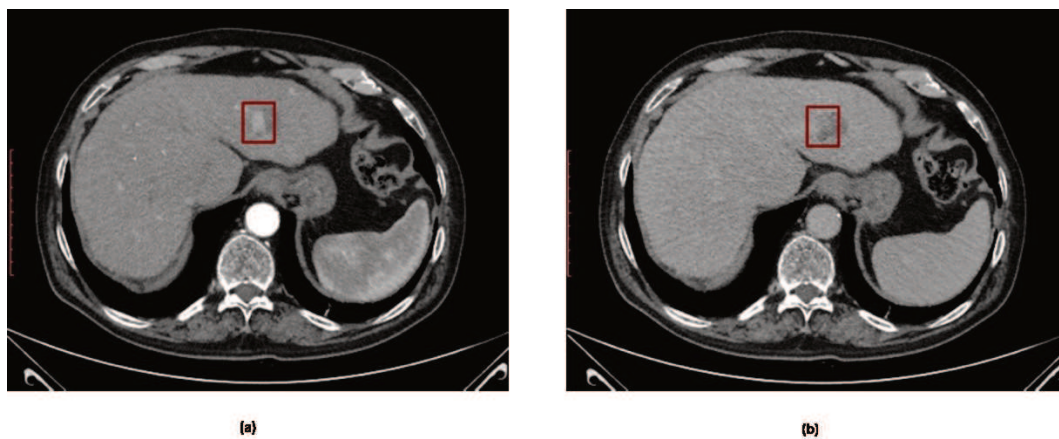
Figure 61 - CT images acquired in the different phases: (a) Arterial phase; (b) Equilibrium phase. The square indicates the lesion in both phases

3.3.3.1.1 Materials and Methods

A double-step segmentation is carried out, after a pre-processing image phase performed through contrast enhancement, in order to improve the contrast of the CT images, and a cropping phase to reduce the amount of data to be processed. In particular, liver and HCC segmentations are performed. Concerning liver segmentation, the histogram of the slice with the largest connected portion of the liver is analysed to obtain the typical liver grey intensity. By means of this evaluation, local thresholding and morphological operations are performed, allowing to remove all the structures external to the liver. The segmentation result of the first considered CT slice (generally, the slice worth the maximum liver extension is considered) is dilated and used as a binary mask both for previous slices and following ones. Those slices are further segmented, and the method is then iteratively propagated in both directions until final slices are reached. A similar procedure is performed for HCC segmentation. Each Hepatocellular carcinoma is subsequently segmented using an innovative two-dimensional region growing algorithm which takes into account images from both arterial and equilibrium phases. Some morphological operations are performed to refine the obtained ROIs. Textural features are then extracted using grey level co-occurrence matrices to describe ROIs. Each HCC is texturally described taking information from the two corresponding slices in both

arterial and delayed phases. Three subsets of features are generated from the dataset, where:

1. 44 features are obtained considering ROIs extracted from the two considered phases (specifically, 22 features extracted from each phase);
2. 22 features come from an algorithm of ranking based on the relative entropy, also known as Kullback-Leibler distance or divergence [345];
3. 5 features of the work of Haralick et al. [340] (Contrast, Correlation, Energy, Homogeneity and Entropy), which have been used in similar previous work for blood vessels and tubules classification and have shown good discrimination capabilities.

3.3.3.1.2 Innovative Results

HCC grades are grouped into two classes: grade 1/2 addressed as Negative Class, and grade 3/4 addressed as Positive Class. The binary classifier is designed to discriminate the above mentioned two groups using a mono-objective genetic algorithm (GA) [289]. In Table 8 obtained results, which are expressed for accuracy, specificity, and sensitivity in terms of mean values (± standard deviation) considering 100 iterations are reported.

Dataset	Accuracy	Sensitivity	Specificity
44 features	0.758 ± 0.062	0.755 ± 0.122	0.730 ± 0.141
22 features	0.763 ± 0.063	0.824 ± 0.089	0.698 ± 0.156
10 features	0.799 ± 0.073	0.795 ± 0.015	0.804 ± 0.126

These results show that HCC classes can be discriminated by using the proposed set of extracted features: the HCC wash-in and wash-out dynamic suggests that this type of lesion can be characterized by processing textural differences considering the most important phases in the HCC dynamics.

3.3.3.2   Deep Learning Approach

Also, in this case, the acquisition protocol is a triphasic CT acquisition characterized by an hyper-enhancement in the arterial phase followed by portal venous or delayed phase washout appearance. For a better understanding of the grading process, the following block diagram of the approach proposed is reported (Figure 62).
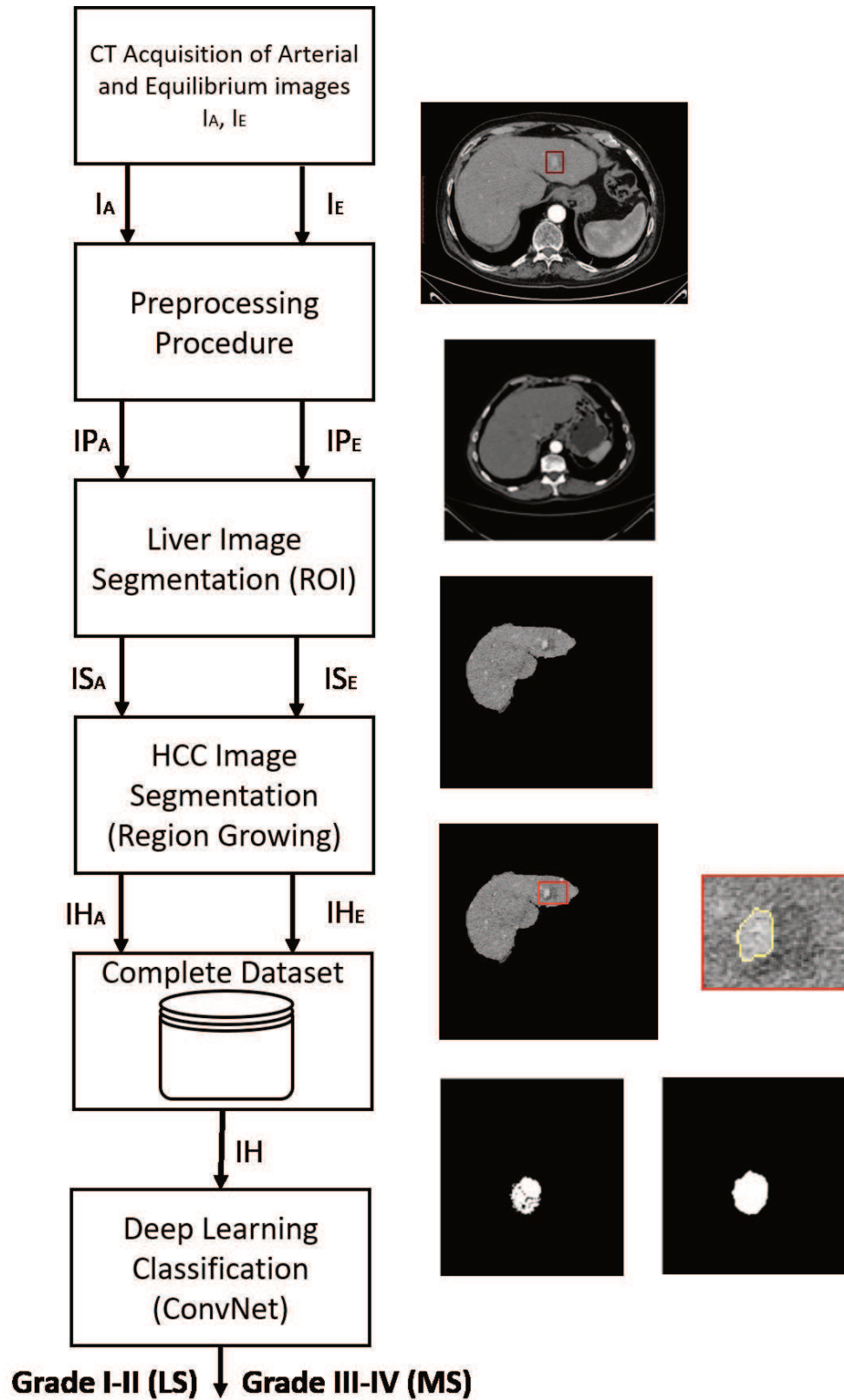
Figure 62 - Block diagram of the proposed approach for hepatocellular carcinoma grading with samples of output images at each step

3.3.3.2.1   Materials and Methods

As far as liver and HCC segmentations are concerned, the same procedures reported in 3.3.3.1.1 are applied thus obtaining binary masks that are applied to CT images acquired during arterial phases. A Convolutional Neural Network, more specifically the Google Inception v3 implementation reported in [379], is used by performing a retrain of the model using the created dataset of images as input. The implemented CNN is trained, validated and tested 100 times considering different permutations of the input dataset.

3.3.3.2.2   Innovative Results

Results reported in Table 24, obtained following the workflow in Figure 62, show that the implemented approach shows high generalization performance regardless the input permutation; in fact, Accuracy, Sensitivity and Specificity are higher than 90%, albeit maintaining a low value of standard deviation.

Table 24 - Results obtained for CNN classification

	Accuracy	Sensitivity	Specificity
Mean	0.928	0.935	0.921
Standard Deviation	0.055	0.075	0.089

3.3.4 Blood Neoplasia

The design of CAD systems for supporting the clinical diagnosis of blood neoplasias reveals of fundamental importance since, in the most of cases, invasiveness of diagnostic procedures is considerably reduced [380, 381].

In [382] a Super-Resolution Convolutional Neural Network (SRCNN) is proposed, which surpasses the double-cubic baseline with just a few training iterations, and out-performs the Sparse Coding-based method (SC) with moderate training. Performance may be further improved adding training iterations. In the reported work, different network structures are investigated, as well as parameter settings, to achieve a trade-off between performance and speed. Moreover, the proposed network is extended to cope simultaneously with three-colour channels and show a better overall reconstruction quality. Then, a deep learning method for single image super-resolution (SR) is proposed in [383]. The suggested method directly learns an end-to-end mapping between the low/high-resolution images and the mapping is represented as a deep Convolutional Neural Network that takes the low-resolution image as the input and outputs the high-resolution one. Moreover, in the same paper, traditional Sparse Coding-based SR methods are viewed as a deep convolutional network that jointly optimizes all layers, differently from traditional methods that handle each component separately. The considered CNN achieves fast speed for practical on-line usage, besides having a lightweight structure and presenting state-of-the-art restoration quality. As for the previous work, in [383] different network structures are also investigated, together with parameter settings to achieve an optimal trade-off between performance and speed.

In the following sections, two approaches for detecting and classifying white blood cells (leukocytes) from Peripheral Blood Smears (PBS) will be analysed and discussed. In particular, the first approach is based on the extraction of hand-crafted features for a subsequent neural classifier, whereas the second approach considers CNNs as feature extractors. A comparison between SVM classification and CNN classification considering images as inputs is performed.

3.3.4.1 Hand-crafted Features

Observation under the microscope of PBS is fundamental in haematology, as an analysis both of leukocyte formula and of morphological characteristics of blood cells (red blood cells, white blood cells, and platelets) provides useful information from a clinic point of view. The morphological evaluation of the WBC can help specialists diagnosing haematological pathologies such as leukaemia and non-haematological ones such as infectious mononucleosis. In this section, image processing techniques with low computational requirements have been designed, together with a CAD system able to recognize all the five types of leukocytes (Figure 63), named Neutrophils, Lymphocytes, Monocytes, Eosinophils and Basophils.
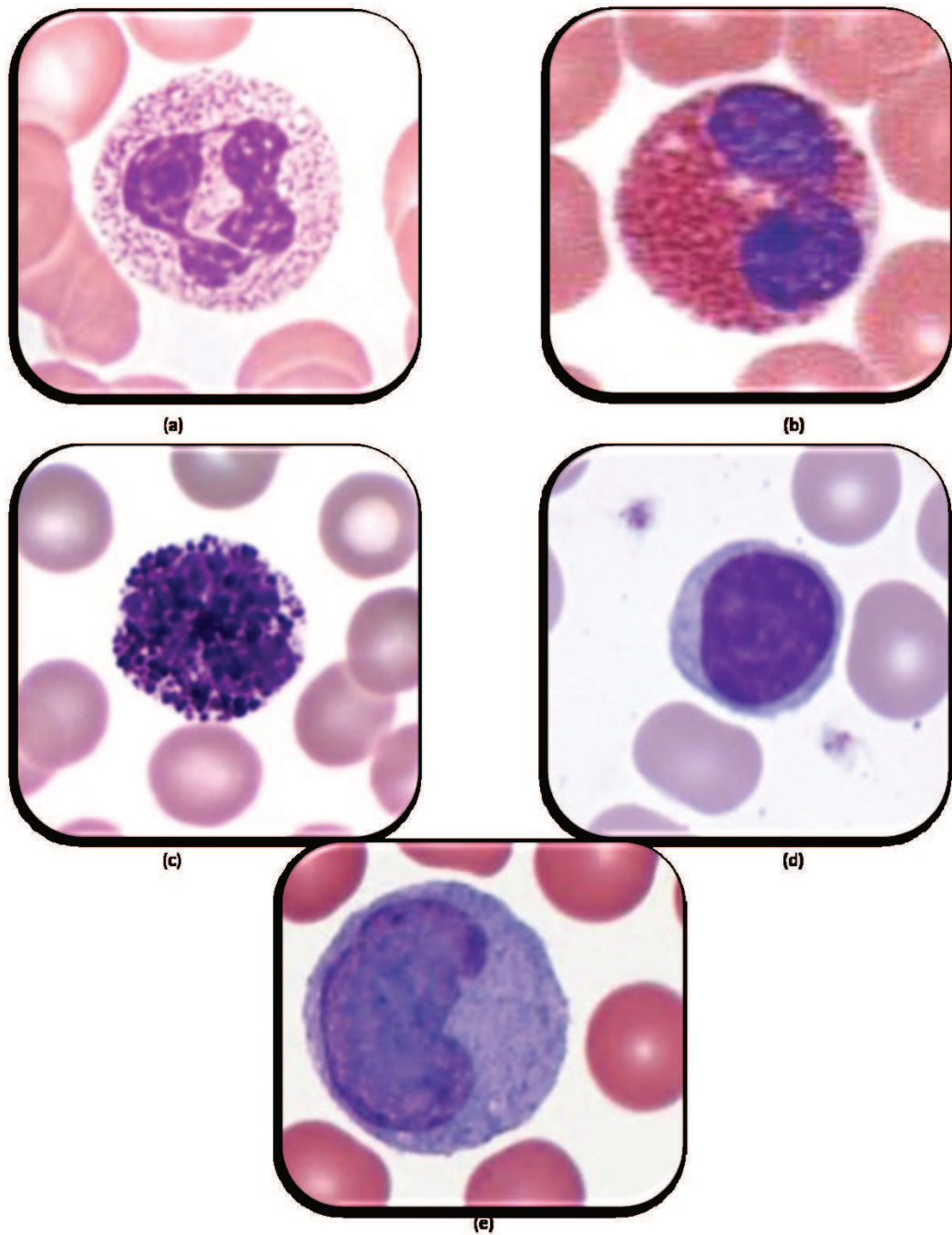
Figure 63 - The five types of leukocytes to be classified: (a) Neutrophils, (b) Eosino-phils, (c) Basophils, (d) Lymphocytes, (e) Monocytes

The workflow followed in this approach is represented in Figure 64.
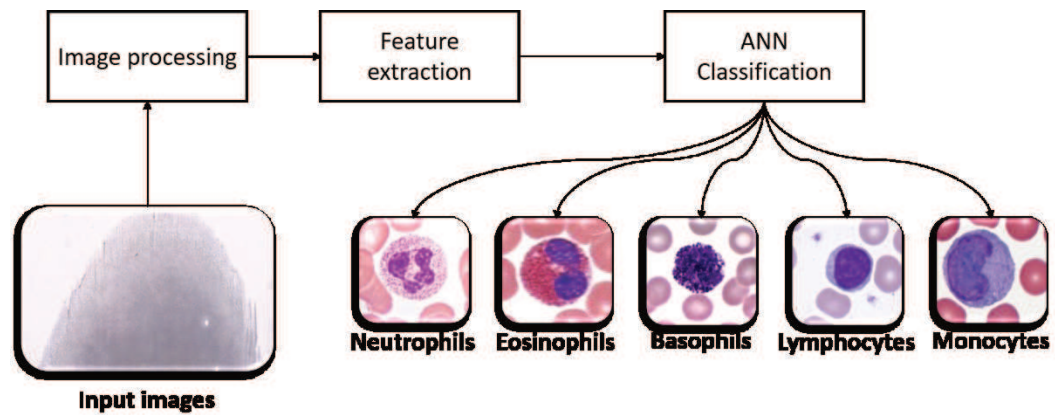
Figure 64 - Workflow for leukocytes classification considering hand-crafted features

3.3.4.1.1 Materials and Methods

Blood Smears are digitally acquired using the microscope D-Sight 200 (www.menarinidiagnostics.it) featuring a 40x optical zoom, with a resolution of 0.25 µm/pixel and a JPEG 2000 compression. The leukocytes segmentation consists of three main steps able to detect leukocytes position, plasma and leukocyte edge, respectively. In details, a colour space conversion into a Hue Saturation Value (HSV) space, a thresholding operation and a morphological dilatation allow generating a mask for the detection of nuclei positions in considered images (Figure 65 and Figure 66).
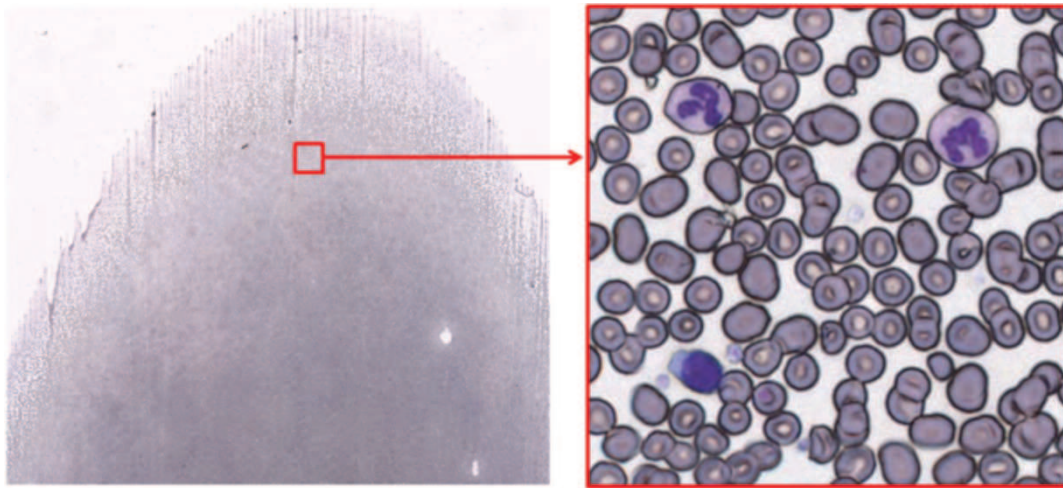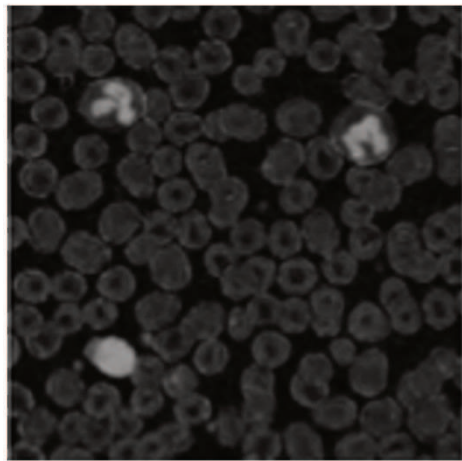
Figure 65 - A representation of steps to obtain the nuclei mask; (a) Sub-image extraction, (b) S channel of HSV sub-image, (c) Obtained Nuclei Mask
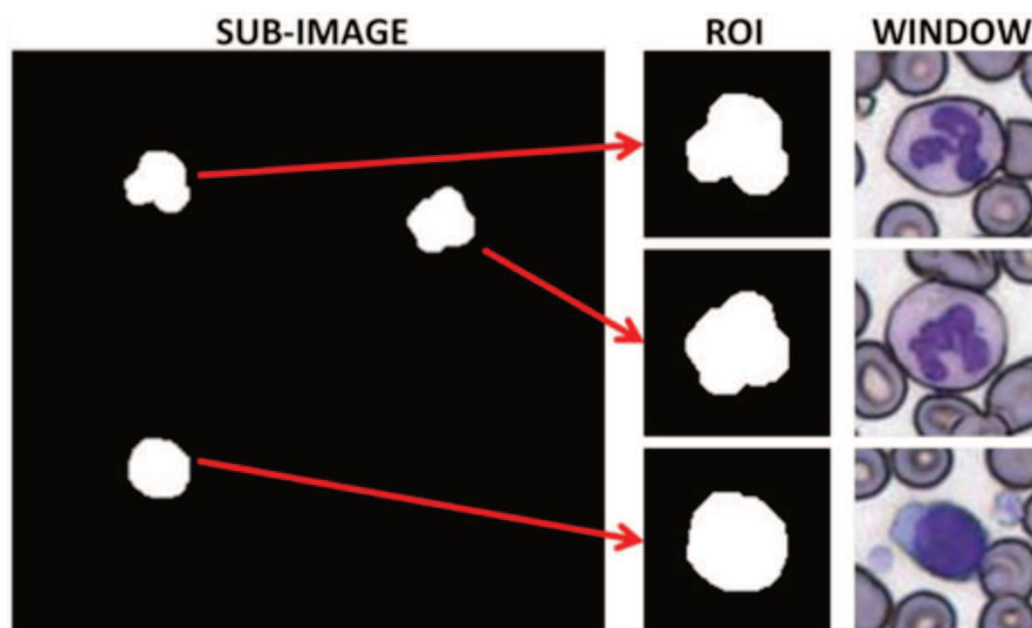
Figure 66 - Leukocyte's ROI and window extraction in one sub-image

A thresholding operation considering the grey-scale histogram of each window containing a leukocyte allows subsequently to separate plasma (background) from the cell; finally, leukocytes edges are detected performing morphological operations on a mask obtained after a thresholding operation considering the blue channel of the RGB window. Thus, geometric, chromatic and texture-based features for blood cells representation have been firstly extracted; an Artificial Neural Network and a Decision Tree have been then designed to discriminate among the five classes of leukocytes.

3.3.4.1.2   Innovative Results

Results are reported in Table 25 expressed in terms of values of Accuracy, Sensitivity and Precision on the test set only for the implemented ANN classifier.

Table 25 - Accuracy, Sensitivity and Specificity for a leukocyte classification evaluated via a 1-vs-all approach

	Accuracy	Sensitivity	Specificity
Neutrophils vs all	96.78%	95.55%	99.73%
Lymphocytes vs all	96.78%	98.81%	96.06%
Monocytes vs all	99.61%	92.59%	99.76%
Eosinophils vs all	99.45%	90%	99.53%
Basophils vs all	100%	100%	100%

The reason relies on the fact that the value of Accuracy for the Decision Tree is almost equal to 70%, that is, a much lower value than the one corresponding to the developed ANN. Reported results show that the proposed approach is suitable for a white blood cell classification; it has to be noted that performances reveal very high, even though the developed image processing procedure is quite simple.

3.3.4.2 Deep Learning Approach

In this section, Convolutional Neural Networks is proposed to perform leukocyte discrimination by means of two approaches.

3.3.4.2.1 Materials and Methods

In a first approach, a pre-trained Convolutional Neural Network is deployed to extract features from the same set of segmented images of the previous work, and it is subsequently combined with an SVM to perform the desired classification. The workflow followed in this approach is represented in Figure 67.
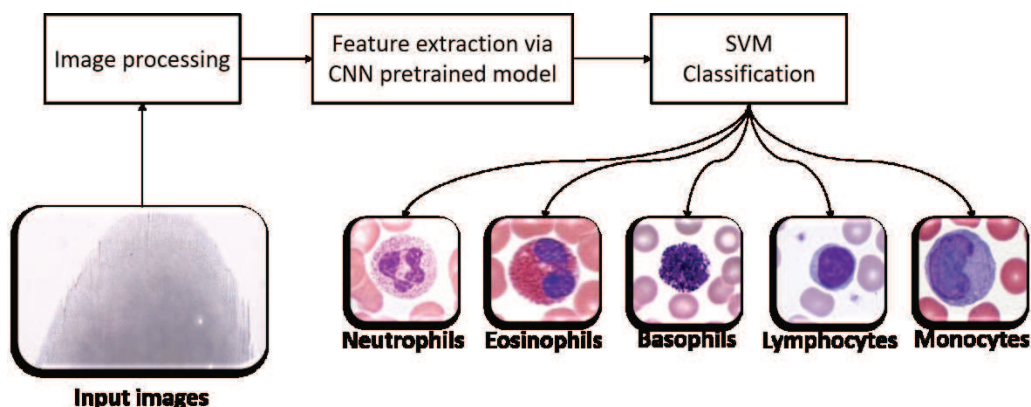
Figure 67 - Workflow for leukocyte classification considering CNNs as feature extractors

Then, the classification capabilities of the CNN is investigated to classify leukocytes using the segmented images as inputs. In this section, the considered model is the AlexNet by Krizhevsky et al. [384]. Differently, from previous approaches, the workflow represented in Figure 68 where the CNN is used for classification, shows that the feature extraction step is skipped.
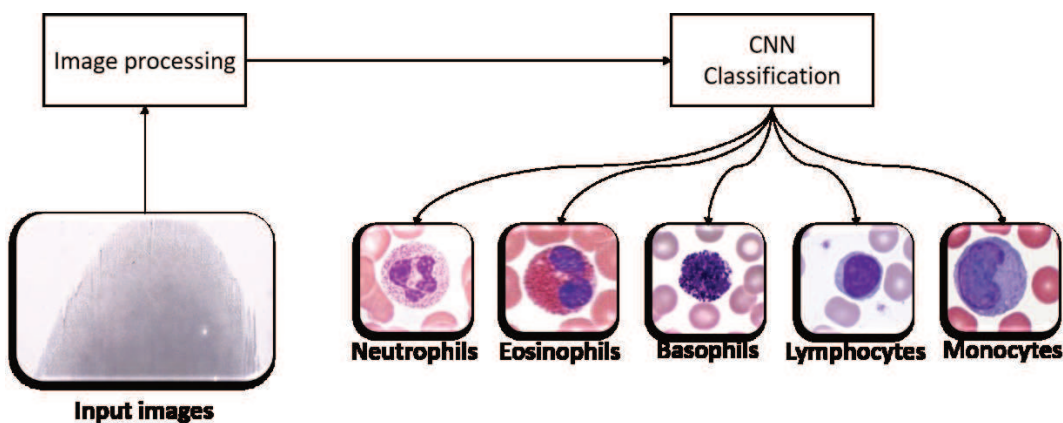
Figure 68 - Workflow for a leukocyte classification using CNN as a classifier

3.3.4.2.2   Innovative Results

As for the previous work, the following Table 26 and Table 27 report all obtained results expressed in terms of Accuracy, Sensitivity and Precision on the considered test set. Reported results show that both the proposed approaches based on CNNs seem to be very promising; in fact, the reported values of Accuracy are always higher than 95%. At the same time, the Sensitivity and Specificity values for both the considered approaches fluctuate depending on the kind of cells. However, this result is understandable by considering the number of samples for particular cells, such as Neutrophils and Lymphocytes, which is greater than the number of the other kinds of cells.

Table 26 - Values of Accuracy, Sensitivity and Specificity for a leukocyte classification evaluated via a 1-vs-all approach with an SVM classifier

	Accuracy	Sensitivity	Specificity
Neutrophils vs all	97.89%	98.78%	95.76%
Lymphocytes vs all	98.59%	97.93%	98.83%
Monocytes vs all	98.67%	48.15%	99.76%
Eosinophils vs all	99.38%	66.67%	99.61%
Basophils vs all	100%	100%	100%

Table 27 - Accuracy, Sensitivity and Specificity for a leukocyte classification evaluated via a 1-vs-all approach with a CNN classifier

	Accuracy	Sensitivity	Specificity
Neutrophils vs all	97.73%	97.12%	99.20%
Lymphocytes vs all	97.73%	99.70%	97.03%
Monocytes vs all	98.67%	48.15%	99.76%
Eosinophils vs all	99.61%	66.67%	98.84%
Basophils vs all	100%	100%	100%

3.3.5 Discussion and Conclusion

The scientific community is at the moment showing a great interest in identifying diagnostic, and staging protocols for periodic monitoring of the course of the three neoplasias dealt with in this survey, that is, breast cancer, hepatocellular carcinoma and blood tumour, due to their significant incidence in the population. It has to be noted that the cited protocols can be widely available due to their reduced invasiveness. In this chapter, the investigation of scientific papers and the designed, developed and evaluated CAD frameworks, focused on this topic shows that diagnosing through medical imaging currently reveals to be the best strategy, as it does not involve surgical interventions, besides guaranteeing a satisfactory compromise between invasiveness and specificity. Unfortunately, all developed protocols present important drawbacks:

1. CT-based imaging techniques expose patients to ionizing radiations;

2. MR analyses are characterized by huge costs that avoid their availability and diffusion in population;
3. the processing of peripheral blood stripes requires the use of innovative equipment available only into specialized centres.

However, the specificity and sensitivity values reported for the investigated approaches are very promising at the moment, thus leading researchers and clinicians towards the investigation of innovative techniques that can increase the reliability of clinical examinations and, at the same time, can reduce the above-mentioned disadvantages. Thus, taking into account the reported premises, in this chapter four innovative imaging methodologies have been carefully focused, which offer, each one in its own domain, the advantages that will be summarized below. The presented procedures can produce specific case history useful to extract the necessary information to implement decision support systems with very high-performance levels, such those presented in the previous paragraphs, using analogous and well-established CAD frameworks. Concerning with Digital Tomosynthesis for breast cancer, it can surely be affirmed that the herein presented method for identifying lesions of interest reveals quite innovative, as its accuracy and specificity show significant values. Moreover, although the considered technique is based on ionizing radiations, it is characterized by a dose release lower than the radiation released by a traditional CT. Therefore, in the near future, Digital Tomosynthesis for breast cancer could be assumed as a valid alternative to Magnetic Resonance Imaging, which does not exhibit ionizing radiation, but presents huge costs and is less specific than tomographic techniques. Then, by considering the experimental results on the comparison between a method in which several CNNs are used for extracting a set of features vector from an image, and a system based on handcrafted features, it can be noted that performance achieved using the first method are higher than those achievable by using the latter. Taking into account these results, in this chapter analogous results for feature extraction in medical images regarding the comparison between handcrafted approaches and automatic ones have been investigated. In particular, two methods have been compared for breast cancer: in the first one, two ANNs have been designed via an evolutionary approach and all the features extracted by means of a handcrafted procedure are used as inputs for ANNs. The first ANN is designed to discriminate binary class samples and has provided values of accuracy, sensitivity and specificity almost equal to 85%, to 86% and to 83%, respectively; the second ANN, designed for discriminating all different kinds of lesions in a multi-class approach, has shown a lower value of Accuracy almost equal to 75%. In the second method, CNNs have been used as feature extractors (automatic approach for features extraction); for this purpose, several pre-trained models have been considered. Several non-neural classifiers are subsequently trained considering an input dataset constituted by the set of features extracted by the CNN models. The best results are provided by the use of VGG-F, VGG-M and VGG-S as pretrained models and the KNN as nonneural learners. They have shown a value of accuracy almost equal to 92% (greater than the accuracy of the best ANN designed via the first method).

The triphasic CT technique with contrast medium for hepatocellular carcinoma detection and staging represents a novel technique, as it enables to have more observing windows due to its high value of specificity. Unfortunately, this technique is characterized by ionizing radiation exposure and by preliminary protocols for the administration of the contrast medium which result to be nephrotoxic and has to be very carefully submitted to allergic patients. However, the increasing amount of observing windows reduces overall the expected level of exposure to ionizing radiation during the standard period of disease monitoring. Regarding the detection and the classification of

hepatocellular carcinoma, a supervised approach based on the extraction of hand-crafted features and supervised CNN are developed and compared. Obtained results show high generalization performance for the supervised CNN approach; in fact, obtained values of accuracy, specificity and sensitivity are higher than 90%, while maintaining low the value of standard deviation. In comparison, the best result obtained considering the approach based on hand-crafted features shows values of accuracy, sensitivity and specificity almost equal to 80% while maintaining low the value of standard deviation.

Concerning blood tumours, the peripheral blood smear technique is absolutely not invasive but requires the presence of instrumentation and specialized personnel that, nowadays, is not always available in all the centres. Therefore, it is assumed to be a technique that will be used in the immediate future even through remote consulting or telemedicine procedures, which are currently increasing in internal medicine and haematology units. Obtained results in terms of accuracy, sensitivity and specificity for leukocyte classification evaluated through 1-vs-all approach using hand-crafted features and 1-vs-all approach with SVM classifier using CNN as a feature extractor and 1-vs-all approach with CNN classifier, respectively, are reported and discussed. According to the general results discussed in recent works comparing deep learning and traditional approaches for the classification of images or ROIs, also in the case of blood tumours, the best performances seem to be obtained by means of deep learning techniques. According to the results presented, the use of a CNN to detect tumours reaches better results rather than the use of ANN trained with hand-crafted features. As these improvements seem to be consistent across a large variety of domains, and, as it is usually the case, the development of a deep learning solution is found to be relatively straight-forward, this can be viewed as a major step forward in the medical computing field. Still, a major question remains as to how and when these frameworks can reach a substantial leap in performance. Future works in this field could be focused on improving the knowledge base for all tumours described. Moreover, since the presented workflow can be applied to other types of tumours in different organs, this chapter could be furtherly improved by deeply comparing handcrafted and non-handcrafted approaches.

3.4 Mixed Reality Systems for Computer-aided Maxillofacial Oncological Surgery

The field of oral and maxillofacial surgery includes many complex operation procedures in complex anatomical areas within oncologic surgery. As summarized by the American National Institutes of Health (NIH) (https://newsinhealth.nih.gov/2016/02/technologies-enhance-tumor-surgery), currently surgeons have no methods to rapidly visualize intraoperatively if a tumour has to be resected completely. Surgeons rely on the support of pathologists and on local examinations of the removed tissue by means of specialized microscopes [385]. These circumstances may involve a longer duration for the surgery, implying a more difficult work for the medical staff, a shorter availability of the Operating Room (OR) for further patients and higher chances of relapses [386].

The complete surgical removal of the tumour mass is of crucial importance in the treatment of head and neck cancer and – as any other manual task – is not exempt from human mistakes. Technologies like PET-CT provide vital support in the preoperative detection and planning phases. Eventually, all comes down to the surgeon's qualification and ability to operate on the latest techniques once in the surgery room. Despite all precautions, errors cannot always be avoided and for this reason a clear, planned surgical treatment management is of great importance, as it is also described in [387]: for the author a "medical mistake" is defined "[…] as a procedure with a wrong plan, an unfulfilled plan or no surgical plan at all". But assuming that every step is properly planned, and all the best decisions are taken for the patient's health, still "lapses" may occur. A surgeon could take the wrong instrument or pursue a wrong step because of a lack of available information, which could then be seen as a hazard (initializing mistake) for bigger and more serious errors, as described with Reason's Swiss, cheese model: the precautions are represented with Swiss cheese slices, and each hole is a possible weakness of the procedure. When these holes are even temporarily aligned, even a small initial mistake can lead to a failure of the process [388] and must, therefore, be avoided.

This limitation becomes more critical when compared with numbers: despite the good trend shown by the mortality rate falling from 6.2% in 1986 to 3.4% in 2015, the Canadian Cancer Society forecast the number of Head and Neck (H&N) cancer patients in Canada to rise by 58.9% in 2028-2032 from 2003-2007 (http://www.cancer.ca/~/media/cancer.ca/CW/cancer%20information/cancer%20101/Canadian%20cancer%20statistics/Canadian-Cancer-Statistics-2015-EN.pdf?la=en).

In recent years, spatial-aware augmented reality (AR) is already starting its positive trend in the fields of gaming and industrial production, but still, limited and experimental results are reported from the medical field as of early 2018. AR is an integrated technique of image processing, and in AR system, real objects and virtual (computer-generated) objects are combined in a real environment. Furthermore, real and virtual objects are aligned with each other and run interactively in real time [389]. Due to the advantages of AR visualization, an AR system able to superimpose pre-operative scans directly on the body of the patient could help specialists to immediately locate the tissues to be further examined and eventually removed, without relying only on less objective methods like palpation. A noteworthy study was conducted in 2016 by Wang et al. [390]. The study focused on the role of video see-through augmented reality for navigation in maxillofacial surgery. Although the authors present a thematic closer to orthodontics, the discussion of the requirements and limitations is comparable to the ones from oncological surgery. According to their analysis, the main issue, which is currently stopping research to go further, is the necessity of more precise registration

methods. Different studies have already been published in the recent months, but they limit their functionality to a mere visualization, having the specialist position the visualizations manually in the correct position by means of tap or gaze [391] and do not focus on H&N cancer.

As of today, most of the work using mixed reality conducted in the medical field has been done for training purposes. Sappenfield et al. [44] used the mixed reality simulator to perform training on how to access the subclavian vein. This shows the advantages of having a navigable 3D scene to benefit the medical staff. Promising results with regards to training are also provided by [66], where CBCT DICOM files are segmented and rendered as animated 3D models in a HoloLens environment. The presence of 3D animations rendered in the real world is believed to boost the medical understanding in radiology. The important technical outcome of this work is that not only is possible to visualize DICOM content in this environment, but also to apply animations on them without affecting the rendering. Initial trials for the introduction of HoloLens in a surgery room have been advanced by [67], where a full MRI scan of a brain is displayed through the glasses. In order to track the patient during the operation, also an additional tracking sensor was introduced. Although limited, this paper shows great appreciation and interest from the specialists towards new visualization techniques and underlines how visualization is still a bottleneck for biomedical imaging, as of 2017. The application of fiducial marker-based system was analysed by Andress et al. [392], for on-the-fly augmentation of orthopaedic surgery. Although it was not possible to apply the same algorithm to the current study, due to limitations in the acquisition of the dataset, it provides interesting consideration about the possibility to reduce the number of x-ray images and time needed. Other papers focus on medical workflow assistance: Hanna et al. [393] considers the introduction of HoloLens in radiology-pathology. Particularly the devices were utilized to help the specialist locate radiographically-localized metal clips during a biopsy. All of the users rated the technology as beneficial with a score of at least 4 over 5 and generally it was measured that the overall procedure was on average 85.5% compared to the same task performed without the electronic assistance. Similar results were also achieved by Lia et al. [394] when examining the HoloLens as an educational tool for surgical suturing. As of Q3 2017 still, no HoloLens-assisted surgical operations were documented. It is only with Pratt et al. (Q3-Q4 2017) [395] that they were officially and successfully employed during a live operation in London. As for the other cases, the technology received very high appreciation among the medical staff, but limitations are reported especially with regard to automatic registration of the 3D models. During the operation, the doctor had to place the virtual object over the patient's leg manually. Further trials were also conducted in France (Q4 2017), where a team in Paris lead by Dr Grégory in collaboration with Microsoft and TeraRecon used HoloLens for the first time not only to augment the surgical scene but also to share it with specialist around the globe through a Skype call (https://www.aphp.fr/actualite/1ere-intervention-chirurgicale-au-monde-realisee-avec-une-plateforme-collaborative-de). A recording of the operation has also been shared on a YouTube channel at (https://www.youtube.com/watch?v=xUVMeib0qek) for press purposes. An interesting approach, beneficial also for this study, is disclosed by both Cho et al. [396] for augmented craniofacial surgery, and Adabi et al. [397] for augmented plastic surgery. Both the authors also operate the device itself also for error measurement mixing image triangulation and spatial mapping information. [398] also provides a 9-question survey for comfort level, ease of use and satisfaction, graded on a 5-point Likert scale. For this purpose, given the experience of the advisors with the questionnaire from ISO-9241/110 [399], an ad-hoc questionnaire is discussed.

Despite the different medical applications of HoloLens, no one seems to have yet analysed the role that it could have for the resection of head and neck cancer, both in the surgery room as well as during preoperational planning. A comparable study has been performed by Perkins et al., considering breast cancer, where only in the US one-quarter of the women who undergo this operation are subject to relapse. An important contribution of this study is the possibility to compare the accuracy of a marker-based system with the marker-less approach to improve the interactions between domain experts and the system.

3.4.1 Research question

The goal of this part of the chapter regarding the new technologies introduced in the industrial field but also used in bioengineering field to understand the degree of aid that a mixed reality headset such as Microsoft HoloLens can provide to a surgeon during a routine surgical operation for tumour removal. A simple way to automatically overlap a hologram of the patient's PET - CT scan is evaluated. Furthermore, the differences between marker-based and marker-less automatic registration methods are being analysed. Afterwards, the actual application of the technology is analysed with the support of experts from both the fields of AR and surgery. To quantify the analysis, a questionnaire based on the standard ISO-9241/110 was dispensed to each specialist.

3.4.2 Materials and Methods

The software architecture

MevisLab v3.0.1 is a rapid prototyping platform for medical imaging; in this work, it is used to develop algorithms for tumour segmentation, and PET-CT scans 3D reconstruction.

The outputs are used to develop the Microsoft HoloLens Application under the platform of the Integrated Development Environment (IDE) of VS2017 (v151.5.0). The operating system is Windows 10 Pro 1709 with Software Development Kit (SDK) v10.0.16299.0. The AR scene is designed in Unity3D 2017.1.3f1. All the functions are programmed in Microsoft C#, and some famous toolkits are also involved, such as OpenCV for Unity (v2.2.7), Dlib FaceLandmarkDetector (v1.1.9) and Microsoft HoloToolkit (v1.2017.1.2).

Figure 69 shows the system framework and is described as follows: The first three steps of the workflow are developed under MevisLab, an open source rapid prototyping platform for medical application. The other steps are achieved under Unity and Visual Studio 2017 using Microsoft Mixed Reality Toolkit. On the basis of a PET-CT scan the patient, the MevisLab application is used to segment the volume of interest and reconstruct the relative 3D shape based on thresholds and Isosurfaces [133, 400]. The result is then loaded to the HMD and, after a proper calibration to the current user, the registration process is executed: with this step, the positioning of the object will depend both on the current position and rotation of the device, hence of the user, and of the target patient.
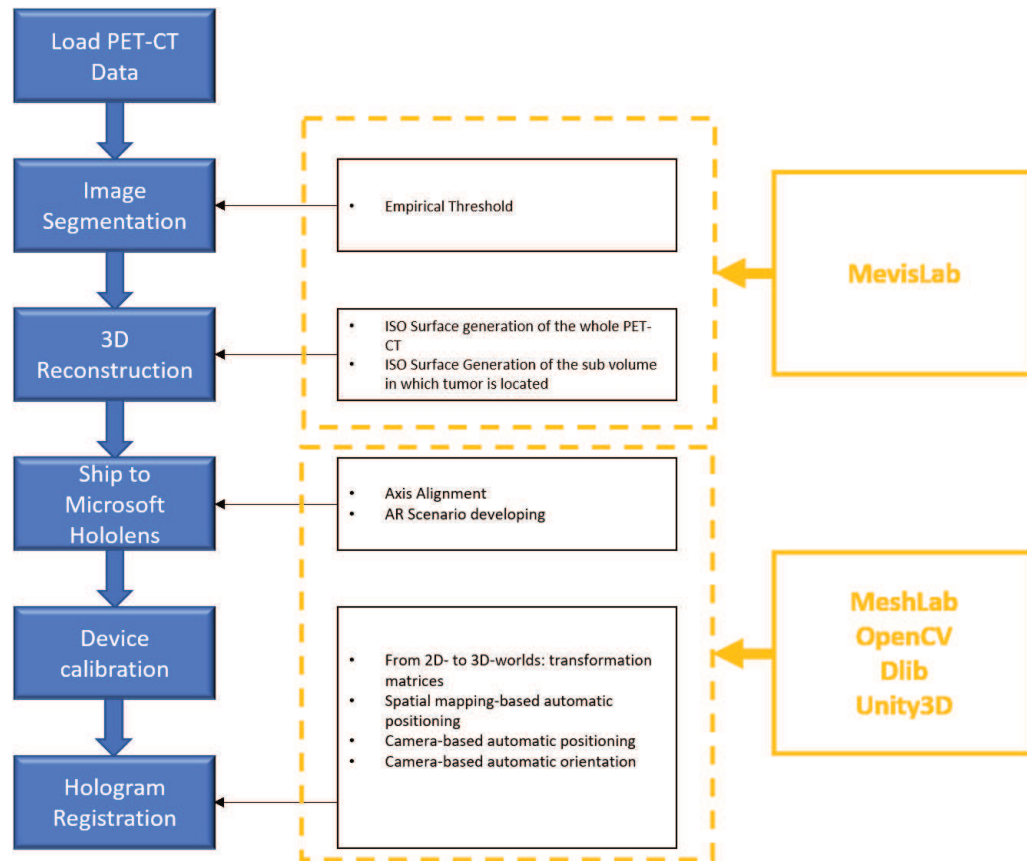
Figure 69 - The system framework

Image segmentation and 3D Reconstruction

Image Segmentation. Multiple studies have already been conducted on the topic of tumour segmentation, including different forms of head and neck cancer. Schinagl et al. in [401] compared five different segmentation techniques on this class of tumours without finding an algorithm being able to segment the complete volume of the tumours generally. For this first study, also considered the limited set of PET-CT scan available (2 of which only 1 could be tested in the real world for the augmented reality applications), it is decided, to consider a colour-based approach which gives sufficient results on the study case. Surgeons are required to check the resected area with microscopes, and the scope of this study is to provide information about the location and shape of a tumour. More detailed information is not necessary as the device would not be able to properly position and visualize it. This is due to both the resolution of the device and the suggested working distance of at least 1.25m. Under a minimum distance of 1.00m, according to documentation, HoloLens does not support stereo-vision. Plus, a more complex mesh would reduce the rendering frame rate, adding more displacement error (https://docs.microsoft.com/en-us/windows/mixed-reality/hologram-stability).

To achieve the task, the DICOM file of the PET is loaded into MevisLab, and the output is then processed through the Threshold module. For the kind of a tumour in the examination, an empirical threshold value of 29.5 provides satisfactory results, as shown in Figure 70.

Figure 70 - Segmented PET-CT of the patient. In orange, the tumour

3D Reconstruction

With the solution of the previous task, it is possible to extract a sub volume from the Region of Interest (ROI) of the PET-CT scan. This work is done mainly with two MevisLab modules, WEMIsoSurface and SoWEMRenderer. Both are based on the Winged-Edge Mesh library. Winged-edge [402] is a data structure typically used for mesh representations, in which for each edge also the symmetrical one is saved.

For the scope of this work only the surficial part of the tumour mesh is needed, therefore first the ISO surface is generated [403].

Figure 71 and Figure 72 show the effect of applying the segmentation algorithm to the images.

Figure 71 - Renderer ISO surface of the original PET-CT
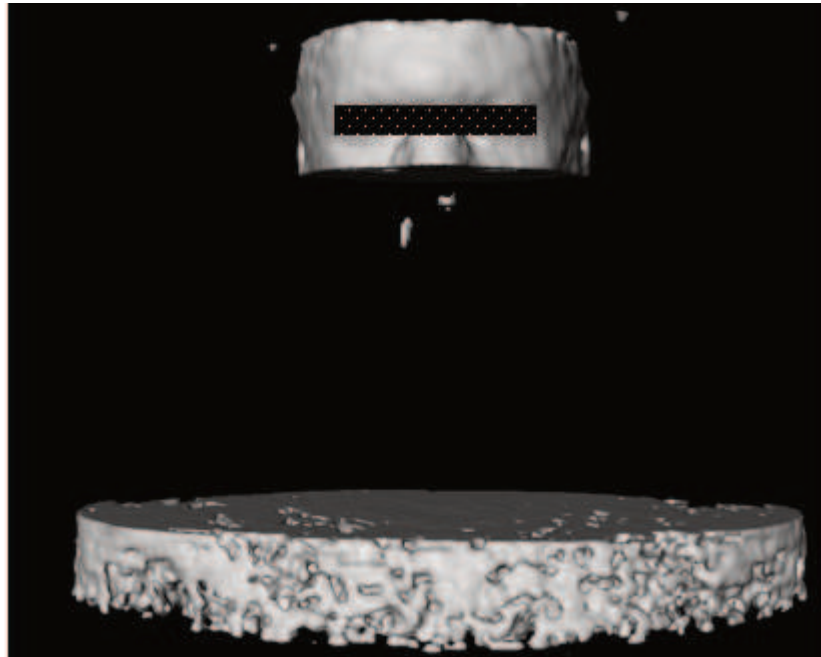
Figure 72 - Renderer ISO surface of the segmented PET-CT

The algorithm is applied only to a sub-region, which is also the portion of the volume where the tumours in the exam could be located, according to the medical advisor. The remaining volumes are used as a control in the mixed reality application, as described in the next paragraphs.

As the last step, WEMSave allows exporting the generated mesh in one of the different formats. Due to compatibility issues and to avoid adding further conversion steps, the selection is limited to the Wavefront format: strong of being the simplest one, and therefore easy to read at runtime.

Design and Development of AR Scenario

Axis alignment. The steps described in the previous paragraph define a way to extract a 3D model of the head tumours' surface starting from a generic PET-CT scan. No considerations have been taken so far regarding the orientation of the model. This is a trivial task, but it helps to keep the holographic app's logic simple:

- the origin of the axes matches with the mass centre of the 3D object,
- the orientation is set accordingly so that the gaze follows the positive direction of the z-axis direction.

This considerably simplifies the object management in the mixed-reality environment.

As these conditions might not be met a priori, a possible way to elaborate these transformations is the introduction of MeshLab (http://www.meshlab.net/).

This step is only needed for the automatic detection of the nose-tip in the 3D model, useful for the registration algorithm described follow.

As a first step, the origin needs to be aligned with the mass centre (Figure 73), this is easily achievable by using a transform filter for translation.
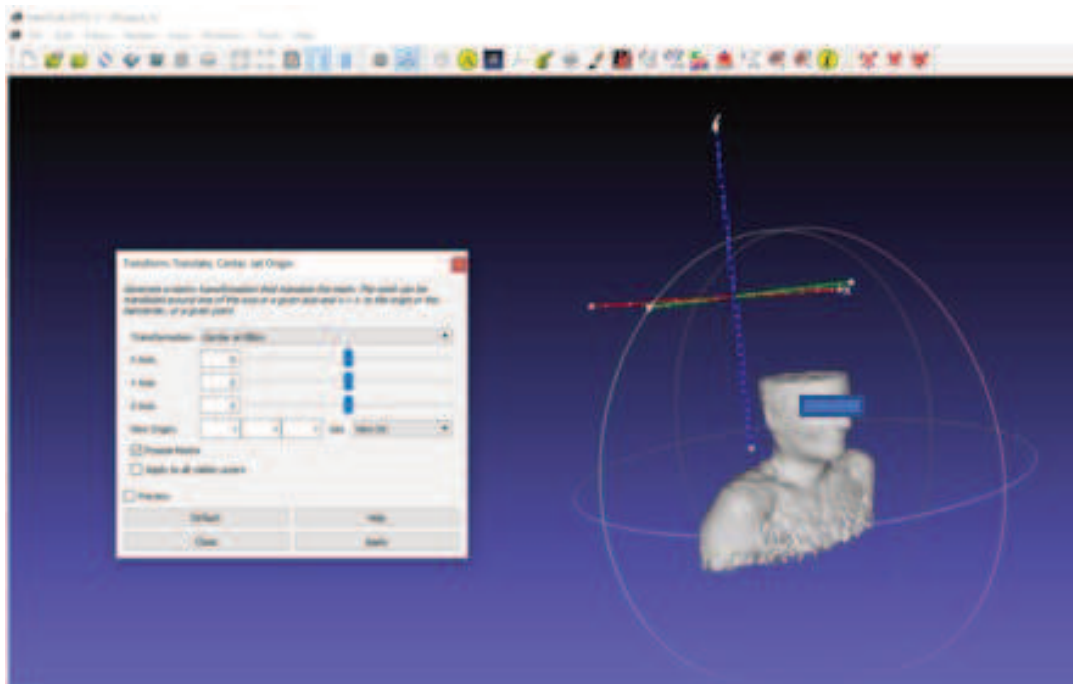
Figure 73 - An example of a 3D model in MeshLab. The origin differs from the centre of mass

The result of the transformation can be observed in Figure 74.
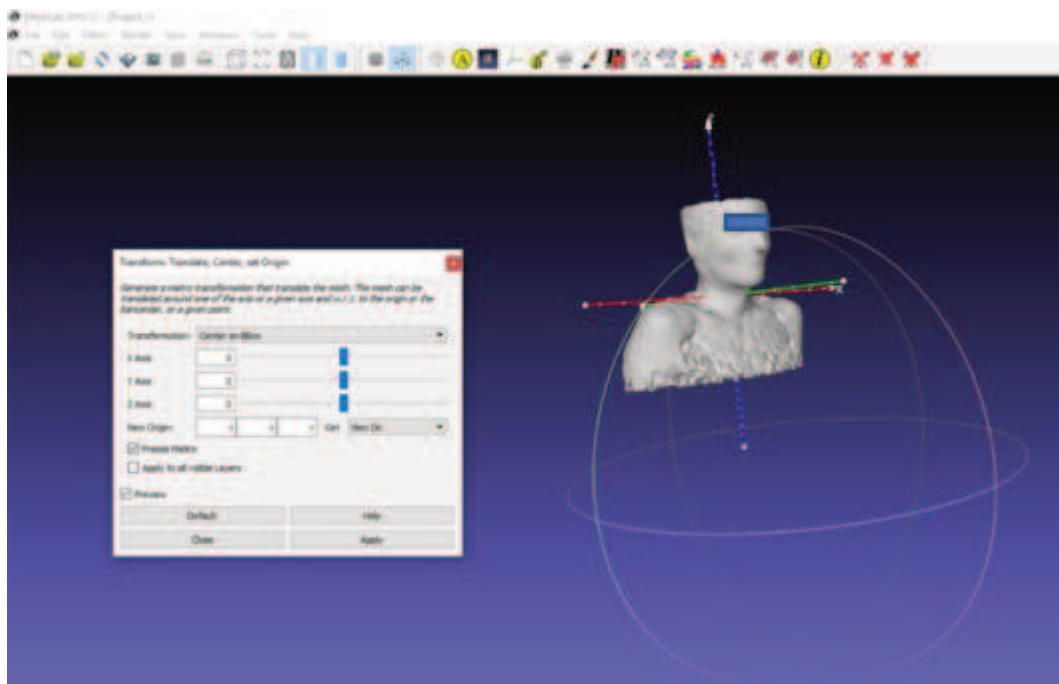
Figure 74 - Effect of the translation transform on the 3D model

Another step needed, as a convention, is the alignment of the gaze direction with the z-axis. In the case reported in Figure 74, this requirement is not met. Thus, a further transform is required: Flip and/or swap axis.

Analysing the case in the exam, both a swap between the Y and Z axes (Figure 75) and a flip of the Z axis (Figure 76) is needed.
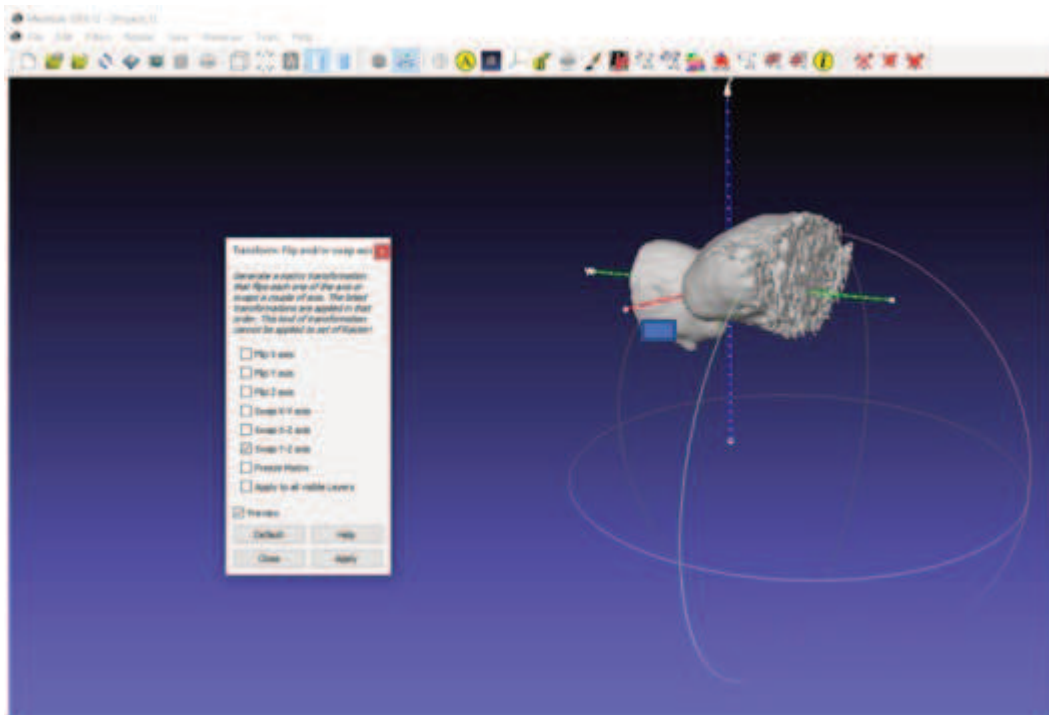
Figure 75 - Example of axes swap with MeshLab
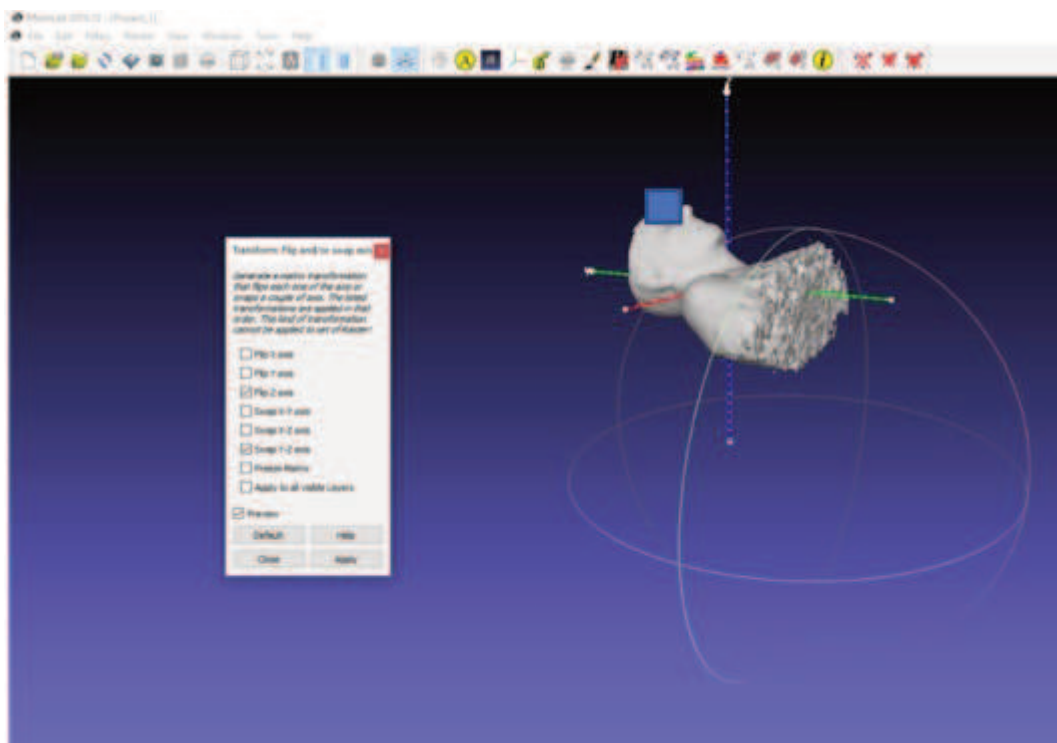
Figure 76 - Example of axis flip in MeshLab

The model now satisfies both the conditions for the automatic extraction of the head features.

Face and Landmark points detection in a holographic environment. In this work, the method suggested by Kazemi and Sullivan [304], already applied in many works in the medical field such as [404], is employed. At the origins of the cited algorithm is a cascade of regressors. Considered a generic landmark point pi = (xi, yi) of an image I, then it is possible to define a further vector

S = (piT, piT, …, piT) T

and with S(t) an estimation of S with the contribution of the t-th regressor:

S(t+1) = S(t) + rt (I, S(t))

The shape S is then cyclically estimated by creating a so-called cascade of regressors. Every single regressor makes predictions on different predefined pixel features, using a gradient tree boosting algorithm [405]. To learn the regression methods rt, first a training dataset of face images and shapes – (I1, S1), …, (In, Sn) – is needed. From this dataset, it is possible to define an initial shape estimate and the so-called target update step for each of the N training elements:

$$k_i \in \{ 1, …, n \}$$

$$\boldsymbol{S}_i^{(0)} \in \{\boldsymbol{S}_1, …, \boldsymbol{S}_n\} \setminus \boldsymbol{S}_{k_i}$$

$$\Delta \boldsymbol{S}_i^{(0)} = \boldsymbol{S}_{k_i} - \boldsymbol{S}_i^{(0)}$$

These data are iterated until the cascade of regressors are learnt with a sufficient ensemble accuracy.

Microsoft HoloLens is equipped with an HD RGB-camera and sensors for environment understanding. To recognise the presence of a face in the user's sight, only the RGB camera is used. The 1280x720p frames are analysed with the face landmarks detection algorithm offered by Dlib (http://dlib.net/).

Figure 77 shows the results of the application of the facial landmark detection algorithm.

Figure 77 - Facial landmark algorithm applied to the phantom, in green

This step only allows understanding if the patient's face is in the user's eyesight. Still, no information has been obtained about the actual spatial location of the patient, apart from the position in the 2-dimensional image.

Registration procedure

From 2D- to 3D-worlds: transformation matrices. The detection algorithm provides information about the pixel-location of particular facial features such as the nose tip. Called PI = (x1, y1) the point with the estimated pixel-coordinates of this feature, it is crucial also to estimate, as reliably as possible, the position of this point in the real world. This is achieved using transformation matrices, based on the intrinsic parameters of the HoloLens camera. The device internally generates a 3D mesh of the environment and allows to obtain distance information by correctly analysing this object. Therefore, it is necessary to convert the pixel-coordinates to an application-specific 3-dimensional coordinate system. As a first step PI is scaled to be, regardless of the actual image size, in a range [-1, 1] for both the axis. This new value, PP, is referred to as projected position. This vector is then un-projected to obtain the position related to the camera space. For this step, the 4x4 projection matrix pm needs to be introduced as follows:

Table 28 - The 4x4 Projection Matrix

Format				Values			
M11	M12	M13	M14	fx	0	0	0
M21	M22	M23	M24	skew	fy	0	0
M31	M32	M33	M34	cx	cy	A	-1
M41	M42	M43	M44	0	0	B	0

Where f is the focal length of the camera and c the optical centre. These values can be retrieved with the Camera API offered by Microsoft. Having now the representation of the projection matrix, and knowing the projected position of the point, it is now possible to perform the inverse operation and un-project the position. For calculation reasons, a 3-dimensional vector is necessary to achieve this step. Hence, a third unitary component is added to the PP vector.

PP3 = (PPx, PPy, 1)

Following the operations beneath, this vector can now be used to retrieve the camera space coordinates using "unproject" method:

```
public static Vector3 unproject(Matrix4x4 pm, Vector3 pp3)
{
  Vector3 up = Vector3.zero;
  var axsX = pm.GetRow(0);
  var axsY = pm.GetRow(1);
  var axsZ = pm.GetRow(2);
  up.z = pp3.z / axsZ.z;
  up.y = (pp3.y - (up.z * axsY.z)) / axsY.y;
  up.x = (pp3.x - (up.z * axsX.z)) / axsX.x;
  return up;
}
```

The unitary value added for the z-component does not alter the overall result of the operation as this value is later corrected by application of a ray-casting algorithm.

Another important element to take into consideration is the camera-to-world matrix. This is a time-dependent element as its values change over time as the camera moves in the space (the headset is not still in the environment). This matrix is already provided by the Mixed Reality Toolkit and needs to be refreshed for each photo or frame acquired with the device. The multiplication of this matrix by the un-projected vector indicates a point Pu in the application-specific coordinates system (https://docs.microsoft.com/en-us/windows/mixed-reality/locatable-camera).

As a doped value is used for the depth component of the vector, this value needs to be further corrected actually to match the desired position. A possible technique, recommended by Microsoft, implies the utilisation of a ray-casting algorithm on the internally generated mesh of the environment. Due to poor results, a further method is then analysed to compensate for the error introduced by the depth sensors partially.

Spatial mapping-based automatic positioning. The point obtained in the previous step does not match exactly with the position of the facial feature, but it has a particular property, which relates it to the real object. It lies on the segment that connects the camera position, at the time of acquisition, with the actual target position (https://docs.unity3d.com/ScriptReference/Physics.Raycast.html).

This condition defines a possible way to find the target position by analysing the spatial mapping mesh. It is possible to feed a ray-casting algorithm with the camera position, C, as the starting point and the difference vector D = Pu – C as a target direction. Furthermore, it is known a-priori that the target is not situated farther than a few meters from the user. This allows setting a maximum distance of, e.g. 3 meters as stop criterion [406].

Summing this explanation up, the algorithm discussed here – excluding any possible optimisation criteria – looks for the particle closest to a given starting point, which satisfies the criterion of lying in a defined direction. The returned value would be the real-world position of the facial feature. Generally, the nose-tip feature provides a good value for this calculation as it is also generally simple to match it in the 3D model of the patient, given the axis orientation is known. Considering a reference system where the z-axis is following the head direction, the nose-tip would generally be the point with the highest z-value. The actual position of the object needs then to be adjusted by summing the vector connecting the nose tip to the mass centre of the object, to the one provided by the ray-cast algorithm. The result of this step will be a PET-CT placed in the right position, but still not with the expected orientation, as the patient could assume any position. This approach is recommended by the headset producer, but it is subject to the measurement error of the environmental sensors which cannot be ignored (see Figure 78).

Figure 78 - Example of evident translation error

To partially reduce this error, the user would have to recalibrate the device every time that it is worn. This step might not always be possible during a surgical operation as it is time-consuming.

Camera-based automatic positioning. To avoid or at least compensate the error introduced by the environmental sensors, a further methodology, already known in computer vision and optics, has been experimentally evaluated with HoloLens. As the size of the patient's head is previously known from the PET-CT scan, which already provides a 1:1 scale model, it is worth to consider the application of triangle similarity for distance evaluation.

Defined with W the distance in meters between the eyes of the patient, and with P the distance in pixels between two facial landmarks corresponding to the left and right eyes. Defined with D the distance from patient. In case of a pin-hole camera it is possible to derive an approximation of the perceived focal length F with the relationship $F = (P \times D)/W$.

As the facial landmarks are retrieved by a heuristic algorithm, P is only an approximation of the actual value. For this reason, this relationship is considered in its simplest form.

Considering the case when P = 10 pixels, D = 1 m, W = 0.1 m, the approximation of the perceived focal length would be $F = (10 \times 1)/0.1 = 100$.

As this value would have to be constant, it is now possible to consider the relation $D' = (100 \times 0.1)/P'$ where D' is the distance of the same object, assuming the eyes are P' pixels apart[407, 408]. This method only provides information regarding the magnitude of the distance from the camera location; no information is given about its direction. The direction information is retrieved applying the transformation matrices. This approximation only provides an alternative to the application of the ray-cast algorithm and not rely uniquely on the spatial information. As this method is subject to measurement errors due to user's inexperience, it is considered a good practice to compare the calculated point with the one provided by the first method. If the difference between the two positions lies outside of a certain confidence level of the first method, then it is highly probable that either the patient's image was acquired with a wrong alignment or the facial landmarks did not accurately enough match the real positions.

Figure 79 shows an example of a completed registration.

Figure 79 - Example of registration with negligible error

The correct registration can also be noticed on the 2D image thanks to the reference points: the red points marked on the printed model are completely overlapped by the green points of the hologram. In this case, the two yellow irregular elements indicate the location and morphology of the tumours, while the bigger element depicts a section of the CT scan to be used as a reference to monitor the location.

Camera-based automatic orientation. Once the hologram is placed in the right position in space, it is necessary to assure that it shares the same facing direction of the patient. As of current state of the art, it is not possible to retrieve this information from the spatial mapping. Following the results achieved by other commercial holographic applications (https://github.com/EnoxSoftware/DlibFaceLandmarkDetector), this step is achieved by relying only on 2-dimensional camera information. Generally, the position of certain facial landmarks is known a priori in the 3D model, but only a 2D projection of the patient's facial landmarks is known. This problem is addressed to as Perspective-n-Point (PNP) problem. This approach requires further information regarding the intrinsic properties of the camera, such as nominal focal length and distortion, which are provided by the Camera API.

From the hypothesis, the position of a particular point in the world space is known, e.g. P3 = (K, J, L). Once the rotation (R) and translation (T) matrices are known, it is possible to convert the point P3 in camera coordinates, and therefore retrieve its projected position.

$$\begin{bmatrix} X \\ Y \\ Z \end{bmatrix} = R \begin{bmatrix} K \\ J \\ L \end{bmatrix} + T = [\, R \,|\, T \,] \begin{bmatrix} K \\ J \\ L \\ 1 \end{bmatrix}$$

In this case, it is necessary to solve the linear system to obtain R and T. This would not be an issue if it is not for the detail that (X, Y, Z) is generally unknown. It is only possible to retrieve the 2D position in the video frame.

In the case of null distortion, this can be achieved by a simple multiplication such as:

$$\begin{bmatrix} x \\ y \\ 1 \end{bmatrix} = s \begin{bmatrix} f_x & 0 & c_x \\ 0 & f_y & c_y \\ 0 & 0 & 1 \end{bmatrix} \begin{bmatrix} X \\ Y \\ Z \end{bmatrix}$$

where fx, fy, cx, and cy are the same constants defined for the projection matrix.

Limitation in this equation is given by the fact that the optical distortion is not taken into account and s, the scale factor, is also unknown. Therefore, it is only possible to calculate s × ⟦(X,Y,Z)⟧ ^T. An equation of this kind, with an unknown scale factor, can now be solved with the Direct Linear Transform (DLT) [409] according to [410].

This approach is subject to a so-called re-projection error, due to a wrong estimation of the rotation matrix. To reduce this error, a common technique is to add an optimisation algorithm that checks if with small changes in the rotation matrix the re-projection error decreases. OpenCV, for instance, implements the Levenberg-Marquardt optimisation algorithm [411, 412] to reduce this error (https://docs.opencv.org/2.4/modules/calib3d/doc/camera_calibration_and_3d_reconstruction.html).

Experiment scenario.

Although the system is designed for working in any environment, a particular test-bed IS reconstructed. The rendering was tested over a 3D-printed version of the unsegmented patient's mesh, which was laid over a green surface to simulate the environment of an operating room (see Figure 80).

Figure 80 - A photo of the 3D-printed model placed in the test-bed environment

To obtain the reproduced phantom, the model was first converted to the STL format (an acronym for Standard Triangulation Language) and then opened with the ad-hoc software provided by the producer of the printer, MakerBot Print. The STL object can be generated both within MevisLab as well as afterwards with MeshLab. The latter was chosen in this case as, to save time and material, the mesh went under a manual, post-processing step. The result was then printed with the MakerBot Replicator+ using a PLA filament.

In this way, it is possible to reconstruct a surgical scene at its very beginning. This is still only a subset of the whole scenario, as during a maxillofacial surgery the patient's face can be not just rotated, but also cut open considerably. According to the location of a tumour, a different area might be interested by the cut, and this not only makes it hard to define a general position for markers but also does not guarantee that enough facial features could be available all over the operation. Therefore, this study considers the initial step of providing support at the beginning of the operation, to avoid initial errors and hence reduce the chances of a surgical mistake.

Figure 81 - DDDr. Jurgen Wallner while trying the mixed reality application during the showcase

3.4.3 Innovative Results and Discussion

Technical Results

One of the settled goals is to compare the performance of the registration algorithm to the results of a marker-based system [399]. The choice of working without markers is dictated by the surgical workflow, which often involves an opening of the whole face area. Nonetheless, results similar to [399] are expected in case the markers would be introduced.

A particularity of the HoloLens device is that it needs to be recalibrated often, and sometimes this would not be possible during operation. For this reason, both the results obtained before and after calibration are reported. This is to give a hint of how much a non-well-done calibration can affect the registration process. In both cases, the measurements were repeated 4 times at a distance of circa 80 cm from the target.

Table 29 - Errors of the marker-based system described in [399]

Error in up-down dimension (mean ± standard deviation)	-1.1 ± 2.0 mm
Error in right-left dimension (mean ± standard deviation)	0.1 ± 1.2 mm
Error in the back-front dimension (mean ± standard deviation)	Not specified

Table 30 - Error of the automatic registration before the calibration

Error in up-down dimension (mean ± standard deviation)	-12.5 ± 2.5 mm
Error in right-left dimension (mean ± standard deviation)	7.0 ± 2.1 mm
Error in the back-front dimension (mean ± standard deviation)	-19.0 ± 2.0mm

Table 31 - Error of the automatic registration after the calibration

Error in up-down dimension (mean ± standard deviation)	-4.5 ± 2.9 mm
Error in right-left dimension (mean ± standard deviation)	3.3 ± 2.3 mm
Error in the back-front dimension (mean ± standard deviation)	-9.3 ± 6.1mm

Analysing the errors from Table 30, the calibration results in a necessary step in case of automatic registration, as it seems to reduce the error by half when comparing with the results of Table 31. Therefore, this step would have to be taken into consideration during the preplanning of an operation.

Furthermore, the utilisation of facial landmarks as markers seems to diminish the accuracy of the system, as can be observed by comparing the results from Table 30 with those from [399] in

Table 29. No comparison can be made regarding the back-front dimension, as this is not tested in the reference study. Anyhow, this appears to be the most relevant shortcoming of the device: as of today, it is not possible to rely on depth information on a millimetre scale, and this forces the specialist to have to look at the hologram from only one direction. A higher average registration error is expected as the face detection algorithm introduces an artificial noise, is it based on a heuristic approach.

Nonetheless, lower average errors are registered when comparing the study with the marker-less video see-through AR system described in [413], this could be thanks to the introduction of integrated spatial understanding capabilities in the HoloLens display, which avoid the necessity to synchronize the display with a third device, an ad-hoc synchronization that can lead to a higher overall measurement error.

Clinical feedback

Two trial sessions have been organized, at the Department of Oral and Maxillofacial Surgery and the Institute of Computer Graphics and Vision, respectively.

During the first showcase, 6 medical experts participated, 2 of which are nurses, 3 doctors and one the lead of the department. They all showed interest and appreciation for the technology. To quantify this appreciation, a questionnaire based on the standard ISO-9241/110 is dispensed to each specialist (Table 32). Each question could be answered with a 6-point Likert scale ranging from 0 (completely disagree) to 5 (completely agree).

Table 32 - ISO-9241/110-based questionnaire and relative answers given by the medical staff

Question	Average answer	Standard deviation
1. The software is easy to use	4.17	±0.69
2. The software is easy to understand without prior training	4.33	±0.75
3. The software is easy to understand after an initial training	4.50	±0.50
4. The software offers all the necessary functionalities (the minimum requirements are met)	3.50	±0.50
5. The software successfully automates repetitive tasks (minimal manual input)	4.00	±0.58
6. The way of interaction is uniform through the operation cycle	4.33	±0.47
7. The introduction of the software considerably reduces the overall operation time (or manual tasks)	3.33	±1.11
8. The introduction of the software can considerably increase the quality of the operation (e.g. less risk of failures)	4.16	±0.89
9. The introduction of similar software in a surgery room would be beneficial	4.67	±0.47
10. The software would be helpful for the educational purpose	5	±0
11. The software would be helpful in an ambulatory and/or doctor's office	4.50	±0.76
12. I am an expert in the medical field	4.66	±0.47
13. I am an expert in the field of human-computer interaction	2.83	±1.57

ENSEMBLE RESULTS - SHOWCASE 1
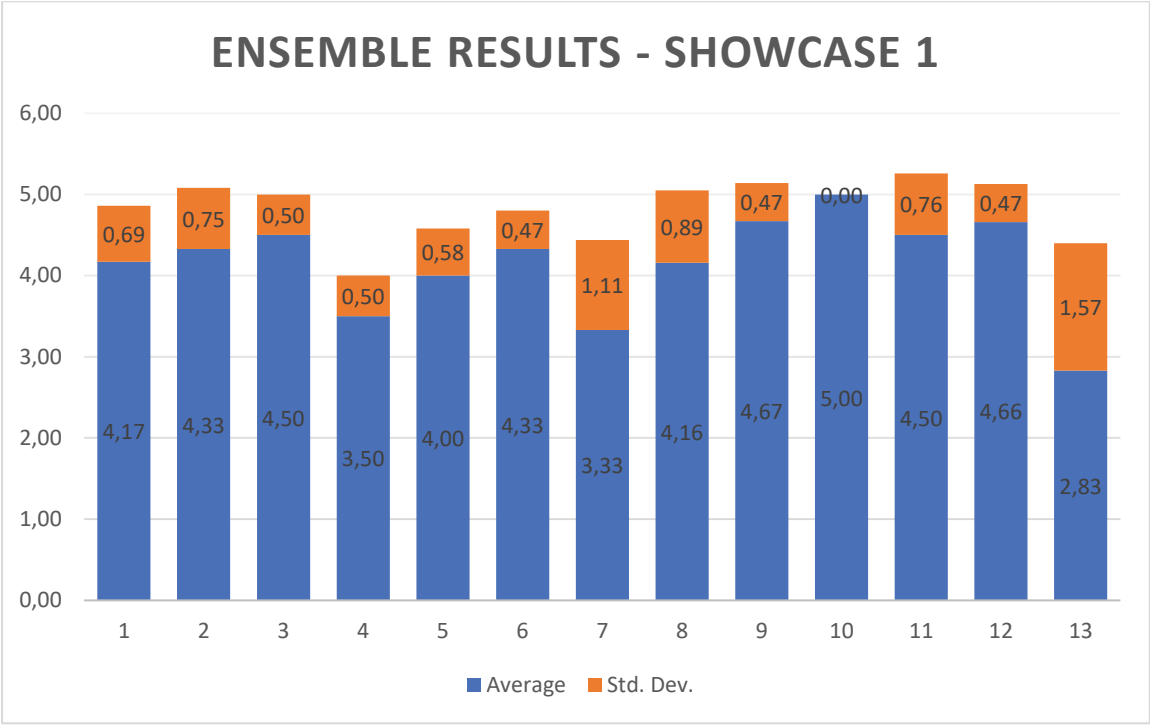
The questionnaire is then proposed also to technical experts (Table 33).

Table 33 - ISO-9241/110-based questionnaire and answers were given by the experts in mixed reality

Question	Average answer	Standard deviation
1. The software is easy to use	4.29	±0.45
2. The software is easy to understand without prior training	4.41	±0.69
3. The software is easy to understand after an initial training	4.71	±0.70
4. The software offers all the necessary functionalities (the minimum requirements are met)	3.71	±1.03
5. The software successfully automates repetitive tasks (minimal manual input)	4.29	±0.70
6. The way of interaction is uniform through the operation cycle	4.00	±1.07
7. The introduction of the software considerably reduces the overall operation time (or manual tasks)*	4.6	±0.49
8. The introduction of the software can considerably increase the quality of the operation (e.g. less risk of failures)*	4.00	±0.71
9. The introduction of similar software in a surgery room would be beneficial*	4.50	±0.87
10. The software would be helpful for the educational purpose	4.43	±0.73
11. The software would be helpful in an ambulatory and/or doctor's office*	4.20	±0.75
12. I am an expert in the medical field	0.86	±1.12
13. I am an expert in the field of human-computer interaction	4.28	±0.70

*Not everyone provided an answer to this question

ENSEBLE RESULTS - SHOWCASE 2
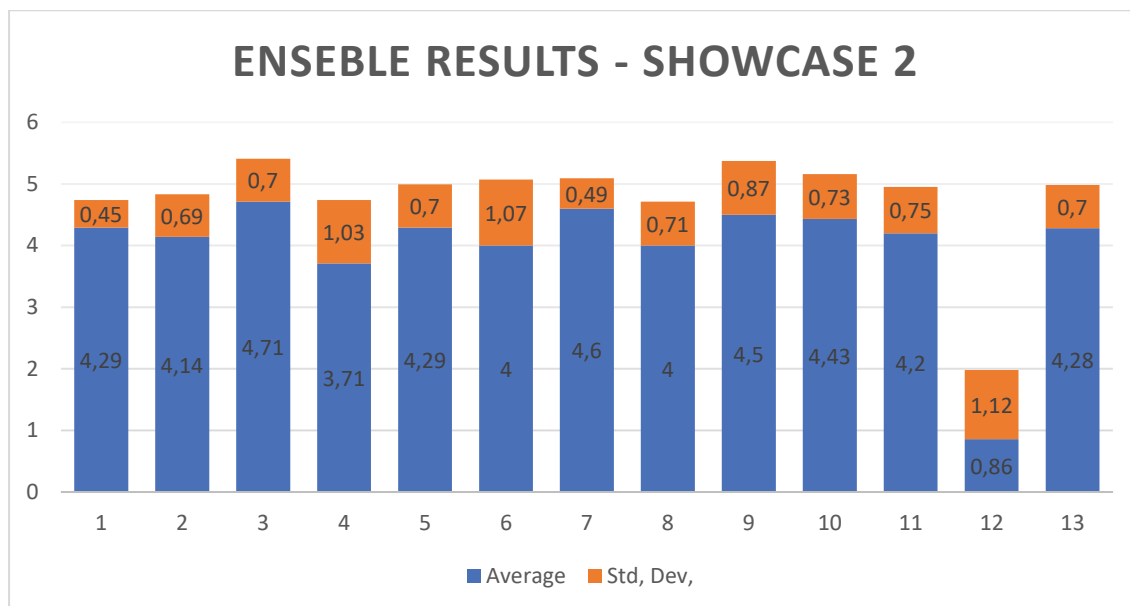
Some of them explicitly asked for not answering those medical related questions as they were not feeling comfortable with them. This group consisted of 7 persons, one professor, two senior researchers and four students of the doctoral school.

During the presentation, three doctors specified that information regarding the position of the bones would be of great help to better address the position of a tumour, this reflects on the average value of 3.50 (somewhat agree – agree) given to question four. The chief surgeon also suggested adding information regarding the position of the blood vessels.

It is also interesting to analyse questions seven, eight, and nine altogether: although they mostly considerably agree on the benefits that this application could bring in an operating room, they consider it more a quality assurance tool than a time-saving method. Noteworthy to mention is also that despite the positioning and rotation errors discussed in the previous paragraph, all participants completely agree on introducing this tool during training.

One more consideration can be done by comparing both Table 32 and Table 33: although all participants agree that the system is easy to use and understand, it can be noticed how it is slightly simpler to use for the engineers, despite the fact that the doctors are more confident with the application already before the initial training. This allows to confirm that the application is well designed for the medical staff, but generally, they need training on how the technology itself works.

3.5   Conclusions

In this chapter, three designed, developed and evaluated use cases are described. For each scenario, innovative results are discussed.

Considering an Industry 4.0 scenario, the described use cases are suitable to support human workers (in these cases physicians) in their decisions. The Technical Assistance principle that describes how the ability of assistance systems could support humans by aggregating and visualising information comprehensively, via immersive and innovative Human-Computer Interfaces, for making informed decisions, solving urgent problems and conducting a range of unpleasant tasks, is satisfied. In fact, in the innovative results paragraphs are discussed, for each use case, the data acquired during the experiments and their elaborations using decision support systems. Concerning the architecture of an Industry 4.0 scenario, the described systems could be introduced as a part of a Medical Cyber-Physical system linked to an IoS and IoT network, to support physicians. In particular, in the first use case, a healthcare network is proposed to link innovative devices uses during the neurological examination, to store all data collected. The data are then processed, and several intelligent algorithms (such as SVM, ANN, etc.) are used to extract some important information about the patient. A final document is then produced to support physicians in the final diagnosis.

Moreover, the second use case described only the core of a future Medical Cyber-Physical system that could be implemented in diagnostic examinations. All the acquisition techniques used in this case are standardised, and the innovative part consists of intelligent systems based on machine learning and deep learning approaches, applied to medical images in the context of blood, liver and breast neoplasias diagnosis. However, a network to link standardised acquisition system and physicians teams should be theorised to improve the quality of the services offered by healthcare institutions. Finally, a realised Mixed reality system is described. The results emphasised how these type of systems are suitable also in an operating room during a surgical operation. These new technologies introduced in the manufacturing environments could also be used in industrial bioengineering field to support human workers (in this case surgeons) during their work. The results are the proof that a combination of CAD frameworks and algorithms used to track features in real-time are suitable to create immersive and intelligent systems that could help, in a non-invasive way, during delicate operations.

4   Conclusion and Future Works

The studies conducted in this PhD work aimed to design, develop and evaluate intelligent systems to support human workers both in the industrial manufacturing and industrial bioengineering fields. The main contributions include the design, development and evaluation of decision support systems via immersive human-computer interfaces using both different innovative and intelligent machine learning and deep learning algorithms and mixed and augmented reality technologies and techniques. A set of experiments for each scenario demonstrated the high level of system accuracy. Therefore, the systems can support human workers following one of the four principles of Industry 4.0: technical assistance. To satisfy other principles (interoperability, information transparency and decentralized decisions) future works should investigate the interconnections between the systems described in this work and the environment's infrastructure consisting of the Internet of Things and Internet of Service networks. Although a healthcare network is theorised in Section 3.2.2 , further investigations must be completed. However, the healthcare network's core is described and evaluated and can be applied to other type of diseases in which the physician should interact with machines by means of human-computer interfaces. The approach is well-known in the manufacturing field in which the Industry 4.0 paradigm was theorised in 2011. Therefore, concerning an Industry 4.0 scenario architecture, the described systems could be placed in the cyber-physical system component (or medical cyber-physical system component if the applications are contextualised in the industrial bioengineering field), demonstrating the versatility of Industry 4.0 principles, techniques and technologies. In particular, five works and relative results were described.

In the first work, an innovative workbench for adaptive maintenance was described. The design and development of a prototype for an effective use of the AR in the industrial world, particularly for manual working stations, was conducted. This prototype consists of an aluminium frame with a camera and a projector that dynamically projects information on the real object to be maintained on the workbench. The camera, using a tracking algorithm, computes (in real time) the position and orientation of the object while the projector displays the information always in the desired position, even moving the object when necessary. The communication between components is performed by means of a database data structure for the management of AR instructions and for interactive access to this information. This work creates the basis for the development of an effective AR application for the industrial environment. Further tests and experiments should be performed to create reliable, user friendly and scalable solutions. The prototype designed in this work still must be optimized, specifically in regard to the use of graphic signs, user interface navigation, frame optimization and the projection of information on undercut points.

The second work presented K2RULA, a real time semi-automatic RULA evaluation system based on Kinect v2. This system speeds up the detection of critical conditions and reduces subjective bias. K2RULA is able to analyse off-line data and save the results for deeper ergonomic studies. The system was validated with two experiments, using as baseline an optical motion capture system and a RULA expert, proving the reliability of K2RULA as a faster alternative to classical visual inspection evaluation. Moreover, the system was compared to commercial software, the Jack-TAT, based on the Kinect v1 sensor. In conclusion, the proposed system can be effectively used as a fast, semi-automatic and low-cost tool for RULA analysis.

The materials and methods used in the first two works contextualised in the manufacturing field can also be used in the bioengineering field to design and implement

systems to support physicians in their work. In fact, in the third work, the proposed model of a healthcare network based on big data analytics for Parkinson's and Blepharospasm's diseases should be capable of transforming the way healthcare providers use sophisticated technologies to gain insight into their clinical and other data repositories and make satisfying decisions. Moreover, the use of machine learning algorithms contextualized in the proposed big data system can support clinicians in their decisions and in monitoring follow ups for each patient's disease. In the future, attention will be focused on issues such as guaranteeing privacy, safeguarding security and establishing standards and governance, thus further improving tools and technologies. The design and development of the motor examination-handwriting analysis acquisition system for Parkinson's disease is described in this work and, in the future, the proposed healthcare network will be more accurately implemented, tested and validated.

In the fourth work, an investigation of scientific papers focused on the computer-aided diagnosis's topic indicated that diagnosing through medical imaging is currently the best strategy, as it does not involve surgical interventions and guarantees a satisfactory compromise between invasiveness and specificity. Unfortunately, all developed protocols present important drawbacks:

- CT-based imaging techniques expose patients to ionizing radiation;
- MR analyses are characterized by huge costs that avoid their availability and diffusion in the population;
- The processing of peripheral blood stripes requires innovative equipment available only in specialized centres.

However, the specificity and sensitivity values reported in literature for the investigated approaches are currently promising, thus leading researchers and clinicians towards the investigation of innovative techniques that can increase the reliability of clinical examinations and, at the same time, reduce the above-mentioned disadvantages. Thus, considering the reports, in this work, four innovative imaging methodologies were carefully analysed, each offering, in its own domain, advantages that are summarized below. The presented procedures can produce specific case histories useful to extract the necessary information to implement decision support systems with high-performance levels, such those presented in the previous paragraphs, using analogous and well-established CAD frameworks. Concerning digital tomosynthesis for breast cancer, it can be affirmed that the presented method for identifying lesions of interest is quite innovative, as its accuracy and specificity have significant values. Moreover, although the considered technique is based on ionizing radiations, it is characterized by a lower dose release than the radiation released by a traditional CT. Therefore, in the near future, digital tomosynthesis for breast cancer could be a valid alternative to MRI, which does not exhibit ionizing radiation but presents huge costs and is less specific than tomographic techniques. Then, by considering the experimental results of the comparison between a method in which several CNNs are used for extracting a set of features vector from an image, and a system based on handcrafted features, performances achieved using the first method are higher than those achievable using the second. Taking into account these results, in this work, analogous results for feature extraction in medical images regarding the comparison between handcrafted and automatic approaches were investigated. In particular, two methods were compared for breast cancer. In the first, two ANNs were designed via an evolutionary approach, and all the features extracted by means of a handcrafted procedure were used as inputs for the ANNs. The first ANN was designed to discriminate binary class samples and provided values of accuracy, sensitivity and specificity almost equal to 85%, 86% and 83%, respectively. The second ANN, designed for discriminating different kinds of lesions in a multi-class approach, had a lower value of

accuracy, almost equal to 75%. In the second method, CNNs were used as feature extractors (automatic approaches for features extraction); for this purpose, several pretrained models were considered. Several non-neural classifiers were subsequently trained considering an input dataset constituted by the set of features extracted by the CNN models. The best results were provided by the VGG-F, VGG-M and VGG-S as pretrained models and the KNN as nonneural learners. They indicated a value of accuracy almost equal to 92% (greater that the accuracy of the best ANN designed via the first method).

The triphasic CT technique with contrast medium for hepatocellular carcinoma detection and staging represents a novel technique, as it enables more observation windows due to its high value of specificity. Unfortunately, this technique is characterized by ionizing radiation exposure and by preliminary protocols for the administration of contrast medium, with nephrotoxic results, and which must be carefully administered to allergic patients. However, the increasing number of observation windows reduces the overall expected level of exposure to ionizing radiation during the standard period of disease monitoring. Regarding the detection and classification of hepatocellular carcinoma, a supervised approach based on the extraction of hand-crafted features and a supervised CNN were developed and compared. Results suggested high generalization performance for the supervised CNN approach; in fact, obtained values of accuracy, specificity and sensitivity were all higher than 90%, while maintaining low values of standard deviation. In comparison, the best result obtained for the approach based on hand-crafted features indicates values of accuracy, sensitivity and specificity almost equal to 80%, while maintaining low values of standard deviation.

Concerning blood tumours, the peripheral blood smear technique is absolutely not invasive, but requires the presence of instrumentation and specialized personnel that, currently, is not always available in all centres. Therefore, this technique is assumed for use in the immediate future even through remote consulting or telemedicine procedures, which are currently increasing in internal medicine and haematology units. In terms of accuracy, sensitivity and specificity, results for leukocyte classification evaluated through a one-versus-all approach using hand-crafted features, a one-versus-all approach with an SVM classifier using CNN as a feature extractor and a one-versus-all approach with a CNN classifier were reported. According to the general results discussed in recent works, which compare deep learning and traditional approaches for the classification of images or ROIs, for blood tumours, the best performance seems to be obtained by means of deep learning techniques. According to the results presented, the use of a CNN to detect tumours has better results than the use of ANN trained with hand-crafted features. As these improvements seem to be consistent across a large variety of domains, and as is usually the case, the development of a deep learning solution was found to be relatively straight-forward, which can be viewed as a major step forward in the medical computing field. Still, a major question remains as to how and when we can reach a substantial leap in performance. Future works in this field could focus on improving the knowledge base for all tumours described in this survey. Moreover, since the presented workflow can be applied to other types of tumours in different organs, this study could be further improved by deeply comparing handcrafted and non-handcrafted approaches.

Finally, the work conducted in Austria at the Technology University of Graz was described. In the proposed work, a marker less mixed reality application for maxillofacial oncologic surgery support was evaluated. The tests focused on a real case of head and neck cancer, under the supervision of a surgeon from the Medical University of Graz. To recreate a test-bed, a 3D model of the patient's head was printed. To generate

the 3D holograms to be rendered, the patient's PET-CT scan was segmented and properly transformed using MevisLab and MeshLab. The resulting object was then managed with the Unity Engine and the APIs for Microsoft HoloLens. The registration of the hologram was achieved automatically by means of a marker less algorithm. Although the manufacturer provides a method to perform registration based on the spatial mapping API, this approach was not considered for real simulations as it was completely unreliable along the depth factor. The environmental 3D mesh recreated by the device is not sufficient for such high precision applications. To overcome this limitation, a simple complementary algorithm was implemented and examined. This combination of the standard API and of the additional algorithm provided results that are comparable to other studies that applied a marker-based registration method, as the order of magnitude of the error is the same, although still lower in the marker-based system. To also understand why having such a system in a medical environment, not only surgery rooms but also in ambulatories and during classes, is important, a questionnaire was provided to a group of experts from the department of maxillofacial surgery at the State Hospital of Graz. The questionnaire was drafted according to the recommendation of the standard ISO-9241/110 Ergonomics of Human-Machine Interaction. All questions could be answered with one of six fixed answers matching a six-point Likert scale. The outcome of this survey, which was conducted during a practical showcase at the hospital, is that generally doctors have great interest in and appreciation for this technology, especially for its potential to ensure higher quality standards. Generally, all study participants felt comfortable with the application, but they needed initial training to understand how the device itself worked. Despite the current limitations with the registration, the overall provided feedback was positive regarding the introduction of the technology in operating rooms and ambulatories with one additional requirement of adding spatial information of bones and blood vessels. The maximum positive feedback was unanimously given for the question of whether study participants would introduce the application in an educational environment, which makes the technology mature enough for this purpose. As an inverse test, the same showcase was then proposed at the Institute of Computer Graphics and Vision, to understand the feeling that someone not familiar with the medical field, but familiar with the technology, has during the fruition of the application. This revealed how a profound knowledge in mixed reality is not necessary to correctly and intuitively understand the application, but it is necessary to have at least a basic knowledge of the target medical field to understand not only the behaviour of the application but also the information provided by its content.

5 My Publications

[1] Carnimeo, L., Trotta, G. F., Brunetti, A., Cascarano, D. G., Buongiorno, D., Loconsole, C., Di Sciascio, E., Bevilacqua, V. A proposal of a Healthcare Network based on Big Data Analytics for Parkinson's disease. Accepted to The Institution of Engineering and Technology (IET) Special Section Industry 4.0: the DIGITAI Transformation in the Engineering findings (DIGITATE).

[2] Trotta, G. F., Pellicciari, R., Boccaccio, A., Brunetti, A., Cascarano, G. D., Manghisi, V. M., Fiorentino, M., Uva, A. E., Defazio, G., Bevilacqua, V. A Neural Network-Based Software to Recognize and Count Blinks, Brief and Prolonged Spasms and Measure Eye Closure Time in Patients with Blepharospasm. To be submitted on Artificial Intelligence In Medicine.

[3] Pepe, A., Trotta, G. F., Schmalstieg, D., Wallner, J., Egger, J., Bevilacqua, V. Study, Implementation and Application of a Mixed Reality System for Computer-aided Maxillofacial Oncological Surgery. To be submitted on PLOS ONE.

[4] Antonio Brunetti, Leonarda Carnimeo, Gianpaolo Francesco Trotta, and Vitoantonio Bevilacqua. Computer-Assisted Frameworks for Classification of Liver, Breast and Blood Neoplasias via Neural Networks: a Survey based on Medical Images. Accepted for publication in Neurocomputing SI 2018.

[5] Brunetti, A., Buongiorno, D., Trotta, G.F., Bevilacqua, V. Computer vision and deep learning techniques for pedestrian detection and tracking: A survey (2018) Neurocomputing, 300, pp. 17-33.

[6] Bevilacqua, V., Brunetti, A., Guerriero, A., Trotta, G.F., Telegrafo, M., Moschetta, M. A performance comparison between shallow and deeper neural networks supervised classification of tomosynthesis breast lesions images (2018) Cognitive Systems Research. Article in Press.

[7] Manghisi, V. M., Uva, A. E., Fiorentino, M., Bevilacqua, V., Trotta, G. F., & Monno, G. (2017). Real time RULA assessment using Kinect v2 sensor. Applied Ergonomics, 65, pp. 481-491.

[8] Bevilacqua, V., Brunetti, A., Trotta, G. F., Carnimeo, L., Marino, F., Alberotanza, V., & Scardapane, A. (2017). A Deep Learning Approach for Hepatocellular Carcinoma Grading. International Journal of Computer Vision and Image Processing (IJCVIP), 7(2), 1-18.

[9] Bortone I., Trotta G.F., Cascarano G.D., Argentiero A., Agnello N., Nicolardi G., Bevilacqua V. Optimal Classifier of Parkinson's Disease based on features selected by Information Gain in 3D Gait Analysis for Differential Diagnosis. Gait & Posture, Volume 57, 205 - 206

[10] Bortone, I., Buongiorno, D., Lelli, G., Di Candia, A., Cascarano, G. D., Trotta, G. F., Fiore, P., and Bevilacqua, V. "Gait Analysis and Parkinson's Disease: Recent trends on main applications in healthcare". Accepted for pubblication International Conference on Neurorehabilitation (ICNR 2018).

[11] Buongiorno, Domenico, Trotta, Gianpaolo Francesco, Bortone, Ilaria, Di Gioia, Nicola, Avitto, Felice, Losavio, Giacomo, Bevilacqua, Vitoantonio: 'Assessment and rating of movement impairment in Parkison's Disease using a low-cost vision-based system', in 'Ac-cepted for pubblication in the Proceedings of the 2018 International

Conference on Intelli-gent Computing' (2018), pp. 777–788, doi: 10.1007/978-3-319-95957-3_82

[12] Gianpaolo Francesco Trotta, Sergio Mazzola, Giuseppe Gelardi, Antonio Brunetti, Nicola Marino, and Vitoantonio Bevilacqua. Reconstruction, Optimisation and Quality Check of Microsoft HoloLens-acquired 3D Points Clouds. Accepted for publication in the Proceedings of the 2018 Italian Workshop on Neural Networks (WIRN 2018).

[13] Caporusso, N., Ding, M., Clarke, M., Carlson, G., Bevilacqua, V., Trotta, G.F. Analysis of the relationship between content and interaction in the usability design of 360o videos (2019) Advances in Intelligent Systems and Computing, 794, pp. 593-602.

[14] Bevilacqua, V., Brunetti, A., Trotta, G.F., De Marco, D., Quercia, M.G., Buongiorno, D., D'Introno, A., Girardi, F., Guarini, A. A novel deep learning approach in haematology for classification of leucocytes (2019) Smart Innovation, Systems and Technologies, 103, pp. 265-274.

[15] Buongiorno, D., Trotta, G.F., Bortone, I., Di Gioia, N., Avitto, F., Losavio, G., Bevilacqua, V. Assessment and Rating of Movement Impairment in Parkinson's Disease Using a Low-Cost Vision-Based System (2018) Lecture Notes in Computer Science (including subseries Lecture Notes in Artificial Intelligence and Lecture Notes in Bioinformatics), 10956 LNAI, pp. 777-788.

[16] Caporusso, N., Biasi, L., Cinquepalmi, G., Trotta, G.F., Brunetti, A., Bevilacqua, V. A wearable device supporting multiple touch- and gesture-based languages for the deaf-blind (2018) Advances in Intelligent Systems and Computing, 608, pp. 32-41.

[17] Loconsole, C., Cascarano, G.D., Brunetti, A., Trotta, G.F., Losavio, G., Bevilacqua, V., Di Sciascio, E. A model-free technique based on computer vision and sEMG for classification in Parkinson's disease by using computer-assisted handwriting analysis (2018) Pattern Recognition Letters. Article in Press.

[18] Bortone, I., Quercia, M.G., Ieva, N., Cascarano, G.D., Trotta, G.F., Tatò, S.I., Bevilacqua, V. Recognition and Severity Rating of Parkinson's Disease from Postural and Kinematic Features During Gait Analysis with Microsoft Kinect (2018) Lecture Notes in Computer Science (including subseries Lecture Notes in Artificial Intelligence and Lecture Notes in Bioinformatics), 10955 LNCS, pp. 613-618.

[19] Invitto, S., Piraino, G., Mignozzi, A., Capone, S., Montagna, G., Siciliano, P. A., Trotta, G.F., ... Brunetti, A. (2018). Smell and Meaning: an OERP study. In Multidisciplinary Approaches to Neural Computing (pp. 289-300). Springer, Cham.

[20] Bevilacqua, V., Simeone, S., Brunetti, A., Loconsole, C., Trotta, G. F., Tramacere, S., ... & Mastronardi, R. (2017, August). A Computer Aided Ophthalmic Diagnosis System Based on Tomographic Features. In International Conference on Intelligent Computing (pp. 598-609). Springer, Cham.

[21] Bevilacqua, V., Altini, D., Bruni, M., Riezzo, M., Brunetti, A., Loconsole, C., Trotta, G.F., ... & Tartaglia, C. (2017, August). A Supervised Breast Lesion Images Classification from Tomosynthesis Technique. In International Conference on Intelligent Computing (pp. 483-489). Springer, Cham.

[22] Loconsole, C., Trotta, G. F., Brunetti, A., Trotta, J., Schiavone, A., Tatò, S. I., ... & Bevilacqua, V. (2017, August). Computer Vision and EMG-Based Handwriting Analysis for Classification in Parkinson's Disease. In International Conference on Intelligent Computing (pp. 493-503). Springer, Cham.

[23] Bortone, I., Trotta, G. F., Brunetti, A., Cascarano, G. D., Loconsole, C., Agnello, N., ... & Bevilacqua, V. (2017, August). A Novel Approach in Combination of 3D Gait Analysis Data for Aiding Clinical Decision-Making in Patients with Parkinson's Disease. In International Conference on Intelligent Computing (pp. 504-514). Springer, Cham.

[24] Bevilacqua, V., Trotta, G. F., Brunetti, A., Caporusso, N., Loconsole, C., Cascarano, G. D. ... & Di Candia, A. (2017, July). A Comprehensive Approach for Physical Rehabilitation Assessment in Multiple Sclerosis Patients Based on Gait Analysis. In International Conference on Applied Human Factors and Ergonomics (pp. 119-128). Springer, Cham.

[25] Bevilacqua, V., Trotta, G. F., Loconsole, C., Brunetti, A., Caporusso, N., Bellantuono, G. M., ... & Di Vietro, M. G. (2017, July). A RGB-D Sensor Based Tool for Assessment and Rating of Movement Disorders. In International Conference on Applied Human Factors and Ergonomics (pp. 110-118). Springer, Cham.

[26] Caporusso, N., Biasi, L., Cinquepalmi, G., Trotta, G. F., Brunetti, A., & Bevilacqua, V. (2017, July). Enabling touch-based communication in wearable devices for people with sensory and multisensory impairments. In International Conference on Applied Human Factors and Ergonomics (pp. 149-159). Springer, Cham.

[27] Caporusso, N., Biasi, L., Cinquepalmi, G., Trotta, G. F., Brunetti, A., & Bevilacqua, V. (2017, July). A Wearable Device Supporting Multiple Touch-and Gesture-Based Languages for the Deaf-Blind. In International Conference on Applied Human Factors and Ergonomics (pp. 32-41). Springer, Cham.

[28] Bevilacqua, V., Brunetti, A., Trotta, G. F., Dimauro, G., Elez, K., Alberotanza, V., & Scardapane, A. (2017, June). A novel approach for Hepatocellular Carcinoma detection and classification based on triphasic CT Protocol. In Evolutionary Computation (CEC), 2017 IEEE Congress on (pp. 1856-1863). IEEE.

[29] Bevilacqua, V., Uva, A. E., Fiorentino, M., Trotta, G. F., Dimatteo, M., Nasca, E., ... & Pellicciari, R. (2016, December). A Comprehensive Method for Assessing the Blepharospasm Cases Severity. In International Conference on Recent Trends in Image Processing and Pattern Recognition (pp. 369-381). Springer, Singapore.

[30] Bevilacqua, V., Carnimeo, L., Brunetti, A., De Pace, A., Galeandro, P., Trotta, G. F., ... & Scardapane, A. (2016, December). Synthesis of a Neural Network Classifier for Hepatocellular Carcinoma Grading Based on Triphasic CT Images. In International Conference on Recent Trends in Image Processing and Pattern Recognition (pp. 356-368). Springer, Singapore.

[31] Bevilacqua, V., Trotta, G. F., Brunetti, A., Buonamassa, G., Bruni, M., Delfine, G., ... & Verrino, L. (2016, October). Photogrammetric Meshes and 3D Points Cloud Reconstruction: A Genetic Algorithm Optimization Procedure. In Italian Workshop on Artificial Life and Evolutionary Computation (pp. 65-76). Springer, Cham.

[32] Uva, A. E., Fiorentino, M., Gattullo, M., Colaprico, M., de Ruvo, M. F., Marino, F., ... & Monno, G. (2016, June). Design of a Projective AR Workbench for Manual Working Stations. In International Conference on Augmented Reality, Virtual Reality and Computer Graphics (pp. 358-367). Springer International Publishing.

[33] Bevilacqua, V., Dimauro, G., Marino, F., Brunetti, A., Cassano, F., Di Maio, A., ... & Guarini, A. (2016, May). A novel approach to evaluate blood parameters using computer vision techniques. In Medical Measurements and Applications (MeMeA), 2016 IEEE International Symposium on (pp. 1-6). IEEE.

[34]   Bevilacqua, V., Brunetti, A., Trigiante, G., Trotta, G. F., Fiorentino, M., Manghisi, V., & Uva, A. E. (2015, September). Design and Development of a Forearm Rehabilitation System Based on an Augmented Reality Serious Game. In Italian Workshop on Artificial Life and Evolutionary Computation (pp. 127-136). Springer International Publishing.

[35]   Bevilacqua, V., Brunetti, A., de Biase, D., Tattoli, G., Santoro, R., Trotta, G. F., ... & Delussi, M. (2015, August). A p300 clustering of mild cognitive impairment patients stimulated in an immersive virtual reality scenario. In International Conference on Intelligent Computing (pp. 226-236). Springer, Cham.

6 Biography

1 Hermann, Mario, Pentek, Tobias, Otto, Boris: 'Design Principles for Industrie 4.0 Scenarios: A Literature Review', in 'Technische Universitat Dortmund' (2015), pp. 4–16, doi: 10.1109/HICSS.2016.488

2 Hofmann, Erik, Rüsch, Marco: 'Industry Industry 4.0 and the current Status as well as Future Prospects on Logistics'*Comput. Ind.*, 2017, **89**, pp. 23–34. , doi: 10.1016/j.compind.2017.04.002

3 Kagermann, Henning, Wahlster, Wolfgang, Helbig, Johannes: 'Securing the future of German manufacturing industry: Recommendations for implementing the strategic initiative INDUSTRIE 4.0' (Forschungsunion, 2013), doi: 10.13140/RG.2.2.14480.20485

4 Lee, Jay, Bagheri, Behrad, Kao, Hung-an: 'ScienceDirect A Cyber-Physical Systems architecture for Industry 4 . 0-based manufacturing systems'*Manuf. Lett.*, 2015, **3**, pp. 18–23. , doi: 10.1016/j.mfglet.2014.12.001

5 Lucke, Dominik, Constantinescu, Carmen, Westkämper, Engelbert: 'Smart Factory - A Step towards the Next Generation of Manufacturing', in 'Manufacturing Systems and Technologies for the New Frontier' (Springer, 2008), pp. 115–118, doi: 10.1007/978-1-84800-267-8_23

6 Zhou, Keliang: 'Industry 4 . 0 : Towards Future Industrial Opportunities and Challenges', in '12th International Conference on Fuzzy Systems and Knowledge Discovery (FSKD)' (2015), pp. 2147–2152

7 Gorecky, Dominic, Schmitt, Mathias, Loskyll, Matthias, Zühlke, Detlef: 'Human-machine-interaction in the industry 4.0 era', in 'Proceedings - 2014 12th IEEE International Conference on Industrial Informatics, INDIN 2014' (2014), pp. 289–294, doi: 10.1109/INDIN.2014.6945523

8 Wan, Jiafu, Cai, Hu, Zhou, Keliang: 'Industrie 4.0: enabling technologies', in 'Intelligent Computing and Internet of Things (ICIT), 2014 International Conference on' (2015), pp. 135–140, doi: 10.1109/ICAIOT.2015.7111555

9 Mueller, Egon, Chen, Xiao Li, Riedel, Ralph: 'Challenges and Requirements for the Application of Industry 4.0: A Special Insight with the Usage of Cyber-Physical System'*Chinese J. Mech. Eng. (English Ed.*, 2017, **30**, (5), pp. 1050–1057. , doi: 10.1007/s10033-017-0164-7

10 Conner, Brett P., Conner, Brett P., Manogharan, Guha P., Martof, Ashley N., Rodomsky, Lauren M., Rodomsky, Caitlyn M., Jordan, Dakesha C., Limperos, James W.: 'Making sense of 3-D printing : Creating a map of additive manufacturing products and services Making sense of 3-D printing : Creating a map of additive manufacturing products and services &'*Addit. Manuf.*, 2014, **1–4**, (September), pp. 64–76. , doi: 10.1016/j.addma.2014.08.005

11 Frazier, William E.: 'Metal Additive Manufacturing: A Review'*J. Mater. Eng. Perform.*, 2014, **23**, (6), pp. 1917–1928. , doi: 10.1007/s11665-014-0958-z

12 Wong, Kaufui V., Hernandez, Aldo: 'A Review of Additive Manufacturing'*ISRN Mech. Eng.*, 2012, **2012**, pp. 1–10. , doi: 10.5402/2012/208760

13 Lumley, Roger N.: 'Aluminium Investment Casting and Rapid Prototyping for

Aerospace Applications', in 'Fundamentals of Aluminium Metallurgy' (Elsevier, 2018), pp. 123–158, doi: 10.1016/B978-0-08-102063-0.00004-7

14 Lopes, P., Flores, P., Seabra, E.: 'Rapid prototyping technology in medical applications: A critical review', in 'Proceedings of the International Symposium CompIMAGE 2006 - Computational Modelling of Objects Represented in Images: Fundamentals, Methods and Applications' (2007), pp. 255–260

15 Regina, Fabrizio, Lavecchia, Fulvio, Galantucci, Luigi Maria: 'Preliminary study for a full colour low cost open source 3D printer, based on the combination of fused deposition modelling (FDM) or fused filament fabrication (FFF) and inkjet printing'*Int. J. Interact. Des. Manuf.*, 2018, **12**, (3), pp. 979–993. , doi: 10.1007/s12008-017-0432-x

16 Sun, Wei, Nam, Jae Hyun, Darling, Andrew Leete, Khalil, Saif.: 'Method and apparatus for computer-aided tissue engineering for modeling, design and freeform fabrication of tissue scaffolds, constructs, and devices.' (Google Patents, 2005)

17 Lv, Shuaishuai, Zhu, Yangyang, Gu, Hai, Ni, Hongjun, Meng, Yue, Wang, Xingxing: 'Structure Optimization of Microbial Fuel Cell Reactor Based on Reverse Engineering and Rapid Prototyping', in 'MATEC Web of Conferences' (2018), p. 1003

18 Kumar, Praveen, Yu, Chris, Yuan, Yang, Foster, Nate, Kleinberg, Robert, Soulé, Robert: 'YATES: Rapid Prototyping for Traffic Engineering Systems', in 'Proceedings of the Symposium on SDN Research' (2018), p. 11:1--11:7, doi: 10.1145/3185467.3185498

19 Park, Su A., Lee, Sang Jin, Seok, Ji Min, Lee, Jun Hee, Kim, Wan Doo, Kwon, Il Keun: 'Fabrication of 3D Printed PCL / PEG Polyblend Scaffold Using Rapid Prototyping System for Bone Tissue Engineering Application'*J. Bionic Eng.*, 2018, **15**, (3), pp. 435–442.

20 Cvetkovic, Caroline, Ko, Eunkyung, Kaufman, Collin, Grant, Lauren, Gillette, Martha, Kong, Hyunjoon, Bashir, Rashid: 'Rapid prototyping of soft bioactuators'*3D Bioprinting Regen. Eng. Princ. Appl.*, 2018.

21 Jiang, Lihong, Zhao, Jiarun, Lian, Jiazhang, Xu, Zhinan: 'Cell-free protein synthesis enabled rapid prototyping for metabolic engineering and synthetic biology'*Synth. Syst. Biotechnol.*, 2018, **3**, (2), pp. 90–96. , doi: 10.1016/j.synbio.2018.02.003

22 Elhayatmy, G., Dey, Nilanjan, Ashour, Amira S.: 'Internet of Things Based Wireless Body Area Network in Healthcare', in 'Internet of Things and Big Data Analytics Toward Next-Generation Intelligence' (Springer, 2018), pp. 3–20, doi: 10.1007/978-3-319-60435-0_1

23 Cowley, Nicholas P., Saraswat, Ruchir, Goldman, Richard J.: 'Biofeedback sensors in a body area network' (Google Patents, 2018)

24 Kargaran, Ehsan, Manstretta, Danilo, Castello, Rinaldo: 'Design considerations for a sub-mW wireless medical body-area network receiver front end'*Micromachines*, 2018, **9**, (1), p. 31. , doi: 10.3390/mi9010031

25 Wang, Dong, Ghosh, Monisha, Smith, Delroy: 'Medical body area network (MBAN) with key-based control of spectrum usage' (Google Patents, 2018)

26 Li, M.G., Tian, X.Y., Chen, X.B.: 'A brief review of dispensing-based rapid prototyping techniques in tissue scaffold fabrication: Role of modeling on scaffold properties

prediction'*Biofabrication*, 2009, **1**, (3), p. 32001. , doi: 10.1088/1758-5082/1/3/032001

27   Töppel, Thomas, Lausch, Holger, Brand, Michael, Hensel, Eric, Arnold, Michael, Rotsch, Christian: 'Structural Integration of Sensors/Actuators by Laser Beam Melting for Tailored Smart Components'*Jom*, 2018, **70**, (3), pp. 321–327. , doi: 10.1007/s11837-017-2725-8

28   Binder, Maximilian, Illgner, Matthias, Anstaett, Christine, Kindermann, Philipp, Kirchbichler, Ludwig, Seidel, Christian: 'Automated Manufacturing of Sensor-Monitored Parts: Enhancement of the laser beam melting process by a completely automated sensor integration'*Laser Tech. J.*, 2018, **15**, (3), pp. 36–39.

29   Uva, Antonio Emmanuele, Fiorentino, Michele, Gattullo, Michele, Colaprico, Marco, De Ruvo, Maria F., Marino, Francescomaria, Trotta, Gianpaolo F., Manghisi, Vito M., Boccaccio, Antonio, Bevilacqua, Vitoantonio, Monno, Giuseppe: 'Design of a projective AR workbench for manual working stations', in 'Lecture Notes in Computer Science (including subseries Lecture Notes in Artificial Intelligence and Lecture Notes in Bioinformatics)' (2016), pp. 358–367, doi: 10.1007/978-3-319-40621-3_25

30   Bevilacqua, Vitoantonio, Brunetti, Antonio, Trigiante, Giuseppe, Trotta, Gianpaolo Francesco, Fiorentino, Michele, Manghisi, Vito, Uva, Antonio Emmanuele: 'Design and development of a forearm rehabilitation system based on an augmented reality serious game', in 'Communications in Computer and Information Science' (2016), pp. 127–136, doi: 10.1007/978-3-319-32695-5_12

31   Porpiglia, Francesco, Fiori, Cristian, Checcucci, Enrico, Amparore, Daniele, Bertolo, Riccardo: 'Augmented Reality Robot-assisted Radical Prostatectomy: Preliminary Experience.'*Urology*, 2018, **115**, p. 184. , doi: 10.1016/j.urology.2018.01.028

32   Porpiglia, F., Bertolo, R., Checcucci, E., Amparore, D., Fiori, C.: 'Robot-assisted radical prostatectomy with 3D-based augmented reality'*J. Urol.*, 2018, **199 (4 Sup**, (4), p. e820.

33   Porpiglia, F., Bertolo, R., Checcucci, E., Amparore, D., Fiori, C.: '3D augmented reality robot-assisted radical prostatectomy'*Eur. Urol. Suppl.*, 2018, **17**, (2), p. e1929. , doi: 10.1016/S1569-9056(18)32334-0

34   Blanco-Novoa, Oscar, Fernandez-Carames, Tiago M., Fraga-Lamas, Paula, Vilar-Montesinos, Miguel: 'A Practical Evaluation of Commercial Industrial Augmented Reality Systems in an Industry 4.0 Shipyard'*IEEE Access*, 2018, **6**, pp. 1–1. , doi: 10.1109/ACCESS.2018.2802699

35   Fernández Del Amo, Iñigo, Erkoyuncu, John Ahmet, Roy, Rajkumar, Wilding, Stephen: 'Augmented Reality in Maintenance: An information-centred design framework'*Procedia Manuf.*, 2018, **19**, pp. 148–155. , doi: 10.1016/j.promfg.2018.01.021

36   Palmarini, Riccardo, Erkoyuncu, John Ahmet, Roy, Rajkumar, Torabmostaedi, Hosein: 'A systematic review of augmented reality applications in maintenance'*Robot. Comput. Integr. Manuf.*, 2018, **49**, (July 2017), pp. 215–228. , doi: 10.1016/j.rcim.2017.06.002

37   Swayze, Jeffrey S., Young, Joshua, Strobl, Geoffrey S., Beckman, Andrew: 'Surgical

system with augmented reality display' (Google Patents, 2018)

38   Broadhead, Eric Wayne, Braasch, Daniel Charles: 'Augmented reality maintenance system' (Google Patents, 2018)

39   Kersten-Oertela, Marta, Jannin, Pierre, Collins, D. Louis: 'The state of the art of visualization in mixed reality image guided surgery'*Comput. Med. Imaging Graph.*, 2013, **37**, (2), pp. 98–112.

40   Lindgren, R., Johnson-Glenberg, M.: 'Emboldened by Embodiment: Six Precepts for Research on Embodied Learning and Mixed Reality'*Educ. Res.*, 2013, **42**, (8), pp. 445–452. , doi: 10.3102/0013189X13511661

41   Gotsis, Marientina, Tasse, Amanda, Swider, Maximilian, Lympouridis, Vangelis, Poulos, Irina C., Thin, Alasdair G., Turpin, David, Tucker, Diane, Jordan-Marsh, Maryalice: 'Mixed reality game prototypes for upper body exercise and rehabilitation', in '2012 IEEE Virtual Reality (VR)' (2012), pp. 181–182, doi: 10.1109/VR.2012.6180940

42   Smilevski, Stephen, Thirunavukkarasu, Gokul Sidarth, Seyedmahmoudian, Mehdi, McMillan, Scott, Horan, Ben: 'Mixed reality tool for training on pressure immobilization treatment of snake bite envenomation', in 'Proceedings of the 23rd International ACM Conference on 3D Web Technology' (2018), p. 3

43   Lima, Tiago França Melo, Beltrame, João Paulo Ferreira, Niquini, Carlos Ramos, Barbosa, Breno Gonçalves, Davis, Clodoveu Augusto: 'Design of a Mixed-Reality Serious Game to Tackle a Public Health Problem', in 'International Conference on Entertainment Computing' (2018), pp. 305–309, doi: 10.1007/978-3-319-99426-0_35

44   Sappenfield, Joshua Warren, Smith, William Brit, Cooper, Lou Ann, Lizdas, David, Gonsalves, Drew B., Gravenstein, Nikolaus, Lampotang, Samsun, Robinson, Albert R.: 'Visualization Improves Supraclavicular Access to the Subclavian Vein in a Mixed Reality Simulator'*Anesth. Analg.*, 2017, **127**, (1), p. 1. , doi: 10.1213/ANE.0000000000002572

45   Gheza, Federico, Raimondi, Paolo: 'Image Fusion and Mixed Reality in Abdominal Surgery'*Ann. Surg.*, 2018. , doi: 10.1097/SLA.0000000000002905

46   Miller, Geoffrey T., Harris, Tyler, Choi, Y. Sammy, DeLellis, Stephen M., Nelson, Kenneth, Magee, J. Harvey: 'Augmented Reality and Telestrated Surgical Support for Point of Injury Combat Casualty Care: A Feasibility Study', in 'International Conference on Augmented Cognition' (2018), pp. 395–405, doi: 10.1007/978-3-319-91470-1_32

47   Schlueter, Jonathan A., Schlueter, Jonathan Andrew: 'Remote maintenance assistance using real-time augmented reality authoring by'2018.

48   Rambach, Jason, Pagani, Alain, Schneider, Michael, Artemenko, Oleksandr, Stricker, Didier: '6DoF Object Tracking based on 3D Scans for Augmented Reality Remote Live Support'*Computers*, 2018, **7**, (1), p. 6. , doi: 10.3390/computers7010006

49   Greenfield, Max J., Luck, Joshua, Billingsley, Michael L., Heyes, Richard, Smith, Oliver J., Mosahebi, Afshin: 'Demonstration of the Effectiveness of Augmented Reality Telesurgery in Complex Hand Reconstruction in Gaza'*Plast. Reconstr. Surgery. Glob.*

Open, 2018, **6**, (3), p. e1708. , doi: 10.1097/GOX.0000000000001708

50   Amir, Yoffe, Cohen, Eitan: 'Remote Distance Assistance System and Method' (2018)

51   Hoppe, Adrian H., Westerkamp, Kai, Maier, Sebastian, van de Camp, Florian, Stiefelhagen, Rainer: 'Multi-user Collaboration on Complex Data in Virtual and Augmented Reality', in 'International Conference on Human-Computer Interaction' (2018), pp. 258–265, doi: 10.1007/978-3-319-92279-9_35

52   Uva, Antonio E., Gattullo, Michele, Manghisi, Vito M., Spagnulo, Daniele, Cascella, Giuseppe L., Fiorentino, Michele: 'Evaluating the effectiveness of spatial augmented reality in smart manufacturing: a solution for manual working stations'*Int. J. Adv. Manuf. Technol.*, 2018, **94**, (1–4), pp. 509–521. , doi: 10.1007/s00170-017-0846-4

53   Al-Ahmari, Abdulrahman, Ameen, Wadea, Abidi, Mustufa Haider, Mian, Syed Hammad: 'Evaluation of 3D printing approach for manual assembly training'*Int. J. Ind. Ergon.*, 2018, **66**, pp. 57–62. , doi: 10.1016/j.ergon.2018.02.004

54   Tang, Qiang, Chen, Yan, Schaefer, Gerald, Gale, Alastair G.: 'The development of an augmented reality (AR) approach to mammographic training: overcoming some real world challenges', in 'Medical Imaging 2018: Image-Guided Procedures, Robotic Interventions, and Modeling' (2018), p. 84, doi: 10.1117/12.2293496

55   Fraga-lamas, Paula, Fernández-caramés, Tiago M., Member, Senior: 'A Review on Industrial Augmented Reality Systems for the Industry 4 . 0 Shipyard'*IEEE Access*, 2018, **6**, pp. 13358–13375.

56   Bimber, Oliver, Raskar, Ramesh: 'Spatial Augmented Reality Merging Real and Virtual Worlds' (AK Peters/CRC Press, 2005), doi: 10.1260/147807708784640126

57   Di Donato, Michele, Fiorentino, Michele, Uva, Antonio E., Gattullo, Michele, Monno, Giuseppe: 'Text legibility for projected Augmented Reality on industrial workbenches'*Comput. Ind.*, 2015, **70**, pp. 70–78. , doi: 10.1016/j.compind.2015.02.008

58   Singh, Konjengbam Jackichand, Saikia, L.P.: 'A Survey on Augmented Reality Technologies and Applications'*Int. Res. J. Eng. Technol.*, 2008, **9001**, p. 791.

59   Liu, Jie, Chen, Chao, Ji, Shenglu, Liu, Qian, Ding, Dan, Zhao, Dan, Liu, Bin: 'Long wavelength excitable near-infrared fluorescent nanoparticles with aggregation-induced emission characteristics for image-guided tumor resection'*Chem. Sci.*, 2017, **8**, (4), pp. 2782–2789. , doi: 10.1039/C6SC04384D

60   Cui, Nan, Kharel, Pradosh, Gruev, Viktor: 'Augmented reality with Microsoft HoloLens holograms for near infrared fluorescence based image guided surgery', in 'Molecular-Guided Surgery: Molecules, Devices, and Applications III' (2017), p. 100490I, doi: 10.1117/12.2251625

61   Stolka, Philipp Jakob, Foroughi, Pezhman, Rendina, Matthew C., Hager, Gregory Donald, Boctor, Emad Mikhail: 'Ultrasound system with stereo image guidance or tracking' (Google Patents, 2017)

62   Kuhl, Christiane K., Strobel, Kevin, Bieling, Heribert, Wardelmann, Eva, Kuhn, Walther, Maass, Nikolaus, Schrading, Simone: 'Impact of Preoperative Breast MR Imaging and MR-guided Surgery on Diagnosis and Surgical Outcome of Women with Invasive Breast Cancer with and without DCIS Component.'*Radiology*, 2017, **284**, (3),

p. 161449. , doi: 10.1148/radiol.2017161449

63   Sharma, Karun V., Yarmolenko, Pavel S., Eranki, Avinash, Partanen, Ari, Celik, Haydar, Kim, AeRang, Oetgen, Matthew, Kim, Peter C.W.: 'Magnetic Resonance Imaging–guided High-intensity Focused Ultrasound Applications in Pediatrics'*Top. Magn. Reson. Imaging*, 2018, **27**, (1), pp. 45–51. , doi: 10.1097/RMR.0000000000000163

64   Vidal-Sicart, S., Valdés Olmos, R., Nieweg, O.E., Faccini, R., Grootendorst, M.R., Wester, H.J., Navab, N., Vojnovic, B., van der Poel, H., Martínez-Román, S., Klode, J., Wawroschek, F., van Leeuwen, F.W.B.: 'From interventionist imaging to intraoperative guidance: New perspectives by combining advanced tools and navigation with radio-guided surgery'*Rev. Española Med. Nucl. e Imagen Mol. (English Ed.*, 2018, **37**, (1), pp. 28–40. , doi: 10.1016/j.remnie.2017.10.009

65   Nishino, Hiroto, Hatano, Etsuro, Seo, Satoru, Nitta, Takashi, Saito, Tomoyuki, Nakamura, Masaaki, Hattori, Kayo, Takatani, Muneo, Fuji, Hiroaki, Taura, Kojiro, Uemoto, Shinji: 'Real-time Navigation for Liver Surgery Using Projection Mapping With Indocyanine Green Fluorescence'*Ann. Surg.*, 2017, **m**, (Xx), p. 1. , doi: 10.1097/SLA.0000000000002172

66   SYED, A.Z., ZAKARIA, A., LOZANOFF, S.: 'Dark Room To Augmented Reality: Application of Hololens Technology for Oral Radiological Diagnosis'*Oral Surg. Oral Med. Oral Pathol. Oral Radiol.*, 2017, **124**, (1), p. e33. , doi: 10.1016/j.oooo.2017.03.041

67   Cristina Marie Morales Mojica C. M. M., Navkar N.V. Tsekos N.V. Tsagkaris D. Webb A. Birbilis T. Seimenis I.: 'Holographic interface for three-dimensional visualization of mri on hololens: a prototype platform for mri guided neurosurgeries'*2017 IEEE 17th Int. Conf. Bioinforma. Bioeng.*, 2017, pp. 21–27.

68   Kovar, Jiri, Mouralova, Katerina, Ksica, Filip, Kroupa, Jiri, Andrs, Ondrej, Hadas, Zdenek: 'Virtual Reality in Context of Industry 4.0', in 'Mechatronika 2016' (2016), p. 7

69   Beier, K.P.: 'Virtual Reality in Automotive Design and Manufacturing'*Converg. 94 Int. Congr. Transp. Electron. SAE Soc. Automot. Eng.*, 1994.

70   Lawson, Glyn, Salanitri, Davide, Waterfield, Brian: 'Future directions for the development of virtual reality within an automotive manufacturer'*Appl. Ergon.*, 2016, **53**, pp. 323–330. , doi: 10.1016/j.apergo.2015.06.024

71   Zimmermann, Peter: 'Virtual Reality Aided Design. A survey of the use of VR in automotive industry', in 'Product Engineering' (Springer, 2008), pp. 277–296, doi: 10.1007/978-1-4020-8200-9_13

72   Gomes De Sá, Antonino, Zachmann, Gabriel: 'Virtual reality as a tool for verification of assembly and maintenance processes'*Comput. Graph.*, 1999, **23**, (3), pp. 389–403. , doi: 10.1016/S0097-8493(99)00047-3

73   Paes, Daniel, Arantes, Eduardo, Irizarry, Javier: 'Immersive environment for improving the understanding of architectural 3D models: Comparing user spatial perception between immersive and traditional virtual reality systems'*Autom. Constr.*, 2017, **84**, pp. 292–303. , doi: 10.1016/j.autcon.2017.09.016

74   Abdullah, Fadzidah, Kassim, Mohd Hisyamuddin Bin, Sanusi, Aliyah Nur Zafirah: 'Go

virtual: Exploring augmented reality application in representation of steel architectural construction for the enhancement of architecture education'*Adv. Sci. Lett.*, 2017, **23**, (2), pp. 804–808. , doi: 10.1166/asl.2017.7449

75 Maga, Dusan; Dudak, Juraj; Pavlikova, Sona; Hajek, Jiri; Simak, Boris: 'Support of technical education at primary and secondary level - IEEE Xplore Document', in 'MECHATRONIKA, 2012 15th International Symposium' (2012), pp. 1–4

76 Altintas, Y., Brecher, C., Weck, M., Witt, S.: 'Virtual Machine Tool'*CIRP Ann.*, 2005, **54**, (2), pp. 115–138. , doi: 10.1016/S0007-8506(07)60022-5

77 Jain, Sanjay, Fong Choong, Ngai, Maung Aye, Khin, Luo, Ming: 'Virtual factory: an integrated approach to manufacturing systems modeling'*Int. J. Oper. Prod. Manag.*, 2001, **21**, (5/6), pp. 594–608. , doi: 10.1108/01443570110390354

78 Sanz Lobera, Alfredo, González, Ignaciof, Castejón, Agustin Javier, Casado, Jose Leopoldo: 'Using Virtual Reality in the Teaching of Manufacturing Processes with Material Removal in CNC Machine-Tools', in 'Materials Science Forum' (2011), pp. 112–119, doi: 10.4028/www.scientific.net/MSF.692.112

79 van den Bogert, Antonie J., Geijtenbeek, Thomas, Even-Zohar, Oshri, Steenbrink, Frans, Hardin, Elizabeth C.: 'A real-time system for biomechanical analysis of human movement and muscle function'*Med. Biol. Eng. Comput.*, 2013, **51**, (10), pp. 1069–1077. , doi: 10.1007/s11517-013-1076-z

80 Delorme, Sébastien, Laroche, Denis, Diraddo, Robert, F. Del Maestro, Rolando: 'NeuroTouch: A physics-based virtual simulator for cranial microneurosurgery training'*Neurosurgery*, 2012, **71**, (SUPPL.1), pp. ons32--ons42. , doi: 10.1227/NEU.0b013e318249c744

81 Rahm, Stefan, Wieser, Karl, Bauer, David E., Waibel, Felix Wa, Meyer, Dominik C., Gerber, Christian, Fucentese, Sandro F.: 'Efficacy of standardized training on a virtual reality simulator to advance knee and shoulder arthroscopic motor skills'*BMC Musculoskelet. Disord.*, 2018, **19**, (1), p. 150. , doi: 10.1186/s12891-018-2072-0

82 Yokoi, Hana, Chen, Jian, Desai, Mihir M., Hung, Andrew J.: 'Impact of Virtual Reality Simulator in Training of Robotic Surgery', in 'Robotics in Genitourinary Surgery' (Springer, 2018), pp. 183–202, doi: 10.1007/978-3-319-20645-5_14

83 Pulijala, Yeshwanth, Ma, Minhua, Pears, Matthew, Peebles, David, Ayoub, Ashraf, Rcs, Fds: 'Effectiveness of Immersive Virtual Reality in Surgical Training - A Randomized Control Trial'*J. Oral Maxillofac. Surg.*, 2017, **76**, (17), pp. 31250–8. , doi: 10.1016/j.joms.2017.10.002

84 McGuire, LS Laura Stone, Neurosurgery, A. Alaraj-Healthcare Simulation:, 2018, undefined, Alaraj, Ali: 'Competency Assessment in Virtual Reality-Based Simulation in Neurosurgical Training', in 'Springer' (Springer, 2018), pp. 153–157, doi: 10.1007/978-3-319-75583-0_12

85 Schulz, Gerald B., Grimm, Tobias, Buchner, Alexander, Jokisch, Friedrich, Casuscelli, Jozefina, Kretschmer, Alexander, Mumm, Jan-Niclas, Ziegelmüller, Brigitte, Stief, Christian G., Karl, Alexander: 'Validation of a High-End Virtual Reality Simulator for Training Transurethral Resection of Bladder Tumors'*J. Surg. Educ.*, 2018. , doi: 10.1016/j.jsurg.2018.08.001

86   Sheikh, Z., Jackson, R., Tharmanathan, P., Keding, A.: 'Virtual Reality Simulation in Minimally Invasive Surgery Training: a Systematic Review and Meta-Analysis', in 'British Journal of Surgery' (2018), p. 31

87   Ricci, Katia, Deulssi, Marianna, Brunetti, Antonio, de Biase, Davide, Tattoli, Giacomo, Trotta, Francesco Gianpaolo, Cassano, Fabio, Santoro, Rosario, Pantaleo, Michele, Mastronardi, Giuseppe, Ivona, Fabio, Bevilacqua, Vitoantonio, de Tommaso, Marina: 'A P300 clustering of old patients stimulated in an immersive virtual reality scenario with Oculus Rift', in 'Neuropsychological Trends' (2015), pp. 142–143

88   Botella, Cristina: 'Virtual Reality in the Treatment of Claustrophobic Fear : A Controlled, Multiple-Baseline Design'*Behav. Ther.*, 2000, **31**, (3), pp. 583–595.

89   Caelho, Carlos M., Waters, Allison M., Hine, Trevor J., Wallis, Guy: 'The use of virtual reality in acrophobia research and treatment'*J. Anxiety Disord.*, 2009, **23**, (1), pp. 563–574.

90   Yuen, E.K., Herbert, J.D., Forman, E.M., Goetter, E.M., Comer, R., Bradley, J.C.: 'Treatment of Social Anxiety Disorder Using Online Virtual Environments in Second Life'*Behav. Ther.*, 2013, **44**, (1), pp. 51–61. , doi: 10.1016/j.beth.2012.06.001

91   Rus-Calafell, M., Gutierrez-Maldonado, J., Botella, C., Banos, R.M.: 'Virtual reality exposure and imaginal exposure in the treatment of fear of flying: a pilot study'*Behav Modif*, 2013, **37**, (4), pp. 568–590. , doi: 10.1177/0145445513482969

92   Shiban, Youssef, Pauli, Paul, Mühlberger, Andreas: 'Author ' s personal copy Behaviour Research and Therapy Effect of multiple context exposure on renewal in spider phobia'*Behav. Res. Ther.*, 2013, **51**, (2), pp. 68–70.

93   Shrouf, F., Ordieres, J., Miragliotta, G.: 'Smart Factories in Industry 4 . 0 : A Review of the Concept and of Energy Management Approached in Production Based on the Internet of Things Paradigm', in 'Ieee Ieem' (2014), pp. 697–701

94   Sadiku, Matthew N.O., Wang, Yonghui, Cui, Suxia, Musa, Sarhan M.: 'Industrial Internet of Things'*Int. J. Adv. Sci. Res. Eng.*, 2017, **3**. , doi: 10.7324/IJASRE.2017.32538

95   Miori, Vittorio, Russo, Dario: 'Domotic evolution towards the IoT', in 'Proceedings - 2014 IEEE 28th International Conference on Advanced Information Networking and Applications Workshops, IEEE WAINA 2014' (2014), pp. 809–814, doi: 10.1109/WAINA.2014.128

96   Mukhopadhyay, Subhas Chandra: 'Internet of Things: Challenges and Opportunities.', in 'Springer eBooks' (2014), pp. 613–614, doi: 10.1007/978-1-4419-8237-7

97   Industrial Internet Consortium: 'Industrial Internet Reference Architecture'*Ind. Internet Consort. (IIC), Tech. Rep*, 2015, pp. 1--101.

98   Crater, K.C., Goldman, C.E.: 'Distributed interface architecture for programmable industrial control systems' (Google Patents, 1999)

99   Engdahl, Jonathan R.: 'Walk-through human/machine interface for industrial control' (Google Patents, 2001)

100   Kretschmann, Robert J.: 'Mobile human/machine interface for use with industrial control systems for controlling the operation of process executed on spatially

separate machines' (Google Patents, 1998)

101 Thames, Lane, Schaefer, Dirk: 'Software-Defined Cloud Manufacturing for Industry 4.0'*Sixth Int. Conf. Chang. Agil. Reconfigurable Virtual Prod.*, 2016, **52**, pp. 12–17. , doi: 10.1016/j.procir.2016.07.041

102 Wu, Dazhong, Rosen, David W., Wang, Lihui, Schaefer, Dirk: 'Cloud-based design and manufacturing: A new paradigm in digital manufacturing and design innovation'*Comput. Des.*, 2015, **59**, pp. 1–14. , doi: 10.1016/j.cad.2014.07.006

103 Pisching, Marcos A., Junqueira, Fabr\'\icio, Santos Filho, Diolino J., Miyagi, Paulo E.: 'Service composition in the cloud based manufacturing focused on the industry 4.0', in 'Doctoral Conference on Computing, Electrical and Industrial Systems' (2015), pp. 65–72

104 Li, Gang, Wei, Mingchuan: 'Everything-as-a-service platform for on-demand virtual enterprises'*Inf. Syst. Front.*, 2014, **16**, (3), pp. 435–452. , doi: 10.1007/s10796-012-9351-3

105 Giménez, Joaqu\in: 'Everything-as-a-Service'no date.

106 Duan, Yucong: 'Value modeling and calculation for everything as a service (XaaS) based on reuse', in 'Proceedings - 13th ACIS International Conference on Software Engineering, Artificial Intelligence, Networking, and Parallel/Distributed Computing, SNPD 2012' (2012), pp. 162–167, doi: 10.1109/SNPD.2012.30

107 Duan, Y.C., Fu, G.H., Zhou, N.J., Sun, X.B., Narendra, N.C., Hu, B.: 'Everything as a Service(XaaS) on the Cloud: Origins, Current and Future Trends', in '2015 Ieee 8th International Conference on Cloud Computing' (2015), pp. 621–628, doi: 10.1109/cloud.2015.88

108 Wu, Dazhong, Thames, J. Lane, Rosen, David W., Schaefer, Dirk: 'Enhancing the Product Realization Process With Cloud-Based Design and Manufacturing Systems'*J. Comput. Inf. Sci. Eng.*, 2013, **13**, (4), p. 041004. , doi: 10.1115/1.4025257

109 Govindan, Kannan, Cheng, Tce, Mishra, Nishikant, Shukla, Nagesh: 'Big data analytics and application for logistics and supply chain management' (Elsevier, 2018), 114, pp. 343–349, doi: 10.1016/j.tre.2018.03.011

110 Kozjek, Dominik, Rihtaršič, Borut, Butala, Peter, others: 'Kozjek, Vrabič - 2018 - Big data analytics for operations management in engineer-to-order manufacturing.pdf'*Procedia CIRP*, 2018, **72**, pp. 209–214.

111 He, Q. Peter, Wang, Jin: 'Statistical process monitoring as a big data analytics tool for smart manufacturing'*J. Process Control*, 2017, **67**, pp. 35–43. , doi: 10.1016/j.jprocont.2017.06.012

112 Attaran, Mohsen, Attaran, Sharmin: 'The Rise of Embedded Analytics: Empowering Manufacturing and Service Industry With Big Data'*Int. J. Bus. Intell. Res.*, 2018, **9**, (1), pp. 16–37. , doi: 10.4018/IJBIR.2018010102

113 Kamble, Sachin S., Gunasekaran, Angappa, Gawankar, Shradha A.: 'Sustainable Industry 4 . 0 framework : A systematic literature review identifying the current trends and future perspectives'*Process Saf. Environ. Prot.*, 2018, **117**, pp. 408–425. , doi: 10.1016/j.psep.2018.05.009

114   Raghupathi, Wullianallur, Raghupathi, Viju: 'Big data analytics in healthcare: promise and potential'*Heal. Inf. Sci. Syst.*, 2014, **2**, (1), p. 3. , doi: 10.1186/2047-2501-2-3

115   Burghard, C.: 'Big Data and Analytics Key to Accountable Care Success'*IDC Heal. Insights*, 2012, (October), pp. 1–9.

116   Abaker, Ibrahim, Hashem, Targio, Yaqoob, Ibrar, Badrul, Nor, Mokhtar, Salimah, Gani, Abdullah, Ullah, Samee: 'The rise of " big data " on cloud computing : Review and open research issues'*Inf. Syst.*, 2015, **47**, pp. 98–115. , doi: 10.1016/j.is.2014.07.006

117   Priyadarshini, Anushree, Agarwal, Sonali: 'A Map Reduce based Support Vector Machine for Big Data Classification'*Int. J. Database Theory Appl.*, 2015, **8**, (5), pp. 77–98. , doi: 10.14257/ijdta.2015.8.5.07

118   IBMAnalytics: 'Big Data Analytics'*IBM Anal.*, 2018, **21**, (8), pp. 695–716. , doi: 10.1002/9781119205005

119   Zaeh, M., Siedl, D.: 'A new method for simulation of machining performance by integrating finite element and multi-body simulation for machine tools'*CIRP Ann. - Manuf. Technol.*, 2007, **56**, (1), pp. 383–386. , doi: 10.1016/j.cirp.2007.05.089

120   Pandy, Marcus G.: 'Computer modeling and simulation of human movement.'*Kinesiology*, 2001, **3**, (1), pp. 245–273. , doi: 10.1146/annurev.bioeng.3.1.245

121   Folgado, E., Rincón, M., Álvarez, JR, Mira, J.: 'Simulating complex robotic scenarios with MORSE', in 'Nature Inspired Problem- …' (2007), pp. 202–211

122   Schrock, P., Farelo, F., Alqasemi, R., Dubey, R.: 'Design, Simulation and Testing of a new Modular Wheelchair Mounted Robotic Arm to Perform Activities of Daily Living', in '2009 IEEE International Conference on Rehabilitation Robotics' (2009), pp. 518–523, doi: 10.1109/ICORR.2009.5209469

123   Pdf, View, Pdf, Download: 'Real time simulation using position sensing' (Google Patents, 2000)

124   Song, Lingguang, Eldin, Neil N.: 'Adaptive real-time tracking and simulation of heavy construction operations for look-ahead scheduling'*Autom. Constr.*, 2012, **27**, pp. 32–39. , doi: 10.1016/j.autcon.2012.05.007

125   Herrmann, Christoph, Thiede, Sebastian: 'Process chain simulation to foster energy efficiency in manufacturing: Life Cycle Engineering'*CIRP J. Manuf. Sci. Technol.*, 2009, **1**, (4), pp. 221–229. , doi: 10.1016/j.cirpj.2009.06.005

126   Mustafaraj, G., Marini, D., Costa, A., Keane, M.: 'Model calibration for building energy efficiency simulation'*Appl. Energy*, 2014, **130**, pp. 72–85. , doi: 10.1016/j.apenergy.2014.05.019

127   Han, L., Xing, K., Chen, X., Xiong, F.: 'A Petri net-based particle swarm optimization approach for scheduling deadlock-prone flexible manufacturing systems'*J. Intell. Manuf.*, 2015, **29**, (5), pp. 1083–1096. , doi: 10.1007/s10845-015-1161-2

128   Shen, Victor R.L., Yang, Cheng Ying, Shen, Rong Kuan, Chen, Yu Chia: 'Application of Petri nets to deadlock avoidance in iPad-like manufacturing systems'*J. Intell. Manuf.*, 2018, **29**, (6), pp. 1363–1378. , doi: 10.1007/s10845-015-1185-7

129 Fiorentino, Michele, Radkowski, Rafael, Stritzke, Christian, Uva, Antonio E., Monno, Giuseppe: 'Design review of CAD assemblies using bimanual natural interface'*Int. J. Interact. Des. Manuf.*, 2013, **7**, (4), pp. 249–260. , doi: 10.1007/s12008-012-0179-3

130 Heckel, B., Uva, A.E., Hamann, B., Joy, K.I.: 'Surface reconstruction using adaptive clustering methods', in 'Computing Supplement' (Springer, 2001), pp. 199–218

131 Boccaccio, Antonio, Uva, Antonio Emmanuele, Fiorentino, Michele, Lamberti, Luciano, Monno, Giuseppe: 'A mechanobiology-based algorithm to optimize the microstructure geometry of bone tissue scaffolds'*Int. J. Biol. Sci.*, 2016, **12**, (1), pp. 1–17. , doi: 10.7150/ijbs.13158

132 Fiorentino, Michele, Uva, Antonio E., Gattullo, Michele, Debernardis, Saverio, Monno, Giuseppe: 'Augmented reality on large screen for interactive maintenance instructions'*Comput. Ind.*, 2014, **65**, (2), pp. 270–278. , doi: 10.1016/j.compind.2013.11.004

133 Bevilacqua, Vitoantonio, Trotta, Gianpaolo Francesco, Brunetti, Antonio, Buonamassa, Giuseppe, Bruni, Martino, Delfine, Giancarlo, Riezzo, Marco, Amodio, Michele, Bellantuono, Giuseppe, Magaletti, Domenico, others: 'Photogrammetric Meshes and 3D Points Cloud Reconstruction: A Genetic Algorithm Optimization Procedure', in 'Italian Workshop on Artificial Life and Evolutionary Computation' (2016), pp. 65–76

134 Smaradottir, Berglind, Martinez, Santiago, Thygesen, Elin, Holen-rabbersvik, Elisabeth, Vatnøy, Torunn, Fensli, Rune: 'Innovative Simulation of Health Care Services in the Usability Laboratory Experiences from the Model for Telecare Alarm Services-project', in 'Proceedings from The 15th Scandinavian Conference on Health Informatics 2017 Kristiansand, Norway, August 29--30, 2017' (2018), pp. 29–30

135 Jewer, Jennifer, Dubrowski, Adam, Hoover, Kristopher, Smith, Andrew, Parsons, Michael: 'Development of a Mobile Tele-Simulation Unit Prototype for Training of Rural and Remote Emergency Health Care Providers'*Proc. 51st Hawaii Int. Conf. Syst. Sci.*, 2018, pp. 2894–2903.

136 Semeraro, Federico, Bergamasco, M., Frisoli, A., Holtzer, M., Cerchiari, Erga L.: 'Virtual reality prototype in healthcare simulation training'*Resuscitation*, 2008, **77**, (Supplement 1), pp. S60–S61. , doi: 10.1016/j.resuscitation.2008.03.187

137 Gaba, D.: 'The future of simulation in health care'*Simul. Healthc. J. Soc. Simul. Healthc.*, 2007, **2**, (2), pp. 126–135.

138 Delisle, Dominik, Schreiber, Markus, Krombholz, Christian, Stüve, Jan: 'Production of fiber composite structures by means of cooperating robots'*Light. Des. Worldw.*, 2018, **11**, (2), pp. 42–47.

139 Jiang, Yuhua, Liu, Keyun, Li, Youxiang: 'Initial Clinical Trial of Robot of Endovascular Treatment with Force Feedback and Cooperating of Catheter and Guidewire.'*Appl. bionics Biomech.*, 2018, **2018**, p. 9735979. , doi: 10.1155/2018/9735979

140 Salmi, Timo, Ahola, Jari M., Heikkilä, Tapio, Kilpeläinen, Pekka, Malm, Timo: 'Human-Robot Collaboration and Sensor-Based Robots in Industrial Applications and Construction', in 'Robotic Building' (Springer, 2018), pp. 25–52

141 Yamamoto, Tomoya, Kawase, Daisuke, Enomoto, Toshifumi, Utsunomiya, Masakazu:

'Robot safety system' (Google Patents, 2018)

142   Wang, Shiyong, Wan, Jiafu, Zhang, Daqiang, Li, Di, Zhang, Chunhua: 'Towards smart factory for industry 4.0: a self-organized multi-agent system with big data base d fee dback and coordination'*Comput. Networks*, 2016, **101**, pp. 158–168. , doi: 10.1016/j.comnet.2015.12.017

143   Wang, W.S., Zhu, X.X., Wang, L.Y., Qiu, Q., Cao, Q.X.: 'Ubiquitous Robotic Technology for Smart Manufacturing System'*Comput. Intell. Neurosci.*, 2016, **2016**. , doi: 10.1155/2016/6018686

144   Wang, Shiyong, Wan, Jiafu, Li, Di, Zhang, Chunhua: 'Implementing Smart Factory of Industrie 4'*Int. J. Distrib. Sens. Networks*, 2016, **2016**, (4), pp. 1–10. , doi: 10.1155/2016/3159805

145   Shu, John, M. Rosenberg, Jason, Upadhyaya, Shambhu, Rao, Hejamadi Raghav: 'The Internet of Things and IT Auditing'*Internet Things A to Z Technol. Appl.*, 2018, pp. 275–292. , doi: 10.1002/9781119456735.ch10

146   Kagermann, Henning: 'Change through digitization - value creation in the age of industry 4.0', in 'Management of Permanent Change' (Springer, 2015), pp. 23–45, doi: 10.1007/978-3-658-05014-6_2

147   Alanne, Kari, Saari, Arto: 'Distributed energy generation and sustainable development'*Renew. Sustain. energy Rev.*, 2006, **10**, (6), pp. 539–558. , doi: 10.1016/j.rser.2004.11.004

148   Billinton, Roy, Acharya, Janak R.: 'Weather-based distribution system reliability evaluation'*IEE Proceedings-Generation, Transm. Distrib.*, 2006, **153**, (5), pp. 499–506.

149   Batista, N.C., Melício, R., Mendes, V.M.F.: 'Services enabler architecture for smart grid and smart living services providers under industry 4.0'*Energy Build.*, 2017, **141**, pp. 16–27. , doi: 10.1016/j.enbuild.2017.02.039

150   Faheem, M., Gungor, V.C.: '[num 1] Energy efficient and QoS-aware routing protocol for wireless sensor network-based smart grid applications in the context of industry 4.0'*Appl. Soft Comput.*, 2017, **68**, pp. 910–922.

151   Bui, Nicola, Castellani, Angelo P., Casari, Paolo, Zorzi, Michele: 'The internet of energy: A web-enabled smart grid system'*IEEE Netw.*, 2012, **26**, (4), pp. 39–45. , doi: 10.1109/MNET.2012.6246751

152   Lom, Michal, Pribyl, Ondrej, Svitek, Miroslav: 'Industry 4.0 as a part of smart cities', in '2016 Smart Cities Symposium Prague (SCSP)' (2016), pp. 1–6, doi: 10.1109/SCSP.2016.7501015

153   Mačiulis, Alminas, Vasiliauskas, Aidas Vasilis, Jakubauskas, Gražvydas: 'The impact of transport on the competitiveness of national economy'*Transport*, 2009, **24**, (2), pp. 93–99. , doi: 10.3846/1648-4142.2009.24.93-99

154   Goldman, Todd, Gorham, Roger: 'Sustainable urban transport: Four innovative directions'*Technol. Soc.*, 2006, **28**, (1–2), pp. 261–273. , doi: 10.1016/j.techsoc.2005.10.007

155   Maslarić, Marinko, Nikoličić, Svetlana, Mirčetić, Dejan: 'Logistics Response to the Industry 4.0: The Physical Internet'*Open Eng.*, 2016, **6**, (1), pp. 511–517. , doi:

10.1515/eng-2016-0073

156 Litman, Todd: 'Developing Indicators for Comprehensive and Sustainable Transport Planning'*Transp. Res. Rec. 2017, TRB*, 2007, (2017), pp. 10–15. , doi: 10.3141/2017-02

157 Brunetti, Antonio, Buongiorno, Domenico, Trotta, Gianpaolo Francesco, Bevilacqua, Vitoantonio: 'Computer vision and deep learning techniques for pedestrian detection and tracking: A survey'*Neurocomputing*, 2018, **300**, pp. 17–33. , doi: 10.1016/j.neucom.2018.01.092

158 BONGIOVANNI R., LOWENBERG-DEBOER J.: 'Precision Agriculture and Sustainability R.'*Precis. Agric.*, 2004, **5**, (4), pp. 359–387.

159 Daberkow, Stan G., McBride, William D.: 'Farm and operator characteristics affecting the awareness and adoption of precision agriculture technologies in the US'*Precis. Agric.*, 2003, **4**, (2), pp. 163–177. , doi: 10.1023/A:1024557205871

160 Whelan, B.M., McBratney, A.B.: '\tThe "Null Hypothesis" of precision agriculture management'\t*Precision Agric.*, 2000, **\t2**, (\t3), pp. 265–279.

161 Yahya, Noorhana: 'Agricultural 4.0: Its implementation toward future sustainability', in 'Green Energy and Technology' (Springer, 2018), pp. 125–145, doi: 10.1007/978-981-10-7578-0_5

162 Knoll, F.J., Czymmek, V.: 'The German Vision of Industry 4.0 Applied in Organic Farming', in 'Automation in Agriculture - Securing Food Supplies for Future Generations' (InTech, 2018), doi: 10.5772/intechopen.72708

163 European Commission: 'Industry 4.0 in Agriculture : Focus on IoT aspects' (Digital Transformation Monitor, 2017)

164 Büttner, Sebastian, Mucha, Henrik, Funk, Markus, Kosch, Thomas, Aehnelt, Mario, Robert, Sebastian, Röcker, Carsten: 'The Design Space of Augmented and Virtual Reality Applications for Assistive Environments in Manufacturing', in 'Proceedings of the 10th International Conference on PErvasive Technologies Related to Assistive Environments - PETRA '17' (2017), pp. 433–440, doi: 10.1145/3056540.3076193

165 Doestzada, Marwah, Vila, Arnau Vich, Zhernakova, Alexandra, Koonen, Debby P.Y., Weersma, Rinse K., Touw, Daan J., Kuipers, Folkert, Wijmenga, Cisca, Fu, Jingyuan: 'Pharmacomicrobiomics: a novel route towards personalized medicine?'*Protein Cell*, 2018, **9**, (5), pp. 432–445. , doi: 10.1007/s13238-018-0547-2

166 Karolak, Aleksandra, Rejniak, Katarzyna A.: 'Mathematical Modeling of Tumor Organoids: Toward Personalized Medicine', in 'Tumor organoids' (Springer, 2018), pp. 193–213, doi: 10.1007/978-3-319-60511-1_10

167 Aguado, Brian A., Grim, Joseph C., Rosales, Adrianne M., Watson-Capps, Jana J., Anseth, Kristi S.: 'Engineering precision biomaterials for personalized medicine'*Sci. Transl. Med.*, 2018, **10**, (424), p. eaam8645. , doi: 10.1126/scitranslmed.aam8645

168 Warnken, Zachary N., Smyth, Hugh D.C., Davis, Daniel A., Weitman, Steve, Kuhn, John G., Williams, Robert O.: 'nasal drug targeting using 3D printed nasal replica casts Personalized medicine in nasal delivery : the use of patient- specific administration parameters to improve nasal drug targeting using 3D printed nasal replica casts'*Mol. Pharm.*, 2018, **15**, (4), pp. 1392–1402. , doi: 10.1021/acs.molpharmaceut.7b00702

169   Kaplan, Henry, Berry, Anna, Rinn, Kristine, Ellis, Erin, Birchfield, George, Wahl, Tanya, Liu, Xiaoyu, Tameishi, Mariko, Beatty, J.D., Dawson, Patricia, others: 'Machine learning approach to personalized medicine in breast cancer patients: Development of data-driven, personalized, causal modeling through identification and understanding of optimal treatments for predicting better disease outcomes' (AACR, 2018)

170   Bevilacqua, Vitoantonio, Dimauro, Giovanni, Marino, Francescomaria, Brunetti, Antonio, Cassano, Fabio, Di Maio, Antonio, Nasca, Enrico, Trotta, Gianpaolo Francesco, Girardi, Francesco, Ostuni, Angelo, Guarini, Attilio: 'A novel approach to evaluate blood parameters using computer vision techniques', in '2016 IEEE International Symposium on Medical Measurements and Applications (MeMeA)' (2016), pp. 1–6, doi: 10.1109/MeMeA.2016.7533760

171   Bevilacqua, Vitoantonio, Carnimeo, Leonarda, Brunetti, Antonio, De Pace, Andrea, Galeandro, Pietro, Trotta, Gianpaolo Francesco, Caporusso, Nicholas, Marino, Francescomaria, Alberotanza, Vito, Scardapane, Arnaldo: 'Synthesis of a neural network classifier for hepatocellular carcinoma grading based on triphasic CT images', in 'Communications in Computer and Information Science' (2017), pp. 356–368, doi: 10.1007/978-981-10-4859-3_32

172   Bortone, Ilaria, Francesco, Gianpaolo, Donato, Giacomo, Argentiero, Alberto, Agnello, Nadia, Nicolardi, Giuseppe, Bevilacqua, Vitoantonio: 'Optimal Classifier of Parkinson's Disease based on features selected by Information Gain in 3D Gait Analysis for Differential Diagnosis'*Gait Posture*, 2017, **57**, pp. 205–206. , doi: 10.1016/j.gaitpost.2017.06.372

173   Bevilacqua, Vitoantonio, Brunetti, Antonio, Trotta, Gianpaolo Francesco, Carnimeo, Leonarda, Marino, Francescomaria, Alberotanza, Vito, Scardapane, Arnaldo: 'A Deep Learning Approach for Hepatocellular Carcinoma Grading'*Int. J. Comput. Vis. Image Process.*, 2017, **7**, (2), pp. 1–18. , doi: 10.4018/IJCVIP.2017040101

174   Bevilacqua, Vitoantonio, Brunetti, Antonio, Trotta, Gianpaolo Francesco, Dimauro, Giovanni, Elez, Katarina, Alberotanza, Vito, Scardapane, Arnaldo: 'A novel approach for Hepatocellular Carcinoma detection and classification based on triphasic CT Protocol', in '2017 IEEE Congress on Evolutionary Computation, CEC 2017 - Proceedings' (2017), pp. 1856–1863, doi: 10.1109/CEC.2017.7969527

175   Bevilacqua, Vitoantonio, Brunetti, Antonio, Trotta, Gianpaolo Francesco, De Marco, Domenico, Quercia, Marco Giuseppe, Buongiorno, Domenico, D'Introno, Alessia, Girardi, Francesco, Guarini, Attilio: 'A Novel Deep Learning Approach in Haematology for Classification of Leucocytes', in 'Italian Workshop on Neural Nets' (2017), pp. 265–274

176   Caporusso, Nicholas, Biasi, Luigi, Cinquepalmi, Giovanni, Trotta, Gianpaolo Francesco, Brunetti, Antonio, Bevilacqua, Vitoantonio: 'A wearable device supporting multiple touch- and gesture-based languages for the deaf-blind', in 'Advances in Intelligent Systems and Computing' (2018), pp. 32–41, doi: 10.1007/978-3-319-60639-2_4

177   Caporusso, Nicholas, Biasi, Luigi, Cinquepalmi, Giovanni, Trotta, Gianpaolo Francesco, Brunetti, Antonio, Bevilacqua, Vitoantonio: 'Enabling touch-based communication in wearable devices for people with sensory and multisensory

impairments', in 'Advances in Intelligent Systems and Computing' (2018), pp. 149–159, doi: 10.1007/978-3-319-60639-2_15

178 Bevilacqua, Vitoantonio, Trotta, Gianpaolo Francesco, Loconsole, Claudio, Brunetti, Antonio, Caporusso, Nicholas, Bellantuono, Giuseppe Maria, De Feudis, Irio, Patruno, Donato, De Marco, Domenico, Venneri, Andrea, Di Vietro, Maria Grazia, Losavio, Giacomo, Tatò, Sabina Ilaria: 'A RGB-D Sensor Based Tool for Assessment and Rating of Movement Disorders', in 'International Conference on Applied Human Factors and Ergonomics' (2018), pp. 110–118, doi: 10.1007/978-3-319-60483-1_12

179 Bevilacqua, Vitoantonio, Trotta, Gianpaolo Francesco, Brunetti, Antonio, Caporusso, Nicholas, Loconsole, Claudio, Cascarano, Giacomo Donato, Catino, Francesco, Cozzoli, Pantaleo, Delfine, Giancarlo, Mastronardi, Adriano, Di Candia, Andrea, Lelli, Giuseppina, Fiore, Pietro: 'A Comprehensive Approach for Physical Rehabilitation Assessment in Multiple Sclerosis Patients Based on Gait Analysis', in 'International Conference on Applied Human Factors and Ergonomics' (2018), pp. 119–128, doi: 10.1007/978-3-319-60483-1_13

180 Loconsole, Claudio, Trotta, Gianpaolo Francesco, Brunetti, Antonio, Trotta, Joseph, Schiavone, Angelo, Tatò, Sabina Ilaria, Losavio, Giacomo, Bevilacqua, Vitoantonio: 'Computer vision and EMG-based handwriting analysis for classification in parkinson's disease', in 'Lecture Notes in Computer Science (including subseries Lecture Notes in Artificial Intelligence and Lecture Notes in Bioinformatics)' (2017), pp. 493–503, doi: 10.1007/978-3-319-63312-1_43

181 Bevilacqua, Vitoantonio, Altini, Daniele, Bruni, Martino, Riezzo, Marco, Brunetti, Antonio, Loconsole, Claudio, Guerriero, Andrea, Trotta, Gianpaolo Francesco, Fasano, Rocco, Di Pirchio, Marica, Tartaglia, Cristina, Ventrella, Elena, Telegrafo, Michele, Moschetta, Marco: 'A supervised breast lesion images classification from tomosynthesis technique', in 'Lecture Notes in Computer Science (including subseries Lecture Notes in Artificial Intelligence and Lecture Notes in Bioinformatics)' (2017), pp. 483–489, doi: 10.1007/978-3-319-63312-1_42

182 Bevilacqua, Vitoantonio, Simeone, Sergio, Brunetti, Antonio, Loconsole, Claudio, Trotta, Gianpaolo Francesco, Tramacere, Salvatore, Argentieri, Antonio, Ragni, Francesco, Criscenti, Giuseppe, Fornaro, Andrea, others: 'A Computer Aided Ophthalmic Diagnosis System Based on Tomographic Features', in 'International Conference on Intelligent Computing' (2017), pp. 598–609

183 Invitto, Sara, Piraino, Giulia, Mignozzi, Arianna, Capone, Simona, Montagna, Giovanni, Siciliano, Pietro Aleardo, Mazzatenta, Andrea, Rocco, Gianbattista, De Feudis, Irio, Trotta, Gianpaolo F., Brunetti, Antonio, Bevilacqua, Vitoantonio: 'Smell and meaning: An OERP study', in 'Smart Innovation, Systems and Technologies' (Springer, 2017), pp. 289–300, doi: 10.1007/978-3-319-56904-8_28

184 Bevilacqua, Vitoantonio, Brunetti, Antonio, Guerriero, Andrea, Trotta, Gianpaolo Francesco, Telegrafo, Michele, Moschetta, Marco: 'A performance comparison between shallow and deeper neural networks supervised classification of tomosynthesis breast lesions images'*Cogn. Syst. Res.*, 2018. , doi: 10.1016/j.cogsys.2018.04.011

185 Buongiorno, Domenico, Trotta, Gianpaolo Francesco, Bortone, Ilaria, Di Gioia, Nicola, Avitto, Felice, Losavio, Giacomo, Bevilacqua, Vitoantonio: 'Assessment and rating of

movement impairment in Parkison's Disease using a low-cost vision-based system', in 'Accepted for pubblication in the Proceedings of the 2018 International Conference on Intelligent Computing' (2018), pp. 777–788, doi: 10.1007/978-3-319-95957-3_82

186   Bortone, I., Quercia, M.G., Ieva, N., Cascarano, G.D., Trotta, G.F., Tatò, S.I., Bevilacqua, V.: 'Recognition and Severity Rating of Parkinson's Disease from Postural and Kinematic Features During Gait Analysis with Microsoft Kinect', in 'Lecture Notes in Computer Science (including subseries Lecture Notes in Artificial Intelligence and Lecture Notes in Bioinformatics)' (2018), pp. 613–618, doi: 10.1007/978-3-319-95933-7_70

187   Trotta, Gianpaolo Francesco, Pellicciari, Roberta, Boccaccio, Antonio, Brunetti, Antonio, Cascarano, Donato Giacomo, Manghisi, Vito Modesto, Fiorentino, Michele, Uva, Antonio Emanuele, Defazio, Giovanni, Bevilacqua, Vitoantonio: 'A Neural Network-based Software to Recognize and Count Blinks, Brief and Prolonged Spasms and Measure Eye Closure Time in Patients with Blepharospasm'*To be Submitt. to Artif. Intell. Med.*, 2018.

188   Pepe, Antonio, Francesco, Gianpaolo, Schmalstieg, Dieter, Wallner, Jürgen, Egger, Jan, Bevilacqua, Vitoantonio: 'Study , Implementation and Application of a Mixed Reality System for Computer-aided Maxillofacial Oncological Surgery'*Submitt. to PLOS ONE*, 2018.

189   Carnimeo, Leonarda, Trotta, Gianpaolo Francesco, Brunetti, Antonio, Cascarano, Giacomo Donato, Buongiorno, Domenico, Loconsole, Claudio, Di Sciascio, Eugenio, Bevilacqua, Vitoantonio: 'A Proposal of a Healthcare Network based on Big Data Analytics for Parkinson's diseases' *Accepted to Inst. Eng. Technol.*, 2018.

190   Bortone, Ilaria, Buongiorno, Domenico, Lelli, Giuseppina, Di Candia, Andrea, Cascarano, Giacomo Donato, Trotta, Gianpaolo Francesco, Fiore, Pietro, Bevilacqua, Vitoantonio: 'Gait Analysis and Parkinson's Disease: Recent trends on main applications in healthcare', in 'International Conference on NeuroRehabilitation (ICNR). Springer. (In press)' (2018)

191   Pepe A., Trotta G.F. Gsaxner C. Schmalstieg D. Egger J. Wallner J. Bevilacqua V: 'Pattern Recognition and Mixed Reality for Computer-Aided Maxillofacial Surgery and Oncological Assessment', in 'Proceedings of the 2018 Biomedical Engineering International Conferece (BMEiCON2018)' (2018)

192   Plaza, Andrea M., Díaz, Jessica, Pérez, Jennifer: 'Software architectures for health care cyber - physical systems : A systematic literature review'*J. Softw. Evol. Process*, 2018, (November 2017), pp. 1–23. , doi: 10.1002/smr.1930

193   Rajabi Shishvan, Omid, Zois, Daphney-Stavroula, Soyata, Tolga: 'Machine Intelligence in Healthcare and Medical Cyber Physical Systems: A Survey'*IEEE Access*, 2018, **6**, pp. 46419–46494. , doi: 10.1109/ACCESS.2018.2866049

194   Gatouillat, Arthur, Badr, Youakim, Massot, Bertrand, Sejdic, Ervin: 'Internet of Medical Things: A Review of Recent Contributions Dealing with Cyber-Physical Systems in Medicine'*IEEE Internet Things J.*, 2018. , doi: 10.1109/JIOT.2018.2849014

195   Plank, Hannes, Steinbaeck, Josef, Druml, Norbert, Steger, Christian, Holweg, Gerald: 'Localization and Context Determination for Cyber-physical Systems based on 3D

Imaging', in 'Handbook of Research on Solutions for Cyber-Physical Systems Ubiquity' (IGI Global, 2018), pp. 1–26

196 Dey, Nilanjan, Ashour, Amira S., Shi, Fuqian, Fong, Simon James, Tavares, João Manuel R.S.: 'Medical cyber-physical systems: A survey'*J. Med. Syst.*, 2018, **42**, (4), p. 74. , doi: 10.1007/s10916-018-0921-x

197 Tang, Arthur, Owen, Charles, Biocca, Frank, Mou, Weimin: 'Comparative effectiveness of augmented reality in object assembly', in 'Proceedings of the conference on Human factors in computing systems - CHI '03' (2003), p. 73, doi: 10.1145/642625.642626

198 Ganier, Franck: 'Factors Affecting the Processing of Procedural Instructions: Implications for Document Design'*IEEE Trans. Prof. Commun.*, 2004, **47**, (1), pp. 15–26. , doi: 10.1109/TPC.2004.824289

199 Watson, G., Curran, R., Butterfield, J., Craig, C.: 'The effect of using animated work instructions over text and static graphics when performing a small scale engineering assembly', in 'Collaborative Product and Service Life Cycle Management for a Sustainable World - Proceedings of the 15th ISPE International Conference on Concurrent Engineering, CE 2008' (Springer, 2008), pp. 541–550

200 Fiorentino, M., Monno, G., Uva, A.E.: 'Interactive ` touch and see ' FEM Simulation using Augmented Reality *'*Comput. Mech.*, 2009, **25**, (6), pp. 1124–1128.

201 Webel, Sabine, Bockholt, Ulrich, Keil, Jens: 'Design criteria for AR-based training of maintenance and assembly tasks', in 'Lecture Notes in Computer Science (including subseries Lecture Notes in Artificial Intelligence and Lecture Notes in Bioinformatics)' (2011), pp. 123–132, doi: 10.1007/978-3-642-22021-0_15

202 TEST TEST TEST Henderson, Steven, Feiner, Steven: 'TEST 22222 TEST TEST Exploring the benefits of augmented reality documentation for maintenance and repair'*TEST TEST TEST, Vis. Comput. Graph. IEEE Trans.*, 2011, **17**, (10), pp. 1355–1368.

203 De Marchi, Luca, Ceruti, Alessandro, Marzani, Alessandro, Liverani, Alfredo: 'Augmented reality to support on-field post-impact maintenance operations on thin structures'*J. Sensors*, 2013, **2013**. , doi: 10.1155/2013/619570

204 Eurofound: 'Sixth European Working Conditions Survey' (European Working and Condition Observatory Dublin, 2015)

205 Luttmann, Alwin, Jager, M., Caffier, G., Liebers, F.: 'Preventing Musculoskeletal Disorders in the Workplace'*World Heal. Organ. Rep. Geneva*, 2003, (5), p. 1–38lu. , doi: http://www.who.int/iris/handle/10665/42651

206 Li, G., Buckle, P.: 'Current techniques for assessing physical exposure to work- related musculoskeletal risks , with em phasis on posture-based'*Ergonomics*, 1999, **42**, (5), pp. 674–695. , doi: 10.1080/001401399185388

207 Balogh, I., Ørbæk, P., Ohlsson, K., Nordander, C., Unge, J., Winkel, J., Hansson, G.Å.: 'Self-assessed and directly measured occupational physical activities—influence of musculoskeletal complaints, age and gender'*Appl. Ergon.*, 2004, **35**, (1), pp. 49–56. , doi: 10.1016/j.apergo.2003.06.001

208 David, G.C.: 'Ergonomic methods for assessing exposure to risk factors for work-related musculoskeletal disorders'*Occup. Med. (Chic. Ill).*, 2005, **55**, (3), pp. 190–199.

, doi: 10.1093/occmed/kqi082

209 Xu, Xu, Mcgorry, Raymond W., Chou, Li-shan, Lin, Jia-hua, Chang, Chien-chi: 'Gait & Posture Accuracy of the Microsoft Kinect TM for measuring gait parameters during treadmill walking'*Gait Posture, Elsevier*, 2015, **42**, (2), pp. 145–151. , doi: 10.1016/j.gaitpost.2015.05.002

210 Xu, Xu, McGorry, Raymond W.: 'The validity of the first and second generation Microsoft Kinect for identifying joint center locations during static postures'*Appl. Ergon.*, 2015, **49**, pp. 47–54. , doi: 10.1016/j.apergo.2015.01.005

211 Kowalski, Jennifer R., Juo, Peter: 'The role of deubiquitinating enzymes in synaptic function and nervous system diseases'*Neural Plast.*, 2012, **2012**. , doi: 10.1155/2012/892749

212 Roman-Liu, Danuta: 'Comparison of concepts in easy-to-use methods for MSD risk assessment'*Appl. Ergon.*, 2014, **45**, (3), pp. 420–427. , doi: 10.1016/j.apergo.2013.05.010

213 BTS Bioengineering: 'Optoelectronic Plethysmography Compedium Marker Setup; A handbook about marker positioning on subjects in standing and supine positions'*Brooklyn, BTS Bioeng.*, 2011.

214 Zamfirescu, Constantin Bala, Pirvu, Bogdan Constantin, Schlick, Jochen, Zuehlke, Detlef: 'Preliminary Insides for an Anthropocentric Cyber-physical Reference Architecture of the Smart Factory Preliminary Insides for an Anthropocentric Cyber-physical Reference Architecture of the Smart Factory'*Stud. Informatics Control*, 2013, **22**, **No.3**, (September), pp. 269–278. , doi: 10.24846/v22i3y201303

215 Gorecky, Dominic, Garcia, Ricardo Campos, Meixner, Gerrit: 'Seamless Augmented Reality Support On The Shopfloor Based On Cyber-Physical-Systems', in 'Proceedings of the 14th International Conference on Human-computer Interaction with Mobile Devices and Services. International Conference on Human-Computer Interaction with Mobile Devices and Services (MobileHCI-12), September 21-24, San Francisco,, CA, U' (2012)

216 Quaranta, Giacomo, Abisset-Chavanne, Emmanuelle, Chinesta, Francisco, Duval, Jean-Louis: 'A cyber physical system approach for composite part: From smart manufacturing to predictive maintenance', in 'AIP Conference Proceedings' (2018), p. 020025, doi: 10.1063/1.5034826

217 Larrinaga, Felix, Fernandez, Javier, Zugasti, Ekhi, Zurutuza, Urko, Anasagasti, Mikel, Mondragon, Mikel, Coop, Goizper S.: 'Implementation of a Reference Architecture for Cyber Physical Systems to support Condition Based Maintenance', in '2018 5th International Conference on Control, Decision and Information Technologies (CoDIT)' (2018), pp. 773–778, doi: 10.1109/CoDIT.2018.8394825

218 Jantunen, Erkki, Di Orio, Giovanni, Hegedus, Csaba, Varga, Pal, Moldovan, Istvan, Larrinaga, Felix, Becker, Matthias, Albano, Michele, Maló, Pedro: 'Maintenance 4.0 World of Integrated Information', in 'Interoperability for Enterprise Systems and Applications, I-ESA'18' (2018)

219 Zhu, Kunpeng, Zhang, Yu: 'A Cyber-Physical Production System Framework of Smart CNC Machining Monitoring System'*IEEE/ASME Trans. Mechatronics*, 2018. , doi: 10.1109/TMECH.2018.2834622

220 Herwan, Jonny, Kano, Seisuke, Oleg, Ryabov, Sawada, Hiroyuki, Kasashima, Nagayoshi: 'Cyber-physical system architecture for machining production line', in 'Proceedings - 2018 IEEE Industrial Cyber-Physical Systems, ICPS 2018' (2018), pp. 387–391, doi: 10.1109/ICPHYS.2018.8387689

221 Villalonga, Alberto, Beruvides, Gerardo, Castano, Fernando, Haber, Rodolfo: 'Industrial cyber-physical system for condition-based monitoring in manufacturing processes', in 'Proceedings - 2018 IEEE Industrial Cyber-Physical Systems, ICPS 2018' (2018), pp. 637–642, doi: 10.1109/ICPHYS.2018.8390780

222 Tuo, Mingfu, Zhou, Cheng, Yin, Zhonghai, Zhao, Xin, Wang, Lei: 'Modelling behaviour of cyber-physical system and verifying its safety based on algebra of event'*Int. J. Intell. Inf. Database Syst.*, 2018, **11**, (2–3), pp. 169–185.

223 Couto, Luis Diogo, Basagianis, Stylianos, Mady, Alie El-Din, Ridouane, El Hassan, Larsen, Peter Gorm, Hasanagic, Miran: 'Injecting Formal Verification in FMI-based Co-Simulation of Cyber-Physical Systems', in '1st Workshop on Formal Co-Simulation of Cyber-Physical Systems' (2017), p. 284

224 Canadas, Nuno, Machado, Jose´, Soares, Filomena, Barros, Carlos, Varela, Leonilde: 'Simulation of cyber physical systems behaviour using timed plant models'*Mechatronics*, 2017, **54**, pp. 175–185. , doi: 10.1016/j.mechatronics.2017.10.009

225 Schmitt, Mathias, Meixner, Gerrit, Gorecky, Dominic, Seissler, Marc, Loskyll, Matthias: 'Mobile interaction technologies in the factory of the future'*IFAC Proc. Vol.*, 2013, **12**, (PART 1), pp. 536–542. , doi: 10.3182/20130811-5-US-2037.00001

226 Vaughan-Nichols, Steven J.: 'New interfaces at the touch of a fingertip'*Computer (Long. Beach. Calif).*, 2007, **40**, (8), pp. 12–15. , doi: 10.1109/MC.2007.286

227 Weber, Dean: 'Conversational Voice Interface of Connected Devices, Including Toys, Cars, Avionics, Mobile, Iot and Home Appliances' (2018)

228 Wigdor, Daniel, Wixon, Dennis: 'Brave NUI World: Designing Natural User Interfaces for Touch and Gesture' (Elsevier, 2011), doi: 10.1016/B978-0-12-382231-4.X0001-9

229 García-Peñalvo, F.J., Moreno, L.: 'Special issue on exploring new Natural User Experiences' (Springer, 2017), doi: 10.1007/s10209-017-0578-0

230 Caporusso, Nicholas, Ding, Meng, Clarke, Matthew, Carlson, Gordon, Bevilacqua, Vitoantonio, Trotta, Gianpaolo Francesco: 'Analysis of the Relationship Between Content and Interaction in the Usability Design of 360 o Videos', in 'International Conference on Applied Human Factors and Ergonomics' (2018), pp. 593–602

231 Plotnick, Rachel: 'Force, flatness and touch without feeling: Thinking historically about haptics and buttons'*New Media Soc.*, 2017, **19**, (10), pp. 1632–1652. , doi: 10.1177/1461444817717510

232 Ranasinghe, Nimesha, Jain, Pravar, Karwita, Shienny, Tolley, David, Yi-Luen Do, Ellen: 'Ambiotherm: Enhancing Sense of Presence in Virtual Reality by Simulating Real-World Environmental Conditions', in 'CHI '17 Proceedings of the 2017 CHI Conference on Human Factors in Computing Systems' (2017), pp. 1731–1742, doi: 10.1145/3025453.3025723

233 Wilson, G.: 'Using Pressure Input and Thermal Feedback to Broaden Haptic

Interaction with Mobile Devices'. University of Glasgow, 2013

234   Wilson, G., Halvey, M., Brewster, S.a., Hughes, S.a.: 'Some Like it Hot: Thermal Feedback for Mobile Devices', in 'Proceedings of the SIGCHI conference on Human Factors in Computing Systems - CHI '11' (2011), pp. 2555–2564, doi: 10.1145/1978942.1979316

235   Sarafoleanu, C., Mella, C., Georgescu, M., Perederco, C.: 'The importance of the olfactory sense in the human behavior and evolution.'*J. Med. Life*, 2009, **2**, (2), pp. 196–198.

236   Brewster, S.A., McGookin, D.K., Miller, C.A.: 'Olfoto: designing a smell-based interaction', in 'Proceedings of the 2006 Conference on Human Factors in Computing Systems CHI 2006 Montréal Québec Canada April 2227 2006' (2010), pp. 653–662, doi: 10.1145/1124772.1124869

237   Matsukura, Haruka, Yoneda, Tatsuhiro, Ishida, Hiroshi: 'Smelling screen: development and evaluation of an olfactory display system for presenting a virtual odor source'*IEEE Trans. Vis. Comput. Graph.*, 2013, **19**, (4), pp. 606–615.

238   Amores, Judith, Maes, Pattie: 'Essence : Olfactory Interfaces for Unconscious Influence of Mood and Cognitive Performance', in 'Chi 2017' (2017), pp. 28–34, doi: 10.1145/3025453.3026004

239   Obrist, Marianna, Tuch, Alexandre N., Hornbaek, Kasper: 'Opportunities for Odor: Experiences with Smell and Implications for Technology', in 'Proceedings of the SIGCHI Conference on Human Factors in Computing Systems' (2014), pp. 2843–2852, doi: 10.1145/2556288.2557008

240   Nimesha, Ranasinghe: 'Digitally stimulating the sensation of taste through electrical and thermal stimulation'. 2012

241   Narumi, Takuji, Nishizaka, Shinya, Kajinami, Takashi, Tanikawa, Tomohiro, Hirose, Michitaka: 'Augmented Reality Flavors: Gustatory Display Based on Edible Marker and Cross-modal Interaction', in 'Proceedings of the SIGCHI Conference on Human Factors in Computing Systems' (2011), pp. 93–102, doi: 10.1145/1978942.1978957

242   Maynes-Aminzade, Dan: 'Edible Bits : Seamless Interfaces between People , Data and Food', in 'Chi 2005' (2005), pp. 2207–2210

243   Fu, Limin Paul, Landay, James, Nebeling, Michael, Xu, Yingqing, Zhao, Chen: 'Redefining Natural User Interface', in 'Extended Abstracts of the 2018 CHI Conference on Human Factors in Computing Systems' (2018), p. SIG19, doi: 10.1145/3170427.3190649

244   Fern, Adso, Salle, La, Ramon, Universitat, Sus, Antonio, Lligadas, Xavier: 'Biomechanical Validation of Upper-body and Lower-body Joint Movements of Kinect Motion Capture Data for Rehabilitation Treatments', in 'Intelligent networking and collaborative systems (INCoS), 2012 4th international conference on' (2012), pp. 656–661, doi: 10.1109/iNCoS.2012.66

245   Kifayat, Kashif, Fergus, Paul, Cooper, Simon, Merabti, Madjid: 'Body area networks for movement analysis in physiotherapy treatments', in '24th IEEE International Conference on Advanced Information Networking and Applications Workshops, WAINA 2010' (2010), pp. 866–872, doi: 10.1109/WAINA.2010.155

246   Brondi, Raffaello, Superiore, Scuola, Anna, Sant, Superiore, Scuola, Anna, Sant: 'I ' m in VR !: Using your own hands in a fully immersive MR system', in 'Proceedings of the 20th ACM Symposium on Virtual Reality Software and Technology' (2016), pp. 73–76, doi: 10.1145/2671015.2671123

247   Elhayek, Ahmed, Aguiar, E., Jain, Arjun, Tompson, Jonathan, Pishchulin, Leonid, Andriluka, Mykhaylo, Bregler, Chris, Schiele, Bernt, Theobalt, Christian: 'MARCOnI - ConvNet-based MARker-less Motion Capture in Outdoor and Indoor Scenes'*IEEE Trans. Pattern Anal. Mach. Intell.*, 2016, **8828**, (c), pp. 1–1. , doi: 10.1109/TPAMI.2016.2557779

248   Nunes, J.F., Moreira, P.M., Tavares, J.M.R.S.: 'Human motion analysis and simulation tools: A survey', in 'Handbook of Research on Computational Simulation and Modeling in Engineering' (IGI Global, 2015), pp. 359–387, doi: 10.4018/978-1-4666-8823-0.ch012

249   Leardini, Alberto, Sawacha, Zimi, Paolini, Gabriele, Ingrosso, Stefania, Nativo, Roberto, Benedetti, Maria Grazia: 'A new anatomically based protocol for gait analysis in children'*Gait Posture*, 2007, **26**, (4), pp. 560–571. , doi: 10.1016/j.gaitpost.2006.12.018

250   Davis III, Rb, Ounpuu, S., Tyburski, Dennis, Gage, Jr: 'A gait analysis data collection and reduction technique'*Hum. Mov. Sci.*, 1991, **10**, (5), pp. 575–587. , doi: 10.1016/0167-9457(91)90046-Z

251   for Standardization (ISO), International Organization: 'Ergonomics--manual handling--part 3: handling of low loads at high frequency' (ISO Geneva, 2007)

252   Mcatamney, Lynn, Corlett, E. Nigel: 'RULA: a survey method for the investigation of world-related upper limb disorders'*Appl. Ergon.*, 1993, **24**, (2), pp. 91–99. , doi: 10.1016/0003-6870(93)90080-S

253   Robertson, Michelle, Amick, Benjamin C., DeRango, Kelly, Rooney, Ted, Bazzani, Lianna, Harrist, Ron, Moore, Anne: 'The effects of an office ergonomics training and chair intervention on worker knowledge, behavior and musculoskeletal risk'*Appl. Ergon.*, 2009, **40**, (1), pp. 124–135. , doi: 10.1016/j.apergo.2007.12.009

254   Dockrell, Sara, O'Grady, Eleanor, Bennett, Kathleen, Mullarkey, Clare, Mc Connell, Rachel, Ruddy, Rachel, Twomey, Seamus, Flannery, Colleen: 'An investigation of the reliability of Rapid Upper Limb Assessment (RULA) as a method of assessment of children's computing posture'*Appl. Ergon.*, 2012, **43**, (3), pp. 632–636. , doi: 10.1016/j.apergo.2011.09.009

255   Bao, Stephen, Howard, Ninica, Spielholz, Peregrin, Silverstein, Barbara, Polissar, Nayak: 'Interrater reliability of posture observations'*Hum. Factors*, 2009, **51**, (3), pp. 292–309. , doi: 10.1177/0018720809340273

256   Lowe, Brian D.: 'Accuracy and validity of observational estimates of shoulder and elbow posture'*Appl. Ergon.*, 2004, **35**, (2), pp. 159–171. , doi: 10.1016/j.apergo.2004.01.003

257   Lowe, Brian D.: 'Accuracy and validity of observational estimates of shoulder and elbow posture'*Appl. Ergon.*, 2004, **35**, (2), pp. 159–171. , doi: 10.1016/j.apergo.2004.01.003

258 Jansen, B., Salvia, P., Bouzahouene, H., Omelina, L., Moiseev, F., Sholukha, V., Cornelis, J., Rooze, M., Jan, S. Van Sint: 'Gait & Posture Validity and reliability of the Kinect within functional assessment activities : Comparison with standard stereophotogrammetry'*Gait Posture*, 2014, **39**, (1), pp. 593–598. , doi: 10.1016/j.gaitpost.2013.09.018

259 Dutta, T.: 'Evaluation of the Kinect sensor for 3-D kinematicmeasurement in the workplace'*Appl. Ergon.*, 2012, **43**, (4), pp. 645–649.

260 Clark, Ross A., Pua, Yong Hao, Fortin, Karine, Ritchie, Callan, Webster, Kate E., Denehy, Linda, Bryant, Adam L.: 'Validity of the Microsoft Kinect for assessment of postural control'*Gait Posture*, 2012, **36**, (3), pp. 372–377. , doi: 10.1016/j.gaitpost.2012.03.033

261 Clark, Ross A., Bower, Kelly J., Mentiplay, Benjamin F., Paterson, Kade, Pua, Yong Hao: 'Concurrent validity of the Microsoft Kinect for assessment of spatiotemporal gait variables'*J. Biomech.*, 2013, **46**, (15), pp. 2722–2725. , doi: 10.1016/j.jbiomech.2013.08.011

262 Plantard, Pierre, Auvinet, Edouard, Pierres, Anne-Sophie, Multon, Franck: 'Pose Estimation with a Kinect for Ergonomic Studies: Evaluation of the Accuracy Using a Virtual Mannequin'*Sensors*, 2015, **15**, (1), pp. 1785–1803. , doi: 10.3390/s150101785

263 Diego-Mas, Jose Antonio, Alcaide-Marzal, Jorge: 'Using Kinect™ sensor in observational methods for assessing postures at work'*Appl. Ergon.*, 2014, **45**, (4), pp. 976–985. , doi: 10.1016/j.apergo.2013.12.001

264 Patrizi, Alfredo, Pennestrì, Ettore, Valentini, Pier Paolo: 'Comparison between low-cost marker-less and high-end marker-based motion capture systems for the computer-aided assessment of working ergonomics'*Ergonomics*, 2016, **59**, (1), pp. 155–162. , doi: 10.1080/00140139.2015.1057238

265 Zennaro, S., Munaro, M., Milani, S., Zanuttigh, P., Bernardi, A., Ghidoni, S., Menegatti, E.: 'Performance Evaluation of the 1st and 2nd Generation Kinect For Multimedia Applications', in 'Multimedia and Expo (ICME), 2015 IEEE International Conference' (2013), pp. 1–6, doi: 10.1109/ICME.2015.7177380

266 Wang, Qifei, Wang, Qifei, Kurillo, Gregorij: 'Evaluation of Pose Tracking Accuracy in the First and Second Generations of Microsoft Kinect Evaluation of Pose Tracking Accuracy in the First and Second Generations of Microsoft Kinect'*arXiv Prepr. arXiv1512.04134*, 2015, (November), pp. 381–390. , doi: 10.1109/ICHI.2015.54

267 Navab, Nassir: 'Developing killer apps for industrial augmented reality'*IEEE Comput. Graph. Appl.*, 2004, **24**, (3), pp. 16–20. , doi: 10.1109/MCG.2004.1297006

268 Fiorentino, Michele, Debernardis, Saverio, Uva, Antonio E., Monno, Giuseppe: 'Augmented reality text style readability with see-through head-mounted displays in industrial context'*Presence Teleoperators Virtual Environ.*, 2013, **22**, (2), pp. 171–190. , doi: 10.1162/PRES_a_00146

269 Debernardis, Saverio, Fiorentino, Michele, Gattullo, Michele, Monno, Giuseppe, Uva, Antonio Emmanuele: 'Text readability in head-worn displays: Color and style optimization in video versus optical see-through devices'*IEEE Trans. Vis. Comput. Graph.*, 2014, **20**, (1), pp. 125–139. , doi: 10.1109/TVCG.2013.86

270   Bajana, Ján, Francia, Daniela, Liverani, Alfredo, Krajčovič, Martin: 'Mobile tracking system and optical tracking integration for mobile mixed reality'*Int. J. Comput. Appl. Technol.*, 2016, **53**, (1), p. 13. , doi: 10.1504/IJCAT.2016.073606

271   Bevilacqua, Vitoantonio, Barone, Donato, Suma, Marco: 'A multimodal fingers classification for general interactive surfaces', in 'Lecture Notes in Computer Science (including subseries Lecture Notes in Artificial Intelligence and Lecture Notes in Bioinformatics)' (2014), pp. 513–521, doi: 10.1007/978-3-319-09339-0_52

272   Wu, Ge, Siegler, Sorin, Allard, Paul, Kirtley, Chris, Leardini, Alberto, Rosenbaum, Dieter, Whittle, Mike, D'Lima, Darryl D., Cristofolini, Luca, Witte, Hartmut, Schmid, Oskar, Stokes, Ian: 'ISB recommendation on definitions of joint coordinate system of various joints for the reporting of human joint motion—part I: ankle, hip, and spine'*J. Biomech.*, 2002, **35**, (4), pp. 543–548. , doi: 10.1016/S0021-9290(01)00222-6

273   Analysis, Biomechanical Motion: 'BTS SMART- D High Frequency Digital System for Biomechanical Motion Analysis BTS SMART- D'*BTS Bioeng.*, no date, pp. 1–2.

274   Colombini, Daniela, Occhipinti, Enrico: 'I disturbi muscolo-scheletrici lavorativi. La causa, l'insorgenza, la prevenzione, gli aspetti medico legali' (Inail, 2000)

275   Wiedemann, L.G., Planinc, R., Nemec, I., Kampel, M.: 'Performance evaluation of joint angles obtained by the kinect V2'*Technol. Act. Assist. Living (TechAAL), IET Int. Conf.*, 2015, pp. 1–6. , doi: 10.1049/ic.2015.0142

276   Mackey, A.H., Walt, S.E., Lobb, G., Stott, N.S.: 'Intraobserver reliability of the modified Tardieu scale in the upper limb of children with hemiplegia'*Dev. Med. Child Neurol.*, 2004, **46**, (4), pp. 267–272. , doi: 10.1017/s0012162204000428

277   Cutti, A.G., Paolini, G., Troncossi, M., Cappello, A., Davalli, A.: 'Soft tissue artefacts assessment in humeral axial rotation'*Gait Posture*, 2005, **21**, (3), pp. 341–349.

278   Aguinaldo, Arnel L., Buttermore, Janet, Chambers, Henry: '<JAB Aguinaldo Effects of upper trunk rotation on shoulder joint torque among baseball pitchers of various levels.pdf>'*J. Appl. Biomech.*, 2007, **23**, (1), pp. 42–51. , doi: 10.1123/jab.23.1.42

279   Ferrari, A; Benedetti, M.G.; Pavan, E.; Frigo, C.; Bettinelli, D.; Rabuffetti, M.; Crenna, P.; Leardini, A.: 'Quantitative comparison of five current protocols in gait analysis'*Gait Posture*, 2008, **28**, (2), pp. 207–216.

280   Formulaire: 'RULA Employee Assessment Worksheet'*Cornell Univ.*, 2001, **24**, (1993), p. 2001.

281   Fleiss, Joseph L., Levin, Bruce, Paik, Myunghee Cho: 'Statistical Methods for Rates and Proportions' (John Wiley & Sons, 2004), doi: 10.1198/tech.2004.s812

282   Landis, J. Richard, Koch, Gary G.: 'The Measurement of Observer Agreement for Categorical Data'*Biometrics*, 1977, **33**, (1), p. 159. , doi: 10.2307/2529310

283   Plantard, P., Shum, H.P.H., Le Pierres, A.S., Multon, F.: 'Validation of an ergonomic assessment method using Kinect data in real workplace conditions'*Appl. Ergon.*, 2016, **65**, pp. 562–569. , doi: 10.1016/j.apergo.2016.10.015

284   Manghisi, Vito Modesto, Uva, Antonio Emmanuele, Fiorentino, Michele, Bevilacqua, Vitoantonio, Trotta, Gianpaolo Francesco, Monno, Giuseppe: 'Real time RULA assessment using Kinect v2 sensor'*Appl. Ergon.*, 2017, **65**, pp. 481–491. , doi:

10.1016/j.apergo.2017.02.015

285 Ahsanul Haque, Shah, Mahfuzul Aziz, Syed, Rahman, Mustafizur: 'Review of Cyber-Physical System in Healthcare.'*Int. J. Distrib. Sens. Networks*, 2014, **10**, (4), pp. 1–20. , doi: 10.1155/2014/217415

286 Hu, Liang, Xie, Nannan, Kuang, Zhejun, Zhao, Kuo: 'Review of cyber-physical system architecture', in 'Object/Component/Service-Oriented Real-Time Distributed Computing Workshops (ISORCW), 2012 15th IEEE International Symposium on' (2012), pp. 25–30

287 B, Krithi Ramamritham, Karmakar, Gopinath, Shenoy, Prashant: 'Big Data Analytics'*TDWI best Pract. report, fourth Quart.*, 2017, **10721**, (4), pp. 3–14. , doi: 10.1007/978-3-319-72413-3

288 Bevilacqua, V., Mastronardi, G., Menolascina, F., Pannarale, P., Pedone, A.: 'A Novel Multi-Objective Genetic Algorithm Approach to Artificial Neural Network Topology Optimisation: The Breast Cancer Classification Problem', in 'The 2006 IEEE International Joint Conference on Neural Network Proceedings' (2006), pp. 1958–1965, doi: 10.1109/IJCNN.2006.246940

289 Bevilacqua, Vitoantonio, Brunetti, Antonio, Triggiani, Maurizio, Magaletti, Domenico, Telegrafo, Michele, Moschetta, Marco: 'An Optimized Feed-forward Artificial Neural Network Topology to Support Radiologists in Breast Lesions Classification', in 'Proceedings of the 2016 on Genetic and Evolutionary Computation Conference Companion - GECCO '16 Companion' (2016), pp. 1385–1392, doi: 10.1145/2908961.2931733

290 Goetz, Christopher G., Fahn, Stanley, Jankovic, Joseph, Olanow, C. Warren: 'Movement Disorder Society-Sponsored Revision of the UnifiedParkinson's Disease Rating Scale (MDS-UPDRS): ScalePresentation and Clinimetric Testing Results'*Mov. Disord.*, 2008, **23**, (15), pp. 2129–2170.

291 Tsanas, Athanasios, Little, Max A., McSharry, Patrick E., Ramig, Lorraine O.: 'Accurate telemonitoring of parkinsons disease progression by noninvasive speech tests'*IEEE Trans. Biomed. Eng.*, 2010, **57**, (4), pp. 884–893. , doi: 10.1109/TBME.2009.2036000

292 Mellone, S., Palmerini, L., Cappello, A., Chiari, L.: 'Hilbert–Huang-Based Tremor Removal to Assess Postural Properties From Accelerometers'*Biomed. Eng. IEEE Trans.*, 2011, **58**, (6), pp. 1752–1761. , doi: 10.1109/TBME.2011.2116017

293 Keijsers, No�l L.W., Horstink, Martin W.I.M., Gielen, Stan C.A.M.: 'Automatic assessment of levodopa-induced dyskinesias in daily life by neural networks'*Mov. Disord.*, 2003, **18**, (1), pp. 70–80. , doi: 10.1002/mds.10310

294 Carmeli, Eli, Patish, Hagar, Coleman, Raymond: 'The Aging Hand'*Journals Gerontol. Ser. A*, 2003, **58**, (2), pp. M146–M152. , doi: 10.1093/gerona/58.2.M146

295 Loconsole, Claudio, Cascarano, Giacomo Donato, Brunetti, Antonio, Trotta, Gianpaolo Francesco, Losavio, Giacomo, Bevilacqua, Vitoantonio, Di Sciascio, Eugenio: 'A model-free technique based on computer vision and sEMG for classification in Parkinson's disease by using computer-assisted handwriting analysis'*Pattern Recognit. Lett.*, 2018. , doi: 10.1016/j.patrec.2018.04.006

296 Petras, Ivo, Bednarova, Dagmar: 'Total Least Squares Approach to Modeling : A

Matlab Toolbox'*Acta Montan. Slovaca*, 2010, **15**, (2), pp. 158–170.

297 Bevilacqua, Vitoantonio, Pannarale, Paolo, Abbrescia, Mirko, Oncologico, Istituto, Paolo, Giovanni, Oncologico, I.R.C.C.S. Ospedale, Bari, Orazio Flacco: 'Comparison of Data-Merging Methods with SVM Attribute Selection and Classification in Breast Cancer Gene Expression', in 'BMC bioinformatics' (2012), pp. 498–507

298 Kanjilal, P.P., Palit, S., Saha, G.: 'Fetal ECG extraction from single-channel maternal ECG using singular value decomposition'*Biomed. Eng. IEEE Trans.*, 1997, **44**, (1), pp. 51–59. , doi: 10.1109/10.553712

299 Tattoli, Giacomo, Buongiorno, Domenico, Bari, Polytechnic, Loconsole, Claudio, Bergamasco, Massimo: 'A novel BCI-SSVEP based approach for control of walking in Virtual Environment using a Convolutional Neural Network', in 'International Joint Conference on Neural Networks (IJCNN)' (2014), pp. 4121–4128, doi: 978-1-4799-1484-5/14/$31.00

300 Bortone, Ilaria, Trotta, Gianpaolo Francesco, Brunetti, Antonio, Cascarano, Giacomo Donato, Loconsole, Claudio, Agnello, Nadia, Argentiero, Alberto, Nicolardi, Giuseppe, Frisoli, Antonio, Bevilacqua, Vitoantonio: 'A novel approach in combination of 3D gait analysis data for aiding clinical decision-making in patients with Parkinson's disease', in 'Lecture Notes in Computer Science (including subseries Lecture Notes in Artificial Intelligence and Lecture Notes in Bioinformatics)' (2017), pp. 504–514, doi: 10.1007/978-3-319-63312-1_44

301 Cortes, Corinna, Vapnik, Vladimir, Saitta, Lorenza: 'Support-Vector Networks Editor'*Mach. Leaming*, 1995, **20**, (3), pp. 273–297. , doi: 10.1023/A:1022627411411

302 Defazio, Giovanni, Hallett, Mark, Jinnah, Hyder A., Stebbins, Glenn T., Gigante, Angelo F., Ferrazzano, Gina, Conte, Antonella, Fabbrini, Giovanni, Berardelli, Alfredo: 'Development and validation of a clinical scale for rating the severity of Blepharospasm'*Mov. Disord.*, 2015, **30**, (4), pp. 525–530. , doi: 10.1002/mds.26156

303 King, Davis. E.: 'Dlib-ml: A Machine Learning Toolkit'*J. Mach. Learn. Res.*, 2009, **10**, (Jul), pp. 1755–1758. , doi: 10.1145/1577069.1755843

304 Kazemi, Vahid, Sullivan, Josephine: 'One Millisecond Face Alignment with an Assemble of Regression Trees', in '27th IEEE Conference on Computer Vision and Pattern Recognition' (2014), pp. 1867–1874, doi: 10.13140/2.1.1212.2243

305 Sagonas, Christos, Tzimiropoulos, Georgios, Zafeiriou, Stefanos, Pantic, Maja: '300 faces in-the-wild challenge: The first facial landmark Localization Challenge', in 'Proceedings of the IEEE International Conference on Computer Vision' (2013), pp. 397–403, doi: 10.1109/ICCVW.2013.59

306 Zhang, Bo, Wang, Wenjun, Cheng, Bo: 'Driver eye state classification based on cooccurrence matrix of oriented gradients'*Adv. Mech. Eng.*, 2015, **7**, (2), p. 707106. , doi: 10.1155/2014/707106

307 Riedmiller, Martin, Braun, H.: 'A direct adaptive method for faster backropagation learning: the RPROP algorithm', in 'Proceedings of the IEEE International Conference on Neural Networks' (1993), pp. 586–591

308 Grandas, F., Elston, J., Quinn, N., Marsden, C.D.: 'Blepharospasm: a review of 264 patients'*J. Neurol. Neurosurg. Psychiatry*, 1988, **51**, (6), pp. 767–772. , doi:

10.1136/jnnp.51.6.767

309   Hallett, Mark, Evinger, Craig, Jankovic, Joseph, Stacy, Mark: 'Update on blepharospasm: Report from the BEBRF International Workshop'*Neurology*, 2008, **71**, (16), pp. 1275–1282. , doi: 10.1212/01.wnl.0000327601.46315.85

310   Jinnah, H.A., Berardelli, Alfredo, Comella, Cynthia, Defazio, Giovanni, Delong, Mahlon R., Factor, Stewart, Galpern, Wendy R., Hallett, Mark, Ludlow, Christy L., Perlmutter, Joel S., Rosen, Ami R.: 'The focal dystonias: Current views and challenges for future research'*Mov. Disord.*, 2013, **28**, (7), pp. 926–943. , doi: 10.1002/mds.25567

311   Berardelli, A., Rothwell, J.C., Day, B.L., Marsden, C.D.: 'Pathophysiology of blepharospasm and oromandibular dystonia'*Brain*, 1985, **108**, (3), pp. 593–608. , doi: 10.1093/brain/108.3.593

312   Peterson, David A., Littlewort, Gwen C., Bartlett, Marian S., Macerollo, Antonella, Perlmutter, Joel S., Jinnah, H.A., Hallett, Mark, Sejnowski, Terrence J.: 'Objective, computerized video-based rating of blepharospasm severity'*Neurology*, 2016, **87**, (20), pp. 2146–2153. , doi: 10.1212/WNL.0000000000003336

313   World Health Organisation (WHO): 'Global status report on noncommunicable diseases 2014' (World Health Organization, 2014), doi: ISBN 9789241564854

314   Ferlay, J., Soerjomataram, I.I., Dikshit, R., Eser, S., Mathers, C., Rebelo, M., Parkin, D.M., Forman, D., Bray, F.: 'Cancer incidence and mortality worldwide: sources, methods and major patterns in GLOBOCAN 2012'*Sect. Cancer Inf. Int. Agency Res. Cancer*, 2012, **136**, (5). , doi: 10.1002/ijc.29210

315   Doi, K., K., Doi: 'Current status and future potential of computer-aided diagnosis in medical imaging'*Br. J. Radiol.*, 2005, **78**, (SPEC. ISS.), pp. S3–S19.

316   Gong, X., Glick, S.J., Liu, B., Vedula, A.A., Thacker, S.: 'A computer simulation study comparing lesion detection accuracy with digital mammography, breast tomosynthesis, and cone-beam CT breast imaging'*Med Phys*, 2006, **33**, (4), pp. 1041–1052.

317   Hendrick, R. Edward: 'Radiation Doses and Cancer Risks from Breast Imaging Studies'*Radiology*, 2010, **257**, (1), pp. 246–253. , doi: 10.1148/radiol.10100570

318   Befeler, Alex S., Di Bisceglie, Adrian M.: 'Hepatocellular carcinoma: diagnosis and treatment'*Gastroenterology*, 2002, **122**, (6), pp. 1609–1619.

319   Mohapatra, S., Patra, D., Satpathy, S.: 'Automated leukemia detection in blood microscopic images using statistical texture analysis', in 'ACM International Conference Proceeding Series' (2011), pp. 184–187, doi: 10.1145/1947940.1947980

320   Bushberg, Jerrold T., Seibert, J. Anthony, Leidholdt, Edwin M. Jr., Boone, John M.: 'The Essential Physics of Medical Imaging' (Lippincott Williams & Wilkins, 2011)

321   Tempany, Clare M.C., Zou, Kelly H., Silverman, Stuart G., Brown, Douglas L., Kurtz, Alfred B., McNeil, Barbara J.: 'Staging of Advanced Ovarian Cancer: Comparison of Imaging Modalities—Report from the Radiological Diagnostic Oncology Group'*Radiology*, 2000, **215**, (3), pp. 761–767. , doi: 10.1148/radiology.215.3.r00jn25761

322   Karssemeijer, N.: 'Computer-aided detection in mammography'*Imaging Decis. MRI*,

2008, **12**, (3), pp. 23–28. , doi: 10.1111/j.1617-0830.2009.00130.x

323 Bankman, Isaac N.: 'Handbook of Medical Image Processing and Analysis', in (2009), p. 984

324 Wang, Xiao-feng, Huang, De-shuang, Xu, Huan: 'An efficient local Chan – Vese model for image segmentation'*Pattern Recognit.*, 2010, **43**, (3), pp. 603–618. , doi: 10.1016/j.patcog.2009.08.002

325 Wang, Xiao Feng, Huang, De Shuang, Du, Ji Xiang, Xu, Huan, Heutte, Laurent: 'Classification of plant leaf images with complicated background'*Appl. Math. Comput.*, 2008, **205**, (2), pp. 916–926. , doi: 10.1016/j.amc.2008.05.108

326 Wang, Xiao-feng: 'A Novel Multi-Layer Level Set Method for Image Segmentation'*Computer (Long. Beach. Calif).*, 2008, **14**, (14), pp. 2428–2452.

327 Kapoor, Luxit, Thakur, Sanjeev: 'A survey on brain tumor detection using image processing techniques', in '2017 7th International Conference on Cloud Computing, Data Science & Engineering - Confluence' (2017), pp. 582–585, doi: 10.1109/CONFLUENCE.2017.7943218

328 Bevilacqua, V., Aulenta, A., Carioggia, E., Mastronardi, G., Menolascina, F., Simeone, G., Paradiso, A., Scarpa, A., Taurino, D.: 'Metallic artifacts removal in breast CT images for treatment planning in radiotherapy by means of supervised and unsupervised neural network algorithms', in 'Lecture Notes in Computer Science (including subseries Lecture Notes in Artificial Intelligence and Lecture Notes in Bioinformatics)' (2007), pp. 1355–1363, doi: 10.1007/978-3-540-74171-8_138

329 Kumar, Nitin: 'Thresholding in salient object detection : a survey'*Multimed. Tools Appl.*, 2017, (January), pp. 1–32.

330 Bevilacqua, Vitoantonio, Piazzolla, Alessandro, Stofella, Paolo: 'Atlas-based segmentation of organs at risk in radiotherapy in head MRIs by means of a novel active contour framework', in 'Lecture Notes in Computer Science (including subseries Lecture Notes in Artificial Intelligence and Lecture Notes in Bioinformatics)' (2010), pp. 350–359, doi: 10.1007/978-3-642-14932-0_44

331 Bengio, Yoshua: 'Deep Learning'*Www*, 2017, **521**, (7553), p. 775. , doi: 10.1561/2000000039

332 Bevilacqua, Vitoantonio, Pietroleonardo, Nicola, Triggiani, Vito, Brunetti, Antonio, Di Palma, Anna Maria, Rossini, Michele, Gesualdo, Loreto: 'An innovative neural network framework to classify blood vessels and tubules based on Haralick features evaluated in histological images of kidney biopsy'*Neurocomputing*, 2017, **228**, pp. 143–153. , doi: 10.1016/j.neucom.2016.09.091

333 Chen, Tao, Xu, Ruifeng, He, Yulan, Wang, Xuan: 'd_Deep Learning in Neural Networks: An Overview'*Expert Syst. Appl.*, 2017, **72**, pp. 221–230. , doi: 10.1016/j.eswa.2016.10.065

334 Oakley, John P., Satherley, Brenda L.: 'Improving image quality in poor visibility conditions using a physical model for contrast degradation'*IEEE Trans. Image Process.*, 1998, **7**, (2), pp. 167–179. , doi: 10.1109/83.660994

335 Kimori, Yoshitaka: 'Mathematical morphology-based approach to the enhancement of morphological features in medical images'*J. Clin. Bioinforma.*, 2011, **1**, (1), p. 33. ,

doi: 10.1186/2043-9113-1-33

336 Nanni, Loris, Ghidoni, Stefano, Brahnam, Sheryl: 'Handcrafted vs. non-handcrafted features for computer vision classification'*Pattern Recognit.*, 2017, **71**, pp. 158–172. , doi: 10.1016/j.patcog.2017.05.025

337 Classification, Texture: 'Completed Local Binary Count for Rotation Invariant Texture Classification'*IEEE Trans. image Process.*, 2012, **21**, (10), pp. 4492–4497.

338 Sahiner, B., Chan, H.P., Petrick, N., Helvie, M.A., Hadjiiski, L.M.: 'Improvement of mammographic mass characterization using spiculation measures and morphological features'*Med. Phys.*, 2001, **28**, (7), pp. 1455–1465. , doi: 10.1118/1.1381548

339 Wu, Wen-Jie, Moon, Woo Kyung: 'ScienceDirect - Academic Radiology : \nUltrasound Breast Tumor Image Computer-Aided Diagnosis With Texture and Morphological Features1'*Acad. Radiol.*, 2008, **15**, (7), pp. 873–80. , doi: 10.1016/j.acra.2008.01.010

340 Haralick, R.M., Shanmugam, K., Dinstein, I.: 'Textural features for image classification'*IEEE Trans. Syst. Man, Cybertinetics*, 1973, **3**, (6), pp. 610–621.

341 Ojala, Timo, Pietikäinen, Matti, Mäenpää, Topi: 'Gray Scale and Rotation Invariant Texture Classification with Local Binary Patterns'*IEEE Trans. Pattern Anal. Mach. Intell.*, 2000, **24**, (7), pp. 404–420. , doi: 10.1007/3-540-45054-8_27

342 Hamilton, N.A., Pantelic, R.S., Hanson, K., Teasdale, R.D.: 'Fast automated cell phenotype image classification'*BMC Bioinformatics*, 2007, **8**, (1), p. 110. , doi: 10.1186/1471-2105-8-110

343 Xu, Anqi, Namit, Gaurav: 'SURF : Speeded - Up Robust Features'*Eur. Conf. Comput. Vis.*, 2008, pp. 1–30. , doi: 10.1007/11744023_32

344 Rangayyan, Rm: 'Biomedical image analysis' (CRC press, 2004)

345 Kullback, S., Leibler, R.A.: 'On Information and Sufficiency'*Ann. Math. Stat.*, 1951, **22**, (1), pp. 79–86. , doi: 10.1214/aoms/1177729694

346 Van Der Maaten, L.J.P., Postma, E.O., Van Den Herik, H.J.: 'Dimensionality Reduction: A Comparative Review'*J. Mach. Learn. Res.*, 2009, **10**, pp. 1–41. , doi: 10.1080/13506280444000102

347 Antonio Brunetti, Leonarda Carnimeo, Gianpaolo Francesco Trotta, Vitoantonio Bevilacqua: 'Computer-Assisted Frameworks for Classification of Liver, Breast and Blood Neoplasias via Neural Networks: a Survey based on Medical Images'*To Appear Neurocomputing 2018*, 2018.

348 Huang, De Shuang, Zhao, Xing Ming, Huang, Guang Bin, Cheung, Yiu Ming: 'Classifying protein sequences using hydropathy blocks'*Pattern Recognit.*, 2006, **39**, (12), pp. 2293–2300. , doi: 10.1016/j.patcog.2005.11.012

349 Metz, C.E.: 'Basic principles of ROC analysis.', in 'Sem Nuc' (1978), pp. 283–289

350 Theodoridis, Sergios: 'Neural Networks and Deep Learning' (Determination Press USA, 2015), pp. 875–936, doi: 10.1016/B978-0-12-801522-3.00018-5

351 Tokarczyk, Piotr, Wegner, Jan D., Walk, Stefan, Schindler, Konrad: 'Beyond hand-crafted features in remote sensing'*ISPRS Ann. Photogramm. Remote Sens. Spat. Inf. Sci.*, 2013, (1), pp. 35–40.

352 Lee, Honglak, Grosse, Roger, Ranganath, Rajesh, Ng, Andrew, Honglak Lee, Roger Grosse: 'Unsupervised learning of hierarchical representations with convolutional deep belief networks'*Commun. ACM*, 2011, **54**, (10), pp. 95–103. , doi: 10.1145/2001269.2001295

353 Ali, Aida, Shamsuddin, Siti Mariyam, Ralescu, Anca L.: 'Classification with class imbalance problem'*Int. J. Adv. Soft Comput. its Appl.*, 2015, **7**, (3), pp. 176–204.

354 Vestito, A., Mangieri, F.F., Gatta, G., Moschetta, M., Turi, B., Ancona, A.: 'Breast carcinoma in elderly women. Our experience'*G Chir*, 2011, **32**, (10), pp. 411–416.

355 Chawla, Nitesh V, Bowyer, Kevin W., Hall, Lawrence O.: 'SMOTE : Synthetic Minority Over-sampling Technique'*J. Artif. Intell. Res.*, 2002, **16**, pp. 321–357.

356 Kallenberg, Michiel, Petersen, Kersten, Nielsen, Mads, Ng, Andrew Y., Diao, Pengfei, Igel, Christian, Vachon, Celine M., Holland, Katharina, Winkel, Rikke Rass, Karssemeijer, Nico, Lillholm, Martin: 'IEEE TMI SPECIAL ISSUE ON DEEP LEARNING Unsupervised deep learning applied to breast density segmentation and mammographic risk scoring'*IEEE Trans. Med. Imaging*, 2016, **35**, (5), pp. 1–10.

357 Samala, Ravi K., Chan, Heang-Ping, Hadjiiski, Lubomir M., Cha, Kenny, Helvie, Mark A.: 'Deep-learning convolution neural network for computer-aided detection of microcalcifications in digital breast tomosynthesis'*SPIE Med. imaging. Int. Soc. Opt. Photonics*, 2016, p. 97850Y. , doi: 10.1117/12.2217092

358 Korhonen, Katrina E., Weinstein, Susan P., McDonald, Elizabeth S., Conant, Emily F.: 'Strategies to Increase Cancer Detection: Review of True-Positive and False-Negative Results at Digital Breast Tomosynthesis Screening'*RadioGraphics*, 2016, **36**, (7), pp. 1954–1965. , doi: 10.1148/rg.2016160049

359 Soh, Leen-kiat, Tsatsoulis, Costas, Member, Senior: 'Texture Analysis of SAR Sea Ice Imagery Using Gray Level Co-Occurrence Matrices Texture Analysis of SAR Sea Ice Imagery Using Gray Level Co-Occurrence Matrices'*Ieee Trans. Geosci. Remote Sens.*, 1999, **37**, (2), pp. 780–795. , doi: 10.1109/36.752194

360 Clausi, David A.: 'An analysis of co-occurrence texture statistics as a function of grey level quantization'*Can. J. Remote Sens.*, 2002, **28**, (1), pp. 45–62. , doi: 10.5589/m02-004

361 Simonyan, Karen, Zisserman, Andrew: 'Very Deep Convolutional Networks for Large-Scale Image Recognition'*arXiv Prepr. arXiv1409.1556*, 2015.

362 Chatfield, Ken, Simonyan, Karen, Vedaldi, Andrea, Zisserman, Andrew: 'Return of the Devil in the Details: Delving Deep into Convolutional Nets'*arXiv Prepr. arXiv1405.3531*, 2014. , doi: 10.5244/C.28.6

363 Lecun, Yann: 'OverFeat : Integrated Recognition , Localization and Detection using Convolutional Networks'*arXiv Prepr. arXiv1312.6229*, 2014.

364 Zeiler, Matthew D., Fergus, Rob: 'Visualizing and Understanding Convolutional Networks arXiv:1311.2901v3 [cs.CV] 28 Nov 2013', in 'Computer Vision–ECCV 2014' (2014), pp. 818–833, doi: 10.1007/978-3-319-10590-1_53

365 Suykens J.A.K. & Vandewalle, J.: ' Least squares support vector machine classifiers'*Neural Process. Lett*, 1999, **9**, (3), pp. 293–300.

366   Mucherino, Antonio, Papajorgji, Petraq J., Pardalos, Panos M.: 'k-Nearest Neighbor Classification'*Scholarpedia*, 2009, **4**, (2), pp. 83–106. , doi: 10.1007/978-0-387-88615-2_4

367   Lewis, David D.: 'Naive (Bayes) at forty: The independence assumption in information retrieval', in 'European conference on machine learning' (1998), pp. 4–15, doi: 10.1007/BFb0026666

368   Safavian, S. Rasoul, Landgrebe, David: 'A Survey of Decision Tree Classifier Methodology A SURVEY OF DECISION TREE CLASSIFIER METHODOLOGY 1'*Electr. Eng.*, 1991, **21**, (3), pp. 660–674. , doi: 10.1109/21.97458

369   Analysis, Linear Discriminant: 'Linear Discriminant Analysis'. Virginia Polytechnic Institute, 1936, doi: 10.1007/978-0-387-78189-1

370   Karlik, Bekir: 'Hepatitis Disease Diagnosis Using Backpropagation and the Naive Bayes Classifiers'*IBU J. Sci. Technol.*, 2011, **1**, (1).

371   Dr. S. Vijayarani1, Mr. S. Dhayanand.: 'Liver Disease Prediction using SVM and Naïve Bayes Algorithms'*Int. J. Sci. Eng. Technol. Res.*, 2015, **4**, (4), pp. 816–820.

372   Gulia, Anju, Vohra, Rajan, Rani, Praveen: 'Liver patient classification using intelligent techniques'*Int. J. Comput. Sci. Inf. Technol.*, 2014, **5**, (4), pp. 5110–5115.

373   Ba-alwi, Fadl Mutaher, Hintaya, Houzifa M.: 'Comparative Study for Analysis the Prognostic in Hepatitis Data: Data Mining Approach'*Spinal Cord*, 2013, **4**, (8), pp. 680–685.

374   Vincey, Ms, Malar, Jeba: 'Computer Aided Diagnosis for liver Cancer Feature Extraction'*Int. J. Eng. Sci.*, 2013, **2**, (11), pp. 27–30.

375   Kumar, S.S., Devapal, D.: 'Survey on recent CAD system for liver disease diagnosis', in '2014 International Conference on Control, Instrumentation, Communication and Computational Technologies, ICCICCT 2014' (2014), pp. 763–766, doi: 10.1109/ICCICCT.2014.6993061

376   Memeo, M., Stabile Ianora, A.A., Scardapane, A., Suppressa, P., Cirulli, A., Sabba, C., Rotondo, A., Angelelli, G.: 'Hereditary haemorrhagic telangiectasia: study of hepatic vascular alterations with multi-detector row helical CT and reconstruction programs'*Radiol.Med.*, 2005, **109**, (0033–8362 (Print)), pp. 125–138.

377   Berman, C.: 'Primary Carcinoma of the Liver A Study of 100 Cases among 48,900 Necropsies'*Cancer*, 1951, **7**, (3), pp. 462–503.

378   Jiang, Wen, Huang, De Shuang, Li, Shenghong: 'Random Walk-Based Solution to Triple Level Stochastic Point Location Problem'*IEEE Trans. Cybern.*, 2016, **46**, (6), pp. 1438–1451. , doi: 10.1109/TCYB.2015.2446198

379   Ahmed, Shan E., Rajpoot, Nasir: 'HANDCRAFTED FEATURES WITH CONVOLUTIONAL NEURAL NETWORKS FOR DETECTION OF TUMOR CELLS IN HISTOLOGY IMAGES Muhammad Nasim Kashif a Muhammmad Arif a Department of Electrical Engineering , Pakistan Institute of Engineering and Applied Sciences , Department of', in 'Biomedical Imaging (ISBI), 2016 IEEE 13th International Symposium on' (2016), pp. 1029–1032

380   Shkolyar, Anat, Gefen, Amit, Benayahu, Dafna, Greenspan, Hayit: 'Automatic

Detection of Cell Divisions (Mitosis) in Live-Imaging Microscopy Images using Convolutional Neural Networks', in 'Engineering in Medicine and Biology Society (EMBC), 2015 37th Annual International Conference of the IEEE' (2015), pp. 743–746, doi: 10.0/Linux-x86_64

381 Tran, Ha, Phan, Hong, Kumar, Ashnil, Kim, Jinman, Feng, Dagan: 'Transfer Learning of a Convolutional Neural Network for Hep-2 Cell Image Classification', in 'Biomedical Imaging (ISBI), 2016 IEEE 13th International Symposium on' (2016), pp. 1208–1211, doi: 10.0/Linux-x86_64

382 Piuri, Vincenzo, Scotti, Fabio: 'Morphological classification of blood leucocytes by microscope images', in '2004 IEEE International Conference onComputational Intelligence for Measurement Systems and Applications, 2004. CIMSA.' (2004), pp. 103–108, doi: 10.1109/CIMSA.2004.1397242

383 Alagappan, M., BanuRekha, B., Arun, R., Kalaikamal, M., Muthukr-ishnan, S., Ganesh, C.S. Sai, Sathishkumar, S.: 'Extreme learning machine (elm) based automated identification and classification of white blood cells', in 'International Conference on Mathematical Modeling and Applied Soft Computing' (no date), pp. 846–852

384 Krizhevsky, Alex, Sutskever, I., Hinton, G.E.: 'ImageNet Classification with Deep Convolutional Neural Networks', in 'Advances in Neural Information Processing Systems (NIPS 2012)' (2012), pp. 1097–1105, doi: 10.1145/3065386

385 Connolly, James L., Schnitt, Stuart J., Wang, Helen H., Longtine, Janina A.: 'Role of the Surgical Pathologist in the Diagnosis and Management of the Cancer Patient - Holland-Frei Cancer Medicine - NCBI Bookshelf Role of the Surgical Pathologist in the Diagnosis and Management of the Cancer Patient Gross Handling of Specimens'2003, (December), pp. 1–21.

386 McCahill, Laurence E., Single, Richard M., Aiello Bowles, Erin J., Feigelson, Heather S., James, Ted A., Barney, Tom, Engel, Jessica M., Onitilo, Adedayo A.: 'Variability in Reexcision Following Breast Conservation Surgery'*Jama*, 2012, **307**, (5), p. 467. , doi: 10.1001/jama.2012.43

387 Harréus, Ulrich: 'Surgical errors and risks - the head and neck cancer patient.'*GMS Curr Top Otorhinolaryngol Head Neck Surg*, 2013, **12**, p. E-pub. , doi: 10.3205/cto000096

388 Stranks, Jeremy: 'Human Factors and Behavioural Safety' (Routledge, 2013), doi: 10.1017/CBO9781107415324.004

389 Chen, X., Xu, L., Wang, Y., Wang, H., Wang, F., Zeng, X., Wang, Q., Egger, J.: 'Development of a surgical navigation system based on augmented reality using an optical see-through head-mounted display'*J Biomed Inf.*, 2015, **55**, pp. 124–131. , doi: 10.1016/j.jbi.2015.04.003

390 Wang, Junchen, Suenaga, Hideyuki, Yang, Liangjing, Kobayashi, Etsuko, Sakuma, Ichiro: 'Video see-through augmented reality for oral and maxillofacial surgery'*Int. J. Med. Robot. Comput. Assist. Surg.*, 2017, **13**, (2), p. e1754. , doi: 10.1002/rcs.1754

391 Hanna, Matthew G., Ahmed, Ishtiaque, Nine, Jeffrey, Prajapati, Shyam, Pantanowitz, Liron: 'Augmented Reality Technology Using Microsoft HoloLens in Anatomic Pathology'*Arch. Pathol. Lab. Med.*, 2018, **142**, (5), p. arpa.2017-0189-OA. , doi: 10.5858/arpa.2017-0189-OA

392   Andress, Sebastian, Johnson, Alex, Unberath, Mathias, Winkler, Alexander, Yu, Kevin, Fotouhi, Javad, Weidert, Simon, Osgood, Greg, Navab, Nassir: 'On-the-fly Augmented Reality for Orthopaedic Surgery Using a Multi-Modal Fiducial', in 'Medical Imaging 2018: Image-Guided Procedures, Robotic Interventions, and Modeling' (2018), p. 105760H, doi: 10.1117/1.JMI.5.2.021209

393   Hanna, Matthew G., Worrell, Stephanie, Ishtiaque, Ahmed, Fine, Jeffrey, Pantanowitz, Liron: 'SIIM 2017 Scientific Session Posters & Demonstrations Pathology Specimen Radiograph Co-Registration Using the HoloLens Improves Physician Assistant Workflow'*SIIM Sci. Sess. Poster Demostr.*, 2017, (Figure 1), pp. 5–7.

394   Lia, Hillary, Paulin, Gregory, Yi, Nelson, Haq, Hassan, Emmanuel, Steve, Ludig, Kristian, Keri, Zsuzsanna, Lasso, Andras, Fichtinger, Gabor, Yeo, Caitlin T., Andrews, Jessica: 'HoloLens in suturing training', in 'Medical Imaging 2018: Image-Guided Procedures, Robotic Interventions, and Modeling' (2018), p. 69, doi: 10.1117/12.2293934

395   Pratt, Philip, Ives, Matthew, Lawton, Graham, Simmons, Jonathan, Radev, Nasko, Spyropoulou, Liana, Amiras, Dimitri: 'Through the HoloLens^{TM} looking glass: augmented reality for extremity reconstruction surgery using 3D vascular models with perforating vessels'*Eur. Radiol. Exp.*, 2018, **2**, (1), p. 2. , doi: 10.1186/s41747-017-0033-2

396   Cho, K., Yanof, J.H., Schwarz, G., West, K., Shah, H., Madajka, M., Drake, R.L., Gharb, B.B., Rampazzo, A., Papay, F.A.: 'Craniofacial Surgical Planning with Augmented Reality: Accuracy of Linear 3D Cephalometric Measurements on 3D Holograms'*Ohio Val. Soc. Plast. Surg.*, 2017, **5**, (9 Suppl).

397   Adabi, K., Rudy, H., Stern, C., Weichman, K., Tepper, O. & Garfein, E.: 'Optimizing Measurements in Plastic Surgery through Holograms with Microsoft Hololens'*Plast. Reconctructive Surg.*, 2017, **5**, (9), pp. 182–183. , doi: 10.1097/01.GOX.0000526428.21421.4a

398   Egger, Jan, Gall, Markus, Tax, Alois, Ücal, Muammer, Zefferer, Ulrike, Li, Xing, Von Campe, Gord, Schäfer, Ute, Schmalstieg, Dieter, Chen, Xiaojun: 'Interactive reconstructions of cranial 3D implants under MeVisLab as an alternative to commercial planning software'*PLoS One*, 2017, **12**, (3), p. e0172694. , doi: 10.1371/journal.pone.0172694

399   Perkins, Stephanie L., Lin, Michael A., Srinivasan, Subashini, Wheeler, Amanda J., Hargreaves, Brian A., Daniel, Bruce L.: 'A mixed-reality system for breast surgical planning', in '2017 IEEE International Symposium on Mixed and Augmented Reality (ISMAR-Adjunct)' (2017), pp. 269–274, doi: 10.1109/ISMAR-Adjunct.2017.92

400   Bevilacqua, Vitoantonio: 'Three-dimensional virtual colonoscopy for automatic polyps detection by artificial neural network approach: New tests on an enlarged cohort of polyps'*Neurocomputing*, 2013, **116**, pp. 62–75. , doi: 10.1016/j.neucom.2012.03.026

401   Schinagl, Dominic A.X., Vogel, Wouter V., Hoffmann, Aswin L., van Dalen, Jorn A., Oyen, Wim J., Kaanders, Johannes H.A.M.: 'Comparison of Five Segmentation Tools for 18F-Fluoro-Deoxy-Glucose-Positron Emission Tomography-Based Target

Volume??Definition in Head and Neck Cancer'*Int. J. Radiat. Oncol. Biol. Phys.*, 2007, **69**, (4), pp. 1282–1289. , doi: 10.1016/j.ijrobp.2007.07.2333

402 Baumgart, Bruce G.: 'A polyhedron representation for computer vision', in 'Proceedings of the May 19-22, 1975, national computer conference and exposition on - AFIPS '75' (1975), p. 589, doi: 10.1145/1499949.1500071

403 Bosma, Marco K., Smit, Jaap, Lobregt, Steven: 'Iso-surface volume rendering', in 'Medical Imaging 1998: Image Display' (1998), pp. 10–20

404 Bevilacqua, Vitoantonio, Uva, Antonio Emmanuele, Fiorentino, Michele, Trotta, Gianpaolo Francesco, Dimatteo, Maurizio, Nasca, Enrico, Nocera, Attilio Nicola, Cascarano, Giacomo Donato, Brunetti, Antonio, Caporusso, Nicholas, others: 'A Comprehensive Method for Assessing the Blepharospasm Cases Severity', in 'International Conference on Recent Trends in Image Processing and Pattern Recognition' (2016), pp. 369–381

405 Mason, Llew, Baxter, Jonathan, Bartlett, Peter, Frean, Marcus: 'Boosting algorithms as gradient descent', in 'Nips' (1999), pp. 512–518, doi: 10.1109/5.58323

406 Salih, Yasir, Malik, Aamir S.: 'Depth and geomtry from a single 2D image using triangulation', in 'IEEE International Conference on Multimedia and Expo Workshops' (2012), pp. 511–515, doi: 10.1109/ICMEW.2012.95

407 P. Alizadeh: 'Object Distance Measurement Using a Single Camera for Robotic Applications'. Laurentian University of Sudbury, 2015

408 Holzmann, Clemens, Hochgatterer, Matthias: 'Measuring distance with mobile phones using single-camera stereo vision', in 'Proceedings - 32nd IEEE International Conference on Distributed Computing Systems Workshops, ICDCSW 2012' (2012), pp. 88–93, doi: 10.1109/ICDCSW.2012.22

409 Abdel-Aziz, Y.I., Karara, H.M.: 'Direct Linear Transformation from Comparator Coordinates into Object Space Coordinates in Close-Range Photogrammetry'*Photogramm. Eng. Remote Sens.*, 2015, **81**, (2), pp. 103–107. , doi: 10.14358/PERS.81.2.103

410 Gamal Seedahmed, and Anton F. Schenk University: 'Direct linear transformation in the context of different scaling criteria', in 'Asprsasprs' (2001), pp. 5–30, doi: 10.13140/2.1.3600.4644

411 Levenberg, Kenneth: 'A method for the solution of certain non-linear problems in least squares'*Q. Appl. Math.*, 1944, **2**, (2), pp. 164–168. , doi: 10.1090/qam/10666

412 Marquardt, Donald W.: 'An Algorithm for the Least-Squares Estimation of Nonlinear Parameters'*SIAM J. Appl. Math.*, 1963, **11**, (2), pp. 431–441.

413 Hsieh, Chung-Hung, Lee, Jiann-Der: 'Markerless Augmented Reality via Stereo Video See-Through Head-Mounted Display Device'*Math. Probl. Eng.*, 2015, **2015**.